Characterization of Heat Shock Protein 70-z (PfHsp70-z) from *Plasmodium falciparum*

by

Tawanda Zininga

submitted in fulfilment of the requirements for the degree of

Doctor of Philosophy

in the subject of Biochemistry

at

the University of Venda

Promoter: Prof Addmore Shonhai

Co-Promoter: Dr. A. Burger

Submitted on November 2015

© University of Venda

ABSTRACT

Malaria is a parasitic disease that accounts for more than 660 thousand deaths annually, mainly in children. Malaria is caused by five Plasmodium species *P. ovale, P. vivax, P. malariae, P. falciparum* and *P. knowlesi.* The most lethal cause of cerebral malaria is *P. falciparum*. The parasites have been shown to up-regulate some of their heat shock proteins (Hsp) in response to stress. Heat shock protein 70 (called DnaK in prokaryotes) is one of the most prominent groups of chaperones whose role is central to protein homeostasis and determines the fate of proteins. Six *Hsp70* genes are represented on the genome of *P. falciparum*. The *Hsp70* genes encode for proteins that are localised in different sub-cellular compartments. Of these two occur in the cytosol, PfHsp70-z and PfHsp70-1; two occur in the endoplasmic reticulum, PfHsp70-2 and PfHsp70-y; one in the mitochondria, PfHsp70-3 and one exported to the red blood cell cytosol, PfHsp70-x. PfHsp70-1 is a well characterized canonical Hsp70 involved in prevention of protein aggregation and facilitates protein folding. Little is known about PfHsp70-z. PfHsp70-z was previously shown to be an essential protein implicated in the folding of proteins possessing asparagine rich repeats. However, based on structural evidence PfHsp70-z belongs to the Hsp110 family of proteins and is thought to serve as a nucleotide exchange factor (NEF) of PfHsp70-1. The main aim of this study is to elucidate the functional roles of PfHsp70-z as a chaperone and its interaction with PfHsp70-1. In the current study, PfHsp70-z was cloned and expressed in *E. coli* JM109 cells. This was followed by its purification using nickel chromatography. The expression of PfHsp70-z in parasites cultured *in vitro* was investigated and its association with PfHsp70-1 was explored using a co-immuno-precipitation assay. PfHsp70-z expression in malaria parasites is up regulated by heat stress and the protein is heat stable based on investigations conducted using Circular Dichroism. Furthermore, the direct interaction between recombinant forms of PfHsp70-z and PfHsp70-1 were investigated using slot blot and surface plasmon resonance assays. PfHsp70-z was observed to exhibit ATPase activity. In addition, the direct interaction between PfHsp70-z and PfHsp70-1 is promoted by ATP. Based on limited proteolysis and tryptophan fluorescence analyses, PfHsp70-z binds ATP to assume a unique structural conformation compared to the conformation of the protein bound to ADP or in nucleotide-free state. PfHsp70-z was able to suppress the heat-induced aggregation of malate dehydrogenase and luciferase *in vitro*. Interestingly, while ATP appears to modulate the conformation of PfHsp70-z, the chaperone function of PfHsp70-z was not influenced by ATP. Altogether, these findings suggest that

© University of Venda

PfHsp70-z serves as an effective peptide substrate holding chaperone. In addition, PfHsp70-z may also serve as the sole nucleotide exchange factor of PfHsp70-1. The broad spectrum of functions of this protein, could explain this PfHsp70-z is an essential protein in malaria parasite survival. This is the first study to show that PfHsp70-z possess independent chaperone activity and that it interacts with its cytosolic counterpart, PfHsp70-1 in a nucleotide dependent fashion. Furthermore, the study shows that PfHsp70-z is a heat stable molecule and that it is capable of forming high order oligomers.

Key words: Malaria, *Plasmodium falciparum*, chaperone, nucleotide exchange factor, PfHsp70-z

© University of Venda

DECLARATION

I Tawanda Zininga hereby declare that the thesis for the Doctor of Philosophy degree at the University of Venda, hereby submitted by me, has not previously been submitted for a degree at this or any other university, and that it is my own work in design and execution and that all reference material contained therein has been duly acknowledged.

Signature……Date…….

© University of Venda

DEDICATION

This thesis is lovingly dedicated to

My Wife Chipo, and our daughters Nadine and Eleora

© University of Venda

PREFACE

This thesis is presented in form of six chapters whose outlines is provided below based on the various thematic areas covered in the study. Some aspects of the thesis have already been published in peer reviewed articles (see list of outputs; page xvii). The outline of the thesis chapters is as follows;

- **Chapter 1**: This is a general introduction encompassing all the background to the suggested broad aim and objectives. The broad problem statement, hypothesis, aim and objectives are highlighted in section 1.5.
- **Chapter 2**: This chapter presents the bioinformatics analyses of the structural features of PfHsp70-z.
- **Chapter 3**: This chapter presents the production of recombinant PfHsp70-z protein and biochemical analysis of its secondary and tertiary features.
- **Chapter 4**: This chapter presents investigation of the association of PfHsp70-z with PfHsp70-1 and assessment of its chaperone activity *in vitro.*
- **Chapter 5**: This chapter represents analysis of the expression, co-localisation and interaction of PfHsp70-z with PfHsp70-1 in parasites maintained at the red blood stage.
- **Chapter 6**. This chapter covers conclusive remarks and future perspectives.

© University of Venda

ACKNOWLEDGEMENTS

I wish to thank God for giving me the strength to complete this study. I am extremely grateful to my supervisor Prof. Addmore Shonhai for his guidance, expertise and mentorship all through the duration of the project. Your support and encouragement indispensably made it possible for me to finish this project.

I also wish to express my gratitude to my co-supervisor Dr. Addelle Burger for her support and guidance.

I also wish to acknowledge the following people for the technical support and for hosting me during research visits:

- Dr. Earl Prinsloo, (Biotechnology Innovation Centre, Rhodes University, South Africa)
- Prof. Heinrich Hoppe (Department of Biochemistry, Microbiology and Biotechnology, Rhodes University, South Africa)
- Dr. Ikechukwu Achilonu, Prof. Heini Dirr (Protein Structure-Function Research Unit, School of Molecular and Cell Biology, University of the Witwatersrand, South Africa)

I wish to extend further acknowledgement to the:

- DFG for Funding the project and study Bursary
- University of Venda Research Committee (South Africa) for student research funding

I would also like to express my gratitude to Mr. Thina Mudau (University of Venda, South Africa), for going out of his way to provide technical support, Mr. Stanley Makumire, (University of Venda, South Africa) for proof-reading my thesis and Dr. David Tinarwo for his support.

Finally, special thanks goes to all the ProBioM research team (University of Venda).

© University of Venda

TABLE OF CONTENTS

© University of Venda

© University of Venda

© University of Venda

© University of Venda

© University of Venda

© University of Venda

LIST OF FIGURES

© University of Venda

LIST OF TABLES

© University of Venda

LIST OF SYMBOLS

Abbreviations of units Symbol Interpretation

%	percent
µl	microlitre
A320	absorbance at 320 nanometres
A360	absorbance at 360 nanometres
A595	absorbance at 595 nanometres
A600	absorbance at 600 nanometres
bp	base pair
kDa	kilodalton
µM	micromolar
pM	picomolar
°C	degree Celsius
µl	microlitre
ml	millilitre
l	litres
w/v	weight per volume
v/v	volume per volume
µg	microgram
g	gram
α	alpha
β	beta

© University of Venda

LIST OF OUTPUTS

JOURNAL ARTICLES:

1. **Zininga, T.** and Shonhai A. (2014) Are heat shock proteins druggable candidates? American Journal of Biochemistry and Biotechnology, 10: 211-213. DOI: 10.3844/ajbbsp.2014.211.213.

2. **Zininga, T**., Achilonu, I., Hoppe, H., Prinsloo, E. Dirr, H.W. Shonhai A. (2015). Overexpression, purification and characterization of the *Plasmodium falciparum* Hsp70-z (PfHsp70-z). PLoS ONE 10(6): e0129445. DOI:10.1371/journal.pone.0129445.

3. **Zininga, T**., Makumire, S., Gitau, G.W., Njunge, J.M., Pooe, O.J., Klimek, H., Scheurr, R., Raifer, R., Prinsloo, E., Przyborski, J.M., Hoppe, H., Shonhai, A (2015). *Plasmodium falciparum* Hop (PfHop) interacts with the Hsp70 chaperone in a nucleotide-dependent fashion and exhibits ligand selectivity. PLoS ONE 10(8): e0135326. DOI:10.1371/journal.pone.0135326.

4. **Zininga, T**., Achilonu, I., Hoppe, H., Prinsloo, E. Dirr, HW. Shonhai A (2015). *Plasmodium falciparum* Hsp70-z (Hsp110c) exhibits independent chaperone activity and interacts with Hsp70-1 in a nucleotide dependent fashion. (In Press)

CONFERENCE PROCEEDINGS

1. **T. Zininga**, I. Achilonu, H. W. Dirr. E. Prinsloo, Hoppe, H., A. Shonhai. Cytosolic *Plasmodium falciparum* heat shock protein 70-z (PfHsp70-z) possesses independent chaperone function and interacts with PfHsp70-1 in a nucleotide dependent fashion. Molecular Approaches to Malaria conference. Lorne, Victoria, Australia (Accepted) 21-25 February 2016.

2. **T. Zininga**, I. Achilonu, H. W. Dirr. E. Prinsloo, Hoppe, H., A. Shonhai. Structure-function analysis of *Plasmodium falciparum* heat shock protein 70-z (PfHsp70-z) reveals a chaperone with multi-faceted functions. Molecular Approaches to Malaria conference. Lorne, Victoria, Australia (Accepted) 21-25 February 2016.

3. **T. Zininga**, I. Achilonu, H. W. Dirr. E. Prinsloo A. Shonhai. Analysis of the chaperone function of cytosolic *Plasmodium falciparum* heat shock protein 70-z (PfHsp70-z). University of Venda Open research day. 3-7 March 2015.

4**. T. Zininga**, I. Achilonu, H. W. Dirr. E. Prinsloo A. Shonhai. *Plasmodium falciparum* heat shock protein 70-z (PfHsp70-z) binds and hydrolyzes ATP. University of Venda, Research Open day. 3-7 March 2015.

5. **T. Zininga**, E. Prinsloo and A. Shonhai. Cytosolic *Plasmodium falciparum* heat shock protein 70-z (PfHsp70-z) interacts with PfHsp70-1 in a nucleotide dependent manner. University of Venda, Research Open day. 3-7 March 2015.

© University of Venda

6. **T. Zininga**, and A. Shonhai. Analysis of the functional interaction between cytosolic *Plasmodium falciparum* heat shock protein 70-z (PfHsp70-z) and PfHsp70-1. The European Molecular Biology Organization (EMBO) Practical Course on Computational Analysis of Protein-Protein Interactions: from Sequences to Networks, September 29th to October 3rd 2014 at the University of Cape Town.

© University of Venda

CHAPTER 1

INTRODUCTION

Literature Review

© University of Venda

1.1 Human Malaria

1.1.1 Epidemiology

Malaria is contracted by more than 198 million people each year and more than 584 thousand people die yearly with the majority being in the tropics (WHO, 2014). Malaria is the most severe public health problem worldwide and largely affects sub-Saharan Africa. Africa accounts for about 90 % of all deaths due to malaria, and of these 78 % are children under 5 years (Orem *et al.,* 2012; WHO, 2014). More than half the world population (3.4 billion people) lives in areas with high risk of malaria transmission spread over 106 countries and regions (CDC, 2014; WHO, 2014). Malaria causes economic and social burdens with a direct estimated cost (illness, treatment and premature death) of US$ 12 billion per year (Sachs and Malaney, 2002; CDC, 2014). The burden on individual countries starts as loss of income which translates to reduced economic growth resulting in reduced economic development of ~1 % per year (CDC, 2014).

Human malaria is caused by *Plasmodium* species which are classified under the phylum Apicomplexan (Figure 1.1; Morrison, 2009). *Plasmodium* species are transmitted by female *Anopheles* mosquitoes. The initial documented description of malaria was made around 2700 BC in ancient Chinese documents. Subsequent studies proving that malaria was caused by protozoa were reported by Laveran in 1880 (Reviewed in Cox, 2010). Malaria was then described on the basis of periodicity (frequency of occurrence) and was thought to be caused by four species responsible for: benign tertian (*Haemamoeba vivax*), malignant tertian (*Laverania malariae*), quartan (*Heamamaeba malariae*) malaria and *P. ovale*. These species are now known as *P. vivax*, *P. falciparum* and *P. malariae,* respectively (Stephens, 1922 in Cox, 2010). *P. knowlesi* was initially considered a parasite for primates (mainly for monkeys) until it was first identified as a human pathogen in Malaysia in 1971 (Singh *et al*., 2004a). It was reclassified as a human pathogen by 2004 when more cases were identified (Singh *et al*., 2004a; Cox-Singh *et al*., 2008). In summary, it has now been established that human malaria is caused by five species of *Plasmodium* (*P. falciparum*, *P. knowlesi, P. malariae, P. ovale,* and *P. vivax*), of which *P. falciparum* is the most deadly form (Figure 1.1; WHO, 2014).

© University of Venda

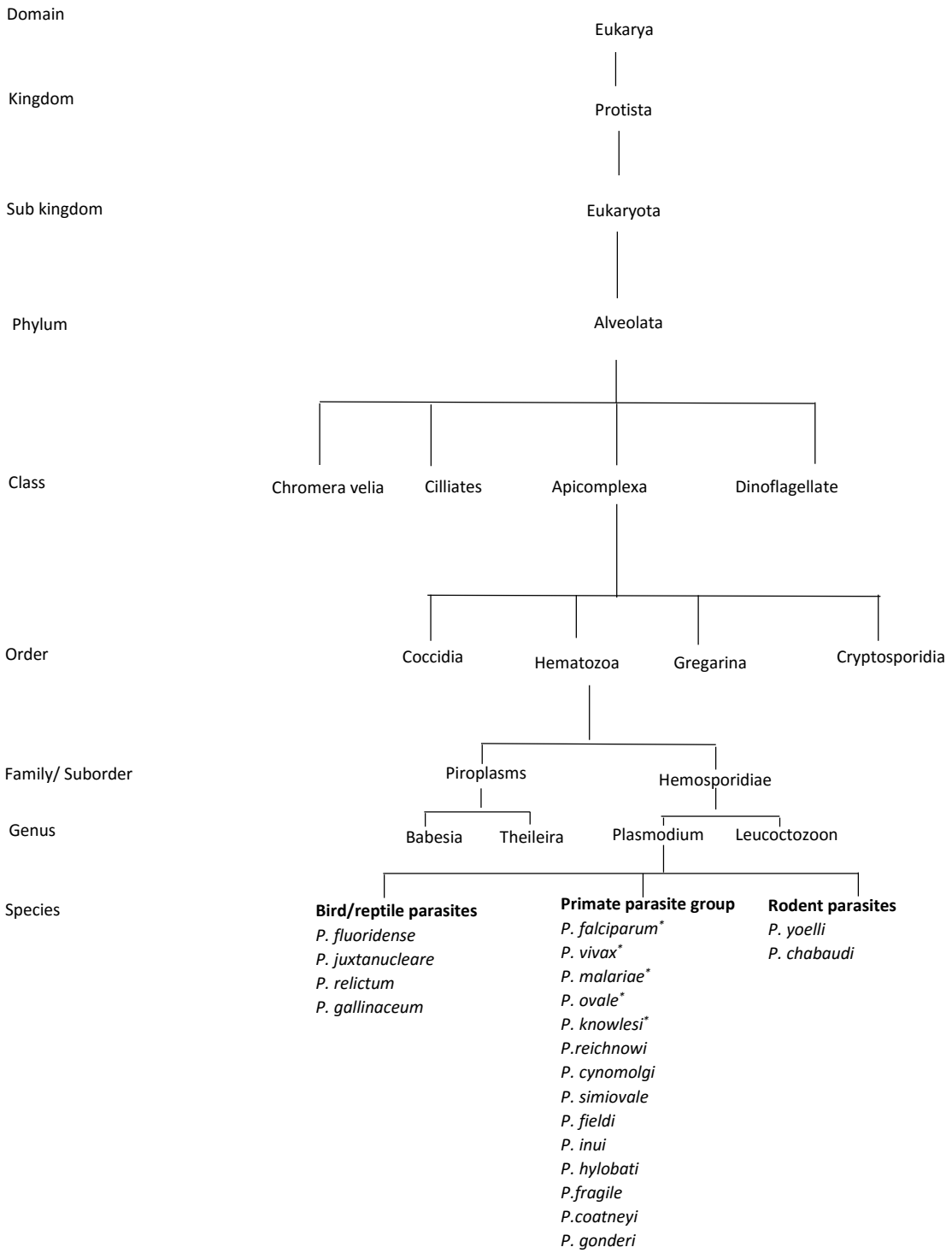

Figure 1.1 Classification of apicomplexans
Genus *Plasmodium* is grouped amongst apicomplexan class that is divided into four groups of coccidia, hematozoa, cryptosporidia and gregarine. The hematozoa group includes hemosporidiae and piroplasms. The piroplasms are subclassified into two genuses *Babesia* and *Theileria*. The hemosproidae are subslassfied into genuses *plasmodium* and *leucocytozoon*. The plasmodium genus is further subclassfied into several species which are grouped according to host (*) represent human parasites (Adapted from Duval *et al.,* 2007; Morrison, 2009; Janouškovec *et al*., 2010).

© University of Venda

1.2.1 *P. falciparum* life cycle

Malaria infection occurs when an infected vector the female *Anopheles* mosquito, takes a blood meal from a host-human and inoculates the *Plasmodium* sporozoites into the blood (Figure 1.2; Koella *et al*., 1998). The sporozoites move in the blood circulation and subsequently infect hepatocytes (Lasonder *et al*., 2008). In the hepatocytes, initial asexual replication takes place and the parasites develop further into exo-erythrocytic shizonts, which rupture releasing merozoites into the blood stream where they infect red blood cells (RBC) (Bannister *et al*., 2000). Entry of the merozoites into the RBC is facilitated by parasite proteins which interact with RBC surface receptors (Boyle *et al*., 2010). The merozoites undergo asexual multiplication (erythrocytic-schizogony) in RBC which ruptures after 48 hours releasing 8-12 merozoites (Fujioka and Aikawa, 2002). The majority of the released merozoites infect more erythrocytes (Bannister and Mitchell, 2003).

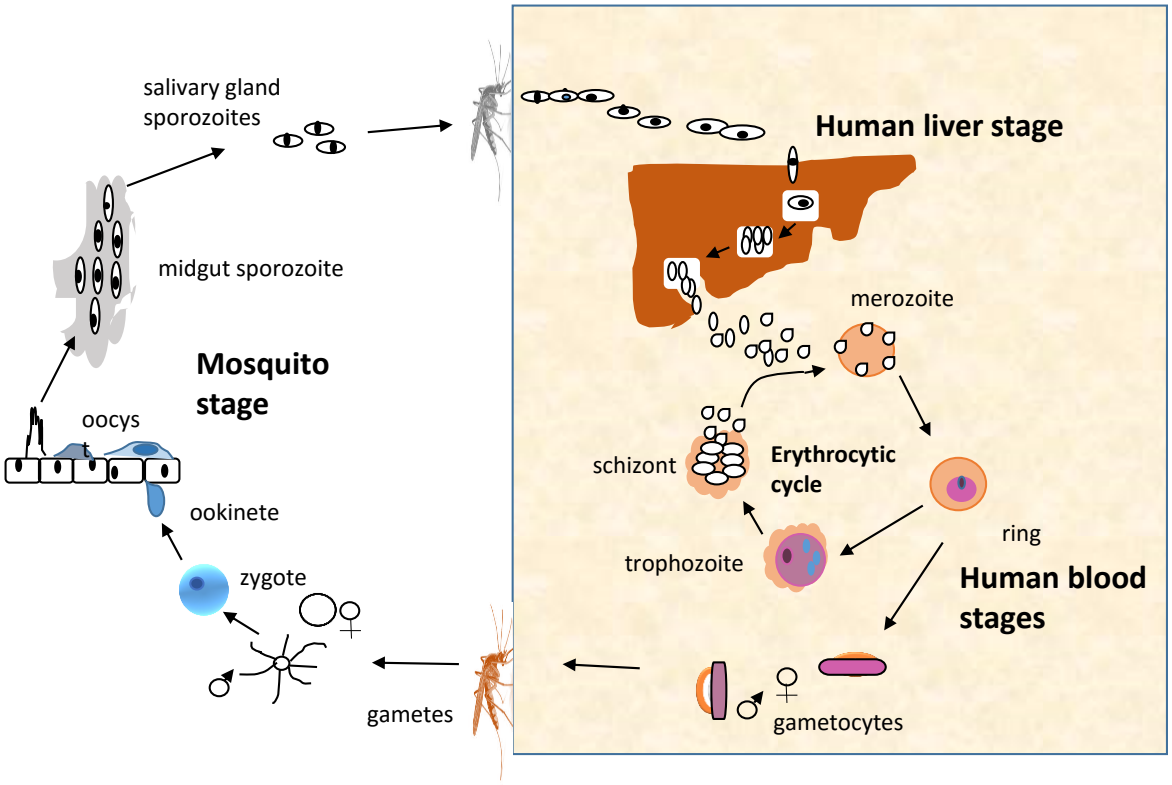

Figure 1.2 The Life cycle of *P. falciparum*
Mosquito stage is characterized by the sporogonic cycle where a mosquito ingests the gametocytes during an infected blood meal (Fujioka and Akiwa, 2002). The Human liver stage starts where the sporozoite migrate to the liver and develop into schizonts. The erythrocytic cycle starts when the merozoites released form hepatocytes infect the RBC, adapted from Cowman *et al* (2012).

© University of Venda

During the febrile episodes, some of the merozoites differentiate into sexual gametocytes; microgametocyte (male) and macrogametocyte (female) (Billker *et al*., 1997), which are ingested by *Anopheles* mosquito when they take a blood meal. The parasites in the mosquito multiply by sexual reproduction. The microgametocytes penetrate macrogametocytes in the mosquito stomach generating zygotes (Figure 1.2). Zygotes are motile and elongated (Ookinetes) and invade the midgut wall and develop into oocysts (Billker *et al*., 1997). The oocysts grow and rupture releasing sporozoites which migrate to the mosquito salivary gland epithelium and are inoculated into the host when the mosquito takes another blood meal and the cycle continues (Crompton *et al*., 2010).

The erythrocytic stages of the Plasmodium life cycle are responsible for the clinical manifestations of clinical malaria characterized by febrile episodes (Pavithra *et al*., 2004). The immune response to the antigenic parasite proteins stimulates release of proinflammatory cytokines among them tumour necrosis factor (TNF) which is responsible for periodic fevers that may elevate body temperature to 41^{o}C (Bannister *et al*., 2000). It is at this crucial stage that the parasites asexually reproduce. During this stage there is increased protein biosynthesis mainly for aiding the rapid multiplication of the parasites.

1.2.2 Treatment and diagnosis

The effectiveness of therapeutic drugs in the control of malaria routinely faces challenges from drug resistant *P. falciparum* parasites. Global reports of Plasmodium strains resistant to quinolines, endoperoxidases and sulfadoxide-pyrimethamine drugs in malaria endemic areas have been documented (Witkowski *et al*., 2009; WHO, 2012). The development of the antimalarial drug Artemisinin derived from *Artemisa annua* plant, ushered in a new hope for the treatment of malaria (Yu, 2011). The promising drug, Artemisinin is also losing its efficacy as resistance to its monotherapy has been reported in the great Mekong sub region (Thailand, Cambodia, Myanmar and Vietnam) (Dordorp *et al*., 2009; Witkowsiki *et al*., 2012). To counter the development of drug resistance, treatment of malaria currently depends on Artemisinin based Combination Therapy (ACT) as the first line treatment endorsed by World Health

© University of Venda

Assembly in 2007 (WHO, 2014). A recent publication reported a *P. falciparum* strain with reduced susceptibility to ACT in the Cambodia region and surrounding areas (van Schalkwyk and Sutherland, 2015). This poses a threat to the future efficacy of ACT with dire public health effects (van Schalkwyk and Sutherland, 2015). There is a high unmet clinical need for new Plasmodium drug targets to produce novel therapeutics against the increasing multidrug resistant strains. It is thought that the multidrug resistance observed in some Plasmodium strains is possibly facilitated by parasite targeted gene mutations (Su *et al*., 1997; Park *et al.,* 2012). The ability of the parasite to thrive under drug selection stress may partly be facilitated by the molecular chaperones whose main function is to refold proteins including their mutated forms thereby enabling the parasite to resist drug pressure (section 1.4; Reviewed in Shonhai, 2010; Zininga and Shonhai, 2014).

1.2.3 Malaria pathology

The pathology of *P. falciparum* malaria is mainly evident during the RBC stage of its life cycle (Le Roch *et al*., 2003). The parasites develop in the infected RBC (iRBC) resulting in their rupture. The intracellular multiplication of the parasite is associated with structural and biochemical changes that alter the functioning of the iRBCs. This leads to the development of the clinical symptoms of *P. falciparum* malaria which gives rise to anemia and/or cerebral malaria (Miller *et al*., 1994). Malaria pathology is influenced by host inflammatory reaction and parasite sequestration in tissues (Miller *et al*., 1994).

Sequestration malaria pathology is linked to iRBCs through their tendency to stick to both capillary endothelial cells and to uninfected RBCs leading to seclusion and rosette formation respectively (Martins and Daniel-Ribeiro, 2013). The iRBCs start showing morphological changes characterized by knob like structures that develop on their surface (Spycher *et al.,* 2003). This normally occurs when the parasites reach the second half of the 48-hour maturation cycle. This is because at this stage the parasites export some of its own proteins to the iRBC membrane where they bind to receptors on endothelial cells that line the microvasculature (Xu *et al*., 2013; Saigal *et al*., 2014). The sequestration of iRBC is thought to

© University of Venda

be facilitated by the binding of *P. falciparum* Erythrocyte Membrane Protein 1 (PfEMP1), present on the membrane of iRBC complexed to the endothelial receptors (Kraemer *et al*., 2006). The endothelial receptors include intracellular adhesion molecule 1 (ICAM-1) and thrombospondin (TSP) (Lucas and Sherman, 1998; Storm and Craig, 2014). The iRBCs can tether and roll on host receptors including ICAM1 and may enhance binding to platelet Glycoprotein IV or Cluster of Differentiation 36 (CD36) leading to sequestration (Reviewed in Angchaisuksiri, 2014). iRBCs are rigid, and this makes them to be sequestered in microvasculature (Dondorp *et al*., 2004). The rosetting and sequestration may lead to mechanical blockage of blood capillaries. These events are thought to result in obstruction of capillary blood flow leading to decreased tissue anoxia and decreased waste removal which may lead to a coma or organ failure (Dondorp *et al*., 2004; Martins and Daniel-Ribeiro, 2013).

The inflammatory pathway is based on host immune response when *P. falciparum* iRBC bursts, releasing both parasite toxins (glycosylphosphatidylinositol, hemozoin) and RBC intracellular molecules (heme) into circulation (Ropert *et al*., 2001; Nebl *et al*., 2005; Martins and Daniel-Ribeiro, 2013). These toxins are recognized by CD1 receptors on monocytes, neutrophils and endothelial cells through Toll-like receptor 2 (TLR2) pattern recognition receptors (Nebl *et al*., 2005). Upon exposure to the toxins the CD1+ (with CD1 receptors) cells are activated and induced to secrete pro-inflammatory cytokines like tumor necrosis factor alpha (TNF-α), Interferon gamma (IFN-γ) and lymphotoxin-alpha (LT-α) (Nebl, 2005; van der Hyde *et al*., 2006). The activated innate immune cells together with released pro-inflammatory cytokines recruit $CD4^+$ and $CD8^+$ cells which further aggravate the inflammation by recruiting more cells to secrete pro-inflammatory cytokines (van der Hyde *et al*., 2006). The inflammation is beneficial at first, in reducing the parasitemia and the release of toxic intracellular molecules. However, later on, the inflammatory response is not properly regulated and consequently mediates damage to the microvascular endothelium resulting in leakage of cytokines, malarial antigens and free radicals resulting in the aggravation of the disease (Hunt *et al*., 2006). Taken together, sequestration and inflammation pathways are complimentary of each other as both are based on processes that occur during *P. falciparum*

© University of Venda

infection. Altogether, these phenomena explain why malaria pathology is multifaceted as it involves both host and parasite factors.

1.2.4 Parasite-host interaction

The invasion of RBC by a parasite is a process that can be described in three distinct stages: (i) attachment with apical reorientation followed by (ii) induction of the parasitophorous vacuole (PV) (Figure 1.3) and subsequently (iii) translocation of parasite into the vacuole. The parasite attaches to the host RBC membrane using the apical end contacts that interact with cell receptors which stimulate parasite reorientation (Baumeister *et al*., 2010). Reorientation involves the gliding motility mediated by the glideosome, an actinomyosin-based protein complex (Baumeister *et al*., 2010). The reorientation results in direct juxta-positioning of parasite apical end and host cell membrane resulting in the formation of a tight junction between the parasite apex and the host RBC (Cowman and Crabb, 2006). This induces the secretion of adhesins from the micronemes that are translocated along the parasite length and are shed on the side of the moving junction (Richard *et al*., 2010). The secretion of PV components from the rhoptries also plays an important role in this event (Baumeister *et al*., 2010; Richard *et al*., 2010). The PV is a compartment that is formed in a circumferential zone of attachment of the orifice of the host cell invagination. The parasite enters the nascent PV by capping the moving junction down its body thought to be facilitated by the *P. falciparum* merozoite-capping protein 1 (MCP-1) (Cowman and Crabb, 2006). The parasite becomes enclosed within the PV (cavity) delimited by the invaginated host membrane (Figure 1.3; Baumeister *et al*., 2010).

The PV is surrounded by the parasitophorous vacuole membrane (PVM) formed during invasion. The PV serves as an interface between the parasite and host iRBC cytosol (Baumeister *et al*., 2010). The PVM has been shown to lack the RBC membrane proteins like glycophorins and anion transporter band 3 (Baumeister *et al*., 2010). This suggests there is selective recruitment of cholesterol-rich sub-domains within the RBC membrane called lipid “rafts” associated membrane proteins (Figure 1.3; Harrison *et al*., 2003; Baumeister *et al*.,

© University of Venda

2010). The recruited erythrocyte proteins associated with the PVM form detergent resistant micro domains which serve as a shield to protect the parasite (Tokumatsu *et al*., 2014).

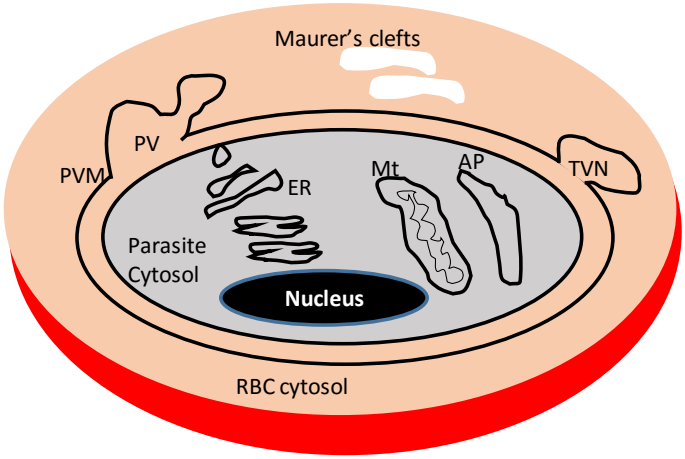

Figure 1.3 Representation of a cross section of the parasite infected erythrocyte
The letters represent the following organelles; ER (endoplamic reticulum), Mt (Mitochondria), AP (Apicoplast), PV (Parasitophorous vacuole), TVN (Tubulovesicular network) and PVM (PV membrane), adapted from Shonhai *et al* (2007).

The transportation of more than 400 parasite proteins beyond the PVM is thought to be mediated by a pentapeptide signal located towards the N-terminus of target proteins (Hiller *et al*., 2004), termed Plasmodium export element (PEXEL) (Marti *et al*., 2005) or the vacuolar transport signal (VTS) (Hiller *et al*., 2004). A second group of exported proteins lack the PEXEL motif and they are termed PEXEL-negative exported proteins (PNEP) (Grüring *et al*., 2012). For PNEPs their export is thought to be mediated through a single hydrophobic region that is located up to 214 amino acids downstream from the N-terminal (Spielmann *et al*., 2006; Spielmann and Gilberger, 2010). The export of both PEXEL and PNEPs is thought to be facilitated by unfolding of proteins thereby suggesting translocation as a common step in export (Gruring *et al*., 2012). There are suggestions that a multimeric protein complex translocon located on the PVM is responsible for the traffic of parasite proteins (Charpian and Pryzborski, 2008). The PVM has non-selective pores that facilitate the transport of nutrients to the parasite (Figure 1.3; Nyalwidhe at al., 2002).

© University of Venda

The exported parasite proteins that mainly associate with the RBC membranes are the ring-infected erythrocyte surface antigen (RESA) (Goel *et al*., 2014), mature-parasite-infected erythrocyte surface antigen (MESA) (Kilili and LaCount, 2011), *P. falciparum* erythrocyte membrane protein 3 (PfEMP-3) (Pei *et al*., 2007), knob-associated histidine-rich protein (KAHRP) (Weng *et al*., 2014) and *P. falciparum* erythrocyte membrane protein 1 (PfEMP1) (Senczuk *et al*., 2001). Amongst these KAHRP and membrane-associated histidine-rich proteins 1 (MAHRP) (Spycher *et al*., 2003) associate beneath the knobs (Spycher *et al*., 2003; Pei *et al*., 2007; Weng *et al*., 2014). The Maurer's clefts are discrete membrane bound appendages that are scatted in the iRBC cytoplasm where they mediate parasite protein assembly (Figure 1.3; Cooke *et al*., 2006). *P. falciparum* skeleton-binding protein 1 (PfSBP1) (Kats *et al*., 2015) and MAHRP are thought to be localized in the Maurer's clefts. RESA is expressed at the ring stage and is thought to contribute to the RBC membrane structural integrity through binding to beta spectrin (Pei *et al*., 2007). MESA facilitates binding of protein 4.1 to glycophorin C, band 3 and p55 (Waller *et al*., 2003; Pei *et al*., 2007). KAHRP is involved in the adhesive interaction of the merozoite to the RBC membrane through binding to the repeat 4 of alpha spectrin (Weng *et al*., 2014). The parasites remodel the RBC as a survival mechanism to evade clearance by the immune system. PFEMP-1 is also implicated in RBC cytoadherance to prevent spleen clearance and also it is implicated in antigenic diversity as a mechanism of immune system evasion (Biggs *et al*., 1991; Buffet *et al* 2011; Merrick *et al*., 2012).

1.2.5 Red blood cell modification by *P. falciparum*

P. falciparum infected RBCs have been found to exhibit increased phosphorylated protein Band 4.1 (Morrissette and Sibley, 2002). Parasite cysteine protease cleaves the iRBC ankyrin and this results in loss of the normal discoid shape of the RBC to spherical orientation (Raphael *et al*., 2000). These modifications together with other exported parasite proteins RESA, MESA and histidine rich protein 1 (HRP-1) (Hayward *et al*., 2002) which are anchored on the RBC membrane associate with spectrin, band 4.1 and band 3 ankyrin binding domain. This association results in altered RBC morphology, a mechanism used by parasites for immune evasion. The integrity of the iRBC cytoskeleton is crucial for parasite development

© University of Venda

(Morrissette and Sibley, 2002). This suggests that the parasite survives indirectly from structural features of the iRBC. At the end of 48 hour asexual cycle, the iRBC membrane is ruptured. This process is thought to be initiated by disruption of the PV and the entry of parasites into the RBC cytoplasm (Morrissette and Sibley, 2002; Mohandas and An, 2012). Parasite serine proteases mediate the destabilization of the iRBC membrane culminating in its rupture releasing new merozoites (reviewed in Mohandas and An, 2012).

1.3 Molecular Chaperones

1.3.1 Heat shock proteins as molecular chaperones

Molecular chaperones are molecules that are involved in the folding of nascent polypeptides, refolding of unfolded proteins, and facilitation of protein transport across membranes, reduce aggregation and facilitate degradation of clients that are beyond refolding as a quality control mechanism (Bukau *et al*., 2006). Molecular chaperones facilitate non-covalent three-dimensional organization of their clients without themselves taking part in the final product.

Heat shock proteins (Hsp) are a group of molecular chaperones, most of which are upregulated in response to stress. Heat shock proteins were named upon their first discovery in *Drosphila* where they were upregulated during heat stress (*Ritosa, 1962*). They are involved in the suppression of stress induced unfolding of client proteins and also refolding of unfolded proteins. Some Hsps have the ability to fold newly formed proteins. Hsps play a central role in proteostasis as they are also involved in determining the fate of misfolded proteins either refolding them or channeling them to the ubiquitin proteolysis pathway for degradation (Kriegenburg *et al*., 2012).

Hsps are ubiquitous molecular chaperones found in all celled organisms. Hsps exhibit high level of conservation across species. Despite the fact that heat shock proteins constitute the bulk of molecular chaperones, not all molecular chaperones are heat shock proteins. There are several ways in which Hsps are named, but generally those that are stress induced are

© University of Venda

referred to as Hsp, and those that are cognatively expressed are termed heat shock cognate (Hsc) proteins. They can also be named according to their functional roles; holding substrate in a folding competent state (holdase), folding the substrate to its native structure (foldase) (Wyn *et al*., 1994) and unfolding aggregated substrates (unfoldase) (Saibil, 2013). Hsps are also classified according to their molecular sizes (Table 1.1; Lindquist and Craig, 1988).

1.4 The Role of Heat Shock Proteins in the Development of *P. falciparum* parasites

1.4.1 Major *P. falciparum* heat shock proteins

There are 7 major families of heat shock proteins from *P. falciparum* denoted according to size; Hsp110, Hsp100, Hsp90, Hsp70, Hsp60, Hsp40 and small Hsps (approximately 15-30 kDa) (Table 1.1).

© University of Venda

Table 1.1: Major shock proteins families and their cellular localisations

Protein name	Monomer size/ kDa	Eukaryotic localisation	Stress function	Comments	References
Hsp110	100-150	cytoplasm ER	nucleotide exchange factors, thermo-tolerance	function as NEFs for Hsp70s, have independent holdase activity	Oh *et al* (1999); Dragovic *et al* (2006); Muralidharan *et al* (2012)
Hsp100	80- 110	cytosol, nucleolus, nucleus, chloroplast	Thermo-tolerance, long term spore viability	assembles into homo-oligomeric proteins in presence of ATP; an ATPase (unfoldase)	Squires, (1992); Sanchez *et al* (1990); Nowicki *et al* (2012)
Hsp90	82- 96	cytosol, nucleus	Thermo-tolerance and viability	associates with steroid hormone receptors, kinases, cyclophilins, actin, tubulin, Hsp70; an ATPase (foldase)	Picard *et al* (1990); Tai *et al* (1992); Yang *et al*., (2015)
Hsp70	67- 76	ER, cytosol, nucleus, mitochondria, chloroplast	chaperone required for protein assembly, secretion, thermo-tolerance	associates with; Hsp60, Hsp40, Hsp90,GrpE; binds unfolded proteins and peptides; an ATPase (foldase)	Kurtz *et al* (1986); Bukau and Walker (1990); Shonhai *et al* (2005)
Hsp60	58- 65	mitochondria, chloroplast.	chaperonin, assembly of oligomeric proteins and folding monomeric proteins	ATPase, hydrolysis stimulated by Hsp10 (foldase)	Martin *et al* (1991); Langer *et al* (1992); Sato and Wilson (2005)
Hsp40	40- 100	cytosol, membranes	co-chaperone of Hsp70	function with Hsp70 and GrpE (holdase)	Cheetham and Caplan (1998); Botha *et al* (2007); Njunge *et al* (2013)

Table legend: ER- endoplasmic reticulum; BiP- binding protein; Grp- glucose-regulated protein; Hsp- heat-shock protein; Clp- Caseinolytic protease, adapted from Lindquist (1992).

1.4.2 Hsp100 family

Hsp100 group of molecular chaperones (Table 1.1) are primarily involved in the dis-assembly of quaternary structure of polypeptide complexes and are crucial elements required for thermotolerance (Sanchez and Lindquist 1990; Pak and Wickner, 1997). Hsp100s, specifically Hsp104 and prokaryotic ClpB (caseinolytic protease B) structurally have two nucleotide binding domains (NBD1 and NBD2; AAA^{+} domains) which are important for chaperone

© University of Venda

function and form functional hexameric complexes (Vale, 2000; Nowicki *et al.,* 2012). The first AAA$^+$ domain of Hsp104 and ClpB contains an additional coil-coil region called the middle domain located on the C-terminus of the ATP binding site (Winkler *et al*., 2012; Mogk *et al*., 2015). Eukaryotic and prokaryotic Hsp100 utilizes an ATP hydrolysis functional cycle which is thought to be stimulated by substrate binding (Nowicki *et al* 2012). The N-terminus serves as the substrate binding domain (Barnet *et al*., 2005). The function of Hsp100 as a disaggregase and ATPase are modulated through a conserved aspartic acid residue D184 in the NBD1 (Hsp104), analogous to ClpB (D178) which is required for both ATPase and dis-aggregation functions (Nowicki *et al*., 2012). This suggests that Hsp100 have a conserved switch that modulates both the ATPase and disaggregase function.

Hsp100 functions in a complex with Hsp70s to form Hsp100/Hsp70 disaggregase complex that entangles polypeptides from mesh of aggregates (Winkler *et al*., 2012; Mogk *et al*., 2015). In this Hsp100/Hsp70 complex, it has been postulated that Hsp100 is the first one to bind to aggregated substrates, pulling them out from the aggregated mesh thereby exposing the hydrophobic patches where Hsp70 subsequently binds allowing the substrate to fold into its native form (Mogk *et al*., 1999; 2015).

P. falciparum encodes eight Clp proteins; five ClpATPases that belong to the AAA$^+$ superfamily (PfClpB1, PfClpB2, PfClpC, PfClpM, PfClpY; El Bakkouri *et al*., 2010; Rathore *et al*., 2011), and three protease like proteins: PfClpP, PfClpR and PfClpQ (El Bakkouri *et al*., 2010; 2013). The Clp AAA$^+$ proteins are localized in the apicoplast with the exception of PfClpB2 (PV) and PfClpY (Mitochondia; El Bakkouri *et al*., 2010). ClpB was shown to be localized in the PV and is thought to facilitate secretion of malarial proteins into the PV (Rathore *et al*., 2011). Clp proteins have also been shown to function as heptemer complexes, whose function is essential in apicoplast development (Rathore *et al*., 2010). There is need for further studies to elucidate possible interactions between Clp ATPases and *P. falciparum* Hsp70s (PfHsp70-3 localized in the mitochondrial and PfHsp70-x in the PV (section 1.4.6.3 and 1.4.6.4, respectively) as this may suggest the formation of functional complexes with an important role in parasite proteostasis.

© University of Venda

1.4.3 Hsp90 family

Heat shock protein 90s (Hsp90) (Table 1.1) are ATP dependent molecular chaperones involved in a variety of cellular processes including cell cycle control, cell survival, hormone and other cell signaling pathways (Jackson, 2013). Hsp90s are widespread in eubacteria and in eukaryotes. They are the most abundant molecules, for example, in the human cell they constitute about 2 % of the total cell protein mass (Finka and Goloubinoff, 2013; Finka *et al*., 2015). As such, Hsp90s have been used as drug targets in neurodegenerative disorders, cancer, and in the development of anti-viral and anti-protozoan infections (reviewed in Zininga and Shonhai, 2014). Hsp90 recognizes substrates from a wide range of protein families (Jackson, 2013). In *S. cerevisae* it was shown that at least 10 % of the proteins require Hsp90 for further folding (Zhao *et al*., 2005).

The Hsp90 family is highly conserved from eubacteria to eukaryotes (Johnson and Brown, 2009). For example, Hsp90 from human and *E. coli* share ~50 % sequence identities (Johnson and Brown 2009; Johnson, 2012). Hsp90 chaperones are essential in eukaryotes but are not essential at all growth conditions in *E coli* (Cao *et al*., 2003; Maynard *et al*., 2010). Hsp90 family is composed of five subfamilies in different cellular locations: cytosolic Hsp90s, ER Hsp90s (Grp94), Mitochondrial TRAP1, chloroplast Hsp90 and bacterial Hsp90 HtpG (Jackson *et al*., 2013). In mammals there are two cytosolic Hsp90s; the constitutively expressed Hsp90β and the inducible isoform Hsp90α (Kampinga *et al*., 2009). These function as homodimers that interact through the C-terminal domain (Figure 1.4; Jackson *et al*., 2013).

Hsp90 are composed of an N-terminal domain that serves as the ATP binding site and is linked to the middle domain through a charged linker. The middle domain is adjacent to the C-terminal domain which ends with an EEVD motif at the C-terminal (Figure 1.4). In *P. falciparum* there are four Hsp90 paralogs; full length cytosolic Hsp90 homologue (PF3D7_0708400), endoplasmic reticulum Grp94 homologue (PF3D7_1222300), mitochondrial TRAP1 (PF3D7_1118200) and a truncated Hsp90 without the cytosolic signal

© University of Venda

(PF3D7_1443900) (Kumar *et al*., 2003; Acharya *et al*., 2007). Similar to the other Hsp90s, they possess the EEVD motif towards the C-terminus (Banumathy *et al*., 2003; Gitau *et al*., 2012).

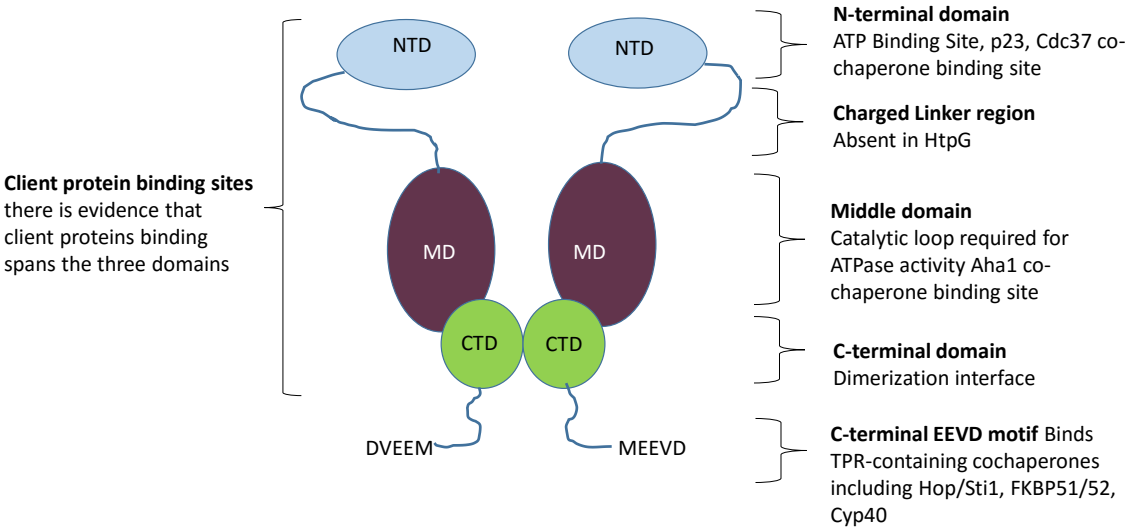

Figure 1.4 Structure and mechanism of Hsp90 homodimer
The NTD is N-terminal domain that has ATPase activity (Prodromou *et al*., 1997) which also bind ATP analogues like geldanamycin (Roe *et al*., 1999), followed by a charged linker that is absent in HtpG. The charged linker can modulate the activity of Hsp90 (Tsutsumi *et al*., 2012) The middle domain (MD) contains a catalytic arginine that is required for ATP hydrolysis, binds to Aha co chaperones and is thought to be the main client binding domain, (CTD) the C-terminal domain contains the major dimerization interface that makes Hsp90 to constitutively function as homodimers. At the c-terminal there is a conserved MEEVD motif that binds to TPR domains on co-chaperones like Hop, CyP40 and FKBP51/52, adapted from Jackson *et al* (2013).

Despite the fact that other Hsp90 homologues have low basal ATPase activity, *P. falciparum* Hsp90 (PfHsp90) has hyper-active basal ATPase activity (Pallavi *et al*., 2010). This activity is sufficient to induce conformation changes resulting in substrate release (Pallavi *et al*., 2010; Krukenberg *et al*., 2011). The high ATPase activity of PfHsp90 imparts the protein with a high substrate turnover as compared to its human homologue (Krukenberg *et al*., 2011). PfHsp90 ATPase domain can be specifically targeted by Geldanamycin and its derivative 17-allylaminogeldanamycin (17-AAG) which inhibits the activity of the chaperone (Pallavi *et al*., 2010). In *P. falciparum* Hsp90 is an essential molecule (Pallavi *et al*., 2010) and this explains why Hsp90 is targeted as a drug candidate (Zininga and Shonhai, 2014).

© University of Venda

The Hsp90 chaperone function is mediated by the assistance of other chaperones and co-chaperones. Hsp90 interacts with Hsp70 (section 1.4.6), to facilitate substrate transfer for further folding (Scheufler *et al*. 2000). This interaction is modulated by Hsp70-Hsp90 organizing protein (Hop/Sti1), which functions as an adaptor protein linking Hsp90 and Hsp70 (Nicolet and Craig, 1989). Hop is characterized by the presence of tetratricopeptide repeat (TPR) domains, TPR1 and TPR2A motifs (Scheufler *et al*. 2000). Both Hsp90 and Hsp70 possess the EEVD motifs towards the C-terminus which are required for interaction with TPR domains on Hop co-chaperone (Banumathy *et al*., 2003; Gitau *et al*., 2012; Schmid *et al.,* 2012). The mechanism of action of Hop has been proposed in two distinct ways: some postulate that Hsp70 binds to substrate first and then interacts with Hop/Sti1 and passes the substrates to Hsp90 for further refolding (Li *et al*., 2013; Röhl *et al*., 2015). Hsp90 exhibits holdase chaperone function as it has the ability to recognize and hold nonnative substrates preventing their aggregation (Weich *et al*., 1992).

A *P. falciparum* Hop homology has been described and it is thought to mediate the interaction between PfHsp90 and PfHsp70-1 complex similar to that of mammalian Hsp90 (Banumathy *et al*., 2003; Gitau *et al*., 2012, Röhl *et al*., 2015). The interaction of Hop/Sti1 and Hsp90/Hsp70 is through its multiple tetratrico-peptide repeat domains (TPR1, 2A and 2B) which interact with the C-terminal EEVD motif on both Hsp90 and Hsp70 (Scheufler *et al*., 2000; Gitau *et al*., 2012; Schmid *et al.,* 2012). Hsp90 facilitates the Hsp90/Hop/Hsp70 complex formation and substrate handover (Röhl *et al*., 2015). Binding of Hsp90 on TPR2A causes conformational changes on TPR2B with subsequent increase in the affinity of TPR2B for Hsp70 (Röhl *et al*., 2015). This results in Hsp70 bound on TPR1 shifting and binding to TPR2B when Hsp90 is bound to TPR2A (Röhl *et al*., 2015). Altogether, this suggests that Hsp70 substrate complex binds to Hop TPR1 first, then when Hsp90 is docked on TPR2A subdomain Hsp70 moves to TPR2B during which time it passes the substrate to Hsp90.

© University of Venda

1.4.4 Hsp60 family

The Hsp60 family is mainly composed of two essential prominent proteins the GroEL (chaperonin 60) /GroES (chaperonin 10) in prokaryotes (Table 1.1; Fayet *et al*., 1989; Viitanen *et al*., 1990) and the t-complex polypeptide-1 (TCP-1 complex) (McCallum *et al*., 2000). TCP-1 is structurally comprised of a heterocomplex which mainly facilitates the assembly of actin and tubulin (McCallum *et al*., 2000). TCP-1 closely associates with client polypeptides coming off from the ribosomes. The GroEL are involved in the assembly of multi-protein complexes by forming a central cavity where substrates are isolated (Ellis, 1994). The central cavity acts as an isolation chamber where GroES acts as the lid which closes the central cavity forming the Anfinsen cage (Ellis, 1994; Houry *et al*., 1999). This results in the formation of a double ring composed of 14 subunits whose central cavity binds to substrates through hydrophobic interactions (Ellis, 1994). Each subunit of GroEL is subdivided into three domains, apical; equatorial and the contact for ring binding. The apical domain has the substrate and GroES binding sites and the equatorial domain has ATP binding site (Houry *et al*., 1999; Inobe *et al*., 2008). The apical and equatorial domains are connected by an intermediate subdomain, which acts as a hinge facilitating conformational changes induced by ATP binding (on the equatorial domain) (Villas *et al*., 2014). The conformational changes on the substrate binding surface determine either the surface hydropathy index (indicator of hydrophobicity or hydrophilicity). Substrate binding occurs when TCP-1 is in hydrophobic state. Thus the first ATP binding results in higher affinity (hydrophobic state) for substrate binding and the binding of the subsequent ATP results in an opposite effect of substrate release when it changes to the hydrophilic state (Ueno *et al*., 2004; Inobe *et al*., 2008).

The *P. falciparum* genome encodes for two Hsp60 GroEL like members, PF3D7_123100 (PfCpn60) and PF3D7_1015600 (PfHsp60) localized in the apicoplast and mitochondria, respectively (Sato and Wilson, 2004; Sato *et al*., 2005). The *P. falciparum* genome also encodes for GroES homologues PF3D7_1333000 (PfCpn20) and PF3D7_1215300 (PfCpn10) localized in the apicoplast and mitochondria respectively (Sato and Wilson, 2005). The co-localisation of these Hsp60 chaperonins (PfCpn60 with PfCpn20 in the apicoplast) and

© University of Venda

(PfHsp60 with PfClpn10 in mitochondria) suggests the possibility of a functional complex in the apicoplast and mitochondria.

1.4.5 Hsp40 family

Heat shock protein 40 (Hsp40) family members are approximately 40 kDa in size (Table 1.1). In prokaryotes they are referred to as DnaJ based on the presence of the highly conserved J-domain comprising of approximately 70 amino acids (Laufen *et al*., 1999). There is a variation in the number of Hsp40s in different organisms. They are generally fewer in prokaryotes (*E. coli,* 6; *Synechococchus elongates*, 3; Qiu *et al*., 2006; Kampinga *et al*., 2009). Eukaryotes have expanded Hsp40s members, for example, humans have at least 50; *S. cerevisiae* have at least 22 and at least 49 in *P. falciparum* (Kampinga *et al*., 2009; Njunge *et al*., 2013).

Generally, Hsp40s are grouped into four types (I-IV) mainly based on their structural and functional characteristics (Cheetham and Caplan, 1998; Botha *et al*., 2011; Rug and Maier, 2011). Hsp40s can be classified structurally based on the presence of three typical domains: a J-domain with or without a conserved tripeptide of His, Pro and Asp (HPD) motif; the glycine–phenylalanine (GF) rich region and cysteine rich domain (CRR) (Figure 1.5; Njunge *et al*., 2013). Type I Hsp40s are composed of a J-domain (with a HPD motif); GF region and CRR (Figure 1.5 Botha *et al*., 2007). Type II Hsp40s contain the J-domain (with HPD motif) and the GF region two but lack the CRR (Figure 1.5; Botha *et al*., 2007). Type III Hsp40s are composed of the J-domain with the HPD motif but they lack both the GF rich region and the CRR (Figure 1.5). Type IV contains the J domain (without the HPD motif) whose position is variable and they lack the GF rich region and the CRR (Figure 1.5; Botha *et al*., 2007).

Type I and type II Hsp40s have the capability to bind substrate through the CRR and the C-terminal region (Figure 1.5; Botha *et al*., 2007; 2011), but they cannot refold the substrates. Type I and type II are capable of suppressing aggregation (Botha *et al*., 2011). Type I and Type II Hsp40s functionally associate with Hsp70s to activate its ATPase (Njunge *et al*., 2015). Their interaction with Hsp70s could be described in two distinct functional features: substrate

© University of Venda

recruitment where they bind and bring substrates to Hsp70s and also as Hsp70 ATPase activators (Horne *et al*., 2010; Bascos and Landry, 2015; Njunge *et al*., 2015). The interaction between Hsp70 and Hsp40 is mediated through the J domain of the Hsp40 (Bascos and Landry, 2015).

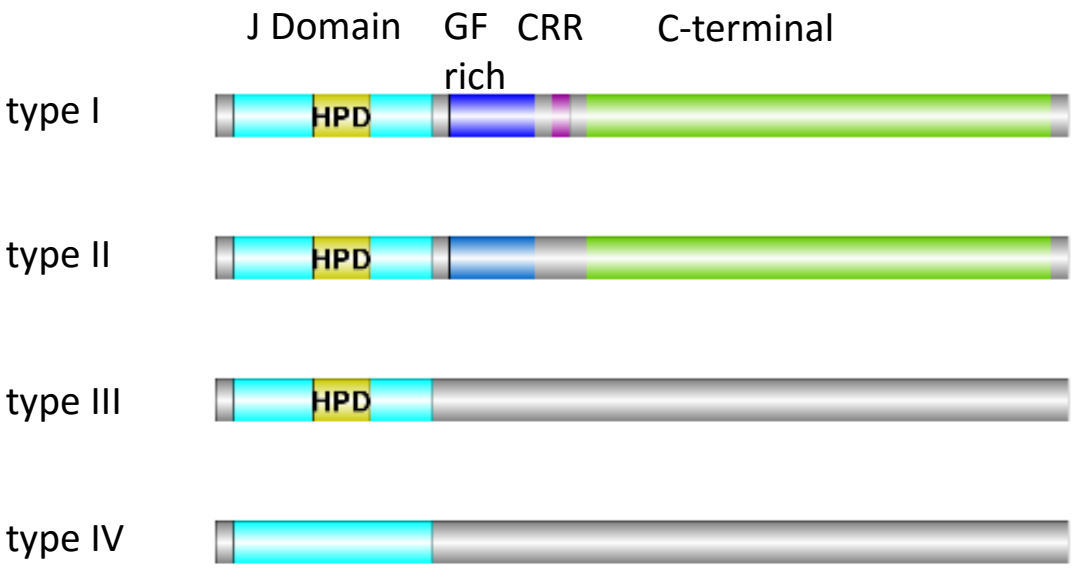

Figure 1.5: Schematic representation of the different Hsp40 types (DnaJ)
The Hsp40s are grouped in four groups using the classification system proposed by Chetham and Caplan, (1998) and Botha *et al*., (2007). The Hsp40 domains are J-Domain, HPD - His, Pro and Asp motif; GF rich - glycine–phenylalanine rich region; cysteine rich domain (CRR) and C-terminal region, adapted from Rug and Maier (2011).

The GF-rich region on Hsp40s is useful for regulation of Hsp70 substrate binding (Walsh *et al*., 2004). Type I and type II Hsp40s bind substrates not only for recruitment to Hsp70 but they also suppress thermally induced misfolding of substrates and assist in multi-complex protein formation (Ansorge *et al*., 1996; Fan *et al*., 2003). Type I and type II, Hsp40s have been shown to interact with Hsp70 in the chaperone cycle involving progesterone receptor (Pratt and Toft, 2003; Young *et al*., 2004). Type I Hsp40; Ydj1 (yeast) and HDj2 (human) bind to substrate with tight stable affinity, whilst type II, HDj1 (human) bind with rapid on/off rates (Cintron and Toft, 2006). This suggests the cysteine rich region (CRR) on type I Hsp40s stabilizes substrate interaction.

© University of Venda

Type III Hsp40s are functionally distinct from type I and type II in that they don't seem to bind non-native substrates, although they present themselves at the Hsp70 site of action (Xiao *et al*., 2006). For example, yeast type III, Swap2p and its mammalian homology axullin, present themselves at the site of action by associating with Hsp70 during uncoating of clathrin-coated vesicles (Xiao *et al*., 2006). Type IV was first described by Botha and colleagues (2007).

Of the 49 members in *P. falciparum* there are two type I Hsp40s, eight type II, twenty-six type III and thirteen type IV (Njunge *et al*., 2013). Nineteen of Hsp40s have the PEXEL sequence, suggesting that they are exported to the iRBC cytosol where they possibly participate in host cell remodeling and interaction with host cell cytoskeleton (section 1.24; 1.2.5; Archarya *et al*., 2012; Njunge *et al*., 2013). This implicates Hsp40s as central chaperones playing an important role during iRBC cell remodeling which characterizes malaria pathology. Some exported type IV Hsp40s have been shown to be essential for parasite survival and pathogenesis for example, PF11_0034 (PF3D7_1102200), RESA (PF3D7_0102200) and PF10_0382 (PF3D7_1039100; Maier *et al*., 2008; Njunge *et al*., 2013).

Comparative functional assays conducted by Botha and colleagues (2011) showed possible functional conservation of *P. falciparum* Hsp40s type 1 with their human (HspA1A) and yeast (DnaJA1) equivalents. Interestingly, biochemical assays have also shown that a type I PfHsp40 (PF3D7_1437900) interacts with PfHsp70-1 (section 1.4.6.5.1) forming a functional PfHsp70-1-PfHsp40 complex (Botha *et al.,* 2007). This functional complex promoted PfHsp70-1 ATPase hydrolysis. Furthermore, there is evidence of co-localization of PfHsp70-1 and PfHsp40 within the parasite cytoplasm (Botha *et al*., 2011). It should be noted that Hsp70-Hsp40 partnerships tend to exhibit functional specificity across species. PfHsp70-1 and PfHsp40 complex was differentially inhibited with Hsp70 inhibitor pyrimidinone when compared to human (HspA1A) and yeast (DnaJA1) counterparts showing selective inhibition (Botha *et al*., 2011). This suggests that *P. falciparum* Hsp40s can be specifically inhibited and it makes them potential drug targets (Botha *et al*., 2011; Cockburn *et al*., 2011; Zininga and Shonhai, 2014).

© University of Venda

1.4.6 Hsp70 family

Hsp70 is one of the most evolutionary conserved superfamily of Hsps that occur in all domains of life archaea, eubacteria and eukaryotes (Table 1.1; Lindquist and Craig 1988). In archaea and eubacteria Hsp70s, are referred to as DnaK. In yeasts, they are named as Ssa, in mammals including humans they are named as HSPA (Kampinga *et al*., 2009). Hsp70 is one of the most prominent molecular chaperones required for several cellular activities, which include folding of nascent polypeptides (Szabo *et al*., 1994), formation of multiprotein complexes (Song *et al* 2005), regulation of kinases (Asea *et al*., 2002), denaturation of protein (Bercovich *et al*., 1997), trafficking of proteins (Gambill *et al*., 1993), protein translocation, assembly and disassembly of oligomeric complexes (Lüders *et al*. 2000; Mayer and Bukau, 2005; Mayer, 2010). Hsp70s are ubiquitous molecules, and some of their homologues are stress inducible. Furthermore, canonical Hsp70s (DnaK like) are capable of both suppressing protein aggregation and refolding misfolded peptides (Kurt *et al*., 2006; Mayer, 2013).

Hsp70 are generally composed of an N-terminal 44 kDa-Nucleotide binding domain (NBD) ($Hsp70_{NBD}$) with ATPase activity, substrate binding domain (SBD) ($Hsp70_{SBD}$) and a C-terminal lid (Figure 1.6). There is high sequence conservation on the $Hsp70_{NBD}$ and the $Hsp70_{SBD}$ is less conserved (Easton *et al*., 2000). These two domains are connected by a highly conserved 7-residue linker region (Sharma and Masison, 2009). Hsp70s are divided into two sub-families: DnaK-like (canonical Hsp70s) and Hsp110 (Figure 1.6; Section 1.4.6.2.5; Easton *et al*., 2000). DnaK is capable of refolding misfolded protein and suppressing protein aggregation (Mogk *et al*., 1999). DnaK and DnaK-like Hsp70s from other species are considered to be canonical Hsp70s. On the other hand, Hsp110 members are specialized proteins that are structurally distinct from canonical Hsp70s. They have been described as nucleotide exchange factors (NEF) of canonical Hsp70s (Dragovic *et al*., 2006; Andreasson *et al*., 2008).

© University of Venda

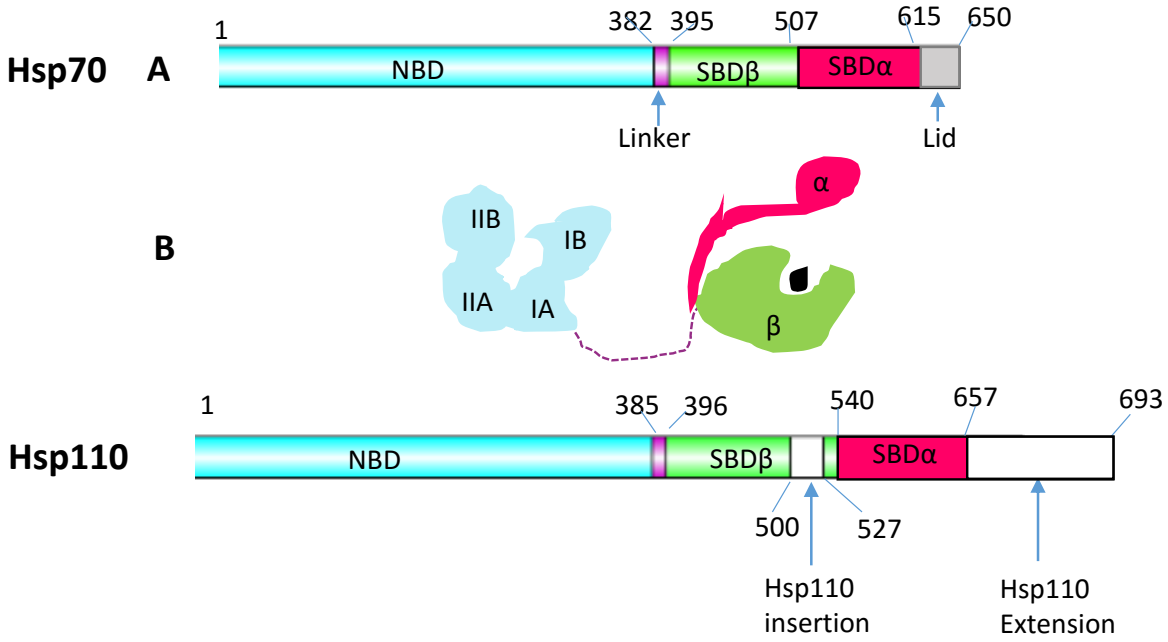

Figure 1.6: The structure of Hsp70 and Hsp110
The schematic representation of Hsp70 and Hsp110, showing the NBD, Linker, SBD and the lid in linear (A) and in folded structure (B). The illustration shows the peptide substrate in the binding cleft of the SBDβ and enclosed by SBDα, and closed by the lid, adapted from Dragovic *et al*., (2006).

Hsp70 domains are connected by a highly conserved linker segment whose mutation leads to functional abrogation, suggesting that inter-domain communication of Hsp70 is crucial for their function (Vogel, 2006). The linker motif of canonical Hsp70s is composed of the residues, DVLLLDV (Easton *et al*., 2000; Vogel, 2006). Allosteric signals from the linker are sent in two directions; binding of nucleotide to the N-terminal NBD is followed by transmission of the signal to the SBD via the linker segment; and similarly binding of misfolded peptide to the SBD alters the conformation of NBD and subsequently the rate of ATP hydrolysis (Zhuravleva and Gierasch, 2011).

1.4.6.1 Hsp70 substrate binding

Hsp70s possess a highly conserved NBD which is related to actin and is composed of four domains IA, IB, IIA, and IIB. These are arranged in two lobes that are linked and create a crevice for nucleotide binding (Figure 1.6B). The crevice has a rather hydrophilic pocket that specifically binds to the adenosine and the phosphates on ATP. $Hsp70_{SBD}$ is composed of a unique two layered twisted β-sandwich (SBDβ) that has a hydrophilic cleft where the

© University of Venda

hydrophobic patches on substrates are bound (Flaherty *et al*., 1990; Kityk *et al*., 2012). The helical SBDα ends with a rather unstructured stretch of about 30 residues (Flaherty *et al*., 1990). X-ray crystallographic studies have shown that in the open conformation the two SBD domains (SBDα/β) are detached from each other and both are anchored onto the different faces of the NBD (Kityk *et al*., 2012; Zhang *et al*., 2014). The association of the SBDα and SBDβ in the closed conformation is controlled by allostery and substrate binding (Kityk *et al*., 2012; Zhang *et al*., 2014).

In the closed conformation of $Hsp70_{SBD}$ SBDα acts as the lid to SBDβ and promotes the stable binding of substrate (Figure 1.6B; Kityk *et al*., 2012; Mayer *et al*., 2013). The poly-peptide binding cleft contacts hydrophobic patches comprised of 7-8 residues of the bound peptide mostly through hydrophobic interactions (Kityk *et al*., 2012; Mayer, 2013). Hsp70 interacts with substrates from different sources. For example, it interacts with nascent polypeptides, polypeptides in complex formation, misfolded polypeptides and polypeptides during transport (Mayer, 2013). This versatility in binding is achieved through the recognition and binding of degenerative motif consisting of a core with five residues which are highly hydrophobic and flanked by positively charged amino acids (Mayer and Bukau, 2005). These motifs are known to occur after every 30 - 40 residues in virtually all proteins (Mayer, 2013). These hydrophobic patches are only exposed in newly synthesized polypeptide awaiting *de novo* folding and in denatured or unfolded proteins (Mayer and Bukau, 2005).

Substrate binding on $Hsp70_{SBD}$ is specifically achieved through the center of the hydrophobic pocket constituted by five residues. The residues implicated are located on the SBD; β1, β3 and β4 which bind a single substrate side chain (Figure 1.7; Mayer, 2013). The backbone of the substrate side chain is enclosed by strands 1 and 2 including loop $L_{1,2}$ and the upward protruding loop $L_{3,4}$. These form hydrogen bonds and hydrophobic interactions with the substrate (Kityk *et al*., 2012). Substrate interaction is further stabilized by a layer of Loops $L_{4,5}$ and $L_{5,6}$ (Kityk *et al*., 2012; Mayer, 2013). The vicinity of the peptide binding cleft has a net negative charge which is consistent with the observation that the substrate binding patch is

© University of Venda

a hydrophobic structure that is flanked by positively charged residues (Kityk *et al*., 2012; Mayer, 2013).

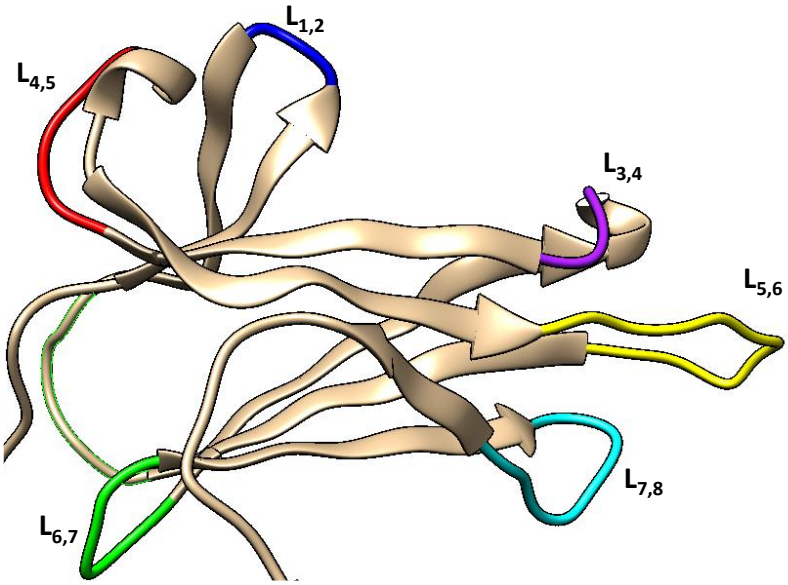

Figure 1.7: Hsp70 substrate binding domain complexes with ATP
Substrate enclosing loops are more distant from the substrate binding pocket of human Hsp70 (1DKX, Zhu *et al* 1996) the loops are numbered from the N-terminal towards C-terminal (1-8), adapted from Kityk *et al* (2012).

Upon ATP binding, Hsp70s undergo structural changes which register as a rotation on NBD lobe I relative to lobe II resulting in closure of the nucleotide binding crevice (Liu and Hendrickson, 2006). This results in opening of the lower lobes IA and IIA allowing their binding to the conserved inter-domain linker which results in ATP stimulated peptide release from the SBD and ATP hydrolysis (Vogel *et al*., 2006; Kumar *et al*., 2011; Kityk *et al*., 2012). Peptide release is achieved through the effects of the rotation of the lobe on the NBD which displaces two residues by about 2 Å in the SBD catalytic center, Lys70 and Glu171 (numbering according to *E. coli* DnaK) (Kityk *et al*., 2012). Lys70 coordinates the γ-phosphate in the ATP bound state which stabilizes the pentavalent transition of the phosphate (Kityk *et al*., 2012). This is then disrupted by Glu171 which together with Thr199 position water for the attack on the γ-phosphate (Kityk *et al*., 2012; Mayer, 2013). This is the reason why ATP binding causes lobe rotation on the NBD which results in docking of the SBD. The docking of SBD on NBD lowers affinity for substrate resulting in substrate release (Mayer, 2013).

© University of Venda

1.4.6.2 Hsp40-Hsp70 partnership

Hsp70 (section 1.4.6.1) has low basal ATPase activity where one molecule of ATP is hydrolyzed by one Hsp70 protein in ~25 minutes at 30 °C (Mayer *et al*., 2000; Alderson *et al*., 2014). This somehow slow activity has been shown to be activated by the binding of a substrate in the $Hsp70_{SBD}$ (Mayer *et al*., 2000). Hsp70 has lower affinity for substrates in its ATP bound state (section 1.4.6.1), then the synergy of bound substrate and Hsp40, results in up to 1000 fold ATP hydrolysis up-regulation compared to basal Hsp70 activity (Silberg *et al*., 2000; Kampinga and Craig, 2010; Needham *et al*., 2015). Hsp70 in the ADP bound state has higher affinity for substrates and exhibits longer substrate dwelling time.

Hsp40s are thought to strategically position themselves where client polypeptides are coming from. For example, at the ribosomal exit tunnel or the translocation pore, where they then bind client polypeptides and pass them over to Hsp70 for binding and subsequent folding (Kampinga and Craig, 2010). In this case, they act as 'targeting factors' for Hsp70 clients (Kampinga and Craig, 2010). Interestingly, Hsp40s are also thought to be responsible for recruiting Hsp70 to sites of protein aggregates. This role is essential with respect to the function of Hsp70 as a disaggregase (Torrente and Shorter, 2013). Upon its recruitment to the site (location of aggregate), Hsp70 subsequently partners with Hsp100 (section 1.4.2), in disentangling the aggregated polypeptides ultimately facilitating their refolding (Mogk *et al*., 2015). This is one hallmark of the function of Hsp70 in reducing toxicity of aggregates as in the case of neurodegenerative diseases which are characterized by accumulation of toxic aggregates (Voss *et al*., 2012). Hsp70s are also involved in the suppression of toxicity induced by aggregated reactive proteins. In this case, Hsp70 diffuses the aberrant accumulation of hyper-phosphorylated microtubules associated protein *tau* called *tau-tangles* (Voss *et al*., 2012), whose accumulation results in central nervous system (CNS) disorders such as Alzheimer's disease and Pick's disease (Sergeant *et al*., 2005).

© University of Venda

1.4.6.3 The functional cycle of Hsp70s

The functional cycle of Hsp70s is known to be driven by ATP hydrolysis (Figure 1.8; Patury *et al*., 2009). The switches between ATP- and ADP bound states of Hsp70 regulates the off and on rates of peptide binding (Buchberger *et al*., 1995). In the ATP bound state Hsp70 has fast on-off rates resulting in low affinity for substrate and in the ADP bound state there is slow on-off rates that results in overall high affinity for substrate (Liberek *et al*., 1991; Kampinga and Craig, 2010). These events are triggered by the inter-domain communication of the protein (Figure 1.6).

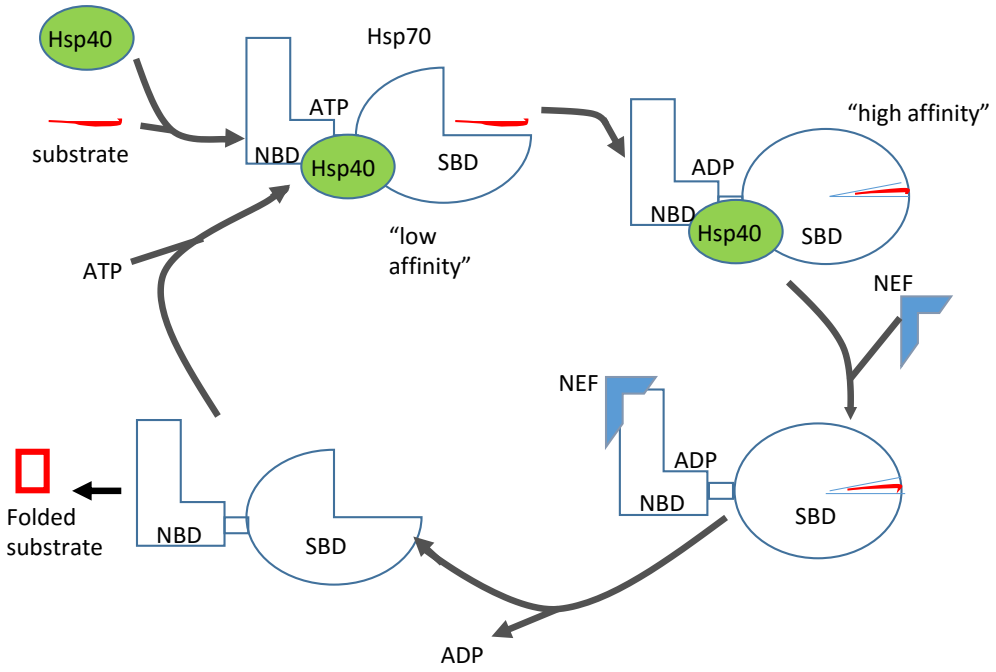

Figure 1.8: The functional cycle of Hsp70
Chaperone mediated folding by the Hsp70-Hsp40 chaperone complex. ATP hydrolysis and nucleotide exchange mediates the Hsp70 folding cycle of substrate release and binding. Substrates are recruited by Hsp40 and they activate ATP hydrolysis which then translates to ADP bound state with high affinity substrate binding, this stage where the substrate is allowed to refold. After which the NEFs exchange ADP for ATP resulting in folded substrate release, adapted from Patury *et al* (2009).

When ATP is bound on the $Hsp70_{NBD}$ allosteric communication triggers signals to the $Hsp70_{SBD}$ facilitating substrate release (section 1.4.1). Subsequently, hydrolysis of bound ATP causes conformational changes which results in a closed conformation with high affinity for substrate (slow on-off rates) (Figure 1.8; Buchberger *et al*., 1995; Kiytk *et al*., 2014). The chaperone cycle of Hsp70 is regulated by two co-chaperones J-domain proteins (Hsp40) (section 1.4.5.1) and

© University of Venda

nucleotide exchange factors (NEFs). Of these the most studied co-chaperones are Hsp40 (section 1.4.5) which recruits the substrate and activates ATP hydrolysis on the $Hsp70_{NBD}$ (Figure 1.8).

1.4.6.4 Nucleotide exchange factors of Hsp70

Nucleotide exchange factors (NEF) improves Hsp70 operational efficiency and acts as substrate release factors (Figure 1.8; Dragovic *et al*., 2006; Raviol *et al*., 2006; Sadlish *et al*., 2008). The NEFs used in prokaryotes and eukaryotes are structurally unrelated but they serve a common role (Raviol *et al*., 2006). The different types of NEF employed by Hsp70 include; in prokaryotes (and mitochondria); GroP-like gene E (GrpE) (Packschies *et al*., 1997); in eukaryotes Bcl2-associated athanagene-1 (Bag-1) (Bimston *et al*., 1998), heat shock protein binding protein 1 (HspBP1) (Patury *et al*., 2009) and Hsp110 (Dragovic *et al*., 2006).

NEFs belong to one of the three groups which are the Hsp110/Grp170, HspBp1/Sil1, and Bag domain proteins (Sondermann *et al*., 2001; Steel *et al*., 2004, Dragovic *et al*., 2006). The diversity of NEFs is crucial for functional specialization of Hsp70s as they determine substrate dwell time (Kabani *et al*., 2008; reviewed in Bracher and Verghese, 2015). The Eubacteria genome encodes for only one Hsp70 NEF which has also been described in organelles such as mitochondria and chloroplasts (Packschies *et al*., 1997). Eukaryotic genomes encode for several NEFs for example, the human genome encodes for at least thirteen NEFs; four Hsp110, two HspBP/Sil1, five Bag domain proteins and two mitochondrial GrpE (Kampinga *et al*., 2009).

There are three different nucleotide release mechanisms facilitated by NEF on Hsp70; (i) the action of GrpE, which depends on the formation of β-strand subdomain dimer (Figure 1.9B) which contact subdomains IB and IIB resulting in the rotation of the $Hsp70_{NBD}$ lobe IIB (Harrison *et al*., 1997); (ii) in contrast, Hsp110 utilizes the Bag-1 domain which is a three helix bundle where helices 2 and 3 contact subdomains IB and IIB resulting in a 14° rotation of $Hsp70_{NBD}$ lobe IIB releasing bound ATP (Figure 1.9C) (Sondermann *et al*., 2001; Andreasson *et al*., 2008); (iii) HspBP1 embraces $Hsp70_{NBD}$ lobe IIB and this results in steric conflict which

© University of Venda

displaces lobe IB thereby resulting in nucleotide release (Figure 1.9D) (Shomura *et al*., 2005). In summary, there are two types of nucleotide releases on Hsp70 which are (i) nucleotide release due to global loss of the tertiary structure of $Hsp70_{NBD}$ (HspBP1/Fes1); (ii) nucleotide release through the opening of nucleotide binding cleft of $Hsp70_{NBD}$ lobe IIB (Bag-1/GrpE/Hsp110) (Sondermann *et al*., 2001; Andreasson *et al*., 2008). The function of NEFs is regulated by a nucleotide ATP promotes NEF function (Buchberger *et al*., 1994; Andreasson *et al*., 2008).

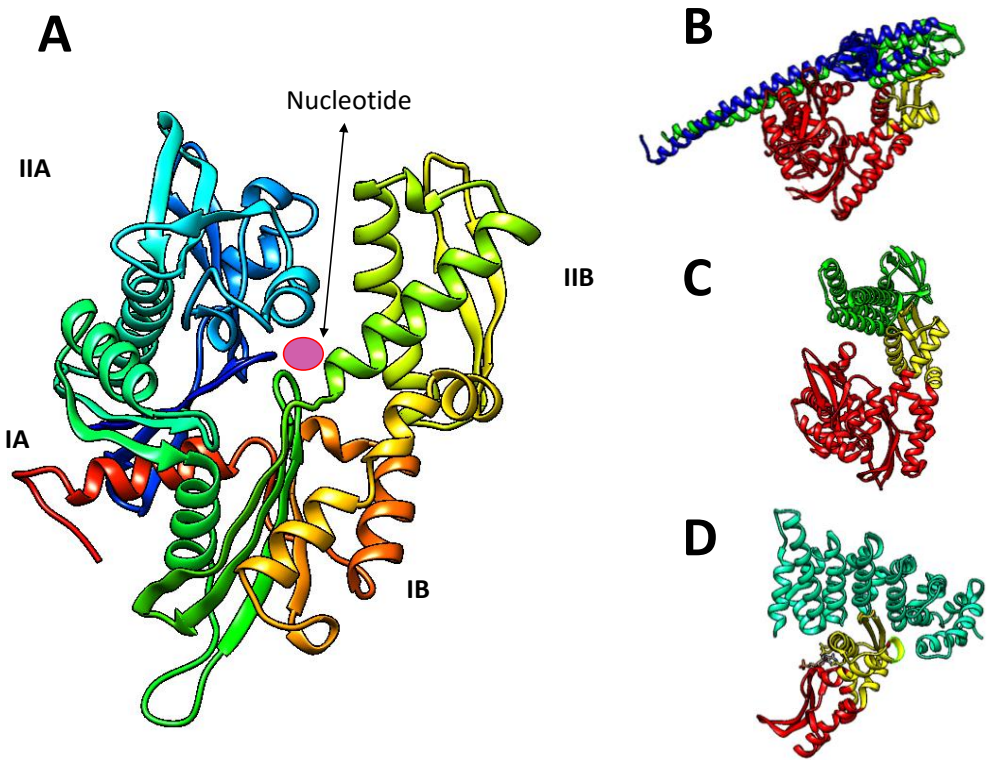

Figure 1.9: The 3D-Model of the human Hsp70 nucleotide binding domain and nucleotide exchange factors
The NBD of hHsp70 (**A**) showing the channel of nucleotides ADP (purple) movement (arrow) (Wisniewska *et al*., 2010). The model of nucleotide exchange factors complexed to the $Hsp70_{NBD}$ (Red) with the IIB subdomain highlighted (yellow) (**B**) GrpE - blue and green helices (Harrison *et al*., 1997), (**C**) Bag1- green helices (Sondermann *et al*., 2001) and (**D**) HspBP1-blue (Shomura *et al*., 2005).

Genomes of metazoans, plants and some protists harbour a special Hsp70 co-chaperone, Hsp70-interacting protein (Hip) that antagonizes NEFs function on Hsp70 (Connell *et al*., 2001). Hip binds to the $Hsp70_{NBD}$ forming a bracket that locks the $Hsp70_{NBD}$, preventing the release of ADP from the nucleotide binding cleft (Li *et al*., 2013). Hip regulates the release of substrates that are to be passed over to downstream chaperones like Hsp60 (section 1.4.4)

© University of Venda

or Hsp90 (sections 1.4.4; Li *et al*., 2013). Hence Hip is also involved in the suppression of aggregation, in that it allows substrates whose reactive patches are exposed to remain locked in the $Hsp70_{SBD}$ until the environment is conducive for their refolding enabling selective substrate release from Hsp70 complex (Li *et al*., 2013).

1.4.6.5 *P. falciparum* Hsp70s

The *P. falciparum* genome encodes for six Hsp70s which are localized in specific cellular compartments (Table 1.2; Shonhai *et al*., 2007). The different localization profiles of Hsp70s help to serve for role specialization. Based on bioinformatics data and yeast two hybrid assays, *P. falciparum* Hsp70s are thought to interact with proteins in virtually every stage of its life cycle, facilitating protein folding, refolding and for degradation (Table 1.2; Shonhai *et al*., 2007; Przyborski *et al*., 2015).

Table 1.2: PfHsp70 and their characteristics

Features	Molecular mass	Chromosome	Location	Signal sequence	Expression phase (mRNA)
PfHsp70-1[a] (PF3D7_0818900)	74	8	nucleus and cytosol[b]	C terminal EEVD motif[a]	exo-erythrocytic stage[a]
PfHsp70-2[b,c] (PF3D7_0917900)	73	9	ER[b]	carboxylic ER sequence[d]	exo-erythrocytic stage[c]
PfHsp70-3[a] (PF3D7_1134000)	73	11	mitochondrial[d,e] NC	mitochondrial transit sequence[d,e]	NE
PfHsp70-x (PF3D7_0831700)	76	7	Rbc cytosol, J-dots[f]	C terminal EEVN motif iRbc export signal motif ASNNAEES; ER signal sequence MKTKICSYIHYIVLFLISTTVHT[f]	intra-erythrocytic stage[f]
PfHsp70-y (PF3D7_1344200)	108	13	ER[d]	carboxylic ER sequence[d]	ER
PfHsp70-z (PF3D7_0708800)	100	7	cytosol[g]	NE	NE

ER (Endoplasmic Reticulum), , NE (Not Established), PlasmoDB ascession numbers are in brackets next to protein, the super script letters represent the following references: **a**- Sharma *et al* (1992); **b**- Kumar *et al* (1991); **c**- Nyalwidhe and Lingelbach (2006); **d**- Sargent *et al* (2006); **e**- Sato and Wilson (2003); **f**- Külzer *et al* (2012); **g**-Muralidharan *et al* (2012), adapted from Shonhai *et* al (2007).

© University of Venda

1.4.6.5.1 *P. falciparum* Hsp70-1

One of the most prominent chaperones PfHsp70-1, localises mainly in the cytosol and nucleus (Table 1.2; Shonhai *et al*., 2007). PfHsp70-1 is stress inducible and is expressed at the blood stages of the parasite (Sharma, 1992; Kappes *et al*., 1993). PfHsp70-1 is known to function as a chaperone responsible for thermotolerance (Shonhai *et al*., 2005; Bell *et al*., 2011). *In vitro* studies using the recombinant form of PfHsp70-1, it was shown that the protein suppresses heat induced aggregation of model substrate malate dehydrogenase (Shonhai *et al*., 2008). Stephens and colleagues (2011), showed that PfHsp70-1 is required for folding of heterologous expressed recombinant *P. falciparum* GTP cyclohydrolase. This suggests that PfHsp70-1 facilitates protein folding, which defines its chaperone cytoprotective role in parasite survival during febrile episodes.

1.4.6.5.2 *P. falciparum* Hsp70-2

PfHsp70-2/*P. falciparum* immunoglobulin heavy chain binding protein (PfBiP) is stress inducible and is expressed during the blood stages of the parasite life cycle (Table 1.2) (Kumar *et al*., 1991; Sharma, 1992; Sommer *et al*., 2007). PfHsp70-2 protein shares 53 % sequence identity with PfHsp70-1 and as such it is the ER resident member of PfHsp70s (Shonhai *et al*., 2007; Hempel *et al*., 2009). PfHsp70-2 facilitates the import of proteins into the ER and to ensure they are folded properly. The importation of proteins into the ER is thought to be through the prominent translocon composed of *P. falciparum* Sec (PfSec) complex (Sommer *et al*., 2007; Reviewed in Shonhai, 2014). PfHsp70-2 binds to and detaches from the translocon on the ER lumen thus allowing extended proteins to pass through the PfSec complex translocon in a nucleotide dependent fashion (Sommer *et al*., 2007). In the ADP bound state, PfHsp70-2 binds to the translocon preventing compact proteins to enter the ER lumen and in the ATP bound state it detaches from the translocon allowing entry of extended protein into the ER lumen (Saridaki *et al*., 2008). Once it opens up the translocon it binds to the extended peptide and it is thought that it pulls the peptide into the ER thus avoiding it sliding back into the cytoplasm (reviewed in Shonhai, 2014). In the ER the protein quality control is thought to be centrally controlled by PfHsp70-2 which is responsible for maintaining

© University of Venda

proteins in native functional state. The proteins which are damaged are thought to be channeled for degradation through the ER-associated degradation (ERAD) pathway.

1.4.6.5.3 *P. falciparum* Hsp70-3

PfHsp70-3 is localized in the matrix side of the mitochondrion (Table 1.2) (Sato and Wilson *et al*., 2004), and has been shown to interact with asparagine rich proteins (La Count *et al*., 2005). The mitochondrion genome encodes for only two functional proteins, this suggests that most of the proteins that function in the matrix are nuclear encoded (Gardner *et al.*, 2002). These proteins are translocated through the two mitochondrion membranes with the assistance of PfHsp70-1 on the cytosol side and facilitated by PfHsp70-3 on the mitochondrion matrix (Figure 1.10).

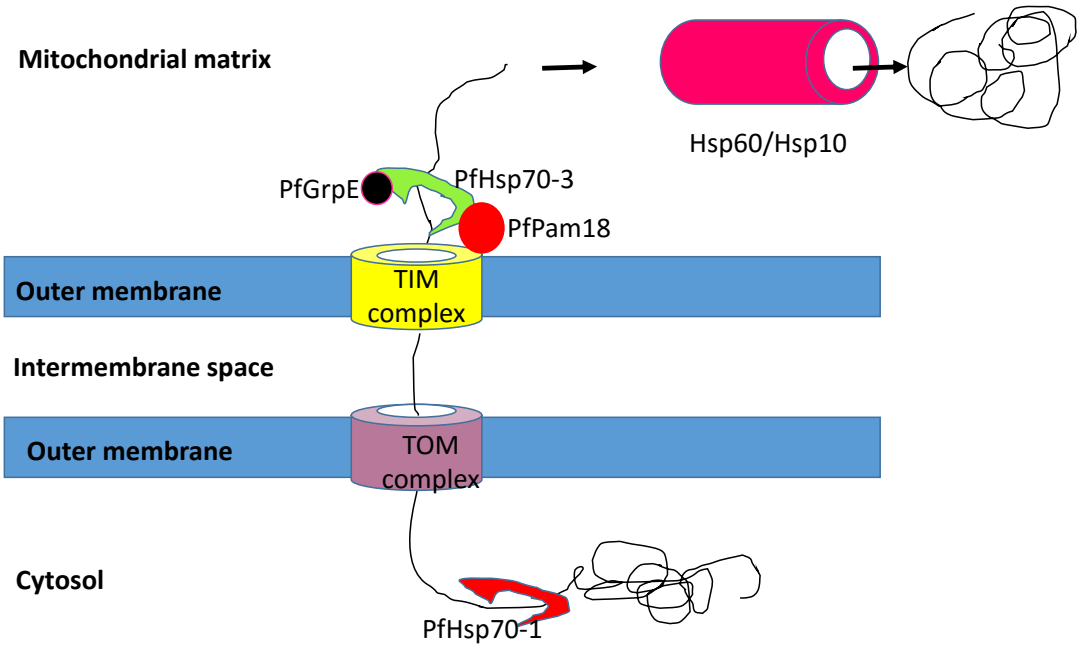

Figure 1.10: The role of PfHsp70-3 during import of proteins into mitochondria
Preproteins coming from the translational machinery are bound by PfHsp70-1 and allowed to thread into the TOM complex through the assistance from the receptors on the outer membrane complex. The preproteins then translocase the intermembrane space and thread through the Tim complex where they are sequestered with the assistance of PfHsp70-3 and PfPam18. The activity of PfHsp70-3 is modulated by GrpE and Hsp40s resident in the mitochondria. The preproteins are refolded by the Hsp60/hsp10 complex, adapted from Shonhai (2014).

© University of Venda

To traverse these two membranes peptides are first extended and kept in folding competent conformation by PfHsp70-1 then passed through the Translocase of the outer membrane complex (Tom) (Njunge *et al*., 2013) and they thread through the inter-membrane space into the translocase of the inner membrane (Tim23) complex (Pfanner and Wiedemann, 2002), possibly by the pulling from PfHsp70-3. GrpE and Hsp40 co-chaperones in the mitochondrion modulate the function of PfHsp70-3 (Figure 1.10). The pre-proteins are then folded to functional proteins by the PfHsp60/10 chaperonin system (Sato and Wilson, 2004).

1.4.6.5.4 *P. falciparum* Hsp70-x

PfHsp70-x is a close homologue of PfHsp70-1 that localizes in the PV and is exported to the iRBC cytosol (Table 1.2; Külzer *et al*., 2012). PfHsp70-x was shown to be expressed and exported during all the developmental stages of the parasite blood stage (Figure 1.11; Külzer *et al*., 2012). The export of parasite proteins to the host RBC cytosol is thought to be mediated by the presence of an export signal of the protein sequence (PEXEL/VTS; Hiller *et al*., 2004; Marti *et al*., 2004). Interestingly, PfHsp70-x lacks the PEXEL/VTS signal. This suggests that its export to the iRBC cytosol is mediated through another signal mechanism. The Przyborsky group proposed that the first 25 amino acids on the N-terminus of PfHsp70-x represent a form of an ER signal sequence (MKTKICSYIHYIVLFLISTTVHT), followed by 8 residues that come after the iRBC export signal motif (ASNNAEES; Külzer *et al*., 2012). This suggests that there is post translational modification to PfHsp70-x where the N-terminus MKTKICSYIHYIVLFLISTTVHT signal sequence targets PfHsp70-x translocation by the classical ER targeting. PfHsp70-x is thought to be packaged into vesicles that will fuse with parasite membrane moving into the PV. When PfHsp70-x is in the PV, it is thought that the signal sequence ASNNAEES targets the protein to the iRBCs cytosol (Figure 1.11; Külzer *et al*., 2012).

© University of Venda

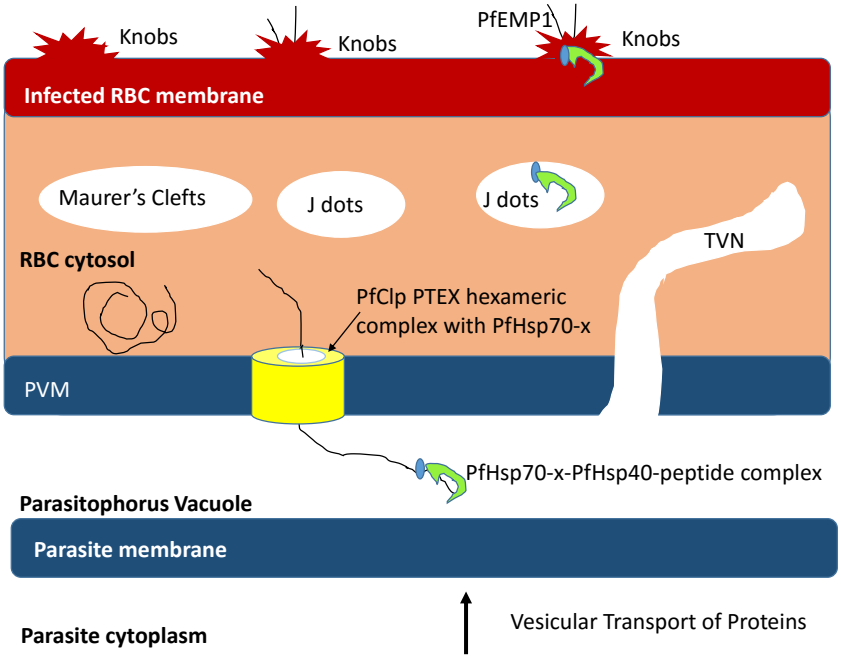

Figure 1.11. A model of the role of PfHsp70-x in the translocation of proteins of parasitic origin to the erythrocyte
This is a summarized representation of the current knowledge of the different roles of different heat shock proteins in *P. falciparum* infected erythrocyte, adapted from Shonhai (2014).

Hsp70s are functionally regulated by Hsp40s (section 1.4.5.1; Kampinga and Craig, 2010). Several reports show evidence that parasite encoded DnaJ/Hsp40 proteins are exported to the iRBC cytosol including PfEMP1 (sections 1.2.4; Hiller *et al*., 2004; Maier *et al*., 2008; Külzer *et al*., 2010). It was shown that PfHsp70-x co-localizes with type II Hsp40s (PF3D7_0113700 and PF3D7_0501100.1) in structures termed 'J-dots' (Külzer *et al*., 2010). J dots are mobile parasitic derived structures present in the iRBC cytosol (Külzer *et al*., 2010). This suggests the presence of Hsp70-Hsp40 functional complexes in the iRBC cytosol (Külzer *et al*., 2012). The deployment of parasite proteins to the iRBC membrane is thought to be facilitated by parasite heat shock proteins. For example, PfHsp70-x is thought to facilitate the deployment of PfEMP1 (Wickham *et al*., 2001). This process may be facilitated through the co-operative function of the Hsp70-Hsp40 complex. PfHsp70-x is thought to be the chaperone that is central to the folding of exported parasite proteins (Külzer *et al*., 2010).

The presence of PfHsp70-x in the PV suggests that it may function as a chaperone which maintains the extended peptides folding competent form in the PV unfolded (Külzer *et al*., 2010; Grüring *et al*., 2012). The PfClp (section 1.4.2) is part of the Plasmodium translocon of

© University of Venda

exported proteins (PTEX) on the PVM (Figure 1.10; de Koning-Ward *et al*., 2009). As shown in other species that Hsp70 and Clp (section 1.4.2) interact in their role as disaggregase it is not clear if in *P. falciparum* PVM context they interact in assisting the translocation of proteins through the PVM. Banumathy and colleagues, (2003) have demonstrated the presence of human Hsp90 and human Hop in iRBCs. The absence PfHop in the iRBC suggest that the EEVN motif of PfHsp70-x may be to facilitate its interaction with human Hop and Hsp90. This suggests that PfHsp70-x interacts with human Hsp90 and Hop in facilitating proper folding of parasite driven proteins exported to the RBC cytosol.

1.4.6.5.5 Hsp110 family of proteins

Heat shock protein 110 (Hsp110) is a member of the Hsp70 super-family of molecular chaperones (Table 1.1; Oh *et al*., 1999; Raviol *et al*., 2005). Hsp110s have been identified in the cytosol while Grp170 occurs in ER (Oh *et al*., 1999; Saxena *et al*., 2012; Xu *et al*., 2012). Like canonical Hsp70s, the structure of Hsp110 comprises of N-terminal nucleotide binding domain ($Hsp110_{NBD}$), followed by substrate binding domain ($Hsp110_{SBD}$) (Figure 1.6). Hsp110s have larger substrate binding domains and have significant sequence divergence from the archetypical Hsp70 (Oh *et al*., 1999). The $Hsp110_{SBD}$ is divided into three sub-domains; the β sandwich which is responsible for peptide binding (Domain B), followed by long acidic loop subdomain (Domain L), and then the three helix sub-domain (Domain H) at the C-terminal domain which function as the cap for large substrate holding capability also called the 'lid' (Figure 1.12; Oh *et al*., 1999; Polier *et al*., 2010). Hsp110 proteins possess a fairly conserved NBD (Domain A; Figure 1.12). However, Hsp110 linker segment and $Hsp110_{SBD}$ are divergent from those of the canonical Hsp70s (Polier *et al*., 2010). Hsp110s are reported to lack allosteric coupling between the $Hsp110_{NBD}$ and $Hsp110_{SBD}$ (Mayer, 2010). Consequently, Hsp110s have been found to exhibit chaperone function limited to holdase function (protein aggregation suppression; Goeckeler *et al*., 2002; Polier *et al*., 2010).

Hsp110s exhibit similar domain architecture as Hsp70 with an extra insertion on SBDβ and longer C-terminal loop both of which are thought to be dispensable for holdase function

© University of Venda

(Shaner *et al*., 2004; Liu and Hendrickson, 2007). Hsp110 lack refolding activity but they have been described as exhibiting more efficient holdase function than canonical Hsp70s (Oh *et al*., 1997; Goeckeler *et al*., 2002). Hsp110s' holdase activity has been suggested to be responsible for their contribution in prion formation and propagation (Sadlish *et al*., 2008), ER degradation (Hrizo *et al*., 2007) and tumour antigen presentation (Manjili *et al*., 2002; Wang *et al*., 2001).

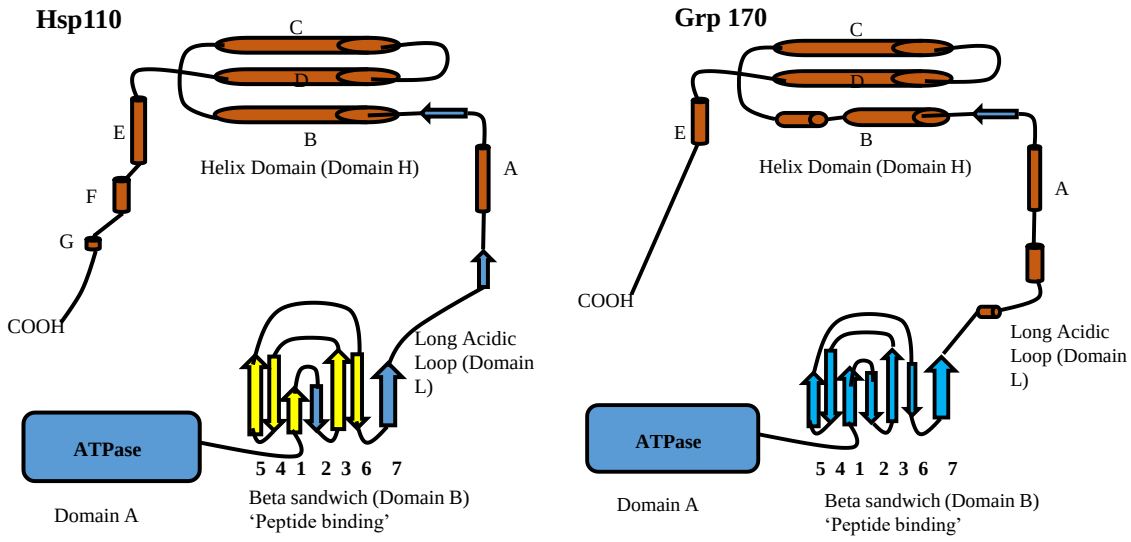

Figure 1.12: The domain arrangement for Hsp110 and Grp170
The domain arrangement of Hsp110s. ATPase/NBD the nucleotide binding - **Domain A**; SBD 7 beta strands substrate binding subdomain - **Domain B**; Long acidic subdomain –**Domain L**; α-helicases subdomain- **Domain H**. Additional helices on Hsp110 E, F, G towards the C-terminal, adapted from Oh *et al* (1999).

In humans and mice three distinct cytosolic Hsp110 homologs exist; Hsp105 (splice variants α and β); Apg-1 and Apg-2 (Easton *et al*., 2000; Kampinga *et al*., 2009). Hsp105 variants are similar to *S. cerevisiae* Hsp110 isoforms where Hsp105α is constitutively expressed and Hsp105β is expressed under heat stress (Easton *et al*., 2000; Hatayama *et al*., 2001). On the other hand, Apg1 and Apg-2 are developmentally expressed in various tissues (Kaneko *et al*., 1997a; Kaneko *et al*., 1997b). Yeasts express two cytosolic Hsp110/Sse isoforms (Sse1p and Sse2p) which are functional under different conditions. Sse1p has been shown to function both as a NEF and a holdase at normal growth temperature ~ 37 ^{o}C (mild heat stress; Polier *et al*., 2008). Interestingly, at elevated heat stress, Sse1p has reduced NEF functionality as

© University of Venda

compared to its isoform Sse2p (Polier *et al*., 2008). This suggests that, these isoforms may functionally complement each other at different temperatures.

1.4.6.5.5.1 Hsp110 substrate binding

The crystal structure of the Hsp110 is complex with substrates unravelled that both the Hsp110 NBD and the SBD β-sandwich are required for substrate binding (Polier *et al*., 2010). The Sse1p crystal structure showed the presence of a rift between the NBD and SBD interfaces. This rift is thought to grasp substrates; consequently, hiding the hydrophobic patches of misfolded proteins (Polier at al., 2010). The mechanism of binding is similar to the binding of trigger factor (a ribosome associated prolyl isomerase of prokaryotes) (Hesterkamp *et al*., 1996; Hoffman *et al*., 2010), prefoldin (a hexameric molecular chaperone complex; Seigert *et al*., 2000) and Skp (a molecular chaperone of the periplasmic space of *E. coli*; Schäfer *et al*., 1999).

The second mechanism proposed to be used for substrate binding by Hsp110 is partial thermal unfolding of Hsp110 through the creation of an intermediate conformation under heat stress with high affinity for substrate binding (Haslbeck *et al*., 2005; Polier *et al*., 2010). In this conformation the hydrophobic motifs of N- and C-terminal extensions of Hsp110 are able to efficiently bind to hydrophobic patches on partially unfolded substrates (Haslebeck *et al*., 2005). Thus, Hsp110 keeps the substrates in a folding competent state during heat stress (Polier *et al*., 2010). This possibly explains the ability of Hsp110 to hold larger substrates (Polier *et al*., 2010). In support of this mechanism of action, Sse1p was embedded in the three dimensional meshwork of aggregated luciferase, and thus shielding luciferase molecules from each other, hence reducing aggregation (Polier *et al*., 2010). When the thermal stress was removed, luciferase was made available to Hsp70 for refolding (Raviol *et al*., 2006; Polier *et al*., 2010).

© University of Venda

1.4.6.5.5.2 Hsp110 functional cooperation with Hsp70

Shorter (2011) reported that in the absence of Hsp100, the mammalian cytosol harbours an ATP-depended disaggregase complex composed of Hsp110, Hsp70 and Hsp40. This functional complex was shown to slowly dissolve large disordered aggregates and recover natively folded protein from two model proteins; urea denatured luciferase that form aggregated structures of approximately 500 - 2000 kDa (Glover and Lindquist, 1998) and heat denatured Green Fluorescence Protein (GFP) which forms continuous aggregated sequences of approximately 500 kDa (Doyle *et al*., 2007). The co-operation of Hsp70, Hsp110 and Hsp40 in entangling aggregated proteins required ATP to function (Shorter, 2011).

Hsp110s regulates yeast prion formation and propagation (Sadlish *et al*., 2008). Yeast productively utilises prion as epigenetic translation regulators which in other systems are cytotoxic and lead to cell death (Sondermann *et al*., 2002). Some prions are used as signals for translation termination in regulating gene expression (Sadlish *et al.*, 2008). The most studied prion is PSI^{+}, the altered form of the translational release factor Sup35 (Sadlish *et al.*, 2008). Several studies have demonstrated that Hsp110 is essential for efficient *de-novo* PSI^{+} prion formation and PSI^{+} phenotype propagation (Fan *et al*., 2007; Kryndushkin and Wickner, 2007; Sadlish *et al*., 2008). Here Hsp110 possibly functions both as a NEF for Hsp70 (Goeckeler *et al*., 2002) and as a holdase stabilising folding intermediates in an active form for prion Sup35 propagation (Yam *et al*., 2005; Sadlish *et al*., 2008).

1.4.6.5.5.3 *P. falciparum* Hsp70-y

PfHsp70-y (Table 1.2) belongs to the Hsp110 group and it is the ER localized member Grp170 (Shonhai *et al*., 2007). PfHsp70-y is likely to serve as a NEF for the ER localized PfHsp70-2 (Shonhai, 2014). In the ER, there is a high rate of generation of hydrogen peroxide through the degradation of hemoglobin coupled with the action of antimalarial drugs that induce oxidative stress (Akide-Ndinge *et al*., 2009; Hartwig *et al*., 2009). For survival the parasite needs a robust protein quality control system.

© University of Venda

1.4.6.5.5.4 *P. falciparum* Hsp70-z

PfHsp70-z (Table 1.2) belongs to the Hsp70 superfamily but is phylogenetically a close member of Hsp110 protein family (Shonhai *et al*., 2007). The Hsp110 protein family members are thought to exhibit NEF activity on Hsp70 (Dragovic *et al*., 2006). PfHsp70-z has not been biochemically characterised but is thought to function as a chaperone (Muralindaran *et al*., 2012). It is predicted to interact with PfHsp70-1 (section 1.4.6.5.1), PfHsp90 (section 1.4.3; La Count *et al*., 2005) and is also proposed to serve as a NEF (Shonhai *et al*., 2007; Bhartiya *et al*., 2015). Hsps are essential for the survival of *P. falciparum* parasite in both othotherm and homoeothermic hosts. *P. falciparum* proteome is thought to comprise of at least 25% of proteins with asparagine repeats (Singh *et al*., 2004b). These repeats increase the propensity of these proteins to aggregate under heat stress. It is thought that PfHsp70-z prevents the aggregation of asparagine rich parasitic proteins under stressful conditions (Muralindaran *et al*., 2012). Some heat shock proteins have been shown to be essential in parasite development. PfHsp90 (section 1.4.3) is essential for the development of the parasite (Banumathy *et al*., 2003; Shonhai *et al*., 2007). Further elucidation of the role of PfHsp70-z in parasite survival will enhance the understanding of its role in protein folding and as a potential drug target.

1.5 Problem Statement, Hypothesis, Aim and Objectives

1.5.1 Problem statement

P. falciparum Hsp70-1 (PfHsp70-1; section 1.4.6.5.1), which primarily localizes to the cytosol and nucleus is thought to confer cytoprotection to the parasite (Shonhai *et al*., 2007). The regulation of PfHsp70-1 activity by Hsp40 co-chaperones has been presented as a prospective pathway for drug design (Shonhai, 2010; Njunge *et al*., 2013). However, little is known about how PfHsp70-1 is regulated by NEFs. Nucleotide exchange defines the life-span of the interaction of Hsp70 with its substrate and has an influence on whether the substrates are refolded or channelled towards degradation. The successful design of inhibitors targeting the function of Hsp70 in *P. falciparum* (Shonhai *et al*., 2010), requires knowledge on how the nucleotide exchange function Hsp70 is regulated. NEFs found in the cytosol of eukaryotic cells include, homologues of BAG domain proteins; HspBP1, and Hsp110 families (Maier *et al*.,

© University of Venda

2008; Sondermann *et al*., 2001). Although PfHsp70-1 possesses putative binding motifs for NEFs based on bioinformatics analysis (Shonhai *et al*., 2007), BAG1 and HspBP1 homologues have not been identified in *P. falciparum*. However, *P. falciparum* Hsp70-z (PfHsp70-z) [cg4] (section 1.4.6.5.5.4), a member of the Hsp110 family was reportedly expressed by parasites isolated from clinical cases (Pallavi *et al*.., 2010). This suggests that PfHsp70-z is the sole NEF for cytosolic PfHsp70-1.

The PfHsp70-z encoding gene occurs on chromosome 7 (Shonhai *et al*., 2007) which houses antigenic *var* and drug-resistant *pfcrt* genes. Hence, PfHsp70-z may play a role in parasite virulence and drug resistance. The function of cytosolic Hsp110 is essential in yeast (Moran *et al*., 2013). Human and yeast Hsp110 proteins exhibit variable functional features (Polier *et al*., 2010). Thus Hsp110 proteins may present species specific functional features appropriate for possible drug design.

1.5.2 Hypothesis

PfHsp70-z is an independent chaperone that interacts with PfHsp70-1 to facilitate the nucleotide exchange function of the latter.

1.5.3 The main aim of this study

To biochemically characterise the role of *P. falciparum* heat shock protein 70-z.

1.5.4 Objectives

1.5.4.1 To utilise bioinformatics analysis to identify the structure-function features of PfHsp70-z.

Approach

© University of Venda

a) Retrieval of PfHsp70-z sequence from plasmoDB, and BLAST searches to identify homologues;

b) Sequence alignments with retrieved homologues to identify conserved functional domains using BioEdit/MAFFT;

c) Generation of three dimensional model of the protein to predict possible interaction sites with PfHsp70-1; and

d) Predict possible PfHsp70-z interactors using STRING.

1.5.4.2 To investigate chaperone activity of PfHsp70-z and its interaction with nucleotides using biochemical analysis.

Approach

a) Heterologous expression and purification of recombinant PfHsp70-z protein from *E. coli;*

b) Investigate nucleotide binding kinetics using surface plasmon resonance (SPR) and ATPase activity of recombinant PfHsp70-z using colorimetric assay;

c) Investigate the effect of nucleotides (ATP/ADP) on PfHsp70-z structure using limited proteolysis and tryptophan fluorescence;

d) Investigate the capability of PfHsp70-z to suppress heat induced aggregation of model substrates luciferase and malate dehydrogenase; and

e) Investigate the interaction of recombinant PfHsp70-z and PfHsp70-1 using slot blot and SPR analyses.

1.5.4.3 To investigate the localisation of PfHsp70-z and PfHsp70-1 in parasite infected erythrocyte.

Approach

a) Investigate the localisation of PfHsp70-z in parasite infected erythrocytes using immunofluorescence microscopy.

© University of Venda

1.5.4.4 To investigate the expression of PfHsp70-z in parasites subjected to heat stress.

Approach

a) Investigate the expression levels of PfHsp70-z in *P. falciparum* 3D7 infected cells grown at 37 °C and heat shocked at 42 °C; and

b) Investigate the stability of recombinant PfHsp70-z to heat stress using circular dichroism (CD).

1.5.4.5 To explore the association of PfHsp70-z and PfHsp70-1 using co-immunoprecipitation assays.

Approach

a) Immuno-precipitation assays will be conducted using α-PfHsp70-z antibodies.

© University of Venda

CHAPTER 2:

BIOINFORMATICS ANALYSES OF THE STRUCTURAL FEATURES OF PFHSP70-Z

© University of Venda

2.1 Introduction

Bioinformatics has been at the forefront in the analysis of DNA and protein sequences. It has been useful in the prediction of the secondary structure and the three dimensional structure of protein. Bioinformatics is also employed to predict protein-protein interactions. Protein-protein interactions reveal the possible role of unknown proteins through their interaction with functional partners. Due to the growth in genomic information mining, several databases have been created which are dedicated to housing species specific genomic data. For example, PlasmoDB (http://plasmodb.org/plasmo/; Aurrecoechea *et al*., 2009) contains extensive genome, proteome and metabolome information relating to malaria parasites (Table 2.1). PlasmoDB is an interactive database that allows inter and intra species genome comparisons (Otto *et al*., 2014). The *P. falciparum* strains represented in online databanks include HB3, DD2, D10, 7G8 and 3D7 (Mu *et al*., 2002). PlasmoDB houses *P. falciparum* genome sequence and annotation as well as draft sequences emerging from several *Plasmodium* sequencing projects. PlasmoDB also houses eight plasmodium parasite species with full sequences and annotated genomes (Table 2.1).

P. falciparum genome sequencing was started in 1996 and completed in 2002 and was recently updated (Gardner *et al*., 2002; Otto *et al*., 2014). The genome consists of 14 chromosomes distributed into three compartments, the nucleus, mitochondrion and the apicoplast, with 8 % being nuclear genome. The genome has high AT composition, with 54 % composed of introns which results in about 2.3 kb of gene length. The nucleus genome codes for both tRNA and ligases. The mitochondrial genome comprises of 5.8 kb and has limited protein coding genes (Gardner *et al*., 2002). This suggests that most of the proteins functioning in the mitochondria are imported from the parasite cytosol.

In silico analysis revealed that of the ~ 5300 protein genes, the *P. falciparum* genome appears to code for approximately 95 different chaperones (Pavithra *et al*., 2007). At least six *Hsp70*

© University of Venda

genes have been identified in *P. falciparum*, amongst these, two belong to the Hsp110 family PfHsp70-z (section 1.4.6.5.4) and PfHsp70-y (section 1.4.6.5.3) (Table 1.2; Shonhai *et al*., 2008). An *Hsp110* homologue (*PfHsp70-z*), has been identified on the genome (Shonhai *et al*., 2007; Muralidharan *et al*., 2012). Identification of the residues that are implicated in PfHsp70-z nucleotide exchange and chaperoning function will help elucidate the role of PfHsp70-z in parasite survival. Hsp110 are known to function as NEFs for canonical Hsp70s (Dragovic *et al*., 2006). There is a possibility that PfHsp70-z may function as both NEF and as a chaperone.

The main aim of this study was to utilise bioinformatics analyses to identify structural and functional motifs and domains in PfHsp70-z. The structural features of PfHsp70-z will be compared to those of its homologues. The specific objectives of this study were to:

i. Identify and compare the cytoplasmic PfHsp70-z protein homologues in *Plasmodium spp*, *Trypanosomes*, human, yeast and mouse;
ii. Map out the phylogeny of PfHsp70-z and putative homologues;
iii. Generate the three dimensional model of PfHsp70-z;
iv. Identify a unique peptide on PfHsp70-z against which a specific antibody was generated;
v. Assess the genomic neighbourhood of PfHsp70-z by chromosomal gene locus analysis; and
vi. Predict and construct the predicted interactome of PfHsp70-z.

© University of Venda

2.2 Experimental Procedures

2.2.1 Multiple sequence alignment of Hsp110 homologues

The amino acid sequence representing PfHsp70-z retrieved from PlasmoDB (Accession number: PF3D7_0708800) was aligned to sequences of other cytosolic Hsp110 homologues from the following: *Plasmodium* species retrieved from PlasmoDB in FASTA format (www.PlasmoDB.org); Tritryps Hsp110 retrieved from TritrypDB in FASTA format (http://tritrypdb.org); *Homo sapiens* and *Mus muclulus* Hsp110 sequences were retrieved in FASTA format from National Centre for Biotechnology Information (NCBI) (http://www.ncbi.nlm.nih.gov). The retrieved protein sequences and their respective accession number are as follows; *P. falciparum,* PfHsp70-z (PF3D7_0708800); *P. vivax,* PvHsp110 (PVX_087970); *P. knowlesi,* PkHsp110 (PKH_010690); *P. chabaudi*, PcHsp110 (XP_745506.1); *P. berghei*, PbHsp110 (PBANKA_121930); *P. yoelii*, PyHsp110 (PlasmoDB accession number PYYM_1222000); *P. cynamolgi*, PcyHsp110 (PCYB_011590); *Trypanosoma brucei*, TbHsp110 (TB927.10.12710); *T. cruzi*, TcHsp110 (TcCLB.507831.60); *Leishmania major*, LmHsp110 (LmjF.18.1370); *L. brazilienze*, LbHsp110 (LbrM.18.1400); *Homo sapiens*, HSPH1 (NP_006635.2); *Mus musculus*, mHsp110 (NP_038587) and *Saccharomyces cerevisiae,* Sse1 (Q875V0). The retrieved protein sequences were analysed using MAFFT version 7 (Katoh *et al*., 2013) and Boxshade (http://www.ch.embnet.org/software/BOX_form.html).

2.2.2 PfHsp70-z homology modelling

The PfHsp70-z sequence retrieved from PlasmoDB was used to conduct a BLAST search to identify the best possible template sequence for homology modeling. Sse1 sequence was identified as it shared the highest possible sequence identity with PfHsp70-z. Template sequence of Sse1 and crystal structure were used to construct three dimensional models of the PfHsp70-z nucleotide binding domain and substrate binding domains using PHYRE2 (http://www.sbg.bio.ic.ac.uk/phyre2/html/page.cgi?id=index; Kelley *et al*., 2015). The images were visualized using Chimera version 1.9 (Pettersen *et al*., 2004). The resulting PDB files were used for Chimera match making PfHsp70-z onto Sse1.

© University of Venda

2.2.3 Secondary structure prediction of PfHsp70-z

The prediction of the secondary structure of PfHsp70-z C-terminal was achieved by identifying a template sequence from multiple sequence alignment conducted using amino acid sequences derived from PlasmoDB. The template sequence and crystal structure were analysed and used to predict the secondary structure using PHYRE2 (http://www.sbg.bio.ic.ac.uk/phyre2/html/page.cgi?id=index; Kelly *et al*., 2015).

2.2.4 Design of peptide for anti-peptide PfHsp70-z antibody

To design a peptide to be used to generate the antibody for PfHsp70-z, the DNASTAR (http://www.dnastar.com) composite analysis was used. The analysis was conducted to determine antigenic regions that are surface exposed and unique to PfHsp70-z using DNASTAR (Proteone, Proteon3D and Novafold) plugins. The epitope determination analysis included assessment of antigenicity using Jameson-Wolf Index plots (Jameson and Wolf, 1988); secondary structure prediction using Chou-Fasman plots (Chou and Fasman, 1978); charge density analysis using Lehninger plots (Lehninger, 2005); chain flexibility using the Karplus-Schultz plots (Karplus *et al*., 1978) and hydrophobicity and hydrophilicity using Kyte-Doolittle plots (Kyte and Doolitle, 1982). To determine the overall antigenicity the Jameson-Wolf Antigenic index which combines data from existing protein structural predictions was used (Jameson and Wolf, 1988). An antigenic region with the lowest similarity to any other Plasmodium protein was assessed using BLAST and the region with high antigenicity and lowest similarities to human and other Plasmodium homologues was selected. The peptide sequence (CSLQEQEKNKPLYEP) corresponding to amino acids 768–782 of the PfHsp70-z amino acid sequence was selected and submitted to the GenScript corporation (Piscataway, New Jersey, USA) to be synthesized. Once synthesized, GenScript used the peptide to produce polyclonal antibody against PfHsp70-z in a rabbit.

2.2.5 PfHsp70-z genome neighbourhood analysis

Genes in close proximity are more likely to undergo similar epigenetic modifications, interactions and transcriptional activity (Overbeek *et al*., 1999; De and Babu, 2010). *PfHsp70-*

© University of Venda

z gene location was assessed to determine important gene neighbours using data retrieved from PlasmoDB (Aurrecoechea *et al*., 2008).

2.2.6 Mapping out the predicted interactome of PfHsp70-z

The interactome prediction for PfHsp70-z was conducted using data downloaded from STRING 10 (http://string-db.org/) database. STRING works as a meta-database which integrates data collected from several sources including gene neighbourhood, co-expression experiments, databases and text mining (Jensen *et al*., 2009). The network was constructed displaying nodes and edges with a median confidence of 0.7. The nodes and edges were analysed on Cytoscape (Shannon *et al*., 2004). A NetworkAnlayzer tool (Brandes, 2001) was used to establish betweenness centrality and closeness centrality. The node size was mapped to the betweenness centrality of PfHsp70-z to reflect the level of control it exerts over the interactions of other proteins in the network (Yoon *et al*., 2006). The node colours were mapped to closeness centrality as a measure of the speed information spreads from PfHsp70-z to other reachable nodes in the network (Newman, 2003).

© University of Venda

2.3 Results

2.3.1 Analysis of sequence similarity between PfHsp70-z, *Plasmodium, Trypanosoma, Leishmania*, human, yeast and mouse homologues

Multiple sequence alignments were conducted on the predicted cytosolic full length Hsp110 proteins from Plasmodium species and Tritryps (*T. cruzi*, *T. brucei*, *L. major*, *and L. brasienz*) were compared to human, mouse and yeast orthologues (Figure 2.1; 2.2). PfHsp70-z possesses an N-terminal NBD (PfHsp70-z_{NBD}) composed of residues 1 - 420 (Figure 2.1), a putative linker region at position 421 - 426 (Figure 2.1) and a SBD composed of SBDβ residues 422 - 660 and SBDα residues 661 - 729 and a C-terminal loop, residues 730 - 873 (Figure 2.2) (Oh *et al*., 1999). Hsp110 residues that are known to be important for the interaction with Hsp70 (Figure 2.1) (Schuermann *et al*., 2008), are more highly conserved in the PfHsp70-z_{NBD} compared to those located in PfHsp70-z_{SBD} (Figure 2.1; 2.2).

The proposed linker residues (EYECVE) (section 1.4.6) of Hsp110s from Plasmodia species are highly divergent from those of yeast Hsp110 (PFKFED) (Schuermann *et al*., 2008) as well as human Hsp110 and mouse Hsp110 (EFSVTD) (Figure 2.1). On the other hand the EFVVSE representing the linker of Hsp110 from *Trypanosomes* and *Leishmania* is also divergent from yeast Hsp110s (Figure 2.1). The divergent linker sequences may have evolved due to species specific functional needs. These findings are in line with previous findings that yeast and human Hsp110 show functional differences (Oh *et al*., 1999; Goeckeler *et al*., 2008; Polier *et al*., 2008).

The residues that are implicated in the formation of homodimers and heterodimers are conserved in PfHsp70-z (Figure 1.2). This suggests that PfHsp70-z possibly form functional homodimers and form heterodimers with PfHsp70-1. These finding are in agreement with evidence from previous studies that suggest that Hsp110 form functional heterodimers with Hsp70s (Liu and Hendrickson, 2007; Malinverni *et al*., 2015).

© University of Venda

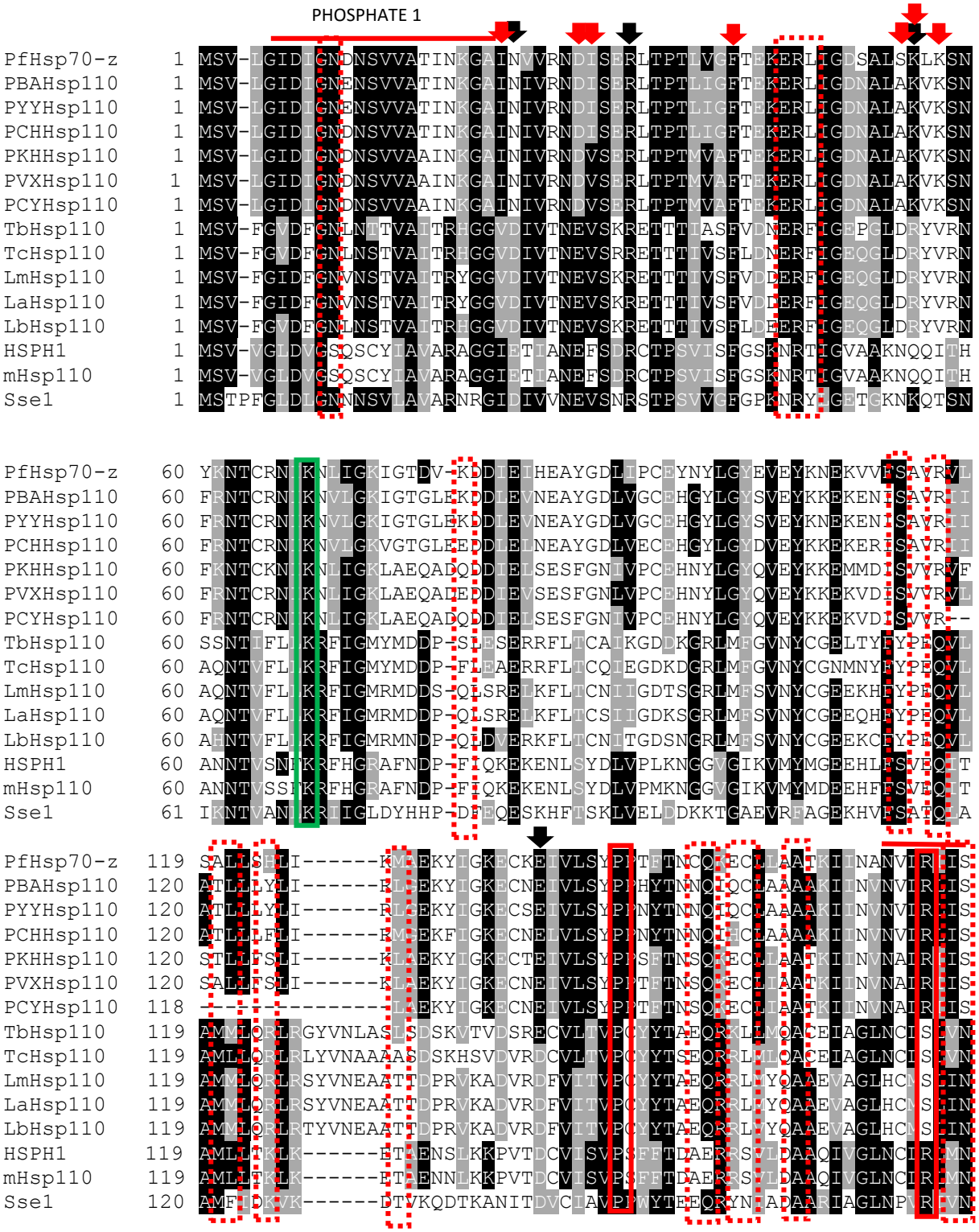

© University of Venda

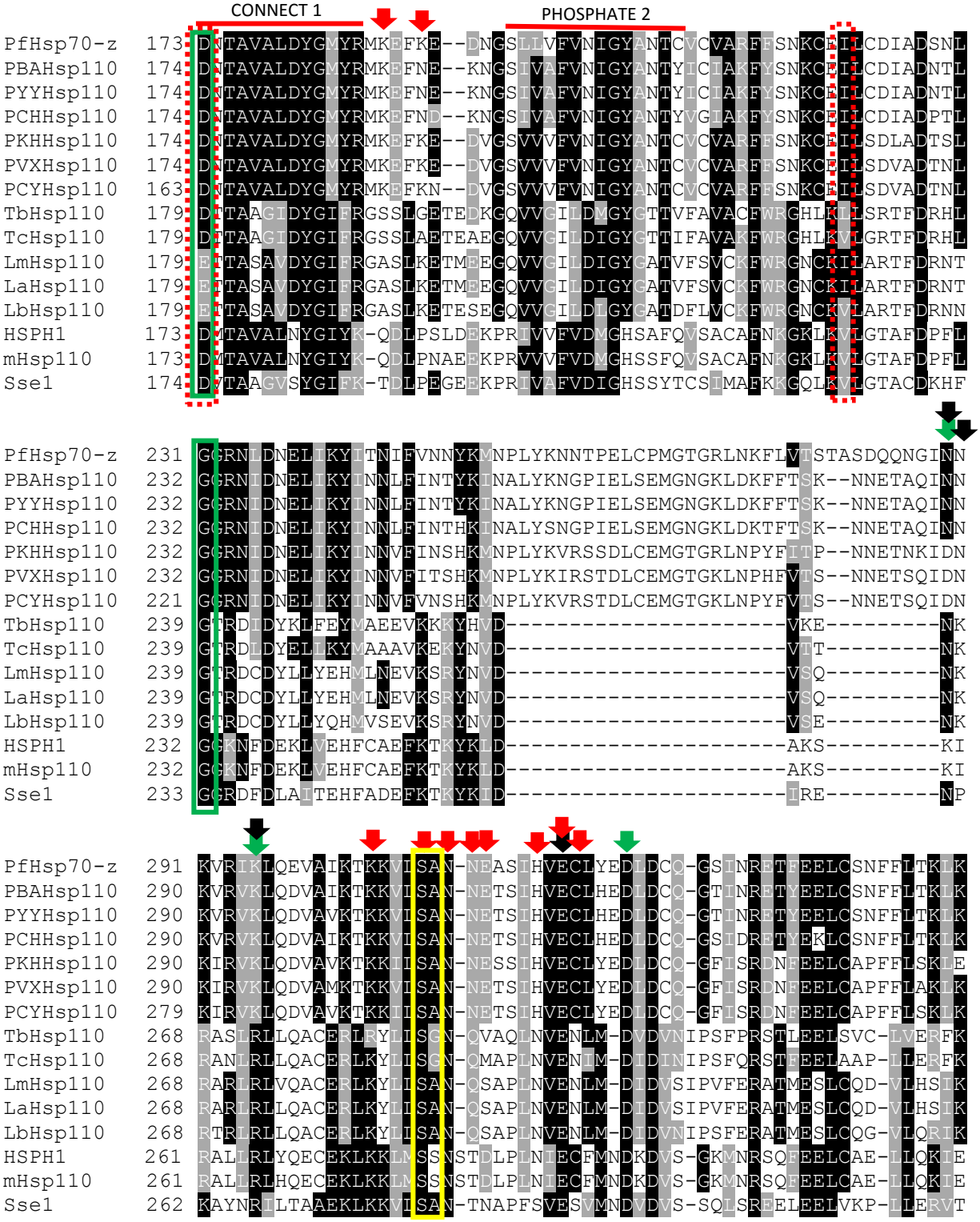

© University of Venda

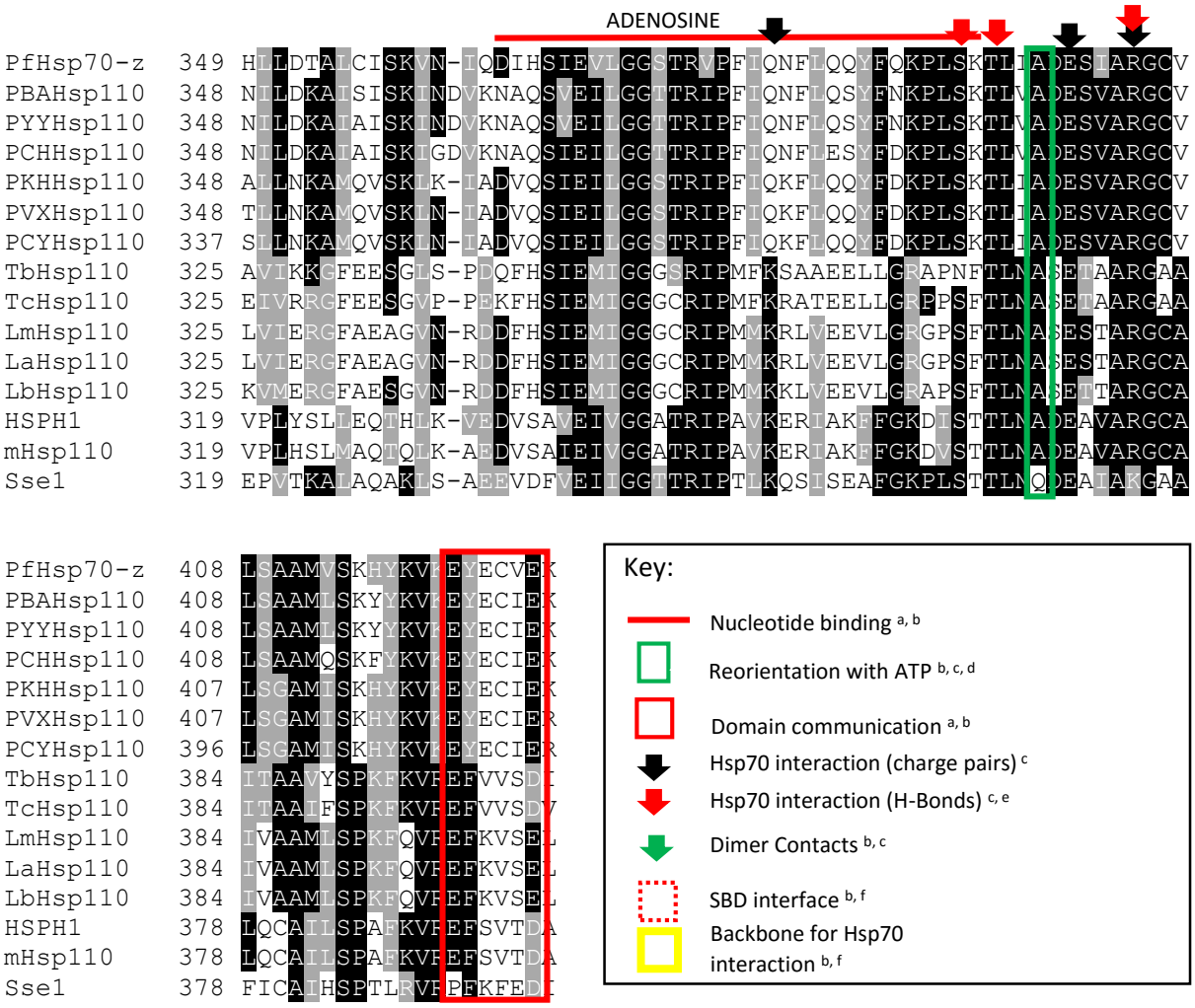

Figure 2.1 Multiple sequence alignment of NBD from Hsp110 homologues
Multiple sequence alignment of $Hsp110_{NBD}$ homologues. Protein sequence accession numbers were obtained from PlasmoDB (Aurrecoechea *et al*. 2008); TritrpDB (Aslett *et al*., 2010) and NCBI (Geer *et al*. 2010). *P. falciparum,* PfHsp70-z (PlasmoDB accession # PF3D7_0708800); *P. vivax,* PVXHsp110 (PlasmoDB accession # PVX_087970); *P. knowlesi,* PKHHsp110 (PlasmoDB accession # PKH_010690); *P. chabaudi*, PCHHsp110 (PlasmoDB accession # XP_745506.1); *P. berghei*, PBAHsp110 (ANKA, PlasmoDB accession # PBANKA_121930); *P. yoelii,* PYYHsp110 (PlasmoDB accession # PYYM_1222000); *P. cynamogi,* PCYHsp110 (PlasmoDB accession # PCYB_011590); *Homo sapiens*, HSPH1 (NCBI accession # NP_006635.2); *Mus musculus,* mHsp110 (NCBI accession # NP_038587); *S. cerevisiae*, Sse1 (NCBI accession # Q875V0); *T. brucei,* TbHsp110 (accession # Tb927.10.12710); *T. cruze* TcHsp110 (accession # TcCLB.507831.60); *L. major,* LmHsp110 (accession # LmjF.18.1370) and *L. brazilienze,* LbHsp110 (accession # LbrM.18.1400). Identical residues are presented in white against a black background, whilst similar residues are shown in white against a grey background the shading was done using Boxshade programme (http://sourceforge.net/projects/boxshade/) ClustalW based alignment was done using MAFFT online tool (http://mafft.cbrc.jp/alignment/software/) to carry out the multiple sequence alignment. The following references represented by superscript (**a**) Shonhai *et al.*, (2008); (**b**) Liu and Hendrickson, (2007); (**c**) Schuermann *et al.*, (2008); (**d**) Moran *et al.*, (2013); (**e**) Wisnieska *et al.*, (2010); (**f**) Kityk *et al.*, (2012).

ATP-bound Hsp110s demonstrate stable interactions with Hsp70s (Andreasson *et al*., 2008). The residues required for ATP binding on the $Hsp110_{NBD}$ are highly conserved; 94.1 % among plasmodial Hsp110 and 72.5 % across all Hsp110 homologues (Figure 2.1). This suggests that nucleotide binding is an important characteristic based on the level of conservation and thus PfHsp70-z possibly interacts with PfHsp70-1 and ATP promotes the interaction. Furthermore,

© University of Venda

the Hsp110 residues implicated in protein reorientation after ATP binding (Figure 2.1) (Moran *et al*., 2013), are well conserved in PfHsp70-z. This suggests that PfHsp70-z possibly exhibits conformational changes in response to nucleotide binding which may be important for regulation its functional cycle.

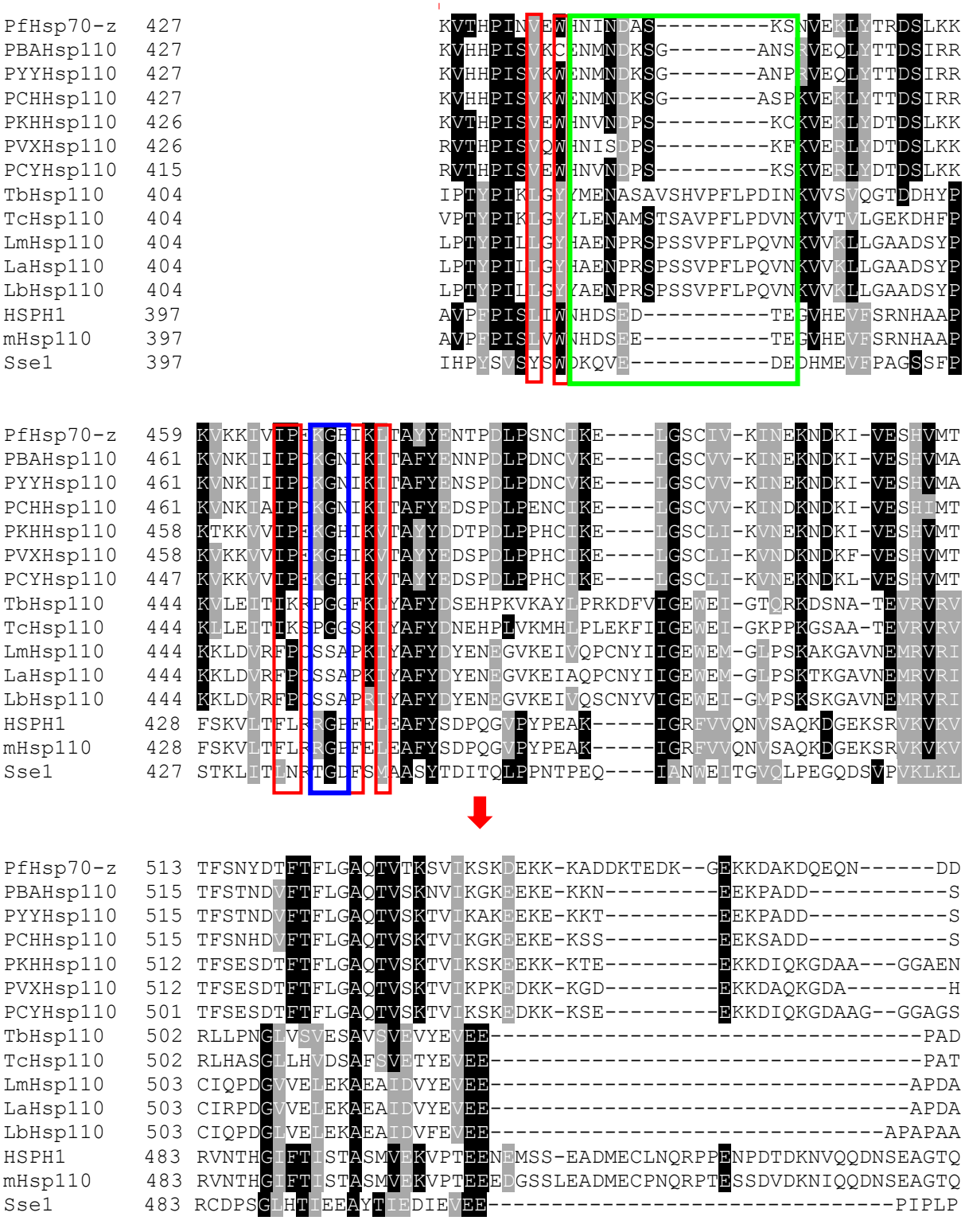

© University of Venda

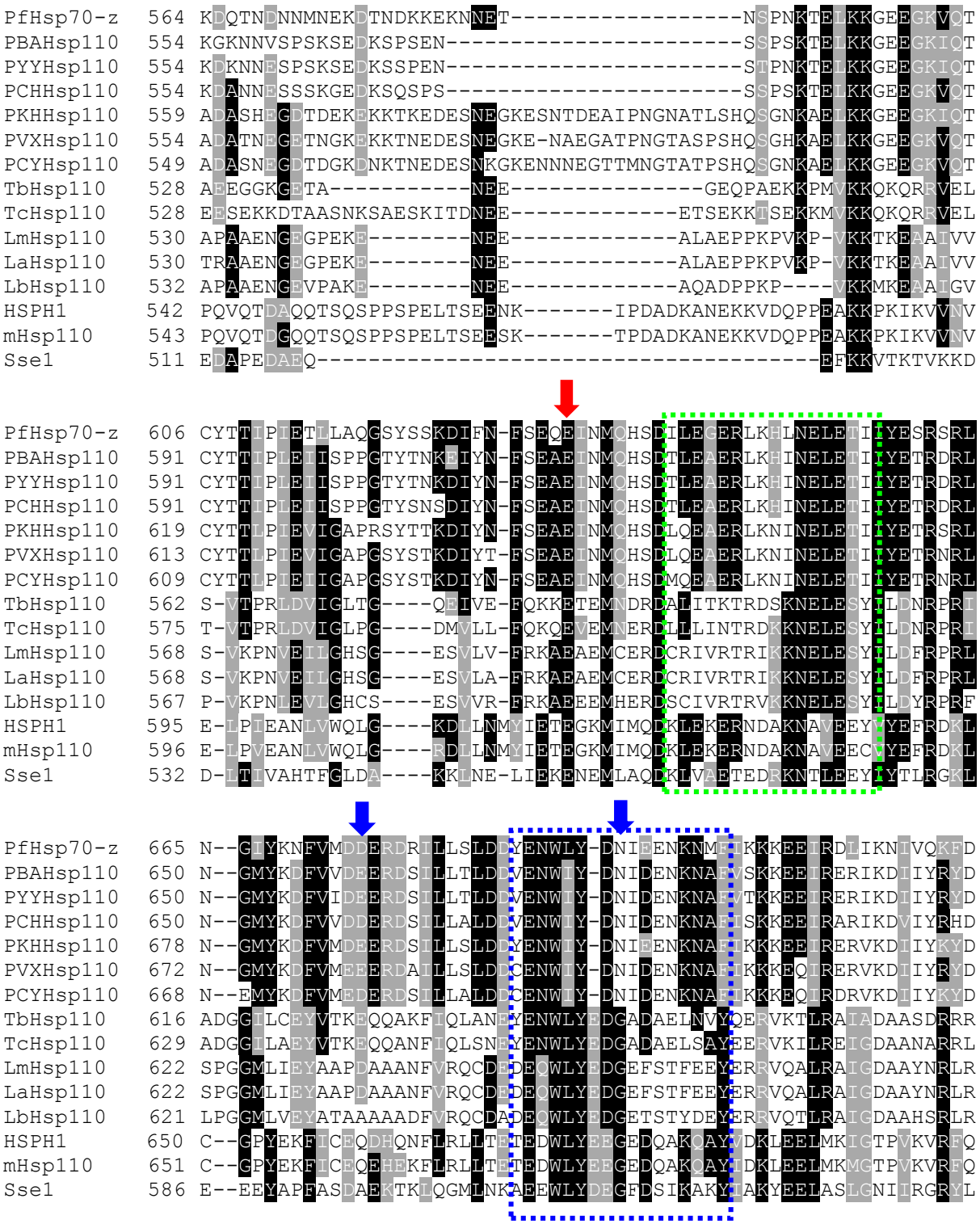

© University of Venda

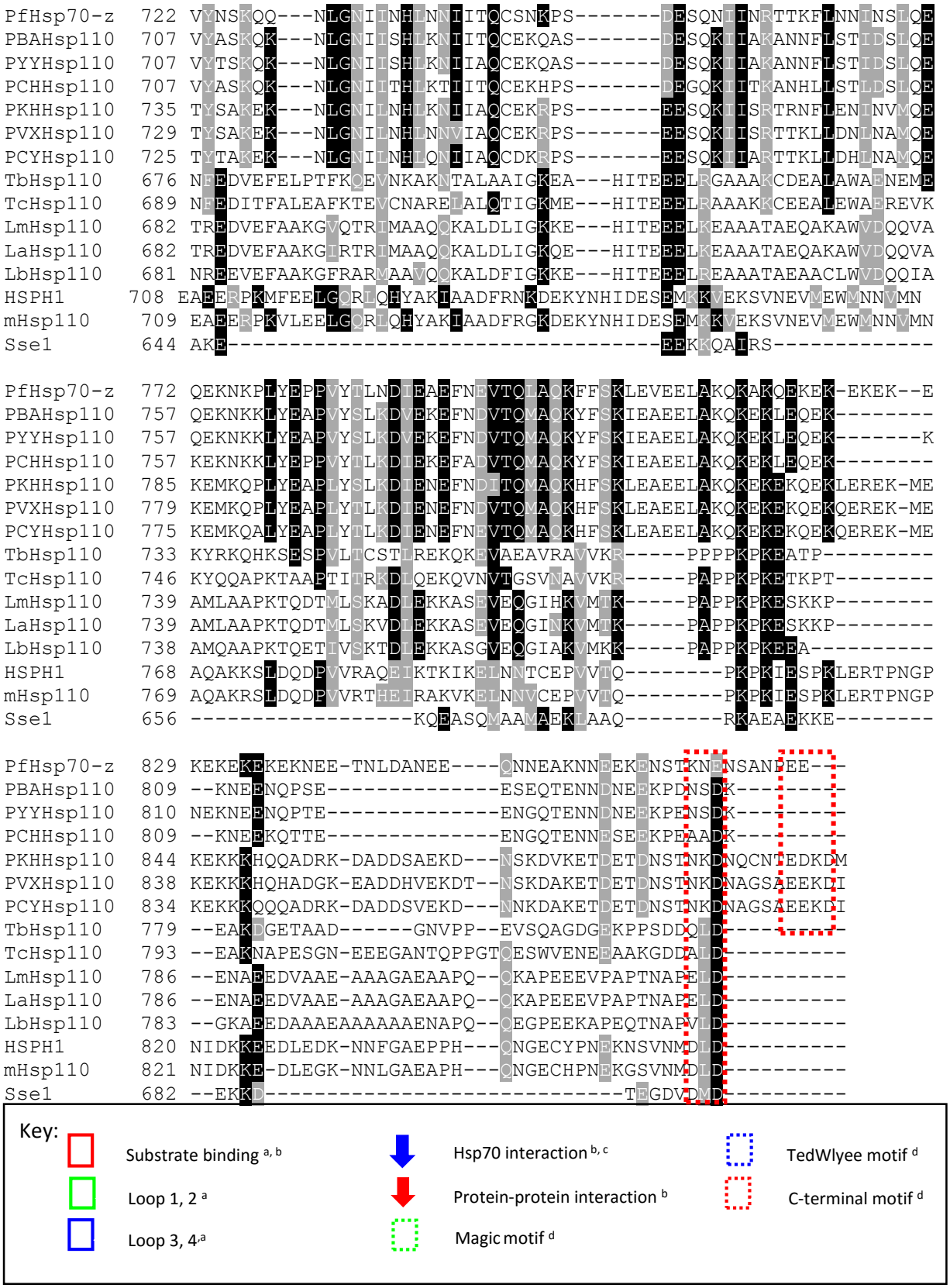

Figure 2.2: Multiple sequence alignment of SBD of Hsp110 homologues
Multiple sequence alignment of Hsp110 SBD othologs and homologues. The accession numbers are as described in figure 2.1. References in superscript (**a**) Xu *et al.*, (2012), (**b**) Moran *et al.*, (2013), (**c**) Dragovic *et al.*, (2006); (**d**) Easton *et al*, (2000).

© University of Venda

Hsp110s have been found to prefer aromatic substrates in contrast to canonical Hsp70s which prefer aliphatic substrates. Sequence alignments of PfHsp70-z_{SBD} show the binding residues flanked by the loops $L_{1,2}$ and $L_{3,4}$ (Figure 2.2;). These residues are thought to be responsible for imparting substrate specificity (Xu *et al*., 2012). The PfHsp70-z substrate binding cleft is in the same orientation as with yeast and human Hsp110s (Xu *et al*., 2012). The sequence on the loops are in reverse orientation when compared to canonical Hsp70s. PfHsp70-z loop $L_{1,2}$ HNININDASKS (Figure 2.2) versus MGG in Hsp70s and loop $L_{3,4}$ KGH (Figure 2.2) versus TAEDNQS. These findings are in line with previous studies suggesting that the loops residues are conserved in Plasmodial Hsp110s (Xu *et al*., 2012). This suggests that PfHsp70-z possibly has similar aromatic substrate preference as other Hsp110s.

Apart from its interaction with substrate the PfHsp70-z_{SBD} is also thought to interact with other proteins to form functional complexes. The residues that are implicated in interaction of $Hsp110_{NBD}$ with $Hsp70_{NBD}$ during nucleotide exchange events are less conserved in PfHsp70-z (Figure 2.2) (Moran *et al*., 2013; Dragovic *et al*., 2006). This suggests that Hsp110 may exhibit species specific nucleotide exchange function. PfHsp70-z is predicted to possess a protein-protein interaction Magic motif (Figure 2.2) and Tedwlyee motifs (Figure 2.2) (Easton *et al*., 2000). Magic and Tedwlyee motifs are the islands with high sequence conservation along the $Hsp110_{SBD}$ sequences and their function is enhanced by the residues implicated in protein-protein interactions (Figure 2.2). Furthermore, Hsp110s exhibit putative C-terminal protein-protein interaction motifs (Figure 2.2). Hsp110 possess D[L/M]D motif and the EEKDI motif on *P. knowlesi*, *P. vivax* and *P. cynamolgi* Hsp110 sequences which aligns to PEE residues on PfHsp70-z. The presence of several protein-protein interaction motifs suggests that PfHsp70-z interacts with Hsps as functional partners.

A high degree of homology in the cytosolic Hsp110 proteins was observed across plasmodial species with PfHsp70-z sharing the highest sequence identity with *P. vivax* homologue (68.4 %) (Appendix B1). However, PfHsp70-z exhibited a lower degree of conservation when compared to human and mouse orthologues (sequence identities of 22.4% and 22.2%,

© University of Venda

respectively) and lowest to orthologues from *S. cerevisiae* 19.4% *T. brucei* 19.2%; *T. cruzi* 20.3%, and *Leishmania major* 19.7%, *L. braziliense* 18.9 % (Appendix B1).

2.3.2 Phylogenetic analysis of PfHsp70-z and its homologues and orthologues

The phylogenetic analysis of PfHsp70z with its cytosolic homologues was conducted by comparison of the amino acid sequences. Plasmodium Hsp110 homologues are phylogenetically closely related as they cluster in a clade that is different from other species. Human and mouse Hsp110 cluster in a clade related to yeast. The TriTryps form two distinct clades that are *Trypanosomes* forming their own clade separate from the *Leishmania spp* (Figure 2.3).

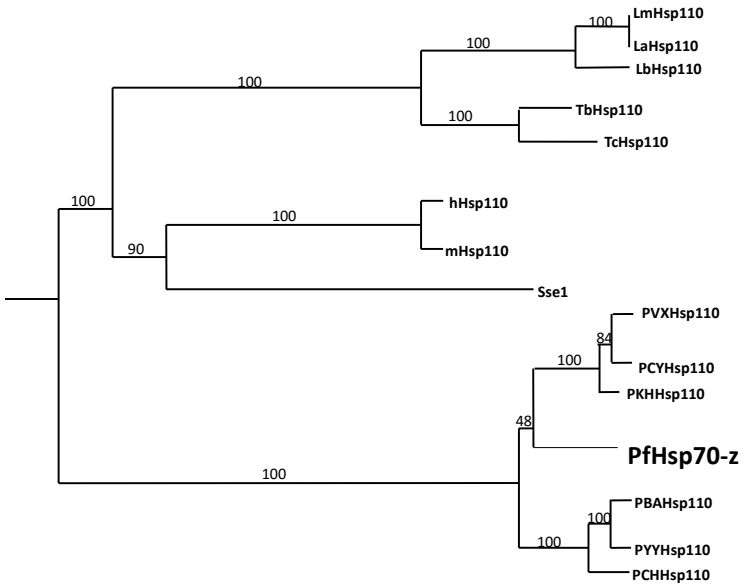

Figure 2.3: Phylogenetic analysis of Hsp110 homologues
The neighbour joining phylogenetic tree of Hsp110 homologues. Dendrograms were constructed using BioEdit (www.mbio.ncsu.edu/Bioedit/bioedit.html) Protdist neighbor phylogenetic analysis tool. The TreeView (Page 1996) option housed on the bioedit programme was used to generate dendrograms (Hall 1999). Boot strap was set at 100. The numbers represent distances. The accession numbers for the proteins are described in figure 2.1.

2.3.3 Generation of PfHsp70-z homology model

Homology modelling of PfHsp70-z subdomains was conducted using Sse1 crystal structures (3c7n.1.A.pdb; Polier *et al*., 2008) as templates for the respective domains. To generate PfHsp70-z_{NBD} three dimensional models, 50 templates were used and a model was built (Figure 2.4). The general $Hsp110_{NBD}$ subdomains IA, IB, IIA, IIB are conserved. Alignment of

© University of Venda

the $Hsp110_{NBD}$ subdomains show structural similarities when aligned to Sse1 subdomains (Figure 2.4A; B).

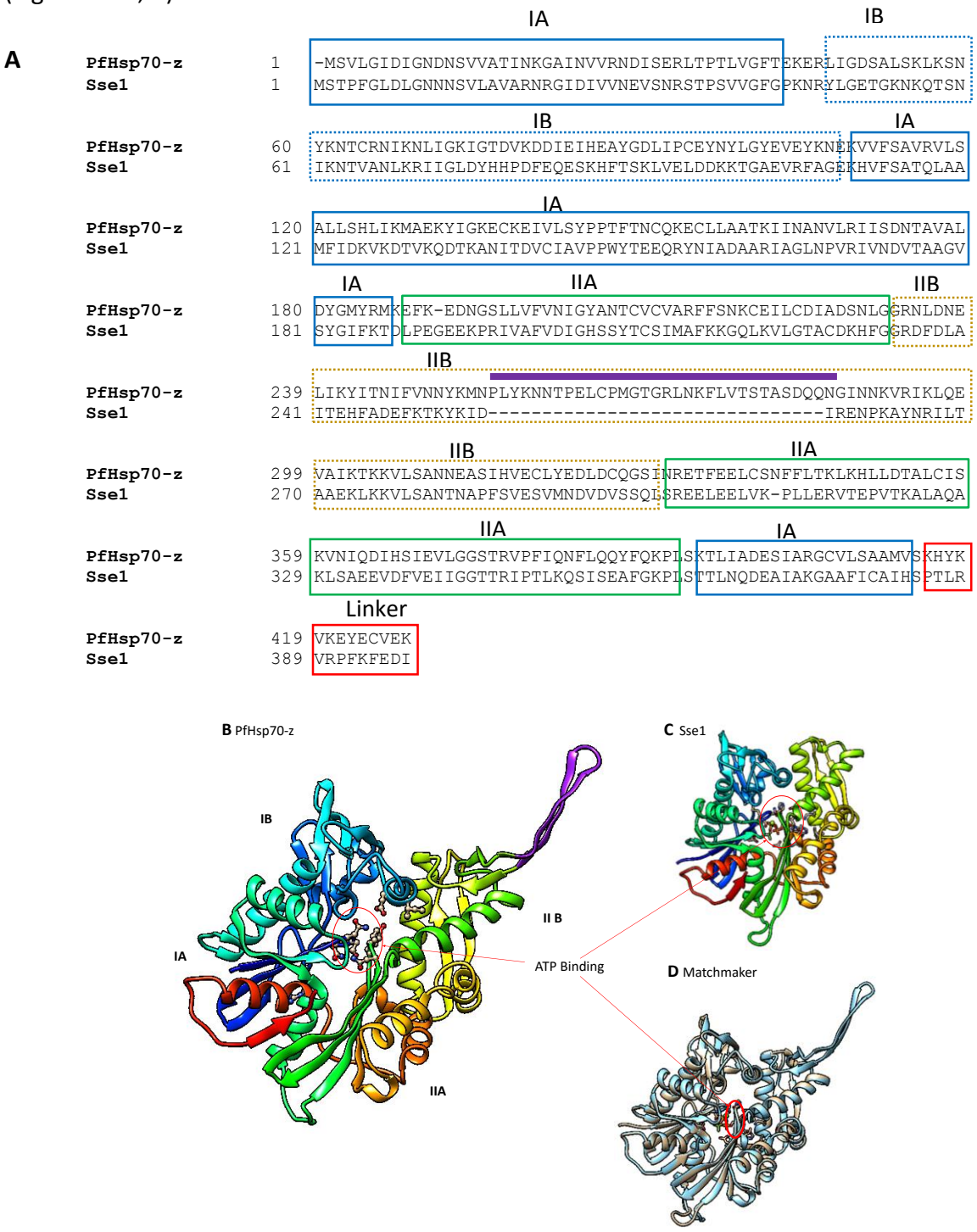

Figure 2.4: A sequence alignment and homology model of the nucleotide binding domain of PfHsp70-z
Multiple sequence alignment between PfHsp70-z and Sse1 (**A**). PfHsp70-z amino acids 1-420 which constitute the putative nucleotide domain were aligned with sse1 amino acids 1-396 which represent the NBD (Oh *et al*., 1999). (**B**) The Homology model of PfHsp70-z. Areas highlighted with ball and stick important for ATP binding in the ATP binding cleft between subdomains IA, IB, IIA and IIB. The two beta sheets highlighted in purple are the insertion segment on the IIB subdomain Sse1 as template (3c7n.1A.pdb; Polier *et al*., 2008). **(C)** The Homology model of $Sse1_{SBD}$ using template (3c7n.1.A.pdb; Polier *et al*., 2008). (**D**) The Chimera matchmaker rendering PfHsp70-z onto Sse1 using Needleman-Wunsch alignment algorithm. The PfHsp70-z model is colored in blue and Sse1 model colored in brown.

© University of Venda

The PfHsp70-z_{NBD} three dimensional model is similar to the known Sse1p_{NBD} which has a conserved nucleotide binding cleft similar to actin ATPase domain (Eason *et al*., 2000; Polier *et al*., 2008). There is structural conservation on PfHsp70-z nucleotide pore formed between subdomain IB and IIB (Figure 2.4B). This pore is thought to be responsible for the movement of nucleotide in and out of the binding cleft (Schuermann *et al.*, 2008). The presence of PfHsp70-z_{NBD} insertion on IIB subdomain results in outstretched beta sheets (Figure 2. 4B); which become more prominent when PfHsp70-z_{NBD} is matched with Sse1$_{NBD}$ (Figure 2.4C; 2.4D; Polier *et al*., 2008). These insertions may have evolved as a mechanism of PfHsp70-z specialisation for possible interaction with PfHsp70-1$_{NBD}$ as a NEF. This is in agreement with predictive studies conducted on *P. falciparum* genome suggesting that PfHsp70-z is possibly the sole cytosolic NEF for PfHsp70-1 (Shonhai *et al*., 2007; Bhartiya *et al*., 2015). The structural predictions suggest that PfHsp70-z has possibly evolved to be a specialised cytosol localised NEF for PfHsp70-1.

The three dimensional model of PfHsp70-z_{SBD} was generated using 80 templates (Figure 2.5). The general subdomain arrangement for Sse1$_{SBD}$ is conserved in PfHsp70-z_{SBD} except the insertion of two beta sheets (β6, β10) (Figure 2.5A). The insertion may possibly suggest that PfHsp70-z exhibits better holdase function as it has more beta sheets which facilitate substrate interaction. Furthermore, the PfHsp70-z loop $L_{1,2}$ in the substrate binding domain exhibits an insertion which is bigger than that of the yeast and human homologues. This suggests that PfHsp70-z possibly interacts with larger substrates as compared to its yeast and human equivalents. This may imply that PfHsp70-z is more effective at suppressing protein aggregation compared to yeast and human equivalence (Muralidharan *et al.,* 2012). Based on observations made on PfHsp70-z_{SBD} multiple sequence alignments (Figure 2.2), the predicted residues implicated in substrate binding are located in β1; β3 and β4 (Figure 2.5B insert) (Polier *et al*., 2010).

© University of Venda

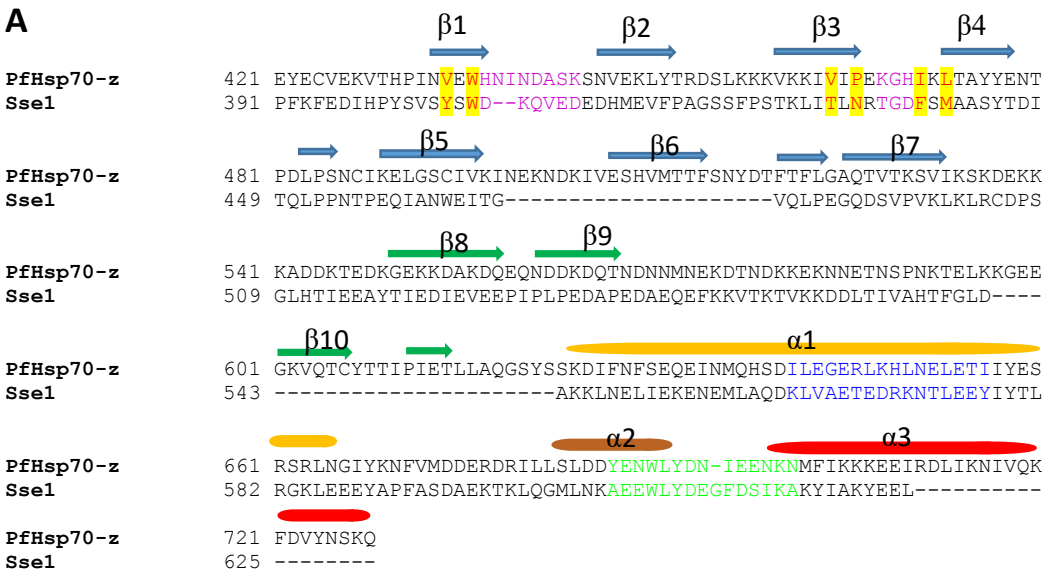

Figure 2.5: A sequence alignment and homology model of the substrate binding domain of PfHsp70-z
Multiple sequence alignment between PfHsp70-z_{SBD} and $Sse1_{SBD}$ (**A**). PfHsp70-z residues 421-728 constitute the putative substrate binding domain aligned with Sse1 residues 391-631 which represent the SBD. Areas highlighted are important for substrate binding residues (Red), substrate binding loops (Purple); Magic motif (Blue) Tedwlyee motif (Green). The three dimensional model of PfHsp70-z_{SBD} (**B**). The highlighted areas are color coded similar to motifs and residues in (A). **Insert** represent the substrate binding cleft magnification and residues implicated. The model was generated using Sse1 as template (3c7n.1.A.pdb; Polier *et al*., 2008; Schuermann *et al*., 2008).

© University of Venda

2.3.4 PfHsp70-z secondary structure prediction

The predictions of a three dimensional homology model for the last 143 residues of the C-terminus were unsuccessful. This may be as a result of this region being predominantly unstructured. Therefore, the PfHsp70-z secondary structure prediction was conducted using an online tool, PHYRE2 (http://www.sbg.bio.ic.ac.uk/phyre2/html/page.cgi?id=index) (Figure 2.6). The secondary structure of PfHsp70-z was predicted to be composed of α-helices and disordered regions (Figure 2.6).

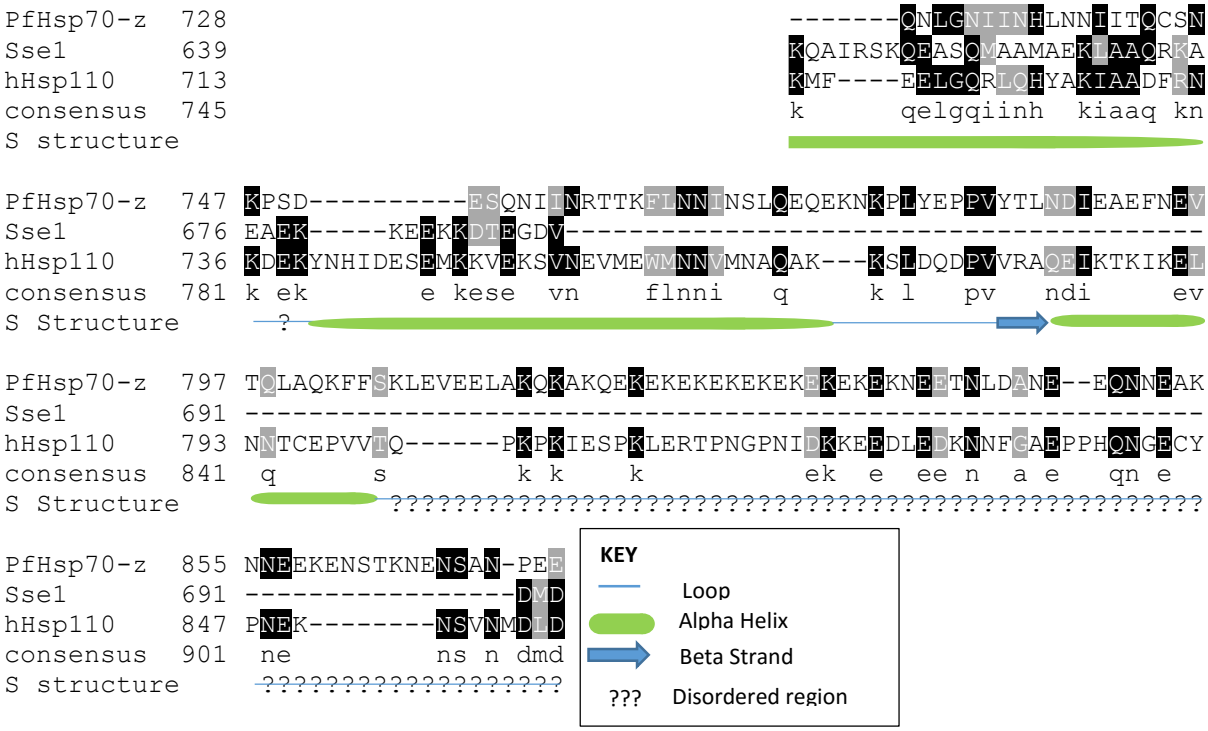

Figure 2.6: Secondary structure prediction of PfHsp70-z
Prediction of the secondary structure of full length PfHsp70-z, Sse1 and HSPH1 was conducted using both PHYRE2. Sequences were retrieved from PlasmoDB and NCBI and the accession numbers are as listed in Figure 2.1.

2.3.5 Composite analysis of the amino acid sequence of PfHsp70-z and design of peptide antibody

Knowledge of the peptide regions of immunogenicity is essential for peptide based antibody design. Composite analysis of PfHsp70-z was conducted using DNASTAR to determine a unique peptide sequence along the protein (Figure 2.7). Thirteen putative epitopes were predicted by GenScript Antigen Design Tool, OptimumAntigenTM design tool. Seven putative peptides were located in the ATPase domain and four within the PfHsp70-z_{SBD} and three were located on the C-terminal domain (Appendix B2). The peptide 768-782 (CSLQEQEKNKPLYEP)

© University of Venda

was selected because it exhibited the lowest degree of sequence conservation in addition to it being surface exposed, possessing appropriate charge, hydophilicity and antigenic indices (Figure 2.7). After the successful design of the antigenic peptide, BLAST analysis was performed on the sequence and no significant similarities to *E. coli*, human, rabbit, goat and mouse protein sequences was detected. The selected peptide sequence was submitted to Genscript (USA) for the antibody production in a rabbit. The antibody was used for subsequent analysis (Section 3.3.4; 5.3.1; 5.3.2; 5.3.3; Zininga *et al*., 2015a).

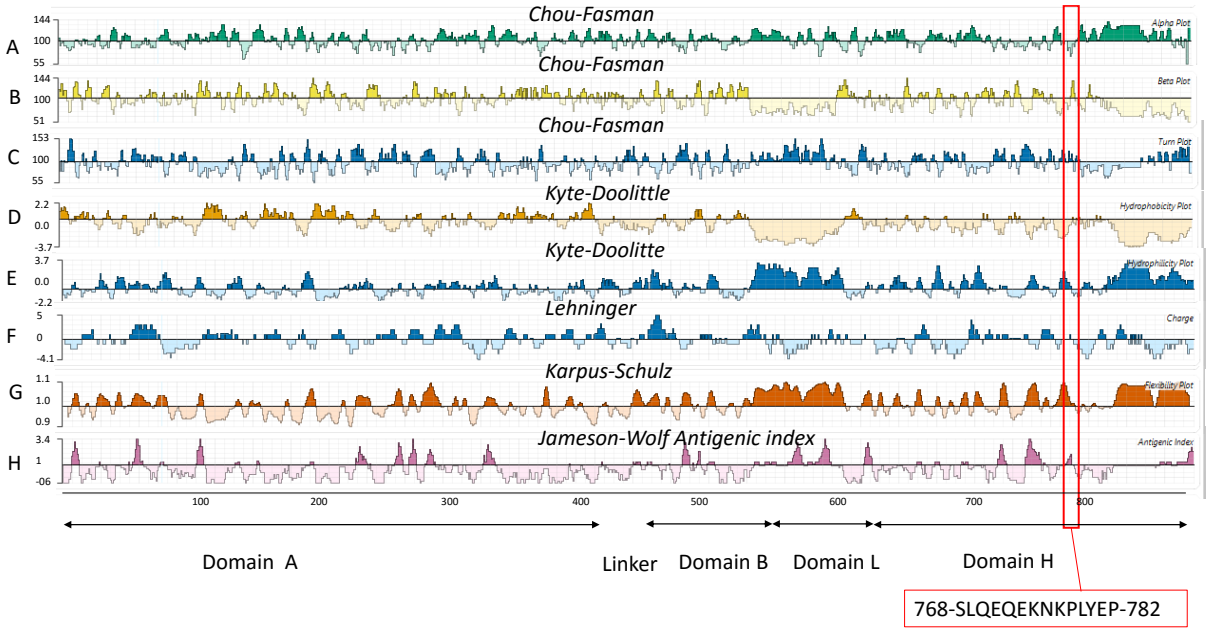

Figure 2.7: Composite analysis of full length PfHsp70-z amino acid sequence
Antigenicity of PfHsp70-z was analysed through the composite analysis of the amino acid sequence using DNASTAR-Proteon 3D. Positioning of residues are specified by numbers along the x-axis. The position of the selected peptide is indicated by a red box, along with the peptide sequence below it. Arrows below the graph indicate the relative positions of the domains of PfHsp70-z. (**A**, **B**, **C**) *Chou-Fasman* – predicts secondary structure (Chou and Fasman, 1978); (**D, E**) *Kyte-Doolittle hydropathy* – plots hydrophilicity and hydrophobicity plots (Kyte and Doolittle, 1982); (**F**) *Lehninger* predicts the surface charge and plots Positive and negative charge plots (Lehninger, 2005). (**G**) *Karpus- Schultz* – predicts chain flexibility and plots enhanced flexibility as a peak (Karplus and Schultz, 1988). (**H**) *Jameson-Wolf antigenic index* – computes an overall antigenicity analysis by combining all the previous analyses, epitopic regions are plotted as peaks. The analysis was conducted using Proteon 3D on DNASTAR Version 12.2.0.80.

2.3.6 Genomic neighbourhood of PfHsp70-z

Eukaryotic genes are thought to be regulated in groups as gene clusters/genomic neighbourhoods based on shared distinct transcriptional activity (De and Babu, 1999). These events are known to affect the expression of several genes simultaneously and as such genes

© University of Venda

within *PfHsp70-z* neighbourhood may be under *cis*-regulatory elements such as transcription factors. The *PfHsp70-z* gene is located on chromosome 7, on *P. falciparum* genome (Figure 2.8A). The members of the gene neighbours of *PfHsp70-z* show similarities with gene neigbours of *Hsp110* from other plasmodial species (Figure 2.8B).

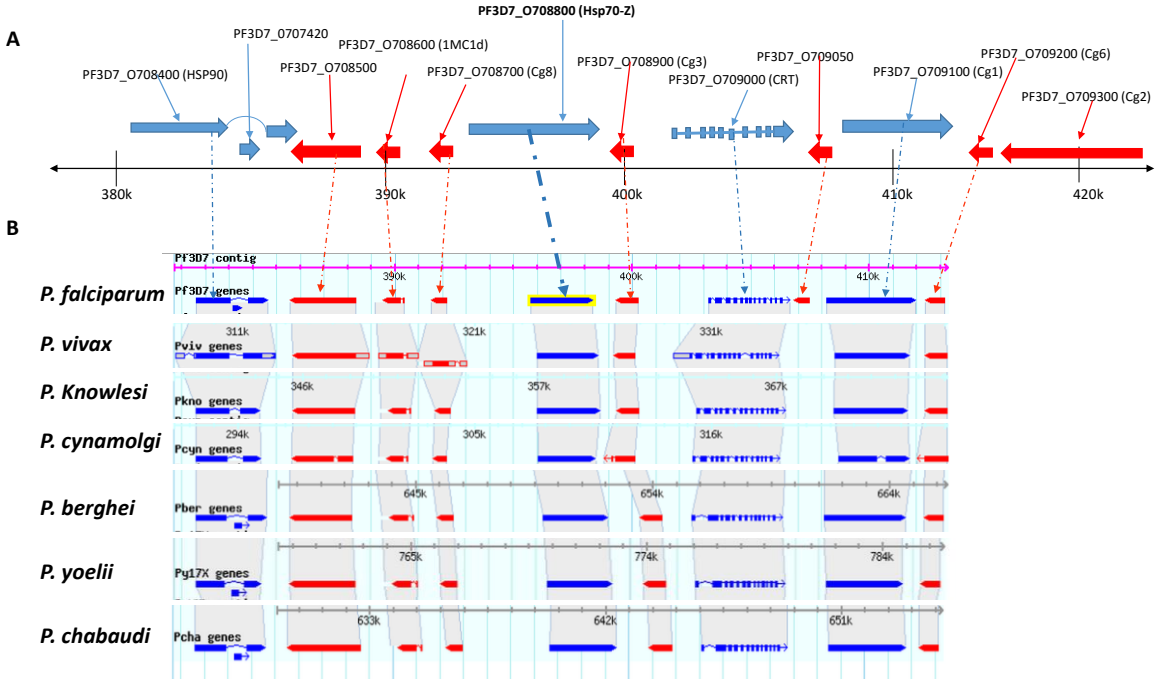

Figure 2.8: Chromosomal location of *PfHsp70-z* gene
The chromosomal location of the gene coding for Hsp70-z on Plasmodia species. PfHsp70-z location on *P. falciparum* chromosome 7 spanning from 380 kbp - 422 kpb (**A**). The chromosomal location of the plasmodium homologues of PfHsp70-z (**B**). Gene code blue arrows and those coded in complement are shown in red arrows, adapted from PlasmoDB.

PfHsp70-z gene neighbours include *PfHsp90* (PF3D7_0708400) and the *chloroquine resistance transporter* (*CRT; PF3D7_0709000*) genes (Figure 2.8). This suggests that among others *PfHsp90* and *Pfcrt* genes are possibly regulated simultaneously with *PfHsp70-z*.

2.3.7 Predicted interaction partners of PfHsp70-z

PfHsp70-z network data was retrieved from STRING database and analysed using Cytoscape (Shannon *et al*., 2004). Betweenness centrality and closeness centrality analyses were conducted using Cytoscape NetworkAnlayzer tool (Brandes, 2001). The node sizes and closeness suggest that PfHsp70z functionally interacts mostly with its interactors in the

© University of Venda

following order: PF3D7_0818900 (PfHsp70-1) > PF3D71437900 (PfHsp40) > PF3D7_0708400 (PfHsp90) > PF3D7_1434300 (PfHop) > PF3D7_0517700 (Eukaryotic translation initiation factor) (Figure 2.8). Mapping of the interactome was conducted based on weighted evidence from direct interaction evidence from *P. falciparum*. The threshold for interactions was set at a confidence level of 0.7. This suggests that the predicted interactions exhibit a set at confidence level which is above 0.7 probability of occurrence (Jensen *et al*., 2009)

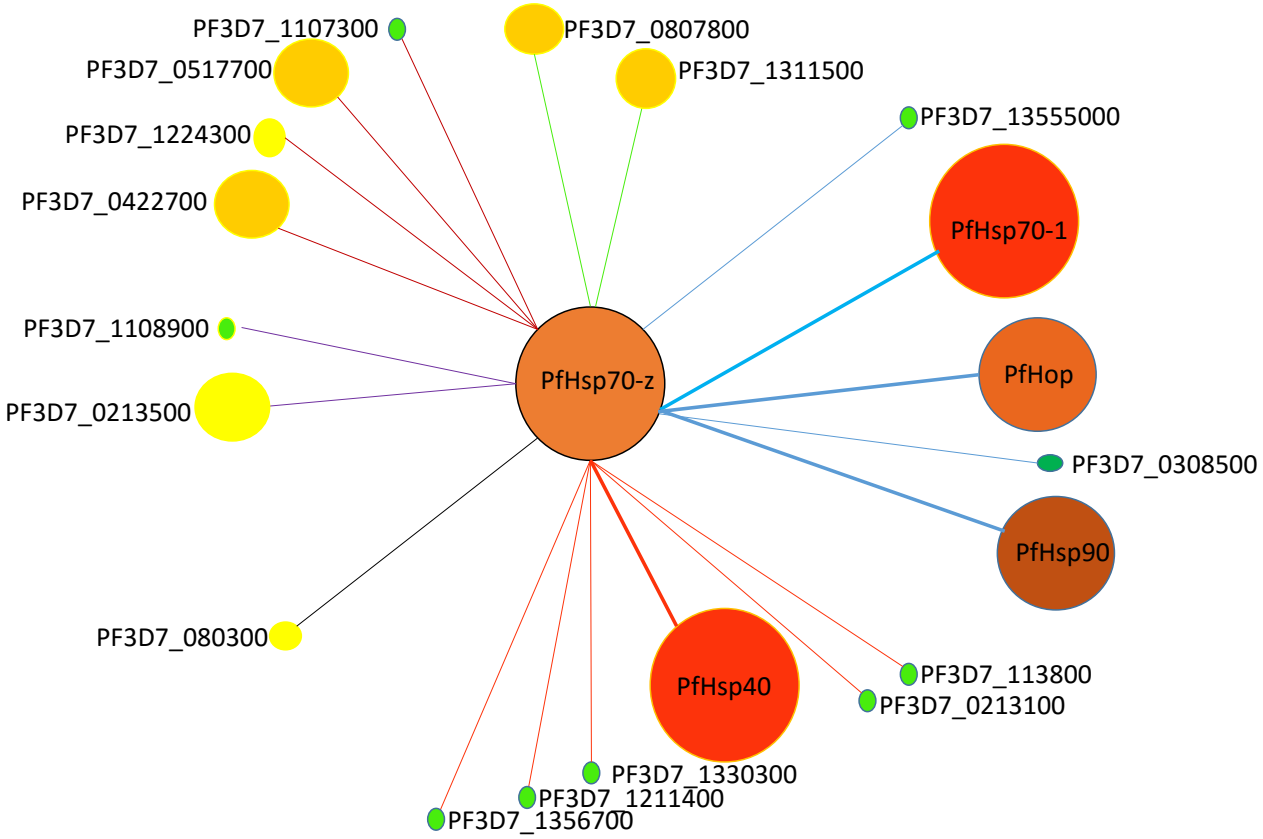

Figure 2.9: PfHsp70-z predicted direct interaction partners

The predicted interactome of PfHsp70-z reflect interaction likelihood using betweeness centrality and closeness centrality. The node size was mapped to betweenness centrality of PfHsp70-z reflecting the amount of control it exerts over the interactions of other proteins in the network (Yoon *et al*., 2006). The node colours were mapped to closeness centrality a measure of communication thus showing how fast (red) or slow (green) information spreads from PfHsp70-z to other reachable nodes in the network (Newman, 2003). The edges represents functional clusters as the red edges (line) represents Hsp40s, Brown edges represent translation factors, blue edges represent known molecular chaperones and co-chaperones forming a complex with Hsp90, Purple edges represent interaction with plasmodial conserved proteins; green edges represent ubiquiting factors, and sky blue edge represent Hsp90 phosphorylation factor.

© University of Venda

2.4 Discussion

The bioinformatics analyses conducted in this study unravelled PfHsp70-z as a structurally divergent Hsp110 protein. PfHsp70-z is predicted to be an NEF of PfHsp70-1 (Shonhai *et al*., 2007). In order to carry out this function, PfHsp70-z must be able to bind nucleotides. This study, using multiple sequence alignments, uncovered the general conservation for residues that are required for ATP binding in PfHsp70-z (Figure 2.1). Based on the three dimensional structure of PfHsp70-z (Figure 2.4), PfHsp70-z possibly functions as a crow bar to open $Hsp70_{NBD}$ IIB and IB subdomains thereby releasing ADP trapped in the $Hsp70_{NBD}$ binding cleft (Dragovic *et al*., 2006).

The orientation of the predicted three dimensional structure of the substrate binding cleft is conserved in PfHsp70-z (Figure 2.5). The loop $L_{1,2}$ in PfHsp70-z in the substrate binding is extended due to the insertion NDAS on loop $L_{1,2.}$ It is plausible that the insertion may have arisen in order to increase the size of the substrate interaction site by enabling PfHsp70-z to bind bigger substrates. This explains PfHsp70-z's competitive advantage as chaperone over human and yeast homologues (Muralidharan *et al*., 2012). Taken together, PfHsp70-z is predicted to possibly function as a robust chaperone with preference for aromatic substrates as previously observed (Muralidharan *et al*., 2012).

PfHsp70-z is predicted to functionally interact with other proteins by the presence of conserved Magic motif and the Tedwlyee motif (Easton *et al*., 2000), that are thought to be involved in protein-protein interaction (Figure 2.2). These two motifs are thought to be at the centre of protein-protein interaction (Easton *et al*., 2000). Interestingly, the conserved Tedwlyee motif is also thought to facilitate the interaction with Hsp70 during NEF function. These data suggest that PfHsp70-z interacts with PfHsp70-1 through both its NBD and SBD in conducting its role as a NEF of PfHsp70-1.

© University of Venda

Hsp110 proteins exhibit unique linker segments that connect the N-terminal $Hsp110_{NBD}$ to the C-terminal $Hsp110_{SBD}$ (Polier 2008). It has been suggested that the linker of Hsp110 is fairly rigid, resulting in the protein exhibiting reduced allosteric function (Liu and Hendrickson, 2007). Based on sequence alignment, Plasmodial Hsp110 proteins exhibit a linker segment that differs from that of canonical Hsp70s (Figure 2.1). Furthermore, the linker of PfHsp70-z is divergent from that of human and yeast Hsp110s (Figure 2.1). Since the linker region is required for Hsp70 allosteric function (Vogel *et al*. 2006), the linker of plasmodial Hsp110 may confer specific functional features to these proteins. Indeed, it has been proposed that Hsp110 from yeast may possess unique structural features compared to the human homologue (Raviol *et al*., 2005). It remains to be experimentally validated, the effects of nucleotide binding assays on the structural conformation of PfHsp70-z (Sections 4.3.1; 4.3.3).

PfHsp70-z has been predicted to associate mostly with chaperones in the following order: PfHsp70-1 > PfHsp40 (PF3D7_1437900) > PfHsp90 (PF3D7_0708400) > PfHop (PF3D7_1434300) (Figure 2.9). Phosphorylation regulates the chaperone function of some chaperones. For example, the inhibition of PfHsp90 phosphorylation results in non-functional PfHsp90 (Banumathy *et al*., 2003). The TPR rich phosphatase PP5 (PF3D7_1355500), a known Hsp90 phosphatase (Dobson *et al*. 2001; Kumar *et al*. 2003) was predicted to interact with PfHsp70-z. This interaction is possibly through the formation of chaperone complexes where PfHsp70-z occurs in complex with PfHsp70-1, PfHsp90-PfHop and it remains to be experimentally validated. Chloroquine resistance in *P. falciparum* is mapped to a 36 kb segment of Chromosome 7, which includes the *PfHsp90* and *PfHsp70-z (PfCg4)* gene (Figure 2.8; Su *et al*., 1997). The gene location data suggest that *PfHsp70-z* may be under the same regulatory mechanism with Chloroquine resistance transporter (*CRT*) genes. Furthermore, it has previously been demonstrated that the expression of yeast Hsp90 and Hsp110 are both induced by heat shock transcription factor carboxyl terminal activation domain (HSF-CTD) (Lui *et al*., 1999). The induction of PfHsp70-z and PfHsp90 is possibly important for cell cycle progression during heat stress conditions. Altogether, this suggests PfHsp70-z and PfHsp90 potential cooperation may facilitate parasite survival during heat stress conditions.

© University of Venda

The interactome data suggest that PfHsp70-z is a potential NEF for PfHsp70-1 as it is the only cytosolic NEF homology (Bhartiya *et al*., 2015). It has been established that PfHsp70-1 interacts with PfHsp90 through PfHop as the adaptor protein (Banumathy *et al*., 2003; Gitau *et al*., 2012; Zininga *et al*., 2015b). Based on the interactome data, this study predicts the possible interaction of PfHsp70-z with the PfHsp70-1-PfHop-PfHsp90 complex (Figure 2.9; Gitau *et al*., 2012). However, the role of PfHsp70-z in this complex remains to be validated. Data from this study, predicts PfHsp70-z to interact with Hsp40s (Figure 2.8). It is known that PfHsp40 (PF3D7_1437900) facilitates PfHsp70-1 functional cycle (Figure 1.8; Botha *et al*., 2011). The predicted functional cooperation of PfHsp70-z and PfHsp40 possibly regulate PfHsp70-1 functional cycle.

PfHsp70-z is also predicted to interact with peptidyl-prolyl cis-trans isomerase (PPI) (PF3D7_0803000) which catalyzes the *cis*-trans isomerization of proline imidic peptide bonds in oligopeptides (Hall *et al*., 2002). PfHsp70-z is possibly involved in the formation of disulphide bond during protein folding through its interaction with PPIs. Furthermore, PfHsp70-z is predicted to interact with proteins involved in translational initiation (Tuteja and Pradhan, 2009). This suggests that PfHsp70-z is involved in virtually every step of a protein life by interacting with translation factors; chaperones and ubiquitin dependant protein degradation factors (Figure 2.9). However, it remains to be validated if the predicted inter-actors are functional partners or potential substrates.

The aim of this study was to utilize available bioinformatics tools to glean the role of PfHsp70-z. PfHsp70-z functional features were mapped and PfHsp70-z inter-actors were established. PfHsp70-z is fairly divergent from human homologue. The divergence makes it prospect for antimalarial possible drug target discovery.

© University of Venda

CHAPTER 3

PRODUCTION OF RECOMBINANT PFHSP70-Z PROTEIN AND ANALYSIS OF ITS SECONDARY AND TERTIARY STRUCTURES

© University of Venda

Production of Recombinant PfHsp70-z Protein and Analysis of its Secondary and Tertiary Structures

3.1 Introduction

Hsp110s belong to an Hsp70 subfamily of eukaryotic chaperones that have been implicated in a variety of cellular functions. Hsp110 like Hsp70, can recognise and bind hydrophobic peptide sequences and exhibits ATPase activity (Goeckeler *et al*., 2008). However, Hsp110s cannot refold denatured substrates and act as 'holdases' binding denatured substrates and supress substrate aggregation (Oh *et al*., 1997; Goeckeler *et al*., 2002). Specific intracellular functions of Hsp110 are poorly characterised (Moran *et al.,* 2013). Hsp110s are thought to serve as NEFs of their respective canonical Hsp70 counterparts (Dragovic *et al*., 2006; Andreasson *et al*., 2008). Nucleotide exchange indirectly determines the substrate dwell time on $Hsp70_{SBD}$ thereby influencing substrate fate (Mandal *et al*., 2010). The premature release of substrates from Hsp70 could result in their aggregation, and ultimate degradation (Mayer and Bukau, 2005). NEFs from prokaryotes and eukaryotes are structurally unrelated but they serve a common role (Raviol *et al*., 2005). In *P. falciparum* only PfHsp70-z, an Hsp110 homologue, is based in the cytosol and thus may function as a potential NEF of the well characterized canonical Hsp70 chaperone, PfHsp70-1 that also occurs in the cytosol (Shonhai *et al*., 2007). Although PfHsp70-z is thought to play an essential role through suppressing aggregation of malarial asparagine repeat-rich proteins (Muralidharan *et al*., 2012), it is possible that its function as NEF of PfHsp70-1 may be crucial for parasite survival. Therefore, this study sought to heterologously express and purify recombinant PfHsp70-z and to investigate its biophysical characteristics.

The objectives of this study were to:

i) Heterologously express and purify recombinant PfHsp70-z protein;

ii) Determine the secondary and tertiary structure of recombinant PfHsp70-z protein;

iii) Assess the heat stability of recombinant PfHsp70-z;

iv) Explore the formation of higher order oligomers by recombinant PfHsp70-z; and

v) Determine the ATPase activity of recombinant PfHsp70-z protein.

© University of Venda

Production of Recombinant PfHsp70-z Protein and Analysis of its Secondary and Tertiary Structures

3.2 Experimental Procedures

3.2.1 Materials

The following plasmids used are summarised in Table 3.1: pQE30 vector (Qiagen, Germany) and pQE30/PfHsp70-z plasmid expressing PfHsp70-z (Zininga *et al.,* 2015a); pQE30/PfHsp70-1 plasmid expressing PfHsp70-1 (Matambo *et al*., 2004; Shonhai *et al*.,2005); pQE30/PfHsp70-1_{NBD} plasmid expressing the PfHsp70-1_{NBD} (Zininga *et al.,* 2015b). The following antibodies were used: the α-PfHsp70-z antibody produced in rabbit against peptide: CSLQEQEKNKPLYEP, corresponding to amino acids 768–782 of the PfHsp70-z amino acid sequence was secured from GenScript (USA) (section 2.3.5; Zininga *et al*., 2015a). Polyclonal rabbit raised antibodies specific for PfHsp70-1 that were previously described (Pesce *et al*., 2008) were used to validate the authenticity of recombinant PfHsp70-1 protein. The rest of the reagents used in the study are listed in Appendix C.

Table 3.1: Description of strains and plasmids used in this study

Strains and plasmids	Description	Supplier/Reference
Strains		
E. coli JM109	e14$^-$ (McrA$^-$) recA1 endA1 *gyr*A96 thi-1 hsdR17 (r_K^- m_K^+) supE44 *rel*A1 Δ(*lac*-proAB) (F´ traD36 proAB *lac*I^q ZΔM15).	Thermofisher Scientific, USA
E. coli XL1 Blue	*rec*A1 *end*A1 *gyr*A96 *thi*1 *hsd*R17 supE44 *rel*A1 *lac* (F´proAB lacI^qZM15 Tn10 (Tetr).	Bullock *et al*., (1987)
Plasmids		
pQE30-PfHsp70-z	pQE30 encoding PfHsp70-z, Amp^R	Zininga *et al*., (2015a)
pQE30-PfHsp70-1	pQE30 encoding PfHsp70-1, Amp^R	Matambo *et al*., (2004)
pQE30/PfHsp70-1_{NBD}	pQE30 encoding PfHsp70-1_{NBD}, Amp^R	Zininga *et al*., (2015b)

3.2.2 Construction of plasmid expressing PfHsp70-z

Codon harmonized form of the gene for *PfHsp70-z* (PlasmoDB accession number: P3D7_088000) was made by Genscript. The DNA segment encoding regions of PfHsp70-z were

© University of Venda

subsequently PCR amplified from pUC57/PfHsp70-z using the forward primer (5'–CATCACGGATCCATGAGC–3') with a *Bam*HI restriction site and reverse primer (5'–GCTAATTAAGCTTTCATTCTTCCGG – 3') with a *Hind*III restriction site. The gene was subsequently cloned in pQE30 (Qiagen) making pQE30/PfHsp70-z construct used to express PfHsp70-z (Zininga *et al*., 2015a) and was verified by DNA sequencing. The pQE30/PfHsp70-z plasmid constructs was purified using the Zymo Research Plasmid Miniprep™ kit (Epigenetics, U.S.A) according to manufactures instructions (Appendix A1). The DNA was digested (Appendix A2) using restriction enzymes, *Hind*III and *Bam*HI (Thermo Scientific, U.S.A). The restriction products were then analysed using 0.8 % agarose gel electrophoresis (Appendix A3).

3.2.3 Confirmation of PfHsp70-1 and PfHsp70-1_{NBD} DNA constructs

A plasmid construct expressing PfHsp70-1 (PlasmoDB accession number: PF3D7_0818900) (pQE30/PfHsp70-1) was used to express PfHsp70-1 as previously described (Matambo *et al*., 2004; Shonhai *et al*. 2008). Another plasmid construct (pQE30/PfHsp70-1_{NBD}) expressing the PfHsp70-1_{NBD} was used to express PfHsp70-1_{NBD} (Zininga *et al*., 2015b). To confirm the integrity of the pQE30/PfHsp70-1 and pQE30/PfHsp70-1_{NBD}, the plasmid constructs were purified as previously described (section 3.2.2) and was digested (Appendix A2) using restriction enzymes, *Hind*III + *Bam*HI for pQE30/PfHsp70-1 and *Bam*HI + *Spe*I for pQE30/PfHsp70-1_{NBD}, respectively (Thermo Scientific, U.S.A). The restriction products were then analysed using 0.8 % agarose gel electrophoresis.

3.2.4. Expression of recombinant proteins

Competent *E. coli* JM109 (DE3) cells were chemically transformed with pQE30/PfHsp70-z (Appendix A4; A5; Zininga *et al*., 2015a). Competent *E. coli* XL1 Blue cells where chemically transformed with either pQE30/PfHsp70-1 or pQE30/PfHsp70-1_{NDB} (Appendix A.4; A5; Shonhai *et al*., 2008; Zininga *et al*., 2014b). The colonies carrying the plasmids were respectively grown for 12 hours in 50 ml 2X yeast/tryptone (2YT) (tryptone 16 g/L, yeast extract 10 g/L and NaCl 5 g/L) broth containing 100 µg/ml ampicillin at 30 °C, then

© University of Venda

subsequently diluted using 450 mL 2YT. The cells were allowed to grow at 30 °C with shaking at 160 rpm using FMH 200 shaker (FMH Electronics, RSA). At A_{600} = 0.6, the expression was induced using 1 mM isopropyl-β-D-1-thiogalactopyranoside (IPTG). After growing for more than 24 hours, the cells were harvested by centrifugation at 5000 g for 20 minutes at 4 °C and the pellet was suspended in lysis buffer (100 mM Tris–HC1, pH 7.4, 300 mM NaCl, 10 mM Imidazole containing 1 mM EDTA, 1 mM phenylmethylsulfonyl fluoride (PMSF) and 1 mg/ml lysozyme) at 23°C for 1 hour. The cell lysates were kept at -80 °C for storage. Protein expression samples were analyzed using 12 % sodium dodecyl sulfate-polyacrylamide gel electrophoresis (SDS-PAGE) and visualised by Coomassie blue (Appendix A6). The production of the His_6-tagged recombinant protein was confirmed by Western analysis using mouse monoclonal anti-His_6-horseradish peroxidase antibodies (α-His) [1 : 2000 dilution] (Sigma-Aldrich, U.S.A). The production of recombinant proteins was confirmed by Western blot (Appendix A.7) using rabbit-raised polyclonal anti-PfHsp70-z (α-PfHsp70-z) [1 : 2000 dilution] as primary antibody for PfHsp70-z. PfHsp70-1 was confirmed using anti-PfHsp70-1 (α-PfHsp70-1) [1: 2000 dilution] as primary antibody for full length and truncated PfHsp70-$1N_{BD}$. The secondary antibody used was goat raised anti-rabbit horseradish peroxidase conjugated antibody (1: 5000 dilution). Imaging of the protein bands on the Western blot was conducted using the ECL kit (Thermoscientific, USA) as per manufacturer's instructions (Appendix A8). Images were captured using ChemiDoc Imaging system (Bio-Rad, USA).

3.2.5 Purification of recombinant proteins

The harvested JM109 and XL1 Blue *E. coli* cells stored at – 80 °C were retrieved and allowed to thaw on ice for one hour. Nucleic acids were precipitated by addition of 0.1 % (w/v) Poly (ethyleneimine) (PEI). The cell lysate was then centrifuged at 5000 g for 20 minutes at 4°C. The supernatant was loaded onto a HisPur™ Nickel-charged nitrilotriacetic acid (Ni-NTA) (ThermoScientific) immobilized metal affinity chromatography column (IMAC) to allow His_6-PfHsp70-z/PfHsp70-1/PfHsp70-1_{NBD} in the soluble cell extract to bind to HisPur™ Ni-NTA at 4°C for four hours. The HisPur™ Ni-NTA IMAC column was then washed using wash buffer

© University of Venda

(100 mM Tris-HCl, pH 7.4, 300 mM NaCl, 25 mM Imidazole, 1 mM EDTA containing 1 mm PMSF). The bound protein was eluted using elution buffer (100 mM Tris-HCl, pH 7.4, 300 mM NaCl, 500 mM Imidazole, 1 mM EDTA, and containing 1 mM PMSF). The protein was extensively dialysed using SnakeSkin tubing 10 000 MWCO (ThermoScientific) in dialysis buffer (100 mM Tris-HCl, pH 7.4, 300 mM NaCl, 10 mM Imidazole, 10 % (v/v) glycerol, containing 1 mM PMSF) and storage buffer buffer (10 mM Tris-HCl, pH 7.4, 150 mM NaCl, 10 % (v/v) glycerol, containing 1 mM PMSF). The purity of the eluted protein was assessed using SDS-PAGE and further confirmed by Western blotting as previously described (section 3.2.5). To validate that the purified PfHsp70-z protein was not contaminated with traces of *E. coli* Hsp70 (DnaK), the protein preparations were probed by Western blotting using α-DnaK antibodies (Stressgen, Germany). The protein was subsequently concentrated with polyethylene glycol. Protein concentrations were estimated by Bradford assay (Sigma-Aldrich) following manufacturer's instructions using bovine serum albumin as protein standard (Appendix A9). The protein concentrations were further confirmed by using the christoph-leidig equation (Appendix A10).

3.2.6 Investigation of the secondary structural organisation of PfHsp70-z

The secondary structure of recombinant PfHsp70-z was analysed using Far-UV circular dichroism (CD). CD spectroscopy experiments were performed using a J-1500 CD spectrometer (JASCO Ltd, UK) equipped with a Peltier temperature controller. PfHsp70-z recombinant protein (0.2 µM) was suspended in 20mM Tris-HCl pH 7.4, 100mM sodium fluoride buffer and analysed using a 0.1 cm path-length quartz cuvette (Hellma). Spectra were averaged for least 15 scans after baseline correction (subtraction of spectrum from buffer in which PfHsp70-z protein was excluded). The CD measurements were normalised to protein concentration and presented as molar ellipticity, (θ) deg.cm^2.dmol^{-1} (Appendix A11). Secondary structure predictions were conducted on the observed CD spectrum at constant temperature set at 19 °C. The spectra were deconvulted to α-helix, β-sheet, β- turn and

© University of Venda

unordered regions, using the Dichroweb server, (http://dichroweb.cryst.bbk.ac.uk) (Sreerama and Woody, 2000; Whitmore and Wallace, 2008).

The effect of heat and urea on PfHsp70-z was investigated, as thermal and chemical denaturants, respectively. The secondary structure of the protein was monitored at 222 nm as the temperature was raised monotonically initially from 19 °C to 65 °C at a rate of 0.5 °C per min. The temperature was restored to 19°C. The experiment was repeated, this time the temperature was raised from 19 °C to 95 °C at a rate of 0.5 °C. The folded state of the PfHsp70-z protein at any given temperature was determined as follows (Misra and Ramachandran, 2009):

$((\theta)_t - (\theta)_h) / ((\theta)_l - (\theta)_h)$ Equation 1

Where $(\theta)_t$ is the molar ellipticity at any given temperature, $(\theta)_h$ at highest temperature, and $(\theta)_l$ at lowest temperature, respectively. The effects of urea on the stability of PfHsp70-z was monitored by assessing the molar residue ellipticity at 222 nm, with temperature set at 19 °C in the absence and presence of varying urea concentration (1 M to 10 M). The folded state of PfHsp70-z protein exposed to various levels of urea was calculated using the Equation 1, described above by substituting the respective urea concentrations for the temperature values.

3.2.7 Investigation of the tertiary structural organisation of PfHsp70-z

Further to the assessment of secondary structure using CD, the tertiary structural organisation of PfHsp70-z proteins was assessed using tryptophan fluorescence. This was conducted by monitoring the changes in tertiary structure of the protein that was subjected to urea denaturation by conducting tryptophan fluorescence based analysis. The recombinant PfHsp70-z protein (0.45 µg/ml) was incubated in assay buffer A (25 mM HEPES-KOH pH 7.5, 100 mM KCl, 10 mM MgOAc) for 20 minutes at 20°C in the presence of the variable urea concentrations (1 M- 8 M). Fluorescence spectra were recorded between 320 nm and 450 nm

© University of Venda

after initial excitation at 295 nm using JASCO FP-6300 spectrofluorometer (JASCO, Tokyo, JAPAN).

3.2.8 Assessment of the capability of PfHsp70-z to form higher order oligomers

The capability of PfHsp70-z molecules to self-associate was conducted using a Proteon XPR36 (BioRad, USA) surface plasmon resonance (SPR) machine. The assays were conducted at room temperature (25 °C), filter sterilised and degassed PBS-Tween (10 mM Phosphate, 137 mM NaCl, 3 mM KCl, 0.005 % (v/v) Tween 20 and 20 mM EDTA; pH 7.4) was used as running buffer. The immobilisation of ligand was achieved through covalent attachment to the modified alginate polymer layer on the GLC sensor chip via amine coupling following a protocol that was provided by the manufacturer (BioRad, USA) (Appendix A12; B4; B5; B6). PfHsp70-z (as ligand) was immobilised at concentrations of 0.5 µg/mL and 1 µg/mL. At these concentrations 187 response units (RU) was achieved for PfHsp70-z per immobilization surface (Moriaty, 2010). As analytes aliquots of PfHsp70-z and BSA (as negative control) were prepared at final concentration of 2000 nM, 1000 nM, 500 nM, 250 nM, and 125 nM and were injected at 50 µl/min into each horizontal channel at a rate of 50µl/min. The analysis was conducted in the absence or presence of 5 mM of either ATP or ADP. Association was allowed for 2 minutes, dissociation was monitored for 8 minutes. The SPR sensorgrams for dimerization were fit to a simple Langmuir kinetic binding model to calculate the association rate constant (k_a in the unit of $M^{-1}s^{-1}$), dissociation rate constant (k_d in the unit of s^{-1}) and the equilibrium constant (K_D in the unit of M). Data analysis was contacted after subtraction of the baseline RU (Buffer with ATP/ADP with BSA and without analyte protein). Association rate constant, dissociation rate constant and equilibrium constant data was processed and analysed using ProteOn Manager™ software version 3.1.0.6 by concatenating the responses of all five analyte concentrations (O'Shannessy *et al*., 1993).

© University of Venda

3.2.9 Investigation of ATPase activity of PfHsp70-z

The ATPase activity of PfHsp70-z was determined by quantifying the amount of released inorganic phosphate based on a previously described approach (Matambo *et al*., 2004) with modifications. Briefly, 0.4 µMPfHsp70-z was incubated for five minutes in buffer HKMD (10 mM HEPES-KOH pH 7.5, 100 mM KCl, 2 mM $MgCl_2$, 0.5 mM DTT). The reaction was started by addition of ATP and samples were collected after every 30 minutes for four hours and reaction was stopped with 10% (w/v) SDS and using 1.25 (w/v) % ammonium molybdate in 6.5 % H_2SO_4 and 9 % (w/v) ascorbic acid to quantitate the release of inorganic phosphate. The reaction mix without the protein was used as a non-enzymatic control. Samples were read at 660nm using SpectraMax M3 spectrometer (Molecular Devices, U.S.A). The absorbance values were extrapolated against a standard calibration curve using Na_2HPO_4 as standard (Appendix B7). The basal ATPase activity was expressed as nmol Pi released/min/mg of recombinant protein. Kinetic plots for the ATPase activities of PfHsp70-z and PfHsp70-1 were determined by generating Michaelis–Menten plots using GraphPad Prism 6.05. At least three independent batches of recombinant protein were used in separate experiments.

© University of Venda

Production of Recombinant PfHsp70-z Protein and Analysis of its Secondary and Tertiary Structures

3.3 Results

3.3.1 Confirmation of the pQE30/PfHsp70-z plasmid

The integrity of pQE30/PfHsp70-z plasmid construct was verified by sequencing and restriction digest (Figure 3.1). Restriction with either *Bam*HI or *Hind*III resulted in linearised plasmid that migrated at 6046 bp (Figure 3.1B). Double digestion using *Bam*HI and *Hind*III resulted in fragments of 3419bp and 2627bp, corresponding to the pQE30 expression vector and PfHsp70-z insert sizes, respectively (Figure 3.1B).

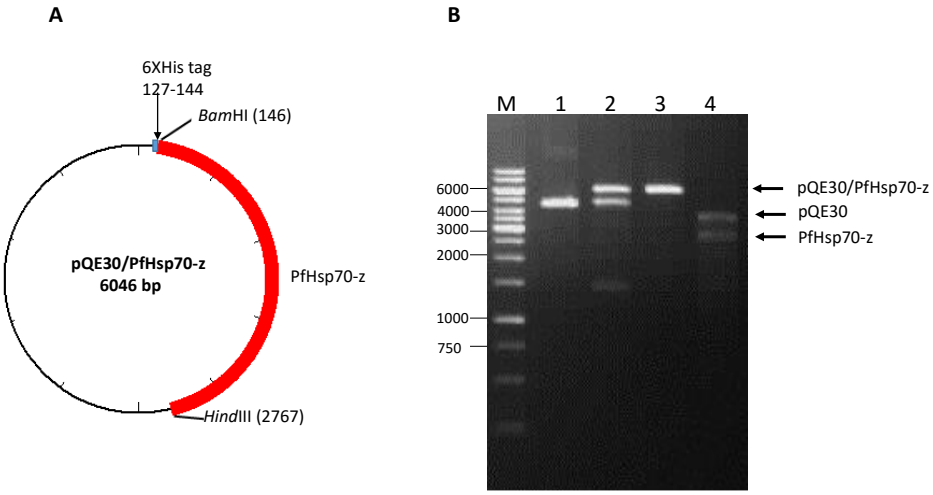

Figure 3.1: pQE30/PfHsp70-z plasmid map and restriction agarose gel

Restriction analysis of pQE30/PfHsp70-z DNA plasmid (**A**) Plasmid map of pQE30/PfHsp70-z showing the *Bam*HI and *Hind*III restriction sites. (**B**) Agarose gel electrophoresis of pQE30/PfHsp70-z: lane M, DNA molecular weight maker in bp; lane 1, undigested pQE30/PfHsp70-z plasmid; lane 2, pQE30/PfHsp70-z digested with *Bam*HI; lane 3, pQE30/PfHsp70-z digested with *Hind*III; lane 4, pQE30/PfHsp70-z digested with both *Bam*HI and *Hind*III.

3.3.2 Confirmation of pQE30/PfHsp70-1 plasmid

The integrity of pQE30/PfHsp70-1 was verified by restriction digest using *Bam*HI and *Hind*III (Figure 3.2; Matambo *et al*., 2004). Single restriction site digestion with either *Bam*HI or *Hind*III resulted in the migration of linearised plasmid of 5471bp (Figure 3.2B). Double digestion using *Bam*HI and *Hind*III excised the PfHsp70-1 coding sequence (2627bp) resulting in fragments of 3419bp and 2052bp, corresponding to the pQE30 expression vector and PfHsp70-1 insert sizes, respectively (Figure 3.2B).

© University of Venda

Production of Recombinant PfHsp70-z Protein and Analysis of its Secondary and Tertiary Structures

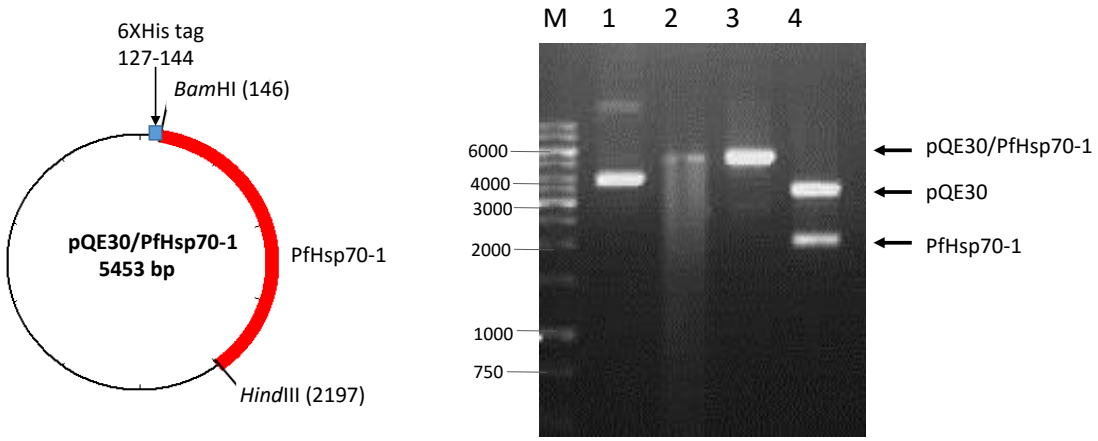

Figure 3.2: pQE30/PfHsp70-1 plasmid map and restriction agarose gel

Restriction analysis of pQE30/PfHsp70-1 DNA plasmid (**A**) Plasmid map of pQE30/PfHsp70-1 showing the *Bam*HI and *Hind*III restriction sites. (**B**) Agarose gel electrophoresis of pQE30/PfHsp70-1: lane M, DNA molecular weight maker; lane 1, undigested pQE30/PfHsp70-1 plasmid; lane 2, pQE30/PfHsp70-1 digested with *Bam*HI; lane 3, pQE30/PfHsp70-1 digested with *Hind*III; lane 4, pQE30/PfHsp70-1 digested with *Bam*HI and *Hind*III.

3.3.3 Confirmation of pQE30/PfHsp70-1_{NBD} plasmid

The plasmid with the truncated version of PfHsp70-1 expressing the nucleotide binding domain pQE30/PfHsp70-1_{NBD} (Zininga *et al*., 2015b) was verified by restriction analysis. Restriction enzymes *Bam*HI and *Spe*I were used for restriction analysis to confirm the integrity of the pQE30/PfHsp70-1_{NBD} (Figure 3.3 B).

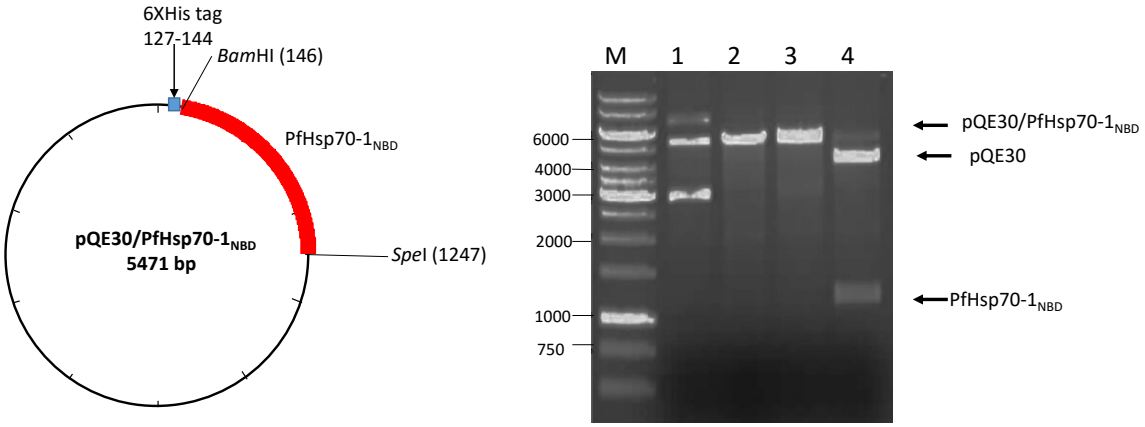

Figure 3.3: pQE30/PfHsp70-1_{NBD} plasmid map and restriction agarose gel

Restriction analysis of pQE30/PfHsp70-1_{NBD} DNA plasmid (**A**) Plasmid map of pQE30/PfHsp70-1_{NBD} showing the *Bam*HI and *Spe*I restriction sites. (**B**) Agarose gel electrophoresis of pQE30/PfHsp70-1_{NBD}: lane M, DNA molecular weight maker; lane 1, undigested pQE30/PfHsp70-1_{NBD} plasmid; lane 2, pQE30/PfHsp70-1_{NBD} digested with *Bam*HI; lane 3, pQE30/PfHsp70-1_{NBD} digested with *Spe*I; lane 4, pQE30/PfHsp70-1 digested with *Bam*HI and *Spe*I.

© University of Venda

Digestion with either *Bam*HI or *Spe*I resulted in the linearised plasmid of 5471bp (Figure 3.3 B). The PfHsp70-1_{NBD} construct (1201bp), was confirmed by digesting the plasmid with both *Bam*HI and *Spe*I, which resulted in the DNA fragments of 4270bp and 1201bp (Figure 3.3 B).

3.3.4 Overexpression and purification of recombinant PfHsp70-z protein

Recombinant PfHsp70-z protein was successfully expressed in JM109 *E. coli* cells (Figure 3.4A). The PfHsp70-z production was analysed by SDS-PAGE and and confirmed by Western blot analysis using α-PfHsp70-z. SDS analysis of the samples retrieved during expression showed an increase in the level of expression of a species at approximately 100 kDa size. The control confirmed the absence of 100 kDa species in untransformed JM109 *E. coli* cells (Figure 3.4A). This suggests that the 100 kDa species were recombinant PfHsp70-z protein and this was confirmed by Western blot. The same 100 kDa species was detected from cells prior to induction (Figure 3.4A) indicating leak expression of the protein. The expression was successfully induced with IPTG (Figure 3.4A). Western analysis confirmed the leaky expression and shown some bands below 70kDa which are possibly breakdown products as their intensity increased in the overnight sample (Figure 3.4A).

PfHsp70-z expressed was purified by affinity chromatography (Figure 3.4B). Before purification it was important to investigate protein solubility the pellet and soluble fractions were analysed. The 100 kDa band in the soluble fraction was thicker than in the pellet fraction (Figure 3.4B). This suggests that recombinant PfHsp70-z protein was soluble and it was loaded on to the IMAC. Some of the PfHsp70-z protein was lost during washes (Figure 3.4B lane W). PfHsp70-z was eluted as a species of approximately 100 kDa (Figure 3.4B). Purifications of PfHsp70-z resulted in a final protein yield of approximately 9.0 µg/L of protein. However, a band running approximately above 200 kDa was also observed which was recognised by both α-His and α-PfHsp70-z antibodies. It was surmised that this band possibly represented a dimer form of PfHsp70-z (section 3.3.10). The purity of the eluted protein was further validated by probing using α-DnaK antibodies and confirmed the assessment that the eluted PfHsp70-z protein was free from DnaK contamination (Figure 3.4B).

© University of Venda

Production of Recombinant PfHsp70-z Protein and Analysis of its Secondary and Tertiary Structures

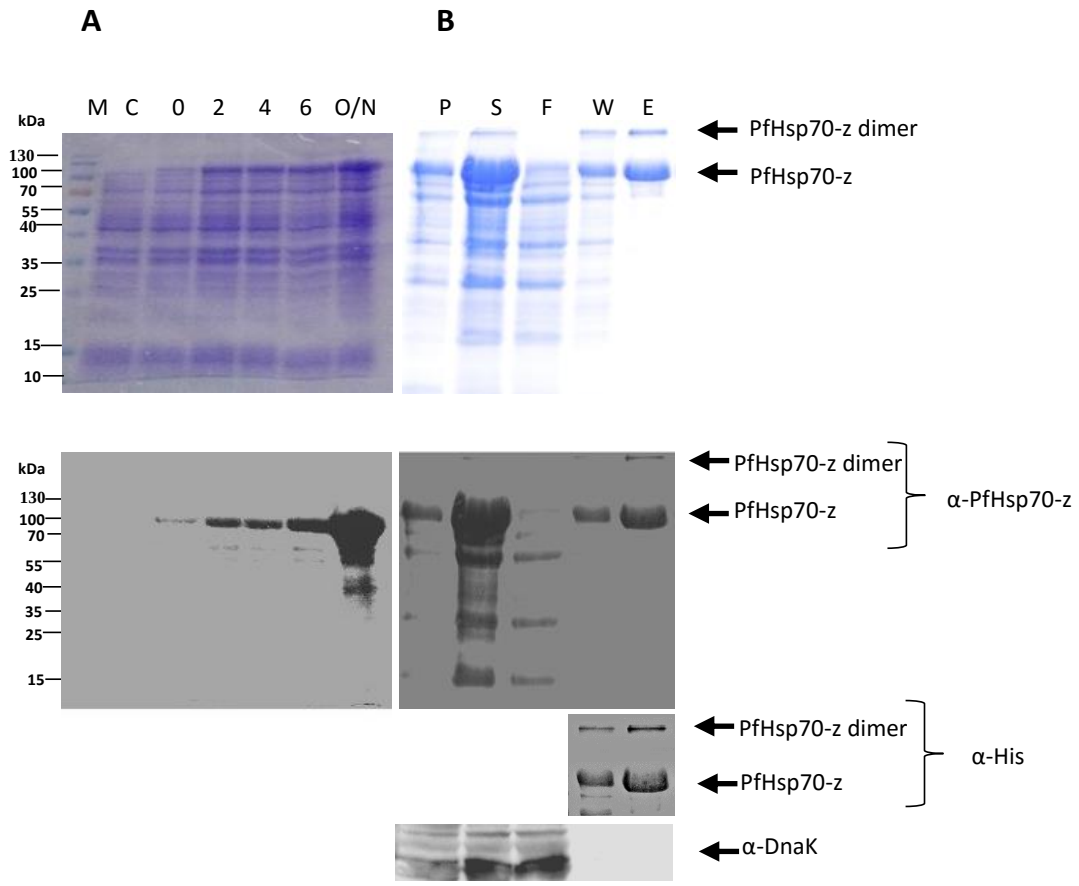

Figure 3.4: Expression and purification of recombinant PfHsp70-z
PfHsp70-z was expressed in *E. coli* JM109 cells transformed with pQE30/PfHsp70-z. SDS-PAGE (12%) and Western analyses of the expression (A) and purification (B) of recombinant PfHsp70-z; lane M–Page ruler (Thermo Scientific) in kDa; lane C—Total extract for cells transformed with a neat pQE30 plasmid; lane 0 –total cell extract transformed with pQE30/PfHsp70-z prior to IPTG induction; lanes 2, 4, 6, O/N–total cell lysate obtained 2, 4, 6 and 16 h post induction, respectively. Lane P, S-pellet and soluble fractions obtained from the total lysate for cells transformed with pQE30/PfHsp70-z, respectively; lane F; flow through; lane W —wash samples, and lane E—PfHsp70-z protein eluted using 500 mM imidazole. Lower panels: Western blot based on use of α-PfHsp70-z and α-His antibodies confirming expression and purification of PfHsp70-z protein. To confirm the purity of PfHsp70-z from DnaK contamination, Western blotting was conducted using α-DnaK antibodies.

3.3.5 Overexpression and purification of recombinant PfHsp70-1 protein

The recombinant form of PfHsp70-1 protein was expressed and purified using previously described protocols (Shonhai *et al*., 2008). Full length PfHsp70-1 represented by a species of 74 kDa on SDS-PAGE analysis was over-expressed (Figure 3.5A) and purified from *E. coli* XL1-Blue cells (Figure 3.5B). Western blotting analysis using antibodies raised against PfHsp70-1 as well as antibodies that recognize the polyhistidine tag, detected PfHsp70-1 (Figure 3.5). The cells started expressing PfHsp70-1 before induction (Figure 3.5A) suggesting leaky

© University of Venda

expression. The cells were able to produce more protein post-induction (Figure 3.5A), with optimum production at 16 hours (Figure 3.5A). Breakdown products of PfHsp70-1 were detected represented by bands of smaller species of 35 kDa, 50 kDa and 60 kDa observed in samples representing protein expression (Figure 3.5A). PfHsp70-1 was purified natively using affinity chromatography (Figure 3.5B).

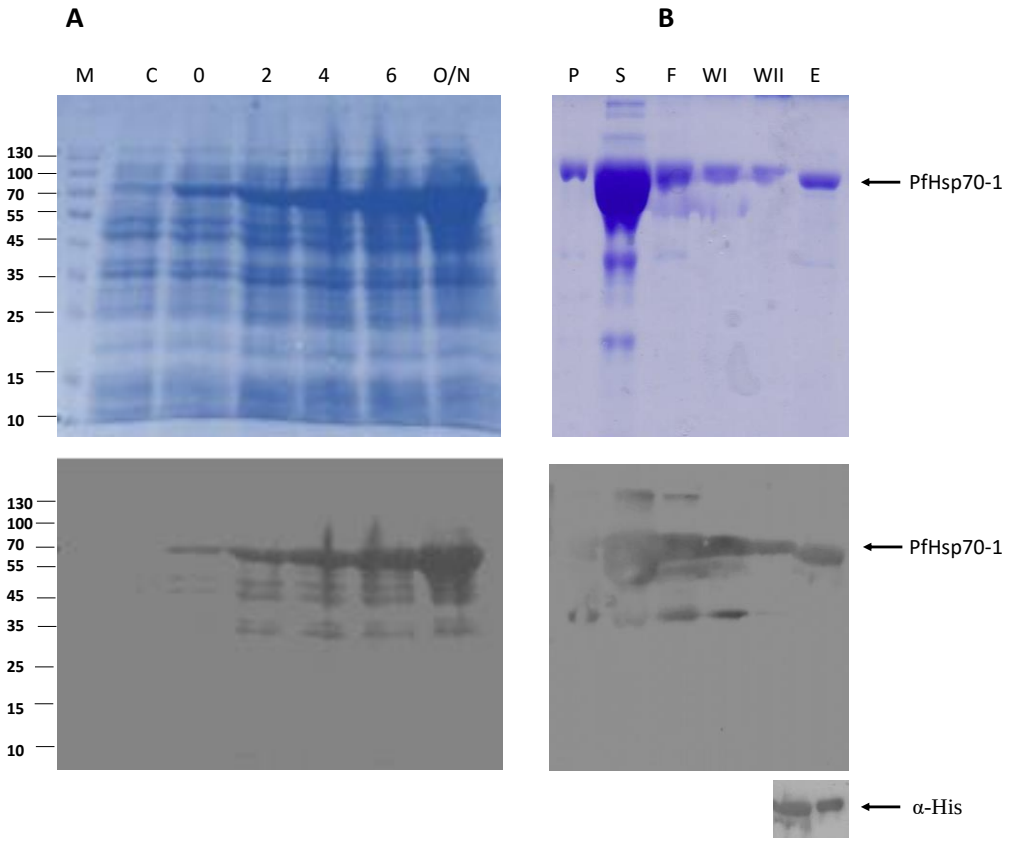

Figure 3.5: Expression and purification of recombinant PfHsp70-1 protein
PfHsp70-1 was expressed in *E. coli* XL1 Blue cells transformed with pQE30/PfHsp70-1. SDS-PAGE (12 %) and Western analyses of **(A)** the expression of recombinant PfHsp70-1, **(B)** the purification of PfHsp70-1. Lane M – Page ruler (Thermo Scientific) in kDa is shown on the left hand side; lane C - the total extract for cells transformed with a neat pQE30 plasmid; lane 0 – total cell extract transformed with pQE30/PfHsp70-1; pQE30/PfHsp70-1_{NBD} prior to IPTG induction; lanes 2, 4, 6, O/N – total cell lysate obtained 2, 4, 6 hours and overnight post induction. Lane P, S-pellet and soluble fractions obtained from the total lysate for cells transformed with pQE30/PfHsp70-1, respectively; lane F; flow through; lane W —wash samples, and lane E— PfHsp70-z protein eluted using 500 mM imidazole. lane E - protein eluted using 500 mM imidazole. *Lower panels*: Western blot confirming expression, purification of PfHsp70-1 based on using α-PfHsp70-1 and α-His antibodies.

Comparison of PfHsp70-1 pellet and soluble fraction (Figure 3.5B) suggests that PfHsp70-1 existed more in the soluble fraction than in the pellet fraction. A significant amount of

© University of Venda

recombinant PfHsp70-1 protein was lost in the flow through (Figure 3.5B) and during the wash steps (Figure 3.5B). Upon purification of PfHsp70-1_{NBD} a yield of approximately 7.0 µg/L protein was obtained.

3.3.6 Overexpression and purification of recombinant PfHsp70-1_{NBD} protein

The truncated PfHsp70-1 (PfHsp70-1_{NBD}) was over expressed and purified from *E. coli* XL1 Blue cells. Western blotting analysis using antibodies raised against PfHsp70-1 as well as antibodies that recognize the polyhistidine tag detected the PfHsp70-1_{NBD}.

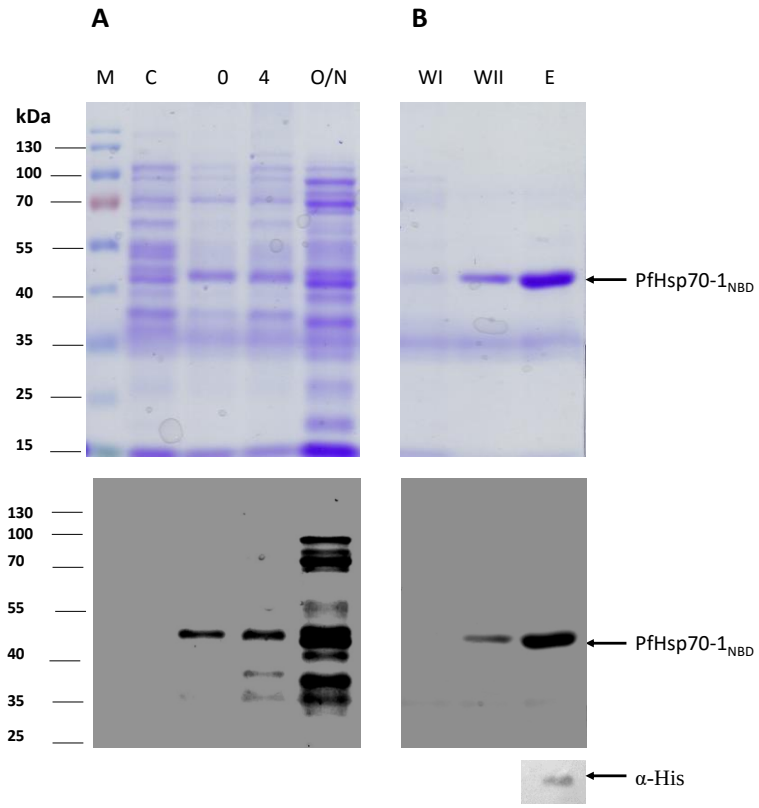

Figure 3.6: Expression and purification of recombinant PfHsp70-1_{NBD} protein
PfHsp70-1_{NBD} was expressed in *E. coli* XL1 Blue cells transformed with pQE30/PfHsp70-1_{NBD}. SDS-PAGE (12 %) and Western analyses of **(A)** the expression of recombinant PfHsp70-1_{NBD}, **(B)** the purification of PfHsp70-1_{NBD}. Lane M – Page ruler (Thermo Scientific) in kDa is shown on the left hand side; lane C - the total extract for cells transformed with a neat pQE30 plasmid; lane 0 – total cell extract transformed with pQE30/PfHsp70-1_{NBD} prior to IPTG induction; lanes 4, O/N – total cell lysate obtained 4 hours and overnight post induction; and lane WI/II- wash samples and lane E - protein eluted using 500 mM imidazole. *Lower panels*: Western blot based on use of α-PfHsp70-1 and α-His confirming expression, purification of PfHsp70-1_{NBD}.

© University of Venda

Production of Recombinant PfHsp70-z Protein and Analysis of its Secondary and Tertiary Structures

The production of PfHsp70-1_{NBD} as a species of 45 kDa was confirmed by SDS-PAGE analysis (Figure 3.6A) and Western blotting (Figure 3.6B). Before IPTG induction, a 45 kDa protein band appearing to represent PfHsp70-1_{NBD} was observed (Figure 3.6A). This suggests leaky expression. However, upon adding IPTG, the cells were able to express PfHsp70-1_{NBD} after 16 hour post induction, after which they were harvested (Figure 3.6A). PfHsp70-1_{NBD} was purified natively using affinity chromatography (Figure 3.6B). Purification of PfHsp70-1_{NBD} resulted in a final yield of approximately 8.0 μg/L of protein.

3.3.7 Secondary structural analysis of PfHsp70-z

To confirm the secondary structure of PfHsp70-z and to investigate the effect of heat stress on its stability, CD spectrophotometric analysis was conducted. The recorded signals (experimental) between 190 nm and 260 nm were superimposed to predicted signals obtained using Dichroweb (Figure 3.7A). The correlation between the two signals that were resolved using the CDSSTR method gave NRMSD values of approximately 0.002, representing a good correlation. The far UV spectra exhibited a positive peak centred at 194 nM and two negative depressions (trough) at 209 and 221 nM, respectively (Figure 3.7A). This spectrum represents the helical character of the recombinant protein. The deconvolution of the CD spectra revealed that full length PfHsp70-z is predominantly composed of α-helices (62 %), followed by β-strands (16 %), β-turns (8 %) and unordered (14 %). The CD spectra measurements were repeated whilst heating the protein to 95 °C (Figure 3.7B), in order to determine if the protein structure is perturbed by temperature changes. Secondary structure stability was subsequently monitored at 221 nm, as the protein was partially heated to 65 °C (Figure 3.7C). The temperature was subsequently restored to 19 °C, allowing the protein to revert to its initial spectral molar residue ellipticity level (Figure 3.7C). On the other hand, when the temperature was raised to 95 °C, the protein failed to regain its original molar residue ellipticity secondary structure (Figure 3.7C). Attempts to refold the protein by reducing the temperature to 19 °C subsequently after heating the protein to 95 °C the protein, failed to refold to its initial molar residue ellipticity level (Figure 3.7C).

© University of Venda

Production of Recombinant PfHsp70-z Protein and Analysis of its Secondary and Tertiary Structures

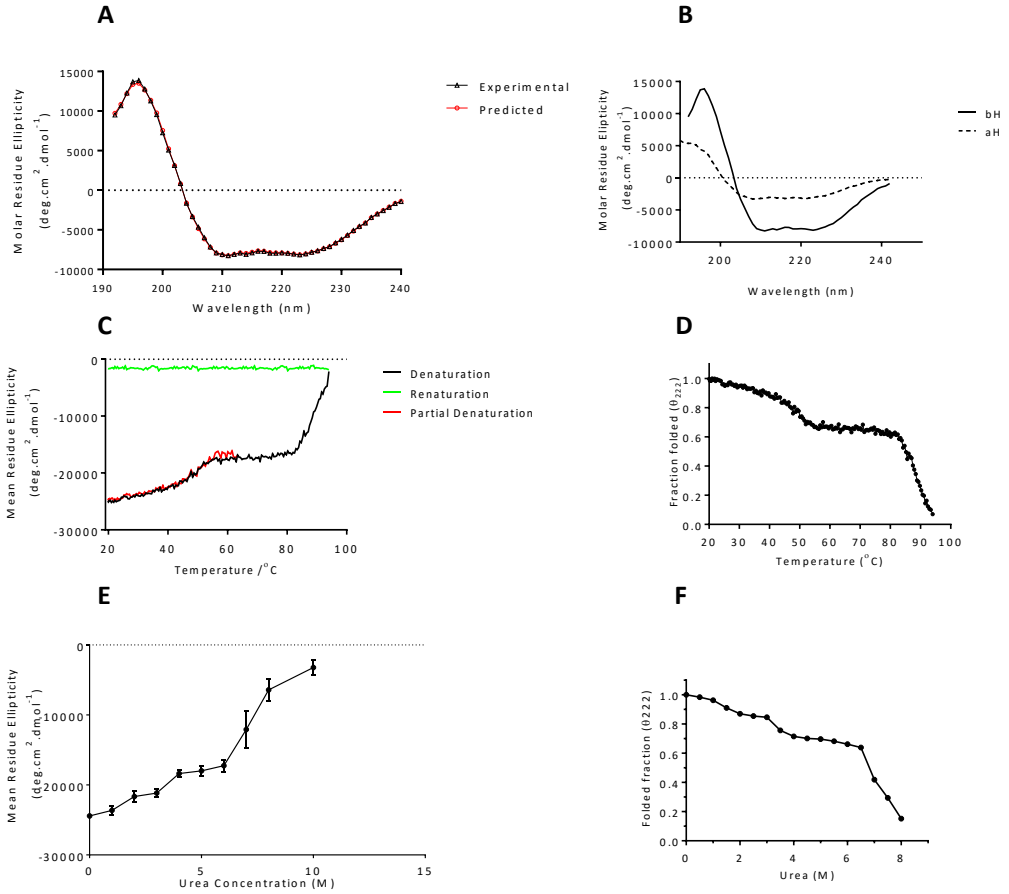

Figure 3.7: Analysis of the secondary structure of PfHsp70-z by circular dichroism
The experimental and predicted CD spectra (using DICHROWEB with CDSSTR as the reference database 4, NRMSD: 0.002) (**A**). The CD spectrum of PfHsp70z was presented as molar residue ellipticity (deg.cm^{2}dmol^{-1}). Assessment of the heat stability of PfHsp70z on the CD spectra (**B**). The temperature was raised from 19 °C to 65 °C, resulting in partial unfolding of PfHsp70z (**C**; **partial denaturation**) and protein was allowed to refold as the temperature was restored back to 19 °C (**C**; **renaturation**). Denaturation of PfHsp70z by raising the temperature above 95 °C permanently abrogated the secondary structure of the protein (**C**, **Denaturation**). The folded fraction of the protein under varying temperatures was calculated using equation 1 (**D**). The secondary structure was also monitored in the presence of varying urea concentration (**E**) and the folded fraction of urea exposed protein was calculated using Equation 1 (**F**) (Zininga *et al.*, 2015a).

The folded fraction assessment of recombinant PfHsp70-z protein showed that more than 60 % of the protein still maintaining its folded state at 80 °C (Figure 3.7D). In a separate experiment, the secondary structure of PfHsp70z was monitored at 221 nm as urea concentration was increased to 10 M (Figure 3.7E). The protein was fairly stable in the presence of up to 6 M urea (Figure 3.7E). Upon increasing the concentration of urea beyond this level, PfHsp70z irreversibly lost its secondary structure (Figure 3.7E). Assessments of the

© University of Venda

folded fraction showed that 60 % of the protein maintained a folded state in the presence of up to 6 M urea (Figure 3.7F). This further demonstrated that the structural conformation of PfHsp70-z was perturbed by urea in a concentration dependent fashion (Figure 3.7E; F).

3.3.8: Tertiary structural organisation of PfHsp70-z

The tertiary structure of PfHsp70-z was evaluated using tryptophan based fluorescence analysis of the protein in the presence of variable levels of urea and variable temperature (Figure 3.8). The tryptophan fluorescence was monitored over different experimental setups. The spectrum reduced in intensity as temperature was raised. This suggests that the tryptophan fluorescence was quenched as the temperature was raised observed as a decrease in relative fluorescence intensity (Figure 3.8A). Analysis of the changes in tryptophan fluorescence peak showed a change in the peak wavelength in response to temperature increase. This change was observed to be following a red shift of fluorescence peak in response to temperature increase (Figure 3.8B). PfHsp70-z tertiary structure assessment in response to increasing urea concentration showed that the tryptophan fluorescence signal decreased with an increase in urea concentration. This suggests quenching of the relative fluorescence dependent on urea concentration (Figure 3.8C). The tryptophan fluorescence changes registered a red shift of emission with maximum peak at 350 nm corresponding to urea concentration of 6.5 M (Figure 3.8D). This finding mirrors the observation that was made by assessing the perturbation of the secondary structure of the protein in response to urea treatment (Figure 3.7E; F).

© University of Venda

Production of Recombinant PfHsp70-z Protein and Analysis of its Secondary and Tertiary Structures

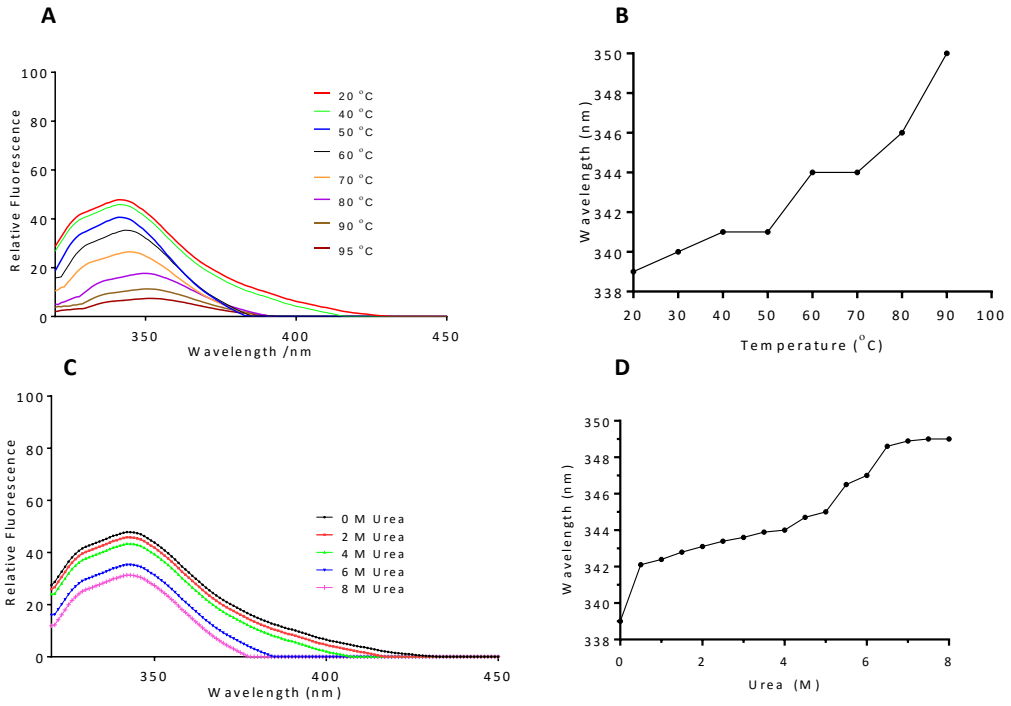

Figure 3.8: Analysis of the tertiary structure of PfHsp70-z by tryptophan fluorescence
The fluorescence emission spectra was monitored at 320 - 450 nm after an initial excitation at 295 nm. The protein tryptophan fluorescence emission spectra was recorded for PfHsp70-z protein exposed to various temperatures (**A**) to assess the effect of temperature on the emission spectra. Assessment of the red shift of PfHsp70z exposed to different temperature on the emission spectra (**B**). The recombinant Pfhsp70-z protein tryptophan fluorescence emission spectra was also recorded under various urea concentrations (**C**). Assessment of the red shift of PfHsp70z exposed to different urea concentrations on the emission spectra (**D**) (Zininga *et al.*, 2015a).

3.3.9 Assessment of the ATPase activity of PfHsp70-z

The basal ATPase activities of both PfHsp70-z and PfHsp70-1 were determined using a colorimetric assay measuring the rate of inorganic phosphate released during ATP hydrolysis (Matambo *et al.*, 2004). The assay was conducted under variable initial ATP concentrations (up to 1500 µM). The Michaelis-Menten plots were generated for at least three independent batches of PfHsp70-z and PfHsp70-1 (Figure 3.9). The turnover rate of PfHsp70-z reported is comparable to that of PfHsp70-1 (Figure 3.9; Table 3. 2); both of which are within the same range as that reported for PfHsp70-1 based on a previous independent study (Matambo *et al.*, 2004; Table 3.2). PfHsp70-z exhibited a lower K_M value (283 µM) compared to that of PfHsp70-1 (428 µM) suggesting that PfHsp70-z has higher affinity for ATP than PfHsp70-1. In

© University of Venda

addition, the catalytic efficiency (K_{cat}/k_M) of PfHsp70-z was nearly two-fold higher than that of PfHsp70-1 (Table 3.2).

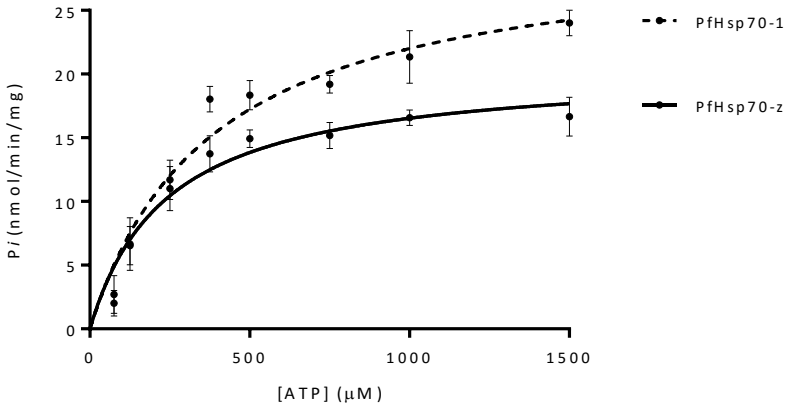

Figure 3.9: PfHsp70-z exhibits intrinsic ATPase activity
Analysis of the basal ATPase activities of PfHsp70-z and PfHsp70-1 and P*i* released was monitored at 595 nm using a direct colorimetric assay.

Table 3.2: Data for kinetics of the ATPase activities of PfHsp70-z and PfHsp70-1

Protein	V_{max} (nmol/min/mg)	K_M (µM)	K_{cat} (mol^{-1})	K_{cat}/K_M	Reference
PfHsp70-z	19.8 (+/- 0.5)	283 (+/-3)	1.9	6.71 E -03	This study
PfHsp70-1	24.6 (+/- 0.8)	428 (+/- 5)	1.6	3.73 E -03	This study
PfHsp70-1	14.6	616.5	1.03	1.67 E -03	Matambo *et al*., 2004

Table 3.2 legends: Values for the V_{max} – the ‚maximum rate of the catalysis reaction; K_M - is the substrate concentration at which the reaction rate is at half-maximum, k_{cat} - is the maximum number of substrate molecules converted to product per enzyme molecule per second; K_{cat}/K_M is the catalytic efficiency were determined as shown. Standard deviations shown represent at least three independent assessment made using separate protein batches.

3.3.10 PfHsp70-z forms higher order oligomers

The purified recombinant PfHsp70-z appeared both as a 100 kDa monomer and a species of approximately 200 kDa based on SDS-PAGE and Western blot analyses (Figure 3.4B). It was speculated that the band representing the species of approximately 200 kDa was that of a detergent resistant PfHsp70-z dimer. To further validate the oligomeric status of PfHsp70-z, SPR analysis was conducted. The SPR raw data (Figure 3.10) were analysed by applying the

© University of Venda

Langmuir kinetic model (Figure 3.10), to generate the k_a, k_d and K_D values for the various SPR sensorgrams (Figure 3.10; Table 3.3).

The ability of PfHsp70-z immobilized on the chip surface to interact with PfHsp70-z in solution was analysed. SPR sensorgrams for specific interactions should show concentration dependence response. Based on the SPR analysis, PfHsp70-z (ligand) associated with its analyte form to generate higher order oligomers in a concentration dependent fashion (Figure 3.10A). The concentration dependence of the association response units suggests that the association was specific. Furthermore, BSA used as a control showed no concentration dependent response when BSA was injected over the immobilised PfHsp70-z. In addition, this association occurred in the absence of a nucleotide (Figure 3.10A) and presence of nucleotides ATP (Figure 3.10B) and ADP (Figure 3.10C) inhibited the association by one order of magnitude when compared to absence of (Table 3.3). Taken together, this suggests that the presence of nucleotides ATP/ADP slightly inhibited self-association of PfHsp70-z forming higher order oligomers.

The fact that this association occurs at nanomolar range (Table 3.3) suggests that the interaction is with fairly high affinity and the absence of ATP/ADP promoted the association. Overall, these findings suggest that PfHsp70-z is capable of forming stable higher order oligomers. It is likely that the protein occurs largely in dimers that are partially resistant to detergents that were resolved by SDS-PAGE and Western analyses (Figure 3.4).

© University of Venda

Production of Recombinant PfHsp70-z Protein and Analysis of its Secondary and Tertiary Structures

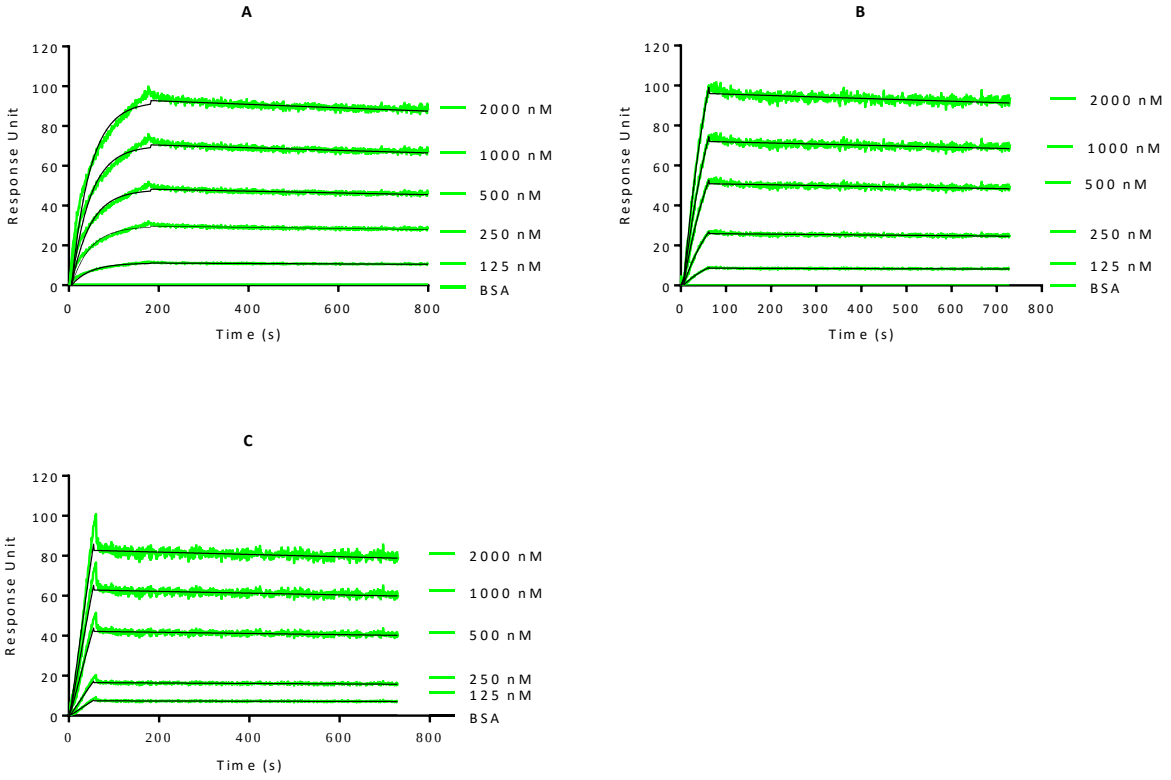

Figure 3.10: PfHsp70-z is capable of forming higher order oligomers
The SPR sensorgrams demonstrating concentration dependent association between PfHsp70-z mounted on the chip and PfHsp70-z introduced in solution. The assay was conducted in the absence of nucleotide (A); and repeated in the presence of 5 mM ATP/ADP (B)/(C), respectively. Association was allowed for 2 min, and the dissociation was monitored for 10 min. The black sensorgram represents the Langmuir kinetic model fit, and the green sensorgrams represent the raw data.

Table 3.3. Kinetics data for the oligomerization of PfHsp70-z

Analyte	Presence of Nucleotide	k_a ($M^{-1}s^{-1}$) (E+03)	k_d (s^{-1}) (E-05)	K_D (nM)	X^2	Reference
PfHsp70-z	-	12.0 (+/-0.3)	9.54 (+/-0.4)	7.97	3.06	This study
PfHsp70-z	5 mM ADP	6.62 (+/- 0.5)	7.60 (+/-0.5)	11.5	2.27	This study
PfHsp70-z	5 mM ATP	2.84 (+/-0.1)	3.20 (+/-0.1)	11.3	4.78	This study
hHsp70	-	ND	ND	4.5	ND	Marcion *et al.*, 2014

Table 1 legends: k_a association rate constant, k_d dissociation rate constant, K_D equilibrium constant, X^2 correlation for SPR sensorgram fitting to the Langmuir model, **ND** not determined. Standard deviations of at least three independent protein batches are shown in parenthesis.

© University of Venda

3.4 Discussion

The recombinant PfHsp70-z protein purified appeared both as a monomer and dimer (Figure 3.4B). SPR analysis conducted to validate that of PfHsp70-z molecules are capable of self-association (Figure 3.10). It was possible that recombinant PfHsp70-z proteins interacted as substrates and chaperone. This was highly unlikely considering that recombinant PfHsp70-z proteins were natively purified (Section 3.3.4). The formation of PfHsp70-z higher order oligomers of PfHsp70-z is nucleotide-independent (ATP/ADP) and the interaction exhibits fairly high affinity (Figure 3.10; Table 3.3). These findings are in agreement with independent studies that have suggested that canonical Hsp70 and Hsp110 homologues are capable of forming functionally important dimers (Liu and Hendrickson, 2007; Marcion *et al*., 2014). Hsp70s in dimer form has been reported to preferentially interact with Hsp40 as compared to monomer state (Marcion *et al*., 2014; Sarbeng *et al*., 2015). Oligomerization of Hsp70 highlights the importance of dimer formation in the functional cycles of these proteins. It is plausible that oligomerisation regulates PfHsp70-z function.

This study also sought to establish the secondary structure of PfHsp70-z. The protein possesses α-helix and β-sheets estimated to be 50 % - 62 %; and 10 % - 16 %, respectively (Figure 3.6 A), which correlates with the predicted structural constitution (Section 2.3.4). This is in line with reported structural constitution of its yeast Hsp110 homologue, Sse1 (Liu and Hendrickson, 2007). PfHsp70-z also possesses β-turns (8 %) and a fairly significant amount of unordered segments (14 %). As predicted the unordered segments (Figure 2.5) covering the Tedwely motif are important for protein-protein interactions. The intrinsically disordered regions on proteins have been reported to be responsible for protein-protein interactions which are transient but specific interactions (Hsu *et al*., 2012; Dyson and Wright, 2015). These findings suggest that apart from interacting with Hsp70-1 as a possible NEF, PfHsp70-z possibly interacts with other functional partners through its disordered regions.

© University of Venda

Production of Recombinant PfHsp70-z Protein and Analysis of its Secondary and Tertiary Structures

The current study findings suggest that at least 60 % of PfHsp70-z is heat stable at temperatures up to 80 °C (Figure 3.6D). The resilience of PfHsp70-z to heat stress is consistent with its possible role as a molecular chaperone as the functions of molecular chaperones is particularly important in response to the development of cellular stress. Since heat shock proteins should be able to keep other proteins in a folding competent form (Shonhai *et al*., 2007), they should themselves be heat stable. This is important as the parasite has been observed to up-regulate some of its heat shock proteins under heat stress (Oakley *et al*., 2007). Furthermore, this study established that PfHsp70-z is an ATPase (Figure 3.9). The protein demonstrated higher catalytic efficiency than PfHsp70-1 (Table 3.2). It has been reported previously that PfHsp70-z provides cytoprotection to malaria parasites by preventing the aggregation of asparagine repeats rich proteins of *P. falciparum* (Muralidharan *et al*., 2012). Taking into account that about 24 % of *P. falciparum* proteins possess asparagine rich repeats (Singh *et al*., 2004), it is not surprising that this protein is essential. Hsp110s are largely thought to act as holdases that are capable of holding client proteins in a folding competent manner under thermal stress (Goeckeler *et al*., 2002). They are thought to subsequently pass their substrates to other chaperones such as canonical Hsp70s that are capable of refolding them. It is for this reason that their ATPase subdomain is thought to be dispensable as the holdase function of Hsp70/Hsp110 chaperones is independent of ATP hydrolysis (Oh *et al*., 1999; Goeckeler *et al*., 2002). On the other hand, some studies have suggested that ATP binding may be important for their holdase function, and not necessarily ATP hydrolysis (Shaner *et al*., 2004; Hrizo *et al*., 2007). Although it remains to be established whether nucleotide binding influences the independent chaperone activity of PfHsp70-z (section 4.3.4), the current findings suggest that it is capable of hydrolysing ATP.

This study demonstrated that PfHsp70-z is a heat stable molecule that is capable of forming dimers. The optimization of the over-production of functional recombinant PfHsp70-z paves way for further biochemical analysis to establish its functions in the development of malaria parasites.

© University of Venda

CHAPTER 4

INVESTIGATION OF THE ASSOCIATION OF PFHSP70-Z WITH PFHSP70-1 AND ASSESSMENT OF ITS CHAPERONE ACTIVITY *IN VITRO*

© University of Venda

Investigation of The Association of PfHsp70-z with PfHsp70-1 and Assessment of its Chaperone Activity *in vitro*

4.1. Introduction

The current study showed that PfHsp70-z is a thermally stable molecule that possesses ATPase activity typical of canonical Hsp70s (Section 3.3.9). Hsp70s are known to play a role in protein quality control (Oh *et al*., 1999; Shonhai *et al*., 2008). PfHsp70-z has been shown to be an essential protein in parasite survival under heat stress (Muralidharan *et al*., 2012). It is plausible that, the thermal stability of PfHsp70-z during heat stress is linked to its involvement in protein quality control. A quarter of the *P. falciparum* proteome is composed of asparagine repeat rich proteins which have an increased propensity to aggregate under heat stress (Singh *et al*., 2004b). The heat stability of PfHsp70-z may enable it to deal with increased demand to minimize heat induced protein aggregation without itself aggregating. The current chapter seeks to establish the chaperone function of PfHsp70-z.

Hsp110s are implicated in nucleotide exchange of canonical Hsp70 counterparts (Dragovic *et al*., 2006). It is important to investigate whether PfHsp70-z could serve as a potential NEF of PfHsp70-1. To function as a NEF, PfHsp70-z must be able to bind and distinguish nucleotides. PfHsp70-z was established to form higher order oligomers (section 3.3.10). The formation of possible heterodimers of PfHsp70-z with PfHsp70-1, may facilitate nucleotide exchange, hence it was important to investigate the ability of PfHsp70-z to associate with PfHsp70-1. Nucleotides are known to regulate nucleotide exchange function of Hsps (Andreasson *et al*., 2008). This study thus partly sought to determine the effect of nucleotides on the possible PfHsp70-z and PfHsp70-1 association. PfHsp70-z's direct chaperone function has not been demonstrated. Its physical association with PfHsp70-1 is yet to be demonstrated.

The main objectives of this study were to:

i) Determine the nucleotide binding affinity of PfHsp70-z;

ii) Assess the effect of nucleotides on PfHsp70-z structural conformation using limited proteolysis and tryptophan fluorescence;

© University of Venda

iii) Explore the chaperone function of PfHsp70-z using MDH and luciferase aggregation assays; and

iv) Investigate the direct interaction between PfHsp70-z and PfHsp70-1.

© University of Venda

Investigation of The Association of PfHsp70-z with PfHsp70-1 and Assessment of its Chaperone Activity *in vitro*

4.2 Experimental Procedures

4.2.1 Materials

Reagents used in this study were purchased from Merck Chemicals (Darmstadt, Germany), Thermo Scientific (Illinois, USA), Zymo Research (USA), Melford (Suffolk, UK), Sigma-Aldrich (USA). The α-PfHsp70-z antibody specific for PfHsp70-z previously described (section 3.2.1; Zininga *et al*., 2015a) was used. Polyclonal rabbit raised antibodies specific for PfHsp70-1 that were previously described (section 3.2.1; Shonhai *et al*., 2008) were used. The other reagents and materials used are listed in Appendix (C1).

4.2.2 Investigation of PfHsp70-z nucleotide binding affinity using SPR

The assay was conducted at room temperature (25 °C) using a ProteOn XPR36 (BioRad, USA). Filter sterilised and degassed PBS-Tween (section 3.2.10) was used as running buffer. PfHsp70-1, PfHsp70-z and PfHsp70-1_{NBD} (as ligands) were immobilised on the HTE chip surface. The immobilisation was achieved through the Tris-NTA complex activated with Ni^{2+}, to enable stable binding of polyhistidine-tagged proteins following manufacturer's protocol (BioRad USA) (Appendix A13; B11; B12). PfHsp70-1 and PfHsp70-z were immobilised at concentrations of 0.5 µg/mL and 1 µg/mL, PfHsp70-1_{NBD} (as ligand) was immobilised at 1 µg/mL. At these concentrations the response units for each immobilised protein achieved were as follows: 187 response units (RU) for PfHsp70-z, 198 for PfHsp70-1 and 180 for PfHsp70-1_{NBD} RU per immobilization surface. As analytes aliquots of ATP/ADP were prepared at final concentration of 1.25 nM, 2.50 nM, 5 nM 10 nM and 20 nM and were injected at 100 µl/min in each horizontal channel. Association was allowed for two minutes and dissociation was monitored for eight minutes. Steady state equilibrium constant data was processed and analysed using ProteOn Manager™ software version 3.1.0.6. by concatenating the responses of all five analyte concentrations.

© University of Venda

4.2.3 Investigation of the effects of nucleotides on the conformation of PfHsp70-z by partial proteolysis

Nucleotide dependent conformational alterations of PfHsp70-z were investigated by partial trypsin proteolysis using a previously described method (Raviol *et al*., 2006) with modifications. Briefly, 0.45 µg/ml recombinant PfHsp70-z was incubated in the absence and presence of 5 mM nucleotide ATP/ADP in buffer A (137 mM NaCl, 2.7 mM KCl, 8 mM Na_2HPO_4, 1.46 mM KH_2PO_4) for 10 minutes at 30 °C. The proteolytic reaction was started by addition of 0.25 ng/ml of trypsin. Samples were taken at 0, 5, 15 and 30 minute time points and added to 4X SDS loading buffer (0.5 M Tris-HCl, pH 6.8, 10 % (v/v) glycerol, 10 % (w/v) SDS, 5 % (v/v) β-mercaptoethanol, 1 % (w/v) Bromophenol Blue) and analysed using SDS-PAGE and stained using the Pierce® silver stain (Appendix A14). Western analysis was used to verify the production of PfHsp70-z using α-His antibodies (1 : 2000). Imaging of the protein bands on the blot was conducted using the ECL kit as per manufacturer's instructions. Images were captured using ChemiDoc Imaging system (Bio-Rad, USA).

4.2.4 Investigation of the nucleotide dependent conformational changes of PfHsp70-z using tryptophan fluorescence based analysis

As a follow-up to the limited proteolysis study, nucleotide dependent conformational alterations of PfHsp70-z were further investigated by tryptophan fluorescence as previously described (Section 3.2.9; Raviol *et al*., 2006). Recombinant PfHsp70-z (0.45 µg/ml) was incubated in the absence and presence of 5 mM nucleotide ATP/ADP in assay buffer A (Section 3.2.9) for 10 minutes at 20 °C and time-course was conducted for 65 minutes. Then fluorescent units were measured as previously described (Section 3.2.9). Relative fluorescence were determined as average for at least 7 spectrum scans after subtraction of baseline (buffer with or without nucleotides in the absence of protein).

4.2.5 Investigation of PfHsp70-z chaperone function using luciferase aggregation assay

The chaperone function of recombinant PfHsp70-z was investigated by analysing its ability to prevent aggregation of heat denatured luciferase from *Photinus pyralis* (Sigma-Aldrich) using

© University of Venda

spectrophotometry. The aggregation suppression assay was conducted as previously described (Xu *et al*., 2012) with minor modifications. The assay was initiated by adding 0.2 µM luciferase and 0.2 µM recombinant chaperone in assay buffer C (25 mM HEPES-KOH, pH 7.5, 5 mM MgCl, 5 mM $NaOA_C$, 50 mM KCl, 5 mM β-mercaptoethanol) heated to 48 °C. Protein aggregation was monitored for 60 minutes at 320 nm using the SpectraMax M3 spectrometer (Molecular Devices, USA). To determine if the chaperone function was dependent on the presence of nucleotides, 5 mM ATP/ADP was added to the reaction mixture 15 minutes after the reaction had started.

4.2.6 Investigation of PfHsp70-z chaperone function using malate dehydrogenase aggregation assay

As a follow-up study, the chaperone function of recombinant PfHsp70-z was further investigated by analysing its ability to prevent aggregation of heat denatured malate dehydrogenase (MDH) from *porcine* heart (Sigma-Aldrich, USA). The aggregation suppression assay was conducted as previously described (Shonhai *et al*., 2008; Luthuli *et al*., 2013; Makumire *et al*., 2014). Briefly, the assay was initiated by adding 0.2 µM MDH and 0.2 µM recombinant PfHsp70-z in assay buffer B (50 mM Tris-HCl, pH 7.5, 100 mM NaCl) and reaction mix was incubated at 48 °C. Protein aggregation was monitored as previously described (Section 4.2.5).

4.2.7 Investigation of the direct association of PfHsp70-z with PfHsp70-1 slot blot analysis

Purified recombinant PfHsp70-z (25, 50, 100 pM) and controls were spotted onto nitrocellulose membrane using Bio-Dot^{TM} SF apparatus connected to a vacuum pump (Sultana and Butterfield, 2008). BSA was used as negative control. The membrane was blocked with 5 % (w/v) fat free milk in TBST (50 mM Tris-HCl pH 7.5, 150 mM NaCl, 0.1 % (v/v) Tween 20) and overlaid with either PfHsp70-1/PfHsp70-1_{NBD} (0.4 µM) in the presence of 5 mM ATP/ADP and incubated overnight at 4 °C, followed by three washes with TBST for 15 minutes. The nucleotide concentrations were maintained in the subsequent steps of the protocol. Protein was detected using α-PfHsp70-1 antibody (1: 2000) (Shonhai *et al*., 2008) and α-PfHsp70-z

© University of Venda

(Genscript, USA) as primary antibodies which were detected using secondary HRP-conjugated α-rabbit IgG antibody (1: 4000) (Sigma-Aldrich, USA). Imaging of the protein bands on the blot was conducted as previously described (Section 3.2.4).

4.2.8 Analysis of the interaction between PfHsp70-z and PfHsp70-1 using surface plasmon resonance

The assay was conducted at room temperature (25 °C), filter sterilised and degassed PBS-Tween (Section 3.2.10) was used as running buffer. The immobilisation of ligands was conducted as previously described (Section 3.2.10) with slight modifications. PfHsp70-1, PfHsp70-z (as ligands) were immobilised at concentrations of 0.5 µg/mL and 1 µg/mL, PfHsp70-1_{NBD} (as ligand) was immobilised as 1 µg/mL. At these concentrations 187 response units (RU) for PfHsp70-z, 196 for PfHsp70-1 and 198 for PfHsp70-1_{NBD} RU were achieved per immobilization surface. As analytes aliquots of PfHsp70-z, PfHsp70-1 and PfHsp70-1_{NBD} were prepared at final concentration of 125 nM, 250 nM, 500 nM 1000 nM and 2000 nM and were injected at 50 µl/min in each horizontal channel. Association was allowed for 2 min, dissociation was monitored for 10 min. Data analysis was conducted as previously described (Section 3.2.10).

© University of Venda

Investigation of The Association of PfHsp70-z with PfHsp70-1 and Assessment of its Chaperone Activity *in vitro*

4.3 Results

4.3.1 Nucleotide equilibrium binding of PfHsp70-z and PfHsp70-1

PfHsp70-z nucleotide binding affinities were determined using SPR analysis (Figure 4.1). At steady state the ATP affinity for the recombinant proteins were analysed by equilibrium analysis (Figure 4.1). The equilibrium analysis was conducted on the SPR sensorgrams at steady state using varying nucleotide (ATP) concentrations as analyte on the following ligands: PfHsp70-z, PfHsp70-1 and PfHsp70-1_{NBD}. BSA was used as a control ligand and no response units were observed. PfHsp70-1 and its truncated form PfHsp70-1_{NBD} obtained ATP binding affinities (K_D values) in the same order of magnitude (Table 4.1). PfHsp70-z exhibited less ATP binding affinity with one order of magnitude when compared to PfHsp70-1 (Table 4.1).

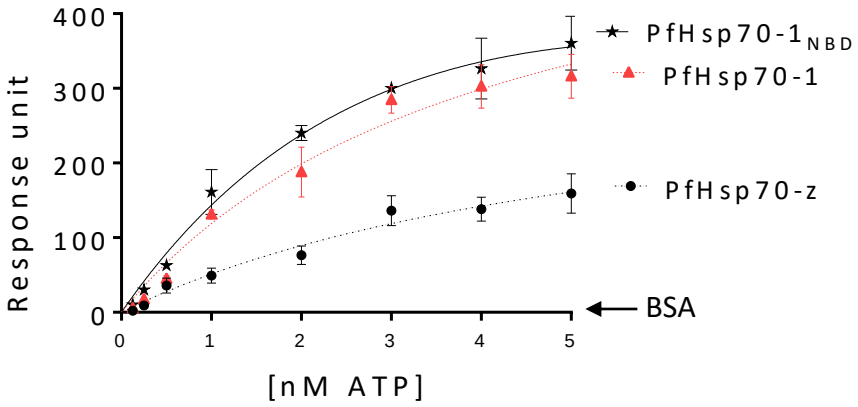

Figure 4.1: Equilibrium analysis of ATP binding by PfHsp70-z and PfHsp70-1/PfHsp70-1_{NBD}
The data represents the equilibrium analysis of ATP binding constants for all three proteins. The equilibrium constant K_D, were obtained for PfHsp70-z, PfHsp70-1 and PfHsp70-1_{NBD} (**A**). The analysis was conducted by plotting total response units from the association curves of PfHsp70-z (**B**), PfHsp70-1 (**C**), and PfHsp70-1_{NBD} (**D**) against ATP concentration. The standard deviations of at least three independent assays are shown.

Table 4.1: Comparative affinities of PfHsp70-1 and PfHsp70-z for nucleotides at equilibrium binding phase

Protein (Ligand)	ATP (analyte)
	K_D (µM) [+/- standard deviation]
PfHsp70-z	25.3 (+/- 1.1)
PfHsp70-1	3.48 (+/- 0.4)
PfHsp70-1_{NBD}	3.47 (+/- 0.2)

Legend: Standard deviation shown in parenthesis are for at least three independent assays

© University of Venda

Investigation of The Association of PfHsp70-z with PfHsp70-1 and Assessment of its Chaperone Activity *in vitro*

4.3.2 Effect of nucleotides on PfHsp70-z as determined using limited proteolysis

PfHsp70-z was subjected to partial proteolysis in the absence of nucleotide and in presence of ATP/ADP to investigate the effect of the nucleotides on the conformation on the protein. The profiles of fragments that were generated from PfHsp70-z digested in the absence and presence of ADP/ATP were analysed on SDS-PAGE and Western blot (Figure 4.2).

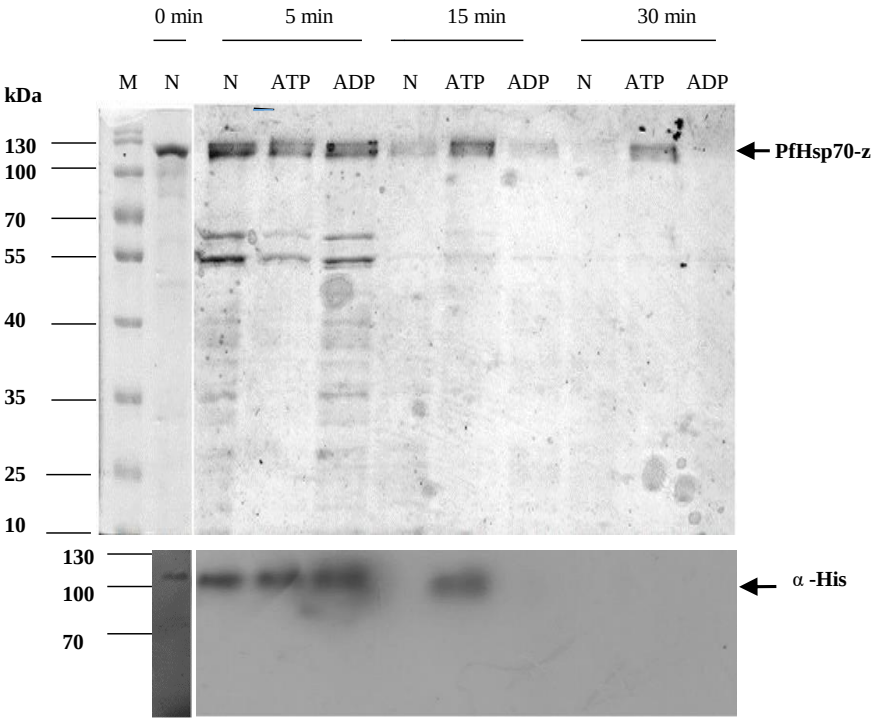

Figure 4.2: Limited proteolysis confirming nucleotide-induced conformational changes in PfHsp70-z
Upper panel - Silver stained SDS-PAGE gel (12 %) representing the partial tryptic digestion of recombinant PfHsp70-z in nucleotide free buffer and in the presence of 5 µM ADP/ATP. **Lower panel**: Western blot representing PfHsp70-z fragments that were detected using α-His_6 antibodies. PfHsp70-z was digested at 30 °C using 0.25 ng/ml trypsin and samples were collected at the indicated time points in the absence of nucleotides (N), presence of 5 mM ATP/ADP.

Prior to proteolytic digestion, it was important to validate protein stability, it was observed that the recombinant PfHsp70-z protein was stable represented by a species of 100kDa. This suggests that PfHsp70-z was stable and did not break into smaller fragments prior to incubation with trypsin. The proteolytic digestion after five minutes of incubation generated species of 55 kDa and 60 kDa fragments (Figure 4.2), in all three samples without nucleotides and with ATP/ ADP (Figure 4.2). The absence of digestion fragments in the purified PfHsp70-z (Figure 4.2; Section 3.3.4), suggests that the fragments observed were generated during proteolysis with trypsin. Furthermore, there were species of approximately 35 kDa that were

© University of Venda

obtained in the absence of nucleotide (Figure 4.2) and in the presence of ADP (Figure 4.2). This suggests that the ADP bound form of PfHsp70-z may assume a conformation that closely resembles that of the protein when it is not bound to nucleotide.

After 15 minutes incubation in the presence of trypsin, the nucleotide free and ADP bound PfHsp70-z were to a greater degree digested (Figure 4.2) compared to protein in the presence of ATP. After 30 minutes, nucleotide-free and ADP-bound PfHsp70-z was completely digested (Figure 4.2). This further confirms that the ADP bound form of PfHsp70-z may assume a conformation that closely resembles that of the protein when it is not bound to nucleotide. However, ATP-bound PfHsp70-z generated digestion fragments that were unique and part of the protein remained undigested after 30 minutes of exposure to trypsin (Figure 4.2). However, the fragment that remained after 30 minutes could not be detected by Western blot analysis suggesting that it may have lost its N-terminal His-tag. Altogether, the findings suggest that ATP induced PfHsp70-z to assume a compact conformation.

4.3.3 Tryptophan fluorescence analysis

PfHsp70-z possesses two tryptophan residues at positions W436 and W690. Urea sensitivity was used as a control experiment validating sensitivity of protein to change (Section 3.3.8). On the basis of urea sensitivity, further enquiries were made using nucleotide presence as variables. The observed tryptophan fluorescence spectra variations suggested different conformational states of PfHsp70-z in nucleotide-free buffer and in the presence of ADP/ATP (Figure 4.3). The changes observed in the tryptophan-based fluorescence spectrum further confirmed that nucleotide free (Figure 4.3A) and ADP-bound (Figure 4.3A) forms of the protein assumed similar conformational states (Figure 4.3A). On the other hand, the ATP-bound form of the protein assumed a unique conformation (Figure 4.3A) as confirmed by tryptophan fluorescence analysis. PfHsp70-z protein was further incubated for at least 65 minutes in the presence of ATP, followed by samples collected after set time intervals for time-course fluorescence analysis (Figure 4.3B). Tryptophan fluorescence spectral changes were observed with increase in time of incubation in the presence of ATP (Figure 4.3B). This

© University of Venda

suggests conformation changes over time, and these may be inferred to reflect hydrolysis of ATP by PfHsp70-z as the tryptophan fluorescence spectra shifted towards that of ADP-bound state over time (Figure 4.3B).

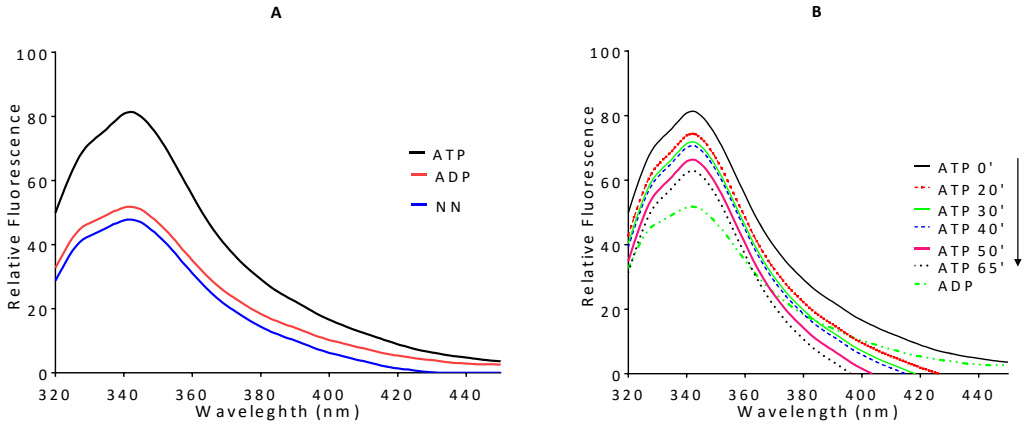

Figure 4.3: The conformation of PfHsp70-z is regulated by nucleotides
Tryptophan fluorescence signals obtained upon incubating PfHsp70-z in the absence of nucleotide or in the presence of 5 µM ATP/ADP (**A**). A time-course assessment of ATP on fluorescence intensity of PfHsp70-z emission peak obtained at 345 nm was conducted (**B**).

4.3.4 PfHsp70-z suppresses heat-induced aggregation of luciferase and Malate dehydrogenase

The chaperone activity of recombinant PfHsp70-z was determined by assessing its ability to prevent heat-induced aggregation of luciferase and malate dehydrogenase (MDH). Based on this assay, heat induced protein aggregation results in increased turbidity which is monitored by taking absorbance readings at 320 nm. First, it was important to establish that PfHsp70-z and PfHsp70-1 were heat-stable. The recombinant proteins did not aggregate at 48 °C, this was in line with findings from secondary and tertiary structure data (Sections 3.3.7; 3.3.8). The model substrates luciferase and MDH were observed to aggregate at 48 °C in the absence of chaperone (Appendix B8; B9). Addition of chaperones to the mixture resulted in suppressed heat induced aggregation (Figure 4.4). As a control, a non-chaperone, BSA, was added to the model substrates but it did not suppress the aggregation of MDH and luciferase resulted in increased heat induced aggregation of model substrates. This validated that the

© University of Venda

suppression of heat induced aggregation on model substrates was specific for chaperones. The aggregation values were calculated based on the level of aggregation observed for luciferase and MDH without chaperone set as 100 % aggregation.

PfHsp70-1 with known chaperone function (Shonhai *et al*., 2008) was used as a control. In order to determine the effective chaperone/substrate ratio, it was important to titrate amounts of chaperone (Figure 4.4A, B). PfHsp70-z suppressed the aggregation of luciferase and MDH (Figure 4.4A, B) in a concentration dependent fashion. The optimum chaperone activity was observed at a 1:1 chaperone to either luciferase/MDH ratio (Figure 4.4A; B). Furthermore, a comparison of the capabilities of PfHsp70-z and PfHsp70-1 in suppressing heat-induced aggregation of proteins *in vitro* was conducted. At the same chaperone concentration, PfHsp70-z suppressed aggregation to a greater degree than PfHsp70-1 (Figure 4.4A, B; $p<0.005$). Based on these findings, PfHsp70-z's protein aggregation suppression capability is marginally higher when compared with that of PfHsp70-1 (Figure 4.4A, B). This suggests that PfHsp70-z is a chaperone with heat induced aggregation suppression activity.

The effect of nucleotides on the chaperone function was determined by repeating the protein aggregation assays in the presence of ATP or ADP. The chaperone function of PfHsp70-z was not influenced by nucleotide (Figure 4.4C, D). On the other hand, addition of ATP to the assay mix inhibited the protein aggregation suppressive function of PfHsp70-1 as previously reported (Shonhai *et al*., 2008) (Figure 4.4C, D). However, ADP did not affect the chaperone function of PfHsp70-1. It is known that ADP enhances substrate binding (holdase) function of Hsp70 (Mayer *et al*., 2000) and therefore this finding is in agreement with this position for both PfHsp70-z and PfHsp70-1.

© University of Venda

Investigation of The Association of PfHsp70-z with PfHsp70-1 and Assessment of its Chaperone Activity *in vitro*

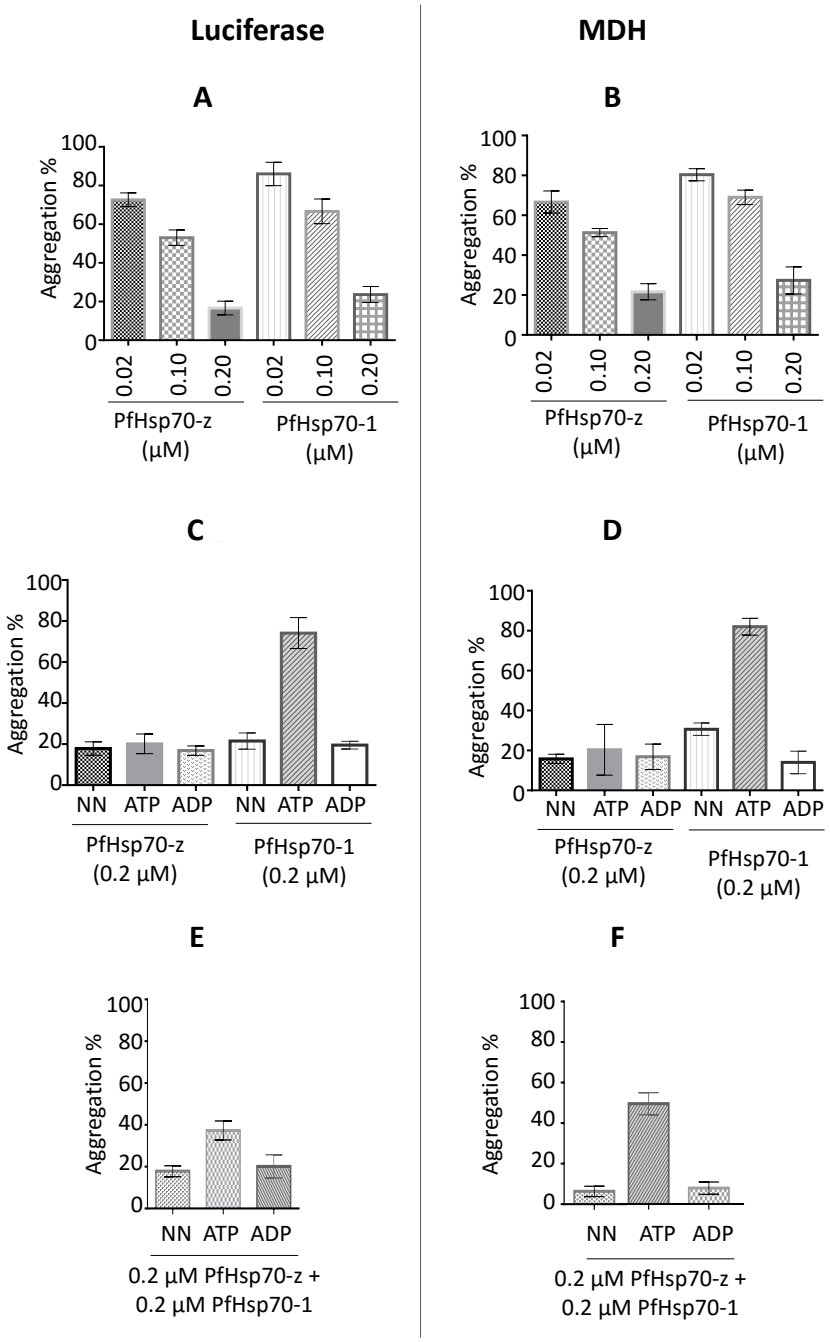

Figure 4.4: PfHsp70-z suppresses heat-induced aggregation of luciferase and Malate dehydrogenase
The heat-induced aggregation of luciferase was assessed *in vitro* at 48 °C. Dose response assessment of the independent capabilities of PfHsp70-z and PfHsp70-1 to suppress heat-induced aggregation of luciferase (**A**); MDH (**B**) the assay was repeated in the presence of 5 µM ADP /ATP for luciferase (**C**) and MDH (**D**). The activity of PfHsp70-1 and PfHsp70-z in the presence of ATP compared to the nucleotide-free state and ADP-bound state, was statistically significant ($p<0.005$), respectively. The assay was repeated for luciferase (**E**) and MDH (**F**) to assess the activity for the combination of PfHsp70-z and PfHsp70-1, under various conditions: nucleotide-free buffer (NN); presence of ADP/ATP, respectively. Standard deviations obtained from three replicate assays are shown.

© University of Venda

Investigation of The Association of PfHsp70-z with PfHsp70-1 and Assessment of its Chaperone Activity *in vitro*

The combined effect of PfHsp70-1 and PfHsp70-z on aggregation suppression of luciferase or MDH was more efficient (Figure 4.4E, F) than what was observed for the individual chaperones. However, there was two-fold reduction in chaperone efficiency (Figure 4.4E, F) in the presence of ATP. The reduction in chaperone efficiency for the PfHsp70-1 and PfHsp70-z combination in the presence of ATP may be attributed to the specific inhibitory effect of ATP on PfHsp70-1 activity (Figure 4.4 C, D; Shonhai *et al*., 2008).

4.3.5 Assessment of the interaction of PfHsp70-z with PfHsp70-1 using slot blot technique

The association of PfHsp70-z and PfHsp70-1 was validated using the recombinant forms of the two molecular chaperones. In order to immobilise the recombinant proteins on nitrocellulose membrane the slot blot technique (Sultana and Butterfield, 2008) was used. Prey protein (PfHsp70-z) was immobilized onto the blot. Firstly, it was important to ascertain whether the α-PfHsp70-1 antibodies to be used in the assay were specific and would not cross-react with PfHsp70-z. The blot with immobilised PfHsp70-z protein and controls BSA; (PfHsp70-1; PfHsp70-1_{NBD}) were used for immunoblotting using α-PfHsp70-1 antibodies (Figure 4.5A). The antibodies detected bands representing both full length PfHsp70-1 and PfHsp70-1_{NBD} in a concentration dependent fashion (Figure 4.5A; B). Furthermore, α-PfHsp70-1 antibodies did not cross react with BSA immobilised on the membrane (Figure 4.5A; B) or PfHsp70-z (Figure 4.5A; B).

The interaction of PfHsp70-z and PfHsp70-1 was established by passing the prey proteins (PfHsp70-1 and PfHsp70-1_{NBD}) over the immobilized bait PfHsp70-z protein (Figure 4.5B). This was followed by conducting immunoblotting to detect PfHsp70-1 bound to immobilised PfHsp70-z using α-PfHsp70-1 antibodies (Shonhai *et al*., 2008). The detected band intensity increased as the amount of PfHsp70-z immobilised on the blot increased (Figure 4.5C). This suggests that PfHsp70-1 was captured on spots where PfHsp70-z was immobilised. Taken together this data suggests that PfHsp70-z interacted with PfHsp70-1 in a concentration dependent manner. The assay was repeated in the presence of nucleotides (ATP/ADP) and it

© University of Venda

appears ADP did not have a significant effect on the interaction (Figure 4.5C). However, ATP appears to enhance the association (Figure 4.5C) of the two proteins.

Densitometric analysis of the immunoblots confirmed the findings that ATP enhances the association between PfHsp70-1 and PfHsp70-z in a dose dependent fashion (Figure 4.5D). The densitometric data suggest that PfHsp70-z interacted with PfHsp70-1_{NBD} and full length PfHsp70-1 under all conditions. These findings suggest that the PfHsp70-1_{NBD} is the primary site through which PfHsp70-z interact with PfHsp70-1.

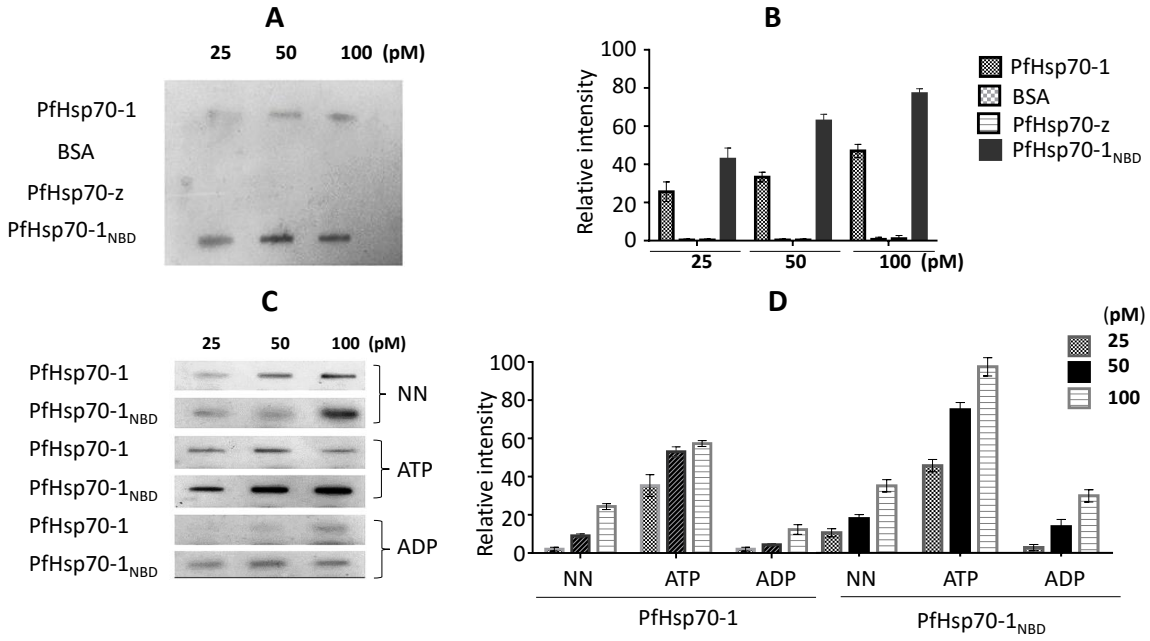

Figure 4.5: Nucleotide dependent interaction of PfHsp70-z and PfHsp70-1
Slot blot analysis (**A**), and accompanying densitometric analysis (**B**) confirming the specificity of α-PfHsp70-1 antibodies; slot blot analysis (**C**) and accompanying densitometric analysis (**D**) demonstrating the interaction of PfHsp70-z with PfHsp70-1/PfHsp70-1_{NBD}. The assay was conducted in the absence of nucleotide (NN) or in the presence of 5 µM ATP/ADP, respectively. The reported data represent at least three independent assays conducted using different protein batches. Standard errors are indicated. Dose-dependent interaction between PfHsp70-z and PfHsp70-1 were ascertained by densitometric analysis using ANOVA ($p<0.001$).

Furthermore, the interaction of PfHsp70-z with PfHsp70-1 occurs in the presence of ATP, it is unlikely that the association is based on PfHsp70-1 acting as chaperone-to PfHsp70-z as substrate since PfHsp70-1 releases its substrates in the presence of ATP (Shonhai *et al*., 2008; Section 4.3.4). It is highly unlikely that PfHsp70-z misfolded during the assay as it was observed that the molecule is thermally stable (sections 3.3.7; 3.3.8), hence it would not

© University of Venda

constitute an appropriate substrate of PfHsp70-1. Furthermore, the natively purified PfHsp70-z protein did not elute complexed with *E. coli* Hsp70 (DnaK) (Section 3.3.4). This further highlights that the purified PfHsp70-z protein was fully folded and not prone to the attention of Hsp70 a through chaperone-substrate association.

In addition, the observed interaction between the NBD subdomain of PfHsp70-1 and PfHsp70-z, further suggests that the association is not based on chaperone-substrate interaction. PfHsp70-1_{NBD} lacks the substrate binding domain and therefore could not interact as chaperone and substrate with PfHsp70-z, respectively (Zininga *et al*., 2015b). However, to rule out that PfHsp70-1_{NBD} constitutes a substrate for PfHsp70-z, the observed chaperone function of PfHsp70-z is not responsive to nucleotides (Section 4.3.4). Based on these findings, it is highly unlikely that PfHsp70-z interacted with PfHsp70-1_{NBD} as a chaperone and substrate association. In addition, during purification, the recombinant PfHsp70-1_{NBD} protein was maintained in native form throughout the purification process (Section 3.3.6). Therefore, these findings suggest that PfHsp70-z interacts with PfHsp70-1, possibly by establishing ionic contacts with specific residues located in the NBD subdomain of the latter.

4.3.6 Assessment of PfHsp70-z interaction with PfHsp70-1 using SPR

To further validate observed association of PfHsp70-1 with PfHsp70-z, interaction kinetics and affinity analysis were conducted using SPR based on a simple Langmuir fit model (Figure 4.6). Based on SPR sensor grams for specific interactions there should be concentration dependent response units. As a control, BSA was injected and resulted in no increase in response units. The concentration dependent observation made on the response units during association of PfHsp70-z with full length PfHsp70-1 suggested a specific interaction (Figure 4.6A). The assay was repeated in the presence of nucleotides ADP (Figure 4.6B), or ATP (Figure 4.6C) and similar concentration dependent response units increase were observed. The interaction of PfHsp70-z with PfHsp70-1_{NBD} was similarly investigated. The array system allowed for analysis to be conducted by reversing ligand and analyte in the absence of nucleotides (Figure 4.6D) or in the presence of nucleotides ADP (Figure 4.6E) and ATP (Figure 4.6F). The observed

© University of Venda

Investigation of The Association of PfHsp70-z with PfHsp70-1 and Assessment of its Chaperone Activity *in vitro*

sensorgrams suggest the interactions between PfHsp70-z with PfHsp70-1/PfHsp70-1_{NBD} as ligands and analytes were specific as evidenced by the concentration dependence of the response units.

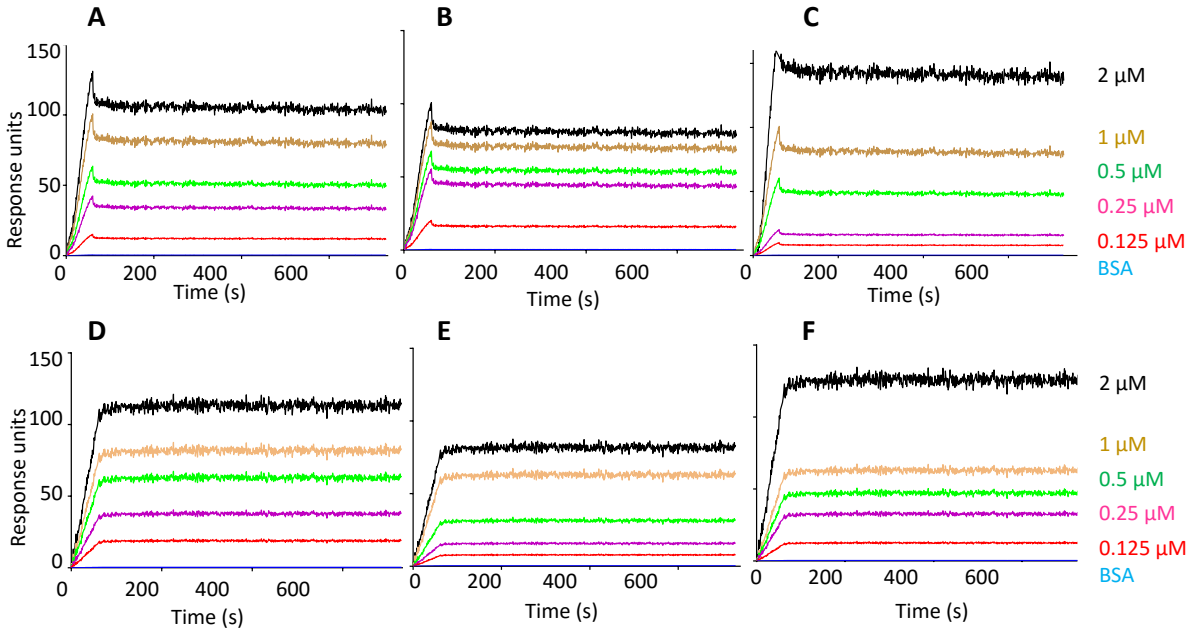

Figure 4.6: PfHsp70-z directly interacts with PfHsp70-1/PfHsp70-1_{NBD}
SPR sensorgrams for the interaction of PfHsp70-z with PfHsp70-1/PfHsp70-1_{NBD}. The interaction between PfHsp70-1 and PfHsp70-z (**A**); the experiment was repeated in the presence of 5 mM ADP (**B**); and 5 mM ATP (**C**). The interaction of PfHsp70-z and PfHsp70-1_{NBD} (**D**); the experiment was repeated in the presence of 5 mM ADP (**E**); and 5 mM ATP (**F**).

The SPR sensorgrams were analysed to generate the SPR kinetics data (Table 4.2). The kinetics data for the interactions were observed for the association and the dissociation phases. The association constant and dissociation constant were determined, respectively. The data was also used to determine the equilibrium constant (binding affinity). The binding affinity data show that ATP promoted interaction in nanomolar range compared to micromolar range in the presence of ADP and absence of nucleotide, respectively (Table 4.2). The interaction kinetics data obtained confirmed the initial results obtained in using slot blot that suggested ATP promoted the interaction between PfHsp70-z with PfHsp70-1/PfHsp70-1_{NBD} (Figure 4.5).

The immobilisation order was reversed and PfHsp70-z was immobilised as ligand and PfHsp70-1/PfHsp70-1_{NBD} injected as the analyte (Table 4.2). The variation observed in the

© University of Venda

interaction kinetics data may be attributed to different orientations of protein immobilisation on GLC surface. Taken together, the SPR interaction kinetics data suggests that PfHsp70-z and PfHsp70-1/PfHsp70-1_{NBD} interacts with higher affinity in the presence of ATP than in the absence of nucleotide or presence of ADP (*p<0.005*). However, in the presence of ATP PfHsp70-1_{NBD} appears to have formed more stable complex with PfHsp70-z than the full length protein (Table 4.2).

Table 4.2. Kinetics and affinities of PfHsp70-z binding by PfHsp70-1 and PfHsp70-1_{NBD} as calculated by langmuir model fitting of sensorgrams

Ligand	analyte	Nucleotide	k_a(Ms^{-1})	k_d (s^{-1})	K_D (M)	χ^2
PfHsp70-1	PfHsp70-z	ATP	9.97 (+/- 0.5) e+02	2.42 (+/-1.0) e-05	2.41 e-08**	1.86
		ADP	2.98 (+/- 0.2) e+2	3.61 (+/-0.7) e-03	1.21 e-05	2.12
		-	4.95 (+/- 0.9) e-01	2.96 (+/-0.1) e-05	5.98 e-05	3.32
PfHsp70-z	PfHsp70-1	ATP	6.08 (+/- 0.8) e+04	7.00 (+/-0.6) e-04	1.15 e-08**	5.67
		ADP	6.52 (+/- 0.3) e+04	1.14 (+/-0.04) e-00	1.75 e-05	2.19
		-	4.94 (+/- 1.0) e+04	4.01 (+/-0.5) e-00	8.11 e-05	6.77
PfHsp 70-z	PfHsp70-1_{NBD}	ATP	4.46 (+/-0.17)e+03	9.43 (+/-0.9) e-06	2.12 e-09**	2.65
		ADP	2.63 (+/-0.7) e+03	2.60 (+/-1.2) e-04	9.86 e-08	6.52
		-	2.39 (+/-0.9) e+00	3.76 (+/-0.6) e-08	1.57 e-08	2.44
PfHsp70-1_{NBD}	PfHsp 70-z	ATP	9.33 (+/- 0.4) e+04	1.58 (+/-0.7) e-04	1.16 e-09**	4.39
		ADP	5.80 (+/-0.12) e+04	8.30 (+/- 0.1) e-04	1.43 e-08	3.12
		-	4.15 (+/- 0.05)e+04	5.15 (+/- 1.5) e-04	1.24 e-08	1.40

Table Legend: The interaction kinetics, represented by the association rate constant (k_a), dissociation rate constants (k_d) and equilibrium constant (K_D) were determined by SPR analysis alternating the status of PfHsp70-z and PfHsp70-1 as ligand and analyte, respectively. The ligand was the immobilised protein on the GLC chip surface and the analyte was the protein injected at a flow rate of 50 µl/min. Data was analysed by using running buffer with or without nucleotides in the absence of protein analyte as baseline. Data are represented as mean plus/minus standard deviation of at least five different repeated assays. Chi square (X^2) values shows the langmuir curve fitting and statistical analysis was done using one way ANOVA *(p<0.005**),* showing that there were statistically significant differences in affinity dependent on the presence or absence of ATP.

The SPR kinetics data generated after swapping the ligand/analyte show some degree of variation although they maintain the same order of magnitude (Table 4.2). These variations may be caused by different orientations of the immobilised proteins thereby making some interaction sites available and vice versa. The immobilised proteins form a monolayer on the chip surface; thereby the protein surface on the chip surface has limited accessibility to

© University of Venda

analyte. Despite these variations the SPR kinetics data are comparable for each data set as indicated by the standard deviation and the goodness of fit (Chi^2) less than 10 on the Langmuir model.

© University of Venda

Investigation of The Association of PfHsp70-z with PfHsp70-1 and Assessment of its Chaperone Activity *in vitro*

4.4. Discussion

The current findings present the first direct evidence that PfHsp70-z possesses independent chaperone function. Furthermore, the study provides evidence confirming that PfHsp70-z interacts with PfHsp70-1 in a nucleotide dependent fashion. The findings indicate that this interaction occurs primarily through the N-terminal ATPase domain of PfHsp70-1.

This study noted that PfHsp70-z binds ATP with high affinity (Figure 4.3.1). This was in line with findings that PfHsp70-z hydrolyses ATP (Section 3.3.9). Therefore, the study enquired the effects of binding nucleotides on the structural conformation of PfHsp70-z. Partial proteolysis which has previously been used as a tool for investigating the conformational changes of Hsp70 induced by nucleotide binding and hydrolysis (Liberek *et al*. 1991, Raviol *et al*. 2006) was employed. The similarity in the profile of fragments generated by trypsin proteolysis between native and ADP-bound PfHsp70-z (Figure 4.2A), suggests that ADP has no effect on the conformation of PfHsp70-z. The variation in the fragments produced upon digestion of PfHsp70-z in the presence of ATP versus ADP further testifies to the fact that PfHsp70-z assumes a unique conformation in the presence of ATP. ATP-bound PfHsp70-z is more stable from proteolysis compared to nucleotide-free or ADP-bound PfHsp70-z. This would suggest that PfHsp70-z is protected from trypsin cleavage by conformational changes introduced by ATP. This finding was in line with a previous study that Hsp110 assumes a compact conformation in the ATP bound state (Raviol *et al*., 2006).

PfHsp70-z possesses two tryptophan residues W436 and W690. The validation of the nucleotide induced conformational changes was conducted using tryptophan fluorescence based study. This study confirms that ATP binding causes PfHsp70-z to assume a distinct conformational state (Figure 4.3A). However, in the presence of ADP, PfHsp70-z assumes a slight conformational shift from the nucleotide free-state.

© University of Venda

Investigation of The Association of PfHsp70-z with PfHsp70-1 and Assessment of its Chaperone Activity *in vitro*

It was demonstrated that PfHsp70-z is a heat-stable molecule (section 3.3.6; Zininga *et al*., 2015a). The heat stability of PfHsp70-z substantiates its ability to suppress heat induced aggregation of luciferase and MDH thereby providing direct evidence of its functioning as a heat stable chaperone. PfHsp70-z aggregation suppression is not affected by the presence of ADP/ATP (Figures 4.4). These results suggest mechanistic functional differences between PfHsp70-1 and PfHsp70-z. In light of this, PfHsp70-z possibly possesses a rigid linker that makes it a more robust holdase than PfHsp70-1 under fluctuating ATP levels.

The current study suggests PfHsp70-z interacts with PfHsp70-1 in a nucleotide-dependent fashion (Figure 4.5; 4.6). It was further observed that the truncated form of PfHsp70-1 (PfHsp70-1_{NBD}) constitutes the minimum subdomain required for interaction with PfHsp70-z. These findings agree with previous reports on human and yeast Hsp110, that the Hsp110:Hsp70 complex is stable with extensive intermolecular contacts encompassing each NBD (residues 1-384 of each molecule; Schuermann *et al*., 2008). Removal of the SBD from PfHsp70-1 may expose the PfHsp70-1_{NBD} to facilitate better interaction with PfHsp70-z. It was going to be interesting to experimentally validate the nucleotide exchange function of PfHsp70-z but technical limitations made it impossible to be conducted in this study.

© University of Venda

CHAPTER 5

ANALYSIS OF THE EXPRESSION, CO-LOCALISATION AND INTERACTION OF PFHSP70-Z WITH PFHSP70-1 IN PARASITES MAINTAINED AT THE RED BLOOD STAGE

© University of Venda

5.1 Introduction

The development of malaria parasites at the blood stage is associated with periodic fever conditions. These fever conditions are known to induce select heat shock proteins which are required for maintaining proteostasis in the parasite (Banumathy *et al*., 2003; Mayer and Bukau, 2005; Pallavi *et al*., 2010). In addition, the up-regulation of some of the heat shock protein genes during fever conditions augments parasite infectivity (Pallavi *et al*., 2010). Genomic studies conducted in *Plasmodium* species suggest that genes that have common expression profiles tend to have similar cellular roles (Section 2.3.6; Le Roch *et al*., 2003). Several heat shock proteins, in *P. falciparum*, are up-regulated in clinical malaria parasite isolates (Pallavi *et al*., 2010). Some of the main heat shock families amongst them PfHsp70-1 and PfHsp90 were reported to overexpress in response to stress (Pallavi *et al*., 2010).The association of PfHsp90 and PfHsp70-1 complex has been reported (Gitau *et al*., 2012; Zininga *et al*., 2015b); it is not known if PfHsp70-z occurs in this complex. Furthermore, PfHsp70-1 has been reported to be heat inducible (Banumathy *et al*., 2003; Pesce *et al*., 2008; Gitau *et al*., 2012). The heat inducibility of PfHsp70-1, suggests that it plays an important role in cytoprotection of the parasite and the subsequent development of malaria. The current study sought to establish the expression and subcellular localization of PfHsp70-z.

Briefly, the specific objectives of the study were to:

i) Investigate the heat inducible expression of PfHsp70-z;

ii) Investigate the sub-cellular localization of PfHsp70-z in intraerythrocytic *P. falciparum; and*

iii) Determine the physical association of PfHsp70-z and PfHsp70-1 by immunoprecipitation and pull-down assays.

© University of Venda

5.2 Experimental Procedures

5.2.1 Materials and special reagents

The following materials and specialised reagents were used in this study: RPMI1640 (containing L-Glutamine, HEPES, 0.2 mM hypoxanthine, 0.1 mg/ml neomycin, 10 % (v/v) plasma (Gibco), albumax II (Invitrogen); protein A/G beads (Pierce, Thermo scientific), α-PfHsp70-1 (Shonhai *et al*., 2008); α-PfHsp70-z antibodies (Zininga *et al*., 2015a); TRITC-conjugates goat anti-rabbit and DAPI were kind donations from Prof Heinrich Hoppe, (Rhodes University Grahamstown, South Africa). The rest of the reagents used in the study are listed in (Appendix C1).

5.2.2 Investigation of heat-induced expression of PfHsp70-z in *Plasmodium falciparum* 3D7 cells

P. falciparum 3D7 cells were cultured as previously described (Trager and Jensen, 1976; Gitau *et al*., 2012; Zininga *et al*., 2015a; b). Sorbitol synchronized parasites were harvested at the trophozoite stage from two fractions. One fraction consisted of parasites that had been subjected to heat shock at 42 °C for two hours and the other were cultured under normal temperature conditions (37 °C) prior to harvesting. RBCs infected with *P. falciparum* 3D7 were lysed with lysis buffer (137 mM NaCl, 2.7 mM KCl, 8 mM Na_2HPO_4, 1.46 mM KH_2PO_4, 0.1 % (w/v) saponin) and incubated at 25 °C for 10 minutes. After lysis the parasites were collected by centrifugation at 5000 x g for 10 minutes. This was followed by an extensive wash step using PBS (137 mM NaCl, 2.7 mM KCl, 8 mM Na_2HPO_4, 1.46 mM KH_2PO_4, pH 7.4). The parasite lysate was subjected to Western analysis to confirm the expression of PfHsp70-z using α-PfHsp70-z antibodies (ThermoScientific, USA). To validate the specificity of the α-PfHsp70-z antibodies rabbit pre-immunization serum was also used. To further validate heat induced expression, a protein with known heat induced expression, PfHsp70-1 was probed with α-PfHsp70-1 (Pesce *et al*., 2008). A host cell protein, glycophorin was also probed as a loading control using goat anti-glycophorin (Sigma-Aldrich, USA) and HRP-conjugated anti-goat secondary antibodies (1: 5000) (Sigma-Aldrich, USA). Furthermore, Western blotting analysis was conducted using α-PfHsp70-z antibodies to confirm the specificity of the antibodies by

© University of Venda

probing their capability to bind recombinant PfHsp70-z as opposed to recombinant PfHsp70-1. Images were acquired as previously described (Section 3.2.4)

5.2.3 Immunofluorescence assay

Immunofluorescence assays (IFAs) were carried out after fixation of the parasite infected RBCs using 4 % paraformaldehyde and 0.0075 % glutaraldehyde at 37 °C for 30 minutes. The fixed cells were permebialised with 125 mM glycine PBS followed by washing with 0.1 % triton-100 in PBS. Blocking was done using 3 % BSA/PBS for 1 hour at room temperature. The cells were incubated with rabbit anti-PfHsp70-z antibodies (diluted 1:1000 in blocking solution) or rabbit anti-PfHsp70-1 antibodies (diluted 1:100 in blocking solution) at 4 °C overnight. After several PBS washes, anti-rabbit-TRITC antibodies (1:2000) were allowed to bind at room temperature and in the dark for 2 hours. The cells were washed three times in PBS and with DAPI (10 µg/ml) included in the last wash. Fluorescence images were captured using Olympus DP72 microscope.

5.2.4 Investigation of the direct association of PfHsp70-z with PfHsp70-1 using a Co-immunoprecipitation and pull down assay

P. falciparum 3D7 cells were cultured, harvested and lysed as previously described (see Section 5.2.2). The parasite lysates were resuspended in 500 µl immunoprecipitation lysis buffer (25 mM Tris-HCl pH 7.5, 150 mM NaCl, 1 mM EDTA, 1 % (v/v) Tween-20, and containing 1 mM PMSF). Immunoprecipitation was carried out using Pierce® Protein A/G Magnetic Beads following the manufacturer's protocol with minor modifications (Pierce, Thermo scientific) (Appendix A15). Briefly, parasite lysates containing approximately 300 µg of total protein were suspended in a protein A/G magnetic resin to which α-PfHsp70-z antibodies had been attached. Binding was allowed to occur for two hours at room temperature (25 °C) with gentle agitation. To investigate the effect of nucleotide on PfHsp70-z binding to PfHsp70-1, the suspension was split into three. The first aliquot was supplemented with 5 mM ATP, the other supplemented with 5 mM ADP and the other no nucleotides were added. Following subsequent washing steps using TBS wash buffer (25 mM Tris-HCl pH 7.5, 500 mM NaCl, 0.05 % Tween 20), the immunoprecipitate was eluted in 150 µl of elution buffer (100 mM glycine,

© University of Venda

pH 2.5) and thereafter neutralized using 100 mM Tris pH 7.5. The immunoprecipitate pulldown was analyzed by Western blot using α-PfHsp70-1.

In addition, to the immunoprecipitation assay, the direct association of PfHsp70-z and PfHsp70-1 was investigated using polyhistidine tagged recombinant PfHsp70-z immobilized on HisPur cobalt affinity resin to facilitate pull down of PfHsp70-1 from parasite lysate. Parasites released by saponin Lysis of the erythrocytes were re-suspended in Pierce lysis buffer (Thermo Scientific).The parasite lysate (Prey) was mixed with purified recombinant PfHsp70-z (Bait) immobilised on HisPur Cobalt resin (Thermoscientific) and binding was allowed for 4 hours at 4 °C. As a control beads without immobilised recombinant PfHsp70-z was used. The samples were washed extensively using TBS: Pierce Lysis buffer. The bait-prey proteins were subsequently eluted in 250 µL elution buffer (TBS: Pierce Lysis buffer, 290 mM imidazole). To investigate the effect of nucleotide on PfHsp70-z binding to PfHsp70-1, the suspension was split into three aliquots. One aliquot was adjusted to 5 mM ATP, the other to 5 mM ADP and the other no nucleotides were added. The pull-down eluates were analysed with Western blot using anti-PfHsp70-1 antibodies.

© University of Venda

5.3 Results

5.3.1 PfHsp70-1 is heat inducible

This study enquired if PfHsp70-z is heat inducible in *P. falciparum* parasites growing at the blood stage. The expression of PfHsp70-z in *P. falciparum* 3D7 cells was analysed by SDS-PAGE (Figure 5.1A). As a control uninfected RBCs were also analysed (Figure 5.1A). The SDS-PAGE analyses was for samples drawn from culture that was maintained at 37 °C for two hours (Figure 5.1A) and the other were from samples drawn from culture heat shocked at 42 °C for two hours before harvesting (Figure 5.1A). The SDS-PAGE did not resolve the proteins as distinct bands which was due to the masking effect of haemoglobin from the lysed red blood cells. To further validate the presence of PfHsp70-z, Western blot analysis using α-PfHsp70-z antibodies was employed (Figure 5.1A). It was important to validate the specificity of the α-PfHsp70-z antibodies. The antibodies did not cross react with human proteins in the uninfected RBC lysates (Figure 5.1A). The antibodies detected PfHsp70-z as a species of approximately 100 kDa in both the lysate from cells cultured at 37 °C and those exposed to 42 °C, (Figure 5.1A), respectively. The densitometric analysis of the Western blot validated up-regulation of PfHsp70-z expression in cells heat shocked at 42 °C compared to protein expressed in parasites maintained at 37 °C (Figure 5.1B) ($P<0.005$). Taken together, this suggests the expression of PfHsp70-z at the erythrocytic stage is heat induced.

To further validate the specificity of the antibodies, serum collected from the rabbit prior to immunisation with PfHsp70-z derived peptide was used to probe for non-specific binding. The pre-immune serum did not cross react with uninfected red blood cells and with the parasite cell lysates (Figure 5.1). In order to validate the specificity of the α-PfHsp70-1 (Section 4.3.5) and α-PfHsp70-z Western blot analysis was conducted (Appendix B10). Western blot analysis of the samples showed that α-PfHsp70-1 antibodies are specific for recombinant PfHsp70-1 protein as they did not cross react with recombinant PfHsp70-z protein. Western analysis using α-PfHsp70-1 to probe for a known heat inducible protein PfHsp70-1 was used as a control (Figure 5.1). A densitometric analysis of the blot confirmed heat inducibility of PfHsp70-z (Figure 5.1 C). It was further enquired if the increase in densitometric analysis was not a loading problem, therefore, a house keeping protein, red blood cell glycophorin C (Pesce

© University of Venda

et al., 2008; Gitau *et al*., 2012) was used. Western analysis was carried out on glycophorin blot as a loading control (Figure 5.1D). Altogether, this validates the findings that PfHsp70-z expression is up-regulated during heat stress.

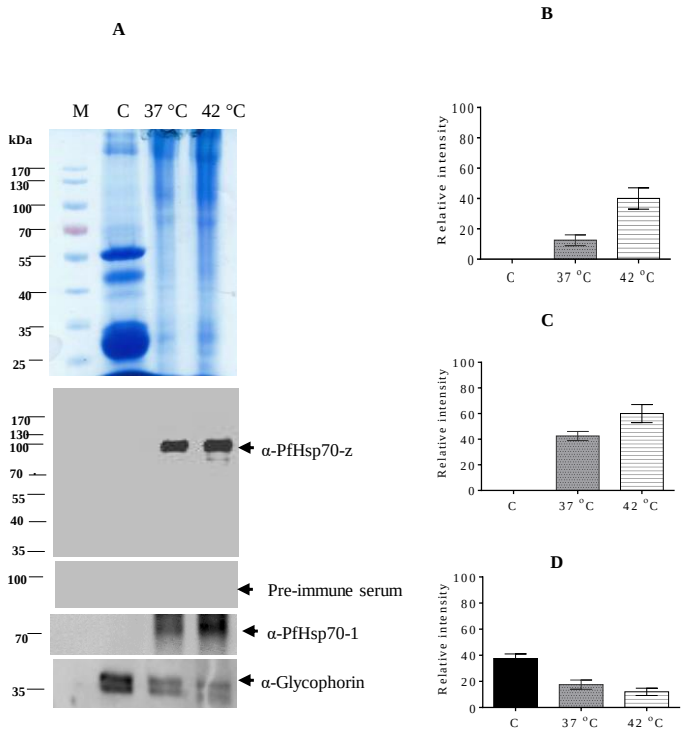

Figure 5.1: PfHsp70-z is induced by heat stress in *Plasmodium falciparum* 3D7 parasites cultured at the blood stage
SDS-PAGE (12%) and western analysis of the expression (A) and densitometric analysis (**B** for α-PfHsp70-z; **C** for α-PfHsp70-1; **D** for α-Glycophorin) of the parasite lysate western blot. Lane M – Page ruler (Thermo Scientific) in kDa is shown on the left hand side; lane C- uninfected human RBC lysate, 37 °C - parasite lysate at incubated at 37 °C and 42 °C -parasite lysate heat shocked at 42 °C for 2 hours, heat induction of PfHsp70-z was ascertained by densitometric analysis using ANOVA (*p<0.0001*).

5.3.2 Localisation of PfHsp70-z

Recombinant PfHsp70-z has been observed to interact with recombinant PfHsp70-1 (Section 4.3.5; 4.3.6). The current study enquired if PfHsp70-z co-localises with PfHsp70-1 in the cytosol. Immunofluorescence experiments were conducted on parasites cultured at 37°C at the trophozoite stage. Despite the poor resolution of the images captured, distinct fluorescence signals were detected suggestive of specific signals. The specificity of the secondary antibodies was validated that they did not bind non-specifically to parasites. The TRITC conjugated secondary antibodies did not cross react with parasite cells evidenced by the absence of a fluorescence signal (Figure 5.2A). PfHsp70-z appear to be cytosol localised

© University of Venda

(Figure 5.2B). This observation correlated with the cellular distribution of PfHsp70-z which was reported by Muralidharan and colleagues (2012), in the parasite cytosol.

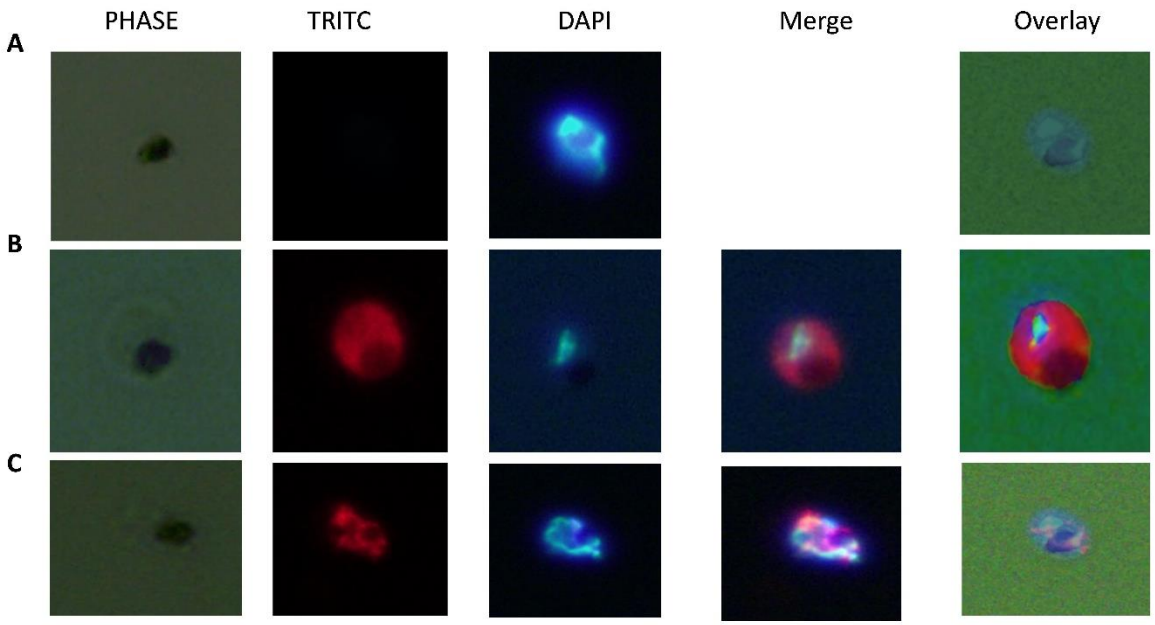

Figure 5.2: Localisation of PfHsp70-z and PfHsp70-1 in *P. falciparum* infected erythrocytes
Panels A, Negative control indicates phase contrast (PHASE) image and nucleus (DAPI), and overlay. **Panels B** indicates a (PHASE) image, localisation of PfHsp70-z (TRITC), nucleus stain (DAPI), merge and overlay of PfHsp70-z. **Panels C** indicates a (PHASE) image, localisation of PfHsp70-1 (TRITC), nucleus stain (DAPI), merge and overlay of PfHsp70-1.

Parasite cells were also probed using α-PfHsp70-1 and it was observed that PfHsp70-1 occurs in the cytosol (Figure 5.2C). These findings suggest the cytosolic co-localisation of PfHsp70-z and PfHsp70-1.

5.3.3 Immunoprecipitation and pull down assays

PfHsp70-z and PfHsp70-1 were reported to localize to the cytosol of the parasite (Section 5.3.2; Pesce *et al*., 2008; Muralidharan *et al*., 2012). This study sought to confirm the physical association of PfHsp70-z and PfHsp70-1 (Section 4.3.5; 4.3.6) in a cell based context. Immunoprecipitation and pull down studies were conducted using the α-PfHsp70-z antibodies and recombinant PfHsp70-z, respectively. The association of PfHsp70-1 and PfHsp70-z has been observed to be nucleotide sensitive (Section 4.3.5; 4.6). As a result, the study sought to establish whether the interaction of the PfHsp70-z and PfHsp70-1 was nucleotide-sensitive. A co-immunoprecipitation and pull down studies were conducted to

© University of Venda

establish the association of PfHsp70-z and PfHsp70-1 from parasite lysate. The α-PfHsp70-z antibodies coupled to protein A/G coupling resin were used for immunoprecipitation. Polyhistidine tagged recombinant PfHsp70-z immobilized on cobalt affinity matrix was used for pull down assay. The co-immunoprecipitation and pull down assays were conducted in the presence of ATP or ADP. The immunoprecipitation assay was analysed under reducing conditions and as such α-PfHsp70-z was reduced to heavy chain and light chains. The heavy chains were detected on the western blot as species of approximately 50 kDa. PfHsp70-1 appeared on the Western blot as a band of approximately 74 kDa (Figure 5.3A, B). These data indicate that PfHsp70-z and PfHsp70-1 may exist in a common complex in *P. falciparum.*

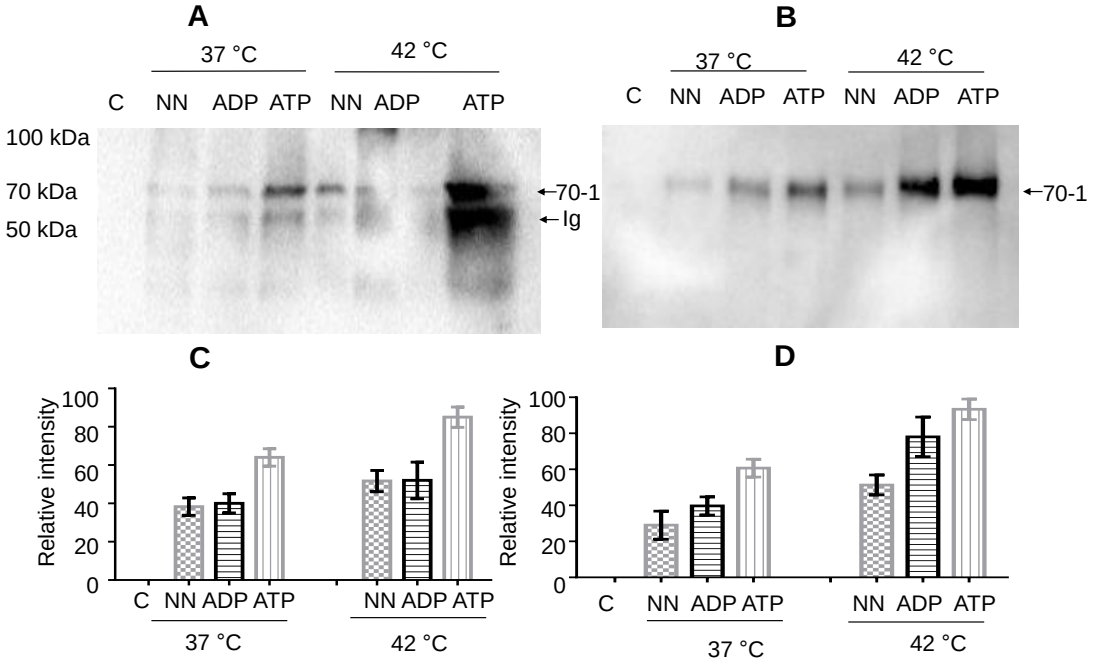

Figure 5.3: Immunoprecipitation and pull-down demonstrating association of PfHsp70-z and PfHsp70-1
Pulldown assays conducted using antibodies against PfHsp70-z and recombinant PfHsp70-z protein. Prey proteins in parasite cell lysate harvested from cultures growing under normal temperature (37 °C) and heat stress (42 °C) conditions. Prey protein was allowed to bind onto columns on which the antibody (A) or recombinant PfHsp70-z (B) were immobilized respectively. Binding was allowed to occur in the absence of nucleotide (NN), or presence of 5 µM ADP/ATP, respectively. The eluate was analysed under reducing conditions and subsequently probed by Western blot using anti-PfHsp70-1 antibodies. The representation of the densitometric analyses for data is provided (lower panels, C, D, respectively). Lane C, control sample (conducted on column with beads minus anti-PfHsp70-z or PfHsp70 recombinant protein); cell lysate used in control assay was obtained from culture incubated at 37 °C; lanes 37 °C, and 42 °C, immunoprecipitation conducted using cell lysate obtained from cells cultured at the respective temperatures which was allowed to bind to beads onto which anti-PfHsp70-z (A) or recombinant PfHsp70-z (B) were immobilized, respectively. Arrows in panel A show bands representing PfHsp70-1 (70-1) and Ig heavy chain (Ig), respectively.

In the current study, PfHsp70-1 appeared to interact with PfHsp70-z both in the presence of either ADP or ATP (Figure 5.3). However, it appears that less PfHsp70-1 associated with

© University of Venda

PfHsp70-z in the presence of ADP than in the presence of ATP from parasite lysates of cells maintained at 37 °C (Figure 5.3). Furthermore, the immunoprecipitation conducted in the presence of ADP show reduced apparent association of PfHsp70-1 with PfHsp70-z which when adjusted to the level of IgG heavy chain suggest that it was possibly a loading problem (Figure 5.3A). The assay was repeated for the lysate from cells that were subjected to heat shock at 42 °C to establish the effects of heat stress on the association of PfHsp70-z with PfHsp70-1. A previous study showed that PfHsp70-1 (Pesce *et al*., 2008) and PfHsp70-z (Section 5.3.1) are up-regulated in parasites under heat stress. The immunoblots of the eluates drawn from immunoprecipitation and pull down assays show enhanced pull down of PfHsp70-1 (Figure 5.3). The observations were confirmed by the densitometric analysis of the immunoblots (Figure 5.3 C; D). The findings suggests that PfHsp70-1 and PfHsp70-z maintain their association under heat stress. The assay was repeated in the presence of nucleotides (ATP/ADP). The observations show increased pull down of PfHsp70-1 with PfHsp70-z in the presence of ATP when compared to ADP (Figure 5.3). The densitometric analysis conducted on the immunoblots further affirms that ATP enhanced association of PfHsp70-z with PfHsp70-1 (Figure 5.3). Taken together, these observations suggest that heat stress and ATP promote the interaction of PfHsp70-1 and PfHsp70-z.

© University of Venda

5.4 Discussion

In light of the possible broad spectrum of functions for PfHsp70-z its importance in the survival of *P. falciparum* cannot be overemphasized. It was observed that PfHsp70-z is induced by heat stress in malaria parasites cultured at the blood stage (Figure 5.1). PfHsp70-z's up-regulation in response to heat stress suggests a key role for this protein in proteostasis.

The PfHsp70-z protein is a heat stable molecule (Sections 3.3.7; 3.3.8), highlighting it as an essential chaperone important for parasite survival under heat stress. PfHsp70-1 is known to be up-regulated during heat stress (Pesce *et al*., 2008). The up-regulation of both proteins suggest that these proteins are required for proteostasis during heat stress.

The current findings demonstrated the co-existence of PfHsp70-z and PfHsp70-1 in the parasite cytosol (Figure 5.2). The cytosolic co-localisation of PfHsp70-1 and PfHsp70-z may suggest that both proteins may functionally interact in close proximity facilitating proteostasis. Furthermore, co-immunoprecipitation and pull down assays validated that PfHsp70-z physically associates with PfHsp70-1 (Figure 5.3). The association of PfHsp70-1 with PfHsp70-z, as observed for recombinant forms of the proteins (Sections 4.3.5; 4.3.6), was enhanced by the presence of ATP. Heat stress induces over-expression of PfHsp70-z and PfHsp70-1, suggesting the formation of functional complexes under heat stress. Furthermore, PfHsp70-1 was found to form heat stable complexes with PfHsp70-z that co-immunoprecipitated (Figure 5.3). A pull down assay showed that recombinant PfHsp70-z associated with PfHsp70-1 from the parasite. This suggests that PfHsp70-1 recognised the recombinant PfHsp70-z partner further highlighting the specific interaction of these two proteins despite the different expression hosts.

In support of the current study, further work on investigation of the direct role of PfHsp70-z as PfHsp70-1 NEF would be essential in understanding the cellular role of this pathway in *P. falciparum*.

© University of Venda

CHAPTER 6

CONCLUSIONS AND FUTURE PERSPECTIVES

© University of Venda

6. Conclusion and Future Work

The current study provided evidence for the physical association between PfHsp70-z and PfHsp70-1. Although, the association of PfHsp70-z with PfHsp70-1 was mostly inferred based on evidence from the recombinant form through slot blot and SPR techniques, the evidence from immunoprecipitation further affirms that PfHsp70-z functionally interacts with PfHsp70-1. The cell based studies indicate that PfHsp70-z is required for survival during heat stress and that it forms stable complexes with PfHsp70-1. This highlights the importance of PfHsp70-z during fever episodes, but as a participant that interacts with PfHsp70-1 in maintaining proteostasis.

PfHsp70-z has been observed to suppress heat induced aggregation of model substrates (Section 4.3.4). *P. falciparum* encodes about 24 % of proteins possessing asparagine rich repeats which are prone to aggregation under heat stress (Singh *et al*., 2004b). PfHsp70-z is an essential molecule whose knock-out is lethal (Muralindaran *et al*., 2012). This highlights that PfHsp70-z's aggregation suppression function is important for parasite survival. Predictive studies previously conducted on *P. falciparum* suggest that PfHsp70-z is possibly the only cytosolic NEF of PfHsp70-1 (Shonhai *et al*., 2007; Bartrya *et al*., 2015). This suggests that the essential role of PfHsp70-z in parasite survival could be attributed to this unique function of the protein, apart from its role as chaperone (Muralindaran *et al*., 2012).

The interaction between PfHsp70-z and PfHsp70-1 may constitute a bottle neck for protein folding in *P. falciparum* which may be ideal for drug targeting. The main NEFs in other systems as in GrpE (Packschies *et al*., 1997), and Bag-1 (Sondermann *et al*., 2001) their cytosolic *P. falciparum* homologues have not been described. It was observed that the two chaperones PfHsp70-1 and PfHsp70-z are both localized in the cytosol of the parasite. Their co-localization in the same cell compartment possibly favours their direct interaction. This concurs with previous reports that cystolic Hsp110 directly interacts with Hsp70 as a NEF (Dragovic *et al*.,

© University of Venda

2006; Andreasson *et al*., 2008). Due to technical limitations this study failed to validate directly the nucleotide exchange function of PfHsp70-z on PfHsp70-1.

Sequence alignment data suggested that PfHsp70-z possesses conserved Hsp110 structural motifs both in the NBD and SBD that might be involved in mediating the PfHsp70-z-PfHsp70-1 partnership. Sequence variation observed between PfHsp70-z and its human orthologue could suggest structural variation; hence possible selective targeting of PfHsp70-z. This may possibly make PfHsp70-z a potential antimalarial drug target. Furthermore, PfHsp70-z, PfHsp70-1 and PfHsp90 are expressed at the clinical phase of malaria and their expression is reported to mirror malaria pathology (Pallavi *et al*., 2010). However, it still remains to be experimentally validated if PfHsp70-z and PfHsp90 directly interact. Chloroquine resistance in *P. falciparum* is mapped to a 50 kb segment of Chromosome 7, which includes the *PfHsp70-z* and *PfHsp90* genes (Su *et al*., 1997). This suggests that PfHsp70-z apart from its potential interaction with PfHsp90 in assisting client protein maturation, it may influence chloroquine resistance. Therefore, further characterisation of PfHsp70-z towards understanding its broad functions is important.

Hsp110-Hsp70 complexes have been implicated in cell division where they modulate the activity of the molecules kenesin-5 motor and cin8, which are required for spindle elongation in yeast and mammalian cells (Makhnevych *et al.,* 2013). The modulation of spindle elongation by molecular chaperones might be a mechanism in which cell division may be controlled under proteostatic stress. The rapid growth cycles of *P. falciparum* in the host facilitates its survival and may influence its pathogenesis (Gerald *et al*., 2011). Although it is unknown whether PfHsp70-z modulates spindle elongation in *P. falciparum*, it cannot be ruled out that its roles as chaperone and NEFs could regulate this pathway.

Previously it has been proposed that Hsp70 modulates actin filament growth (Tardieux *et al*., 1998a; b). Actin is thought to participate in vesicle trafficking facilitating endocytosis (Smythe

© University of Venda

et al., 2008) and the involvement of PfHsp70-1 in actin filament polymerization reinforces the importance of PfHsp70-z its functional partner, in parasite survival. Apart from prevention of aggregation (Muralidharan *et al*., 2012), PfHsp70-z may possibly interact with PfHsp70-1 in fundamental cell division and parasite invasion cycles.

The findings from this study suggest a possible broad spectrum of functions for PfHsp70-z protein. It is important to conduct further studies to elucidate the role of PfHsp70-z in cell cycle regulation and actin filament polymerisation. It is important that work done in this study be followed up with further elucidation of PfHsp70-z structure-functional features using X-ray crystallisation to resolve the protein's three dimensional structure.

© University of Venda

References

Acharya, P., Kumar, R., Tatu, U. (2007). Chaperoning a cellular upheaval in malaria: heat shock proteins in *Plasmodium falciparum*. *Mol Biochem Parasitol.* **153**: 85–94.

Akide-Ndunge, O. B., Tambini, E., Giribaldi, G., McMillan, P. J., Müller, S., Arese, P., Turrini, F. (2009). Co-ordinated stage-dependent enhancement of *Plasmodium falciparum* antioxidant enzymes and heat shock protein expression in parasites growing in oxidatively stressed or G6PD-deficient red blood cells. *Malar J*, **8**: 113.

Alderson, T. R., Kim, J. H., Cai, K., Frederick, R. O., Tonelli, M., Markley, J. L. (2014). The specialized Hsp70 (HscA) interdomain linker binds to its nucleotide-binding domain and stimulates ATP hydrolysis in both cis and trans configurations. *Biochemistry*, **53**: 7148-7159.

Andreasson, C., Fiaux, J. Rampelt, H., Druffel-Augustin, S., Bukau, B. (2008). Insights into the structural dynamics of the Hsp110-Hsp70 interaction reveal the mechanism for nucleotide exchange activity. *Proc Natl Acad Sci U S A,* **105**: 16519-16524.

Ang, D., Georgopoulos, C. (1989). The heat-shock-regulated GrpE gene of *Escherichia coli* is required for bacterial growth at all temperatures but is dispensable in certain mutant backgrounds. *J Bacteriol*, **171**: 2748-2755.

Angchaisuksiri, P. (2014). Coagulopathy in malaria. *Thromb Res*, **133**: 5–9.

Ansorge, I., Benting, J., Bhakdi, S., Lingelbach, K. (1996). Protein sorting in *Plasmodium falciparum*-infected red blood cells permeabilized with the pore-forming protein streptolysin O. *Biochem J,* **315**: 307–314

Archarya, P., Chaubey, S., Grover, M., Tatu, U. (2012). An exported heat shock protein 40 associates with pathogenesis-related knobs in *Plasmodium Falciparum* infected erythrocytes. *PLOS One,* **7**: e44605.

Asea, A., Rehli, M., Kabingu, E., Boch, J. A., Bare, O., Auron, P. E., Stevenson, M. A., Calderwood, S. K. (2002). Novel signal transduction pathway utilized by extracellular HSP70: role of toll-like receptor (TLR) 2 and TLR4. *J Biol Chem*, **277**: 15028-15034.

Ashburner, M., Ball, C.A., Blake, J.A., Botstein, D., Butler, H., Cherry, J.M., Davis, A.P., Dolinski, K., Dwight, S.S., Eppig, J.T., Harris, M.A., Hill, D.P., Issel-Tarver, L., Kasarskis, A., Lewis, S., Matese, J.C., Richardson, J.E., Ringwald, M., Rubin, G.M., Sherlock, G. (2000). Gene ontology: tool for the unification of biology. The gene ontology consortium. *Nat Genet,* **25**: 25-9.

Aslett, M., Aurrecoechea, C., Berriman, M., Brestelli, J., Brunk, B.P., Carrington, M., Depledge, D.P., Fischer, S., Gajria, B., Gao, X., Gardner, M.J., Gingle, A., Grant, G., Harb, O.S., Heiges, M., Hertz-Fowler, C., Houston, R., Innamorato, F., Iodice, J., Kissinger, J.C., Kraemer, E., Li, W., Logan, F.J., Miller, J.A., Mitra, S., Myler, P.J., Nayak, V., Pennington, C., Phan, I., Pinney, D.F., Ramasamy, G., Rogers, M.B., Roos, D.S., Ross, C., Sivam, D., Smith, D.F., Srinivasamoorthy, G., Stoeckert, C.J. Jr., Subramanian, S., Thibodeau, R., Tivey, A., Treatman, C., Velarde, G., Wang,

© University of Venda

H. (2010). TriTrypDB: a functional genomic resource for the Trypanosomatidae. *Nucleic Acids Res,* **38**: D457-D462.

Aurrecoechea, C., Brestelli, J., Brunk, B.P., Dommer, J., Fischer, S., Gajria, B., Gao, X., Gingle, A., Grant, G., Harb, O.S., Heiges, M., Innamorato, F., Iodice, J., Kissinger, J.C., Kraemer, E., Li, W., Miller, J.A., Nayak, V., Pennington, C., Pinney, D.F., Roos, D.S., Ross, C., Stoeckert, C.J. Jr., Treatman, C., Wang, H. (2009). PlasmoDB: a functional genomic database for malaria parasites. *Nucleic Acids Res,* **37**: D539-43.

Bahl, A., Brunk, B., Crabtree, J., Fraunholz, M. J., Gajria, B., Grant, G.R., Ginsburg, H., Gupta, D., Kissinger, J.C., Labo, P., Li, L., Mailman, M.D., Milgram, A.J., Pearson, D.S., Roos, D.S., Schug, J., Stoeckert, C.J. Jr., Whetzel, P. (2003). PlasmoDB: The Plasmodium genome resource. A database integrating experimental and computational data. *Nucleic Acids Res*, **31**: 212–215.

Bannister, L. H., Hopkins, J. M., Fowler, R. E., Krishna, S., Mitchell, G. H. (2000). The plastid in *Plasmodium falciparum* asexual blood stages: a three-dimensional ultra structural analysis. *Parasitol Today,* **16**: 427–433.

Bannister, L., Mitchell, G. (2003). The ins, outs and roundabouts of malaria. *Trends Parasitol,* **19**: 209-213.

Barnett, M. E., Nagy, M., Kedzierska, S., Zolkiewski, M. (2005). The amino-terminal domain of ClpB supports binding to strongly aggregated proteins. *J Biol Chem*, **280**: 34940-34945

Banumathy, G., Singh, V., Pavithra, S. R., Tatu, U. (2003). Heat shock protein 90 is essential for *Plasmodium falciparum* growth in human erythrocytes. *J Biol Chem*, **278**: 18336–18345.

Bascos, N. A. D., Landry, S. J. (2015). Structural rigidity regulates functional interactions in the Hsp40-Hsp70 molecular machine. *Biophys J*, **108**: 210a.

Baum, J., Gilberger, T. W., Frischknecht, F., Meissner, M. (2008). Host-cell invasion by malaria parasites: insights from Plasmodium and Toxoplasma. *Trends Parasitol*, **24**: 557–563.

Baumeister, S., Winterberg, M., Przyborski, J. M., Lingelbach, K. (2010). The malaria parasite *Plasmodium falciparum*: Cell biological peculiarities and nutritional consequences. *Protoplasma*, **240**: 3–12.

Bell, S. L., Chiang, A. N., Brodsky, J. L. (2011). Expression of a malarial Hsp70 improves defects in chaperone-dependent activities in ssa1 mutant yeast. *PLoS ONE*, **6**: 1–10.

Bercovich, B., Stancovski, I., Mayer, A., Blumenfeld, N., Laszlo, A., Schwartz, A. L. Ciechanover, A. (1997). Ubiquitin-dependent degradation of certain protein substrates *in vitro* requires the molecular chaperone Hsc70. *J Biol Chem,* **272**: 9002–9010.

Bhartiya, D., Chandramouli, B., Kumar, N. (2015). Co-evolutionary analysis implies auxiliary functions of HSP110 in *Plasmodium falciparum*. *Proteins,* **83**: 1513-25.

Biggs B.A., Gooze, T.L., Wycherley, K., Wollish, W., Southwell, B., Leech, J.H., G. V. Brown, G.V. (1991). Antigenic variation in *Plasmodium falciparum*. *Proc Natl Acad Sci USA*, **88**: 9171-9174.

© University of Venda

Billker, O., Shaw, M.K., Margos, G., Sinden, R.E. (1997). The roles of temperature, pH and mosquito factors as triggers of male and female gametogenesis of *Plasmodium berghei in-vitro*. *Parasitol,* **115**: 1-7.

Bimston, D., Song, J., Winchester, D., Takayama, S., Reed, J.C., Morimoto, R.I. (1998). BAG-1, a negative regulator of Hsp70 chaperone activity, uncouples nucleotide hydrolysis from substrate release. *EMBO J,* **17**: 6871–6878.

Botha, M., Chiang, A.N., Needham, P.G., Stephens, L.L., Hoppe, H.C., Külzer, S., Przyborski, J.M., Lingelbach, K., Wipf, P., Brodsky, J.L., Shonhai, A., Blatch, G.L. (2011). *Plasmodium falciparum* encodes a single cytosolic type I Hsp40 that functionally interacts with Hsp70 and is upregulated by heat shock. *Cell Stress Chaperones,* **16**: 389–401.

Botha, M., Pesce, E.R., Blatch, G.L. (2007). The Hsp40 proteins of *Plasmodium falciparum* and other apicomplexa: regulating chaperone power in the parasite and the host. *Int J Biochem Cell Biol,* **39**: 1781-803.

Boyle, M.J., Richards, J.S., Gilson, P.R., Chai, W., Beeson, J.G. (2010). Interactions with heparin-like molecules during erythrocyte invasion by *Plasmodium falciparum* merozoites. *Blood,* **115**: 4559-68.

Bracher, A., Verghese, J. (2015). GrpE, Hsp110/Grp170, HspBP1/Sil1 and BAG domain proteins: nucleotide exchange factors for Hsp70 molecular chaperones. *Subcell Biochem,* **78**:1-33.

Brandes, U. (2001). A faster algorithm for betweenness centrality. *J Math Sociol,* **25**: 163-177.

Buchberger, A., Schröder, H., Buttner, M., Valencia, A., Bukau, B. (1994). A conserved loop in the ATPase domain of the DnaK chaperone is essential for stable binding of GrpE. *Nat Struct Biol*, **1**: 95–101.

Buchberger, A., Theyssen, H., Schröder, H., McCarty, J. S., Virgallita, G., Milkereit, P., Reinstein, J., Bukau, B. (1995). Nucleotide-induced conformational changes in the ATPase and substrate binding domains of the DnaK chaperone provide evidence for interdomain communication. *J Biol Chem,* **270**: 16903–16910.

Buffet, P. A., Safeukui, I., Deplaine, G., Brousse, V., Prendki, V., Thellier, M., Turner, G.D., Mercereau-Puijalon, O. (2011). The pathogenesis of *Plasmodium falciparum* malaria in humans: insights from splenic physiology. *Blood*, **117**: 381-392.

Bukau, B., Walker, G. C. (1990). Mutations altering heat shock specific subunit of RNA polymerase suppress major cellular defects of *E. coli* mutants lacking the DnaK chaperone. *EMBO J,* **9**: 4027-4036.

Bukau, B., Weissman, J., Horwich, A. (2006). Molecular chaperones and protein quality control. *Cell*, **125**: 443–451.

Carlton, J. (2003). The *Plasmodium vivax* genome sequencing project. *Trends Parasitol*, **19**: 227–231.

© University of Venda

CDC (2014). Centers for Disease Control and Prevention. President's Malaria Initiative Seventh Annual Report, http://www.africairs.net/wp-content/uploads/2012/08/pmi_annual_report13.pdf.

Chiang, A.N., Valderramos, J.C., Balachandran, R., Chovatiya, R.J., Mead, B.P., Schneider, C., Bell, S.L., Klein, M.G., Huryn, D.M., Chen, X.S., Day, B.W., Fidock, D.A., Wipf, P., Brodsky, J.L. (2009). Select pyrimidinones inhibit the propagation of the malarial parasite, *Plasmodium falciparum*. *Bioorg Med Chem,* **17:** 1527-1533.

Cao, D., Froehlich, J.E., Zhang, H., Cheng, C. (2003). The chlorate-resistant and photomorphogenesis-defective mutant cr88 encodes a chloroplast-targeted HSP90. *Plant J*, **33**: 107- 118.

Charpian, S., Przyborski, J. M. (2008). Protein transport across the parasitophorous vacuole of *Plasmodium falciparum*: Into the great wide open. *Traffic*, **9**: 157–165.

Chatterjee, M., Andrulis, M., Stühmer, T., Müller, E., Hofmann, C., Steinbrunn, T., Heimberger, T., Schraud, H., Kressmann, S., Einsele, H., Bargou, R. C. (2013). The PI3k/Akt signaling pathway regulates the expression of Hsp70, which critically contributes to Hsp90-chaperone function and tumor cell survival in multiple myeloma. *Haematologica*, **98**: 1132–1141.

Cheetham, M. E., Caplan, A. J. (1998). Structure, function and evolution of DnaJ: conservation and adaptation of chaperone function. *Cell Stress Chaperones,* **3**: 28-36.

Chen, B., Retzlaff, M., Roos, T., Frydman, J. (2011). Cellular strategies of protein quality control. *Cold Spring Harb Perspect Biol*, **3**: 1–14.

Chou, P.Y., Fasman, G.D. (1978). Prediction of the secondary structure of proteins from their amino acid sequence. *Adv Enzymol Relat Areas Mol Biol*, **47**: 45-148.

Cintron, N. S., Toft, D. (2006). Defining the requirements for Hsp40 and Hsp70 in the Hsp90 chaperone pathway. *J Biol Chem*, **281**: 26235–26244.

Claessens, A., Hamilton, W.L., Kekre, M., Otto, T.D., Faizullabhoy, A., Rayner, J.C., Kwiatkowski, D. (2014). Generation of antigenic diversity in *Plasmodium falciparum* by structured rearrangement of Var genes during mitosis. *PLoS Genet,* **10**: e1004812.

Cockburn, I.L., E-R. Pesce, J.M. Pryzborski, M.T. Davies-Coleman and P.G.K. Clark, P.G., Keyzers, R.A., Stephens, L.L., Blatch, G.L. (2011). Screening for small molecule modulators of Hsp70 chaperone activity using protein aggregation suppression assays: Inhibition of the plasmodial chaperone PfHsp70-1. *Biol Chem*, **392**: 431-438.

Colvin, T.A., Gabai, V.L., Gong, J., Calderwood, S.K., Li, H., Gummuluru, S., Matchuk, O.N., Smirnova, S.G., Orlova, N.V., Zamulaeva, I.A., Garcia-Marcos, M., Li, X., Young, Z.T., Rauch, J.N., Gestwicki, J.E., Takayama, S., Sherman, M.Y. (2014). Hsp70-Bag3 interactions regulate cancer-related signaling networks. *Cancer Res*, **74**: 4731-40.

© University of Venda

Connell, P., Ballinger, C.A., Jiang, J., Wu, Y., Thompson, L.J., Höhfeld, J., Patterson, C. (2001). The cochaperone CHIP regulates protein triage decisions mediated by heat-shock proteins. *Nat Cell Biol,* **3**: 93–96.

Cooke, B. M., Buckingham, D. W., Glenister, F. K., Fernandez, K. M., Bannister, L. H., Marti, M., Mohandas, M., Coppel, R. L. (2006). A Maurer's cleft–associated protein is essential for expression of the major malaria virulence antigen on the surface of infected red blood cells. *J Cell Biol*, **172**: 899–908.

Cox, F.E.G. (2010). History of the discovery of the malaria parasites and their vectors. *Parasit Vectors,* **3**: 5.

Cox-Singh, J., Davis, T.M., Lee, K.S., Shamsul, S.S., Matusop, A., Ratnam, S., Rahman, H.A., Conway, D.J., Singh, B. (2008). *Plasmodium knowlesi* malaria in humans is widely distributed and potentially life threatening. *Clin Infect Dis,* **46**: 165-71.

Cowman, F., Berry, D., Baum, J. (2012). The cell biology of disease: The cellular and molecular basis for malaria parasite invasion of the human red blood cell. *J Cell Biol*, **198**: 961–971.

Cowman, A. F., Crabb, B. S. (2006). Invasion of red blood cells by malaria parasites. *Cell*, **124**: 755–766.

Crompton, P.D., Pierce, S.K., Miller, L.H. (2010). Advances and challenges in malaria vaccine development. *J Clin Invest,* **120**: 4168-78.

Cyr, D. M. (2008). Swapping nucleotides, tuning Hsp70. *Cell*, **133**: 945–947.

De, S., Babu, M. M. (2010). Genomic neighbourhood and the regulation of gene expression. *Curr Opin Cell Biol*, **22**: 326-333.

de Koning-Ward, T.F., Gilson, P.R., Boddey, J.A., Rug, M., Smith, B.J., Papenfuss, A.T., Sanders, P.R., Lundie, R.J., Maier, A.G., Cowman, A.F., Crabb, B.S. (2009). A newly discovered protein export machine in malaria parasites. *Nature*, **459**: 945–949.

Dobson, S., Kar, B., Kumar, R., Adams, B., Barik, S. (2001). A novel tetratricopeptide repeat (TPR) containing PP5 serine/threonine protein phosphatase in the malaria parasite *Plasmodium falciparum*. *BMC Microbiol,* **1**: 3.

Dodd, K., Nance, S., Quezada, M., Janke, L., Morrison, J.B., Williams, R.T., Beere, H.M. (2015). Tumor-derived inducible heat-shock protein 70 (HSP70) is an essential component of anti-tumor immunity. *Oncogene,* **34**: 1312-22.

Dondorp, A.M., Nosten, F., Yi, P., Das, D., Phyo, A.P., Tarning, J., Lwin, K.M., Ariey, F., Hanpithakpong, W., Lee, S.J., Ringwald, P., Silamut, K., Imwong, M., Chotivanich, K., Lim, P., Herdman, T., An, S.S., Yeung, S., Singhasivanon, P., Day, N.P., Lindegardh, N., Socheat, D., White, N.J. (2009). Artemisinin resistance in *Plasmodium falciparum* malaria. *N Engl J Med*, **361**: 455–467.

© University of Venda

Dondorp, A.M., Pongponratn, E. White, N. J. (2004). Reduced microcirculatory flow in severe *falciparum* malaria: pathophysiology and electron-microscopic pathology. *Acta Tropica,* **89**: 309-317.

Doyle, S.M., Shorter, J., Zolkiewski, M., Hoskins, J.R., Lindquist, S., Wickner, S. (2007). Asymmetric deceleration of ClpB or Hsp104 ATPase activity unleashes protein remodeling activity. *Nat Struct Mol Biol,* **14**: 114–122.

Dragovic, Z., Broadley, S.A., Shomura, Y., Bracher, A., Hartl, F.U. (2006). Molecular chaperones of the Hsp110 family act as nucleotide exchange factors of Hsp70s. *EMBO J.* **25**: 2519-2528.

Duval, L., Robert, V., Csorba, G., Hassanin, A., Randrianarivelojosia, M., Walston, J., Nhim, T., Goodman, S.M., Ariey, F. (2007). Multiple host-switching of Haemosporidia parasites in bats. *Malar J*, **6**: 157.

Dyson, H. J., Wright, P. E. (2005). Intrinsically unstructured proteins and their functions. *Nat Rev Mol Cell Biol*, **6**: 197–208.

Easton, D.P., Kaneko, Y., Subjeck, J.R. (2000). The Hsp110 and Grp170 stress proteins: newly recognized relatives of the Hsp70s. *Cell Stress Chaperones,* **5**: 276–290.

El Bakkouri, M., Pow, A., Mulichak, A., Cheung, K.L., Artz, J.D., Amani, M., Fell, S., de Koning-Ward, T.F., Goodman, C.D., McFadden, G.I., Ortega, J., Hui, R., Houry, W.A. (2010). The Clp chaperones and proteases of the human malaria parasite *Plasmodium falciparum*. *J Mol Biol,* **404**: 456-77.

Ellis, R. J. (1994) Opening and closing the Anfinsen cage. *Curr Biol,* **4**: 633-635.

Fan, C.-Y., Lee, S., Cyr, D. M. (2003). Mechanisms for regulation of Hsp70 function by Hsp40. *Cell Stress Chaperones*, **8**: 309–316.

Fan, Q., Park, K. W., Du, Z., Morano, K. A., Li, L. (2007) The role of Sse1 in the de novo formation and variant determination of the [PSI+] prion. *Genetics,* **177**: 1583–1593.

Fayet, O., Ziegelhoffer, T., Georgopoulos, C. (1989). The GroES and GroEL heat shock gene products of *Escherichia coli* are essential for bacterial growth at all temperatures. *J Bacteriol*, **171**: 1379-85.

Finka, A., Goloubinoff, P. (2013). Proteomic data from human cell cultures refine mechanisms of chaperone-mediated protein homeostasis. *Cell Stress Chaperones,* **18**: 591-605.

Finka, A., Sood, V., Quadroni, M., Rios, P. D. L., Goloubinoff, P. (2015). Quantitative proteomics of heat-treated human cells show an across-the-board mild depletion of housekeeping proteins to massively accumulate few HSPs. *Cell Stress Chaperones*, **20**: 605–620.

Flaherty, K.M., Deluca-Flaherty, C., McKay, D.B. (1990). Three-dimensional structure of the ATPase fragment of a 70K heat-shock cognate protein. *Nature*, **346**: 623–628.

© University of Venda

Fujioka, H., Aikawa, M. (2002). Structural and life cycle. In: *Malaria and parasite and disease*, (eds). Troye-Blomberg, M., and Perlmann, P. pp 1-26.

Gambill, B. D., Voos, W., Kang, P. J., Miao, B., Langer, T., Craig, E. A., and Pfanner, N. (1993). A dual role for mitochondrial heat shock protein 70 in membrane translocation of preproteins. *J Cell Biol,* **123**: 109-17.

Gardner, M. J., Hall, N., Fung, E., White, O., Berriman, M., Hyman, R. W., Carlton, J.M., Pain, A., Nelson, K.E., Bowman, S., Paulsen, I.T., James, K., Eisen, J.A., ,Rutherford, K., Salzberg, S.L., Craig, A., Kyes, S., Chan, M.S., Nene, V., Shallom, S.J., Suh, B., Peterson, J., Angiuoli, S., Pertea, M., Allen, J., Selengut, J., Haft, D., Mather, M.W., Vaidya, A.B., Martin, D.M., Fairlamb, A.H., Fraunholz, M.J., Roos, D.S., Ralph, S.A., McFadden, G.I., Cummings, L.M., Subramanian, G.M., Mungall, C., Venter, J,C., Carucci, D.J., Hoffman, S.L., Newbold, C., Davis, R.W., Fraser, C.M., Barrell, B. (2002). Genome sequence of the human malaria parasite *Plasmodium falciparum*. *Nature*, **419**: 498-511

Gerald, N., Mahajan, B., Kumar, S. (2011). Mitosis in the human malaria parasite *Plasmodium falciparum. Eukaryot Cell,* **10**: 474–482.

Gitau, G.W., Mandal, P., Blatch, G.L., Przyborski, J., Shonhai, A. (2012). Characterization of the *Plasmodium falciparum* Hsp70-Hsp90 organising protein (PfHop). *Cell Stress and Chaperone,* **17**: 191-202.

Glover, J.R., Lindquist, S. (1998). Hsp104, Hsp70, and Hsp40: a novel chaperone system that rescues previously aggregated proteins. *Cell*, **94**: 73–82.

Goeckeler, J. L., Petruso, A. P., Aguirre, J., Clement, C. C., Chiosis, G., Brodsky, J. L. (2008). The yeast Hsp110, Sse1p, exhibits high-affinity peptide binding. *FEBS Lett*, **582**: 2393–2396.

Goeckeler, J.L., Stephens, A., Lee, P., Caplan, A.J., Brodsky, J.L. (2002). Overexpression of yeast Hsp110 homolog Sse1p suppresses ydj1-151 thermosensitivity and restores Hsp90-dependent activity. *Mol Biol Cell*, **13**: 2760–2770.

Goel, S., Muthusamy, A., Miao, J., Cui, L., Salanti, A., Winzeler, E.A., Gowda, D.C. (2014) Targeted disruption of a ring-infected erythrocyte surface antigen (RESA)-like export protein gene in *Plasmodium falciparum* confers stable chondroitin 4-sulfate cytoadherence capacity. *J Biol Chem*, **289**: 34408-21.

Grüring, C. Heiber, A., Kruse, F., Flemming, S., Franci, G., Colombo, S.F., Fasana, E., Schoeler, H., Borgese, N., Stunnenberg, H.G., Przyborski, J.M., Gilberger, T-W., Spielmann, T. (2012) Uncovering common principles of protein export of malaria parasites. *Cell Host Microbe*, **12**: 717-729.

Hall, N., Karras, M., Raine, J. D., Carlton, J. M., Kooij, T. W. , Berriman, M., Florens, L., Janssen, C.S., Pain, A., Christophides, G.K., James, K., Rutherford, K., Harris, B., Harris, D., Churcher, C., Quail, M.A., Ormond, D., Doggett, J., Trueman, H.E., Mendoza, J., Bidwell, S.L., Rajandream, M.A., Carucci, D.J., Yates, J.R. 3rd, Kafatos, F.C., Janse, C.J., Barrell, B., Turner, C.M., Waters, A.P., Sinden, R. E. (2005). A comprehensive survey of the Plasmodium life cycle by genomic, transcriptomic, and proteomic analyses. *Science*, **307**: 82–86.

© University of Venda

Harrison, C. J., Hayer-Hartl, M., Di Liberto, M., Hartl, F., Kuriyan, J. (1997). Crystal structure of the nucleotide exchange factor GrpE bound to the ATPase domain of the molecular chaperone DnaK. *Science*, **276**: 431—435.

Harrison T., Samuel B. U., Akompong T., Hamm H., Mohandas N., Lomasney J. W., Haldar K. (2003). Erythrocyte G protein-coupled receptor signaling in malarial infection. *Science*, **301**: 1734–1736.

Harst, A., Lin, H., Obermann, W. M. J. (2005). Aha1 competes with Hop, p50 and p23 for binding to the molecular chaperone Hsp90 and contributes to kinase and hormone receptor activation. *Biochem J*, **387**: 789–796.

Hartwig, C.L., Rosenthal, A.S., D'Angelo, J., Griffin, C.E., Posner, G.H., Cooper, R.A. (2009). Accumulation of artemisinin trioxane derivatives within neutral lipids of *Plasmodium falciparum* malaria parasites is endoperoxide-dependent. *Biochem Pharmacol,* **77**: 322-36.

Haslbeck, M., Franzmann, T., Weinfurtner, D., Buchner, J. (2005). Some like it hot: the structure and function of small heat-shock proteins. *Nat Struct Mol Biol,* **12**: 842–846.

Hatayama, T., Yamagishi, N., Minobe, E., Sakai, K. (2001). Role of Hsp105 in protection against stress-induced apoptosis in neuronal PC12 cells. *Biochem Biophys Res Commun,* **288**: 528–534.

Hayward, R. E., Derisi, J. L., Kaslow, D. C., Brown, P. O., Rathod, P. K. (2000). Shotgun DNA microarrays and stage-specific® gene expression in *Plasmodium falciparum* malaria. *Mol Microbiol*, **35**: 6-14.

Hempel, F., Bullmann, L., Lau, J., Zauner, S. Maier, U.G. (2009). ERAD-derived pre-protein transport across the second outermost plastid membrane of diatoms. *Mol Biol Evol,* **26**: 1781–1790.

Hennessy, F., Nicoll, W. S., Zimmermann, R., Cheetham, M. E., Blatch, G. L. (2005). Not all J domains are created equal: implications for the specificity of Hsp40-Hsp70 interactions. *Protein Sci*, **14**: 1697–1709.

Hesterkamp, T., Hauser, S., Lütcke, H., Bukau, B. (1996). *Escherichia coli* trigger factor is a prolyl isomerase that associates with nascent polypeptide chains. *Proc Natl Acad Sci U S A*, **93**: 4437–4441.

Hiller, N.L., Bhattacharjee, S., van Ooij, C., Liolios, K., Harrison, T., Lopez-Estrano, C., Haldar, K. (2004). A host targeting signal in virulence proteins reveals a secretome in malarial infection. *Science.* **306:** 1934–1937.

Hoffmann, A., Bukau, B., Kramer, G. (2010). Structure and function of the molecular chaperone Trigger Factor. *Biochim Biophys Acta*, **1803**: 650–661.

Horne, B. E., Li, T., Genevaux, P., Georgopoulos, C., Landry, S. J. (2010). The Hsp40 J-domain stimulates Hsp70 when tethered by the client to the ATPase domain. *J Biol Chem*, **285**: 21679–21688.

© University of Venda

Houry, W. A., Frishman, D., Eckerskorn, C., Lottspeich, F., Hartl, F. U. (1999). Identification of *in vivo* substrates of the chaperonin GroEL. *Nature,* **402**: 147-154.

Hrizo, S.L., Gusarova, V., Habiel, D.M., Goeckeler, J.L., Fisher, E.A., Brodsky, J.L. (2007). The Hsp110 molecular chaperone stabilises apolipoprotein B from endoplamic reticulum-associated degradation (ERAD). *J Biol Chem,* **282**: 32665-32675.

Hsu, W. T., Pang, C. N. I., Sheetal, J., Wilkins, M. R. (2007). Protein-protein interactions and disease: Use of S. cerevisiae as a model system. *BBA-Proteins and proteomics*, **1774**: 838–847.

Hunt, N.H., Golenser, J., Chan-Ling, T., Parekh, S., Rae, C., Potter, S., Medana, I.M., Miu, J., Ball, H.J. (2006). Immunopathogenesis of cerebral malaria. *Int J Parasitol*, **36**: 569-82.

Inobe T, Takahashi K, Maki K, Enoki S, Kamagata K, Kadooka, A., Arai, M., Kuwajima, K. (2008). Asymmetry of the GroEL-GroES complex under physiological conditions as revealed by small-angle X-ray scattering. *Biophys J*, **94**: 1392–1402.

Jackson, S.E. (2013). Hsp90: structure and function. *Top Curr Chem*, **328**: 155-240.

Jameson, B.A., Wolf, H. (1988). The antigenic index: a novel algorithm for predicting antigenic determinants. *Comput Appl Biosci,* **4**: 181-6.

Janouskovec, J., Horák, A., Oborník, M., Lukes, J., Keeling, P. J. (2010). A common red algal origin of the apicomplexan, dinoflagellate, and heterokont plastids. *Proc Natl Acad Sci U S A*, **107**: 10949–10954.

Jensen, L. J., Kuhn, M., Stark, M., Chaffron, S., Creevey, C., Muller, J., Doerks, T., Julien, P., Roth, A., Simonovic, M., Bork, P., von Mering, C. (2009). STRING 8 - A global view on proteins and their functional interactions in 630 organisms. *Nucleic Acids Res*, **37**: 412–416.

Johnson, J. L. (2012). Evolution and function of diverse Hsp90 homologs and cochaperone proteins. *BBA - Molecular Cell Research*, **1823**: 607–613.

Johnson, J.L., Brown, C. (2009). Plasticity of the Hsp90 chaperone machine in divergent eukaryotic organisms. *Cell Stress Chaperones*, **14**: 83-94.

Kappes, B., Suetterlin, B. W., Hofer-Warbinek, R., Humar, R., Franklin, R. M. (1993). Two major phosphoproteins of *Plasmodium falciparum* are heat shock proteins. *Mol Biochem Parasitol*, **59**: 83-94.

Kabani, M., Martineau, C. N. (2008). Multiple Hsp70 isoforms in the eukaryotic cytosol: mere redundancy or functional specificity? *Curr Genomics*, **9**: 338–248.

Kampinga, H. H., Craig, E. (2010). The Hsp70 chaperone machinery: J proteins as drivers of functional specificity. *Nat Rev Mol Cell Biol*, **11**: 579–592.

Kampinga, H. H., Hageman, J., Vos, M. J., Kubota, H., Tanguay, R. M., Bruford, E., Cheetham, M.E., Chen, B., Hightower, L. E. (2009). Guidelines for the nomenclature of the human heat shock proteins. *Cell Stress Chaperones*, **14**: 105–111.

© University of Venda

Kaneko, Y., Kimura, T., Nishiyama, H., Noda, Y., Fujita, J. (1997a). Developmentally regulated expression of APG-1, a member of heat shock protein 110 family in murine male germ cells. *Biochem Biophys Res Commun,* **233:** 113–116.

Kaneko, Y., Nishiyama, H., Nonoguchi, K., Higashitsuji, H., Kishishita, M., Fujita, J. (1997b). A novel Hsp110-related gene, apg-1, that is abundantly expressed in the testis responds to a low temperature heat shock rather than the traditional elevated temperatures. *J Biol Chem,* **272**: 2640–2645.

Karplus, P.A., Schulz, G.E. (1985). Prediction of chain flexibility in proteins: A tool for the selection of peptide antigens. *Naturwissenschaften*, **72**: 212-213.

Katoh, K., Standley, D. M. (2013). MAFFT multiple sequence alignment software version 7: Improvements in performance and usability. *Mol Biol Evolution*, **30**, 772–780.

Kelley, L., Sternberg, M. J. E. (2009). Protein structure prediction on the Web: a case study using the Phyre server. *Nat Protoc*, **4**: 363–371.

Kelley, L.A., Mezulis, S., Yates, C.M., Wass, M.N., Sternberg, M.J. (2015). The Phyre2 web portal for protein modeling, prediction and analysis. *Nat Protoc*, **10**: 845-58.

Kilili, G. K., La Count, D. J. (2011). An erythrocyte cytoskeleton-binding motif in exported *plasmodium falciparum* proteins. *Eukaryot Cell*, **10**: 1439–1447.

Kityk, R., Kopp, J., Sinning, I., Mayer, M. P. (2012). Structure and dynamics of the ATP-bound open conformation of Hsp70 chaperones. *Mol Cell*, **48**: 863–874.

Kriegenburg, F., Ellgaard, L., Hartmann-Petersen, R. (2012). Molecular chaperones in targeting misfolded proteins for ubiquitin-dependent degradation. *FEBS J*, **279**: 532–542.

Koella, J.C., Sørensen, F.L., Anderson, R.A. (1998). The malaria parasite, *Plasmodium falciparum*, increases the frequency of multiple feeding of its mosquito vector, *Anopheles gambiae*. *Proc Biol Sci,* **265**: 763–768.

Kraemer, S.M. (2006). A family affair: var genes, PfEMP1 binding, and malaria disease. *Curr Opin Microbiol*, **9**:374-80.

Krukenberg, K., Street, T. O., Lavery, L., Agard, D. (2011). Conformational dynamics of the molecular chaperone Hsp90. *Q Rev Biophys*, **44**: 229–255.

Kryndushkin, D., Wickner, R. B. (2007) Nucleotide exchange factors for Hsp70s are required for [URE3] prion propagation in *Saccharomyces cerevisiae*. *Mol Biol Cell,* **18**: 2149–2154.

Külzer, S., Charnaud, S., Dagan, T., Riedel, J., Mandal, P., Pesce, E. R., Blatch, G.L., Crabb, B.S., Gilson, P.R., Przyborski, J. M. (2012). *Plasmodium falciparum*-encoded exported Hsp70/Hsp40 chaperone/co-chaperone complexes within the host erythrocyte. *Cell Microbiol*, **14**: 1784–1795.

© University of Venda

Külzer, S., Rug, M., Brinkmann, K., Cannon, P., Cowman, A., Lingelbach, K., Blatch, G.L., Maier, A.G., Przyborski, J.M. (2010). Parasite-encoded Hsp40 proteins define novel mobile structures in the cytosol of the *P. falciparum*-infected erythrocyte. *Cell Microbiol,* **12:** 1398–1420.

Kumar, D. P., Vorvis, C., Sarbeng, E. B., Cabra Ledesma, V. C., Willis, J. E., Liu, Q. (2011). The four hydrophobic residues on the Hsp70 inter-domain linker have two distinct roles. *J Mol Biol*, **411**: 1099–1113.

Kumar, N., Koski, G., Harada, M., Aikawa, M., Zheng, H. (1991). Induction and localisation of *Plasmodium falciparum* stress proteins related to the heat shock protein 70 family. *Mol Biochem Parasitol*, **48**: 47–58.

Kumar, R., Musiyenko, A., Barik, S. (2003). The heat shock protein 90 of *Plasmodium falciparum* and antimalarial activity of its inhibitor, geldanamycin. *Malar J*, **2**: 30

Kurt, N., Rajagopalan, S., Cavagnero, S. (2006). Effect of Hsp70 chaperone on the folding and misfolding of polypeptides modeling an elongating protein chain. *J Mol Bio*, **355**: 809–820.

Kurtz, S., Rossl, J., Petko, L., Lindquist, S. (1986). An ancient developmental induction: Heat-shock proteins induced in sporulation and oogenesis. *Science* **231:** 1154-1157.

Kyte, J., Doolittle, R.F. (1982). A simple method for displaying the hydropathic character of a protein. *J Mol Biol*, **157**:105-32.

LaCount, D.J., Vignali, M., Chettier, R., Phansalkar, A., Bell, R., Hesselberth, J.R., Schoenfeld, L.W., Ota, I., Sahasrabudhe, S., Kurschner, C., Fields, S., Hughes, R.E. (2005). A protein interaction network of the malaria parasite *Plasmodium falciparum*. *Nature,* **438**: 103-7.

Langer, T., Lu, C., Echols, H., Fianagan, J., Hayer, M. K., Hartl, F. U. (1992). Successive action of DnaK, DnaJ and GroEL along the pathway of chaperone-mediated protein folding. *Nature,* **356**: 683-689.

Lasonder E, Janse CJ, van Gemert G-J, Mair GR, Vermunt AMW, Douradinha BG, van Noort V, Huynen MA, Luty AJ, Kroeze H, Khan SM, Sauerwein RW, Waters AP, Mann M, Stunnenberg HG. (2008). Proteomic profiling of Plasmodium sporozoite maturation identifies new proteins essential for parasite development and infectivity. *PLoS Pathog*, **4**: e1000195.

Laufen, T., Mayer, M. P., Beisel, C., Klostermeier, D., Reinstein, J. and Bukau, B. (1999). Mechanism of regulation of Hsp70 chaperones by DnaJ co-chaperones. *Proc Natl Acad Sci USA,* **96**: 5452–5457.

Lehninger, A.L.; Nelson, D.L.; Cox, M.M. (2005). *Lehninger principles of Biochemistry*. New York: W.H. Freeman. ISBN 978-0-7167-4339-2.

Le Roch, K.G., Zhou, Y., Blair, P.L., Grainger, M., Moch, J.K., J. Haynes, D., De la Vega, P., Holder, A.A., Batalov, S., Carucci, D.J., Winzeler, E.A., (2003). Discovery of gene function by expression profiling of the malaria parasite life cycle. *Science,* **301**: 1503-1508.

© University of Venda

Li Z., Hartl, F.U., Bracher, A. (2013). Structure and function of Hip, an attenuator of the Hsp70 chaperone cycle. *Nat Struct Mol Biol,* **20**: 929-35.

Liberek, K., Marszalek, J., Ang, D., Georgopoulos, C. Zylicz, M. (1991). *Escherichia coli* DnaJ and GrpE heat shock proteins jointly stimulate ATPase activity of DnaK. *Proc Natl Acad Sci USA,* **88**: 2874–2878.

Lindquist, S., Craig, E.A. (1988). The heat-shock proteins. *Annu Rev Genet,* **22**: 631– 677.

Liu, Q., Hendrickson, W.A. (2007). Insights into Hsp70 chaperone activity from a crystal structure of the yeast Hsp110 Sse1. *Cell*, **131**: 106–120.

Lucas, J.Z., Sherman, I.W. (1998). *Plasmodium falciparum*: thrombospondin mediates parasitized erythrocyte band 3-related adhesin binding. *Exp Parasitol*, **89**: 78-85

Lüders, J., Demand, J., Höhfeld, J. (2000). The ubiquitin-related BAG-1 provides a link between the molecular chaperones Hsc70/Hsp70 and the proteasome. *J Biol Chem,* **275**: 4613-4617.

Luthuli, S. D., Chili, M. M., Revaprasadu, N., Shonhai, A. (2013). Cysteine-capped gold nanoparticles suppress aggregation of proteins exposed to heat stress. *IUBMB Life*, **65**: 454–461.

Maier, A.G., Rug, M., O'Neill, M.T., Brown, M., Chakravorty, S., Szestak, T., Chesson, J., Wu, Y., Hughes, K., Coppel, R.L., Newbold, C., Beeson, J.G., Craig, A., Crabb, B, B., Cowman, A.F. (2008). Exported proteins required for virulence and rigidity of *Plasmodium falciparum*-infected human erythrocytes. *Cell,* **134**: 46-61.

Makhnevych, T., Wong, P., Pogoutse, O., Vizeacoumar, F.J., Greenblatt, J.F., Emili, A., Houry, W.A. (2012). Hsp110 is required for spindle length control. *J Cell Biol*, **198**: 623–636.

Malinverni, D., Marsili, S., Barducci, A., De Los Rios, P. (2015). Large-scale conformational transitions and dimerization are encoded in the amino-acid sequences of Hsp70 chaperones. *PLoS Comput Biol*, **11**: e1004262.

Mandal, A. K., Gibney, P. A., Nillegoda, N. B., Theodoraki, M. A., Caplan, A. J., Morano, K. A. (2010). Hsp110 chaperones control client fate determination in the Hsp70-Hsp90 chaperone system. *Mol Bio Cell,* **21**: 1439-2448.

Manjili, M. H., Henderson, R., Wang, X. Y., Chen, X., Li, Y., Repasky, E., Kazim, L., Subjeck, J. R. (2002). Development of a recombinant HSP110-HER-2/neu vaccine using the chaperoning properties of HSP110. *Cancer Res*, **62**: 1737–1742.

Marcion, G., Seigneuric, R., Chavanne, E., Artur, Y., Briand, L., Hadi, T., Gobbo, J., Garrido, C., Neiers, F. (2014). C-terminal amino acids are essential for human heat shock protein 70 dimerization. *Cell Stress Chaperones*, **20**: 61–72.

Marti, M., Good, R.T., Rug, M., Knuepfer, E., Cowman, A.F. (2004). Targeting malaria virulence and remodelling proteins to the host erythrocyte. *Science,* **306:** 1930–1933.

© University of Venda

Martin, J., Langer, T., Boteva, R., Schramel, A., Horw1cha, L., Hartl, F. U. (1991). Chaperonin-mediated protein folding at the surface of GroEL through a 'Molten Globule'-like Intermediate. *Nature*, ***352***: 36-42.

Martins, Y. C., Daniel-Ribeiro, C. T. (2013). A new hypothesis on the manifestation of cerebral malaria: The secret is in the liver. *Med Hypotheses*, **81**: 777–783.

Matambo, T. S., Odunuga, O. O., Boshoff, A., Blatch, G. L. (2004). Overproduction, purification, and characterization of the *Plasmodium falciparum* heat shock protein 70. *Protein Expr Purif*, **33**: 214–222.

Mayer, M. P. (2010). Gymnastics of molecular chaperones. *Mol Cell*, **39**: 321–331.

Mayer, M. P. (2013). Hsp70 chaperone dynamics and molecular mechanism. *Trends Biochem Sci*, **38**: 507–514.

Mayer, M.P., Bukau B. (2005). Hsp70 chaperones: cellular functions and molecular mechanism. *Cell Mol Life Sci,* **62**: 670–684.

Mayer, M. P., Schröder, H., Rüdiger, S., Paal, K., Laufen, T., Bukau, B. (2000). Multistep mechanism of substrate binding determines chaperone activity of Hsp70. *Nat Struct Biol*, **7**: 586-593.

Maynard, J.C., Pham, T., Zheng, T., Jockheck-Clark, A., Rankin, H.B., Newgard, C.B., Spana, E.P., Nicchitta, C.V. (2010). Gp93, the Drosophila GRP94 ortholog, is required for gut epithelial homeostasis and nutrient assimilation-coupled growth control. *Dev Biol,* **339**: 295-306.

McCallum, C. D., Do, H., Johnson, A. E., Frydman, J. (2000). The interaction of the chaperonin tailless complex polypeptide 1 (TCP1) ring complex (TRiC) with ribosome-bound nascent chains examined using photo-cross-linking. *J Cell Biol*, **149**: 591-602.

Merrick, C. J., Huttenhower, C., Buckee, C., Amambua-ngwa, A., Gomez-escobar, N., Walther, M., Conway, D.J., Duraisingh, M. T. (2012). Epigenetic dysregulation of virulence gene expression in severe *Plasmodium falciparum* malaria. *J Infect Dis,* **205**: 1593-600.

Miller, L.H., Good, M.F., Milon, G. (1994). Malaria pathogenesis. *Science*, **264**: 1878-83.

Storm, J., Craig, A.G. (2014). Pathogenesis of cerebral malaria—inflammation and cytoadherence. *Front Cell Infect Microbiol,* **4**: 100.

Misra, G., Ramachandran, R. (2009). Hsp70-1 from *Plasmodium falciparum*: protein stability, domain analysis and chaperone activity. *Biophys Chem,* **142**: 55-64.

Mogk, A., Kummer, E., Bukau, B. (2015). Cooperation of Hsp70 and Hsp100 chaperone machines in protein disaggregation. *Front Mol Biosci,* **2**: 22.

Mogk, A, Tomoyasu, T., Goloubinoff, P., Rüdiger, S., Röder, D., Langen, H., Bukau, B. (1999). Identification of thermolabile *Escherichia coli* proteins: prevention and reversion of aggregation by DnaK and ClpB. *EMBO J,* **18**: 6934–6949.

© University of Venda

Mohandas, N., An, X. (2012). Malaria and Human Red Blood Cells. *Med Microbiol Immunol,* **201**: 593–598.

Moran, C., Kinsella, G. K., Zhang, Z.-R., Perrett, S., Jones, G. W. (2013). Mutational analysis of Sse1 (Hsp110) suggests an integral role for this chaperone in yeast prion propagation in vivo. *Genes Genomes Genetics*, **3**: 1409–18.

Morrison, D. (2008). Prospects for elucidating the phylogeny of the Apicomplexa. *Parasite*, **15**, 191–196.

Morrison, D. (2009). Evolution of the Apicomplexa: where are we now? *Trends in Parasitol*, **25**: 375–382.

Morrissette, N. S., Sibley, L. D. (2002). Cytoskeleton of apicomplexan parasites. *Microbiol Mol Biol Rev,* **66**: 21–38.

Mu, J., Myers, R.A., Jiang, H., Liu, S., Ricklefs, S., Waisberg, M., Chotivanich, K., Wilairatana, P., Krudsood, S., White, N.J., Udomsangpetch, R., Cui, L., Ho, M., Ou, F., Li, H., Song, J., Li, G., Wang, X., Seila, S., Sokunthea, S., Socheat, D., Sturdevant, D.E., Porcella, S.F., Fairhurst, R.M., Wellems, T.E., Awadalla, P., Su, X.Z. (2010). *Plasmodium falciparum* genome-wide scans for positive selection, recombination hot spots and resistance to antimalarial drugs. *Nat Genet*, **42**: 268–271.

Murphy, M. E. (2013). The Hsp70 family and cancer. Carcinogenesis, **34**: 1181–1188.

Muralidharan, V., Oksman, A., Pal, P., Lindquist, S., Goldberg, D.E. (2012). *Plasmodium falciparum* heat shock protein 110 stabilizes the asparagine repeat-rich parasite proteome during malarial fevers. *Nat Commun,* **3**:1310.

Nebl, T., De Veer, M.J., Schofield, L. (2005). Stimulation of innate immune responses by malarial glycosylphosphatidylinositol via pattern recognition receptors. *Parasitology,* **130**: S45-62.

Needham, P. G., Patel, H. J., Chiosis, G., Thibodeau, P. H., Brodsky, J. L. (2015). Mutations in the Yeast Hsp70, Ssa1, at P417 Alter ATP Cycling, interdomain coupling, and specific chaperone functions. *J Mol Biol*, **427**: 2948-65.

Newman, M. E. J. (2003). A measure of Betweenness based on random walks. *Social Networks,* **27:** *39–54.*

Nicolet CM, Craig EA (1989) Isolation and characterization of STI1, a stress-inducible gene from *Saccharomyces cerevisiae*. *Mol Cell Biol*, **9**: 3638–3646.

Njunge, J.M, Ludewig, M.H, Boshoff, A., Pesce, E., Blatch, G.L. (2013). Hsp70s and J proteins of Plasmodium parasites infecting rodents and primates: structure, function, clinical relevance, and drug targets. *Curr Pharm Des*, **19**: 387-403.

© University of Venda

Njunge, J. M., Mandal, P., Przyborski, J. M., Boshoff, A., Pesce, E.-R., Blatch, G. L. (2015). PFB0595w is a *Plasmodium falciparum* J protein that co-localizes with PfHsp70-1 and can stimulate its in vitro ATP hydrolysis activity. *Int J Biochem Cell Biol*, **62**: 47–53.

Nowicki, Ł., Leźnicki, P., Morawiec, E., Litwińczuk, N., Liberek, K. (2012). Role of a conserved aspartic acid in nucleotide binding domain 1 (NBD1) of Hsp100 chaperones in their activities. *Cell Stress Chaperones*, **17**: 361–373.

Nyalwidhe, J., Baumeister, S., Hibbs, A.R., Tawill, S., Papakrivos, J., Volker, U., Lingelbach, K. (2002). A nonpermeant biotin derivative gains access to the parasitophorous vacuole in *Plasmodium falciparum*-infected erythrocytes permeabilized with streptolysin O. *J Bioll Chem*, **277**: 40005-11.

Nyalwidhe, J., Lingelbach, K. (2006). Proteases and chaperones are the most abundant proteins in the parasitophorous vacuole of *Plasmodium falciparum*-infected erythrocytes. *Proteomics,* **6**: 1563-1573.

Oakley, M.S.M., Kumar, S., Anantharaman, V., Zheng, H., Mahajan, B., Haynes, J.D., Moch, J.K., Fairhurst, R., McCutchan, T.F., Aravind, L. (2007). Molecular factors and biochemical pathways induced by febrile temperature in intra erythrocytic *Plasmodium falciparum* parasites. *Infect Immun,* **75:** 2012-2025.

Oh, H.J., Chen, X., Subjeck, J.R., (1997) Hsp110 protects heat-denatured proteins and confers cellular thermoresistance. *J Biol Chem*, **272**: 31636–31640.

Oh, H.J., Eston, D., Murawski, M., Kaneneko, Y., Subjeck, J.R., (1999). The chaperoning activity of Hsp110: Identification of functional domains by use of targeted deletions. *J Biol Chem*, **27**: 15712-15718.

Orem, J.N., Kirigia, J.M., Azairwe, R., Kasirye, I., Walker, O. (2012). Impact of malaria morbidity on gross domestic product in Uganda. *Int Arch Med,* **5**: 12.

Orengo, C.A., Jones, D.T., Thornton, J.M. (1994). Protein superfamilies and domain superfolds. *Nature*, **372**: 631-4.

O'Shannessy, D.J., Brigham-Burke, M., Soneson, K.K., Hensley, P., Brooks, I. (1993). Determination of rate and equilibrium binding constants for macromolecular interactions using surface plasmon resonance: use of nonlinear least squares analysis methods. *Anal Biochem,* **212**: 457-468.

Otto, T. D., Böhme, U., Jackson, A. P., Hunt, M., Franke-Fayard, B., Hoeijmakers, W. M., Religa, A.A., Robertson, L., Sanders, M., Ogun, S.A., Cunningham, D., Erhart, A., Billker, O., Khan, S.M., Stunnenberg, H.G., Langhorne, J., Holder, A.A., Waters, A.P., Newbold, C.I., Pain, A., Berriman, M., Janse, C. J. (2014). A comprehensive evaluation of rodent malaria parasite genomes and gene expression. *BMC Biology*, **12**, 1–18.

Overbeek, R., Fonstein, M., D'Souza, M., Pusch, G.D., Maltsev, N. (1999). The use of gene clusters to infer functional coupling. *Proc Natl Acad Sci U S A,* **96**: 2896-901.

© University of Venda

Packschies, L., Theyssen, H., Buchberger, A., Bukau, B., Goody, R.S., Reinstein, J. (1997). GrpE accelerates nucleotide exchange of the molecular chaperone DnaK with an associative displacement mechanism. *Biochemistry,* **36**: 3417–3422.

Pak, M., Wickner, S. (1997) Mechanism of protein remodeling by ClpA chaperone. *Proc Natl Acad Sci USA,* **94**: 4901–4906.

Pallavi, R., Archarya, P., Chandran, S., Daily, J.P., Tatu, U. (2010). Chaperone expression profiles correlate with distinct physiological states of *Plasmodium falciparum* in malaria patients. *Malar J*, **9**: 236.

Park, D.J., Lukens, A.K., Neafsey, D.E., Schaffner, S.F., Chang, H.H., Valim, C., Ribacke, U., Van Tyne, D., Galinsky, K., Galligan, M., Becker, J.S., Ndiayed, D., Mboupd, S., Wieganda, R.C., Daniel, L., Hartl, D.L., Pardis, C., Sabetia, P.C., Dyann, F., Wirtha, D.F., Volkmana, S.K. (2012). Sequence-based association and selection scans identify drug resistance loci in the *Plasmodium falciparum* malaria parasite. *Proc Natl Acad Sci USA,* **109:** 13052–13057.

Patury, S., Miyata, Y., Gestwicki, J.E. (2009). Pharmacological targeting of the Hsp70 Chaperone. *Curr Top Med Chem*, **9**: 1337-1351.

Pavithra, S.R., Banumathy, G., Joy, O., Singh, V., Tatu, U. (2004). Recurrent fever promotes *Plasmodium falciparum* development in human erythrocytes. *J Biol Chem*, **279**: 46692-46699.

Pei, X., Guo, X., Coppel, R., Mohandas, N., An, X. (2007). *Plasmodium falciparum* erythrocyte membrane protein 3 (PfEMP3) destabilizes erythrocyte membrane skeleton. *J Biol Chem*, **282**: 26754–26758.

Pesce, E. R., Acharya, P., Tatu, U., Nicoll, W.S., Shonhai, A., Hoppe, H.C. Blatch, G.L. (2008). The *Plasmodium falciparum* heat shock protein 40, Pfj4, associates with heat shock protein 70 and shows similar heat induction and localisation patterns. *J Biochem Cell Biol*, **40**: 2914–2926.

Pfanner, N., Wiedemann, N. (2002). Mitochondrial protein import: two membranes, three translocases. *Curr Opin Cell Biol,* **14**: 400-11.

Picard, D., Khursheed, B., Garabedian, M. J., Fortin, M.G., Lindquist S, Yamamoto K. R. (1990). Reduced levels of Hsp90 compromise steroid receptor action in vivo. *Nature*, **348**: 166-168.

Pimienta, G., Herbert, K. M., Regan, L. (2011). A compound that inhibits the Hop - Hsp90 complex formation and has unique killing effects in breast cancer cell lines. *Mol Pharm*, **8**: 2252-61.

Polier, S., Dragovic, Z., Hartl, F. U., Bracher, A. (2008). Structural basis for the cooperation of Hsp70 and Hsp110 chaperones in protein folding. *Cell*, **133**: 1068–1079.

Polier, S., Hartl, F.U., Bracher, A. (2010). Interaction of the Hsp110 molecular chaperones from *S. cerevisiae* with substrate protein. *J Mol Biol,* **401**: 696-707.

© University of Venda

Pratt, W. B., Toft, D. O. (2003) Regulation of signaling protein function and trafficking by the Hsp90/Hsp70-based chaperone machinery. *Exp Biol Med,* **228**: 111–133.

Przyborski, J. M., Diehl, M., Blatch, G. L. (2015). Plasmodial Hsp70s are functionally adapted to the malaria parasite life cycle. *Front Mol Biosci,* **2**: 34.

Prodromou, C., Roe, S.M., O'Brien, R., Ladbury, J.E., Piper, P.W., Pearl, L.H. (1997) Identification and structural characterization of the ATP/ADP-binding site in the Hsp90 molecular chaperone. *Cell*, **90**: 65-75.

Qiu, X. B., Shao, Y. M., Miao, S., Wang, L. (2006). The diversity of the DnaJ/Hsp40 family, the crucial partners for Hsp70 chaperones. *Cell Mol Life Sci*, **63**: 2560–2570.

Pettersen, E.F., Goddard, T.D., Huang, C.C., Couch, G.S., Greenblatt, D.M., Meng, E.C., Ferrin, T.E. (2004). UCSF Chimera--a visualization system for exploratory research and analysis. *J Comput Chem,* **25**: 1605-12.

Rampelt, H., Kirstein-Miles, J., Nillegoda, N. B., Chi, K., Scholz, S. R., Morimoto, R. I., Bukau, B. (2012). Metazoan Hsp70 machines use Hsp110 to power protein disaggregation. *EMBO J*, **31**: 4221–4235.

Raphael, P., Takakuwa, Y., Manno, S., Liu, S.C., Chishti, A.H., Hanspal, M. (2000). A cysteine protease activity from *Plasmodium falciparum* cleaves human erythrocyte ankyrin. *Mol Biochem Parasitol*, **110**: 259-72.

Rauch, J. N., Gestwicki, J. E. (2014). Binding of human nucleotide exchange factors to heat shock protein 70 (Hsp70) generates functionally distinct complexes in vitro. *J Biol Chem*, **289**: 1402–1414.

Raviol, H., Bukau, B., Mayer, M.P. (2005). Human and yeast Hsp110 chaperones exhibit functional differences. *FEBS Lett*, **580**: 168–174.

Raviol, H., Sadlish, H., Rodriguez, F., Mayer, M. P., Bukau, B. (2006). Chaperone network in the yeast cytosol: Hsp110 is revealed as an Hsp70 nucleotide exchange factor. *EMBO J,* **25**: 2510–2518.

Recker, M., Buckee, C. O., Serazin, A., Kyes, S., Pinches, R., Christodoulou, Z., Springer, A.L., Gupta, S., Newbold, C. I. (2011). Antigenic variation in *Plasmodium falciparum* malaria involves a highly structured switching pattern. *PLoS Pathogens*, **7**: 1001306

Richard, D., MacRaild, C. a., Riglar, D. T., Chan, J. A., Foley, M., Baum, J., Ralph, S.A., Norton, R.S., Cowman, A. F. (2010). Interaction between *Plasmodium falciparum* apical membrane antigen 1 and the rhoptry neck protein complex defines a key step in the erythrocyte invasion process of malaria parasites. *J Biol Chem*, **285**: 14815–14822.

Ritossa, F. (1996). Discovery of the heat shock response. *Cell Stress Chaperones,* **1**:97-8.

Röhl, A., Wengler, D., Madl, T., Lagleder, S., Tippel, F., Herrmann, M., Hendrix, J., Richter, K., Hack, G., Schmid, A.B., Kessler, H., Lamb, D.C. Buchner, J. (2015). Hsp90 regulates the

© University of Venda

dynamics of its cochaperone Sti1 and the transfer of Hsp70 between modules. *Nat Commun*, **6**: 6655.

Ropert, C., Almeida, I.C., Closel, M., Travassos, L.R., Ferguson, M.A., Cohen, P., Gazzinelli, R.T. (2001). Requirement of mitogen-activated protein kinases and I kappa B phosphorylation for induction of proinflammatory cytokines synthesis by macrophages indicates functional similarity of receptors triggered by glycosylphosphatidylinositol anchors from parasitic protozoa and bacterial lipopolysaccharide. *J Immunol,* **166**: 3423–3431.

Rathore, S., Jain, S., Sinha, D., Gupta, M., Asad, M., Srivastava, A., Narayanan, M.S., Ramasamy, G., Chauhan, V.S., Gupta, D., Mohmmed, A. (2011). Disruption of a mitochondrial protease machinery in *Plasmodium falciparum* is an intrinsic signal for parasite cell death. *Cell Death Dis,* **2**: e231.

Rowe, J.A., Claessens, A., Corrigan, R.A., Arman, M. (2009). Adhesion of *Plasmodium falciparum*-infected erythrocytes to human cells: molecular mechanisms and therapeutic implications. *Rev Mol Med*, **11**: e16.

Roe S.M., Prodromou, C., O'Brien, R., Ladbury, J.E., Piper, P.W., Pearl, L.H. (1999). Structural basis for inhibition of the Hsp90 molecular chaperone by the antitumor antibiotics radicicol and geldanamycin. *J Med Chem*, 42: 260–266.

Rug, M., Maier, A.G. (2011). The Heat shock protein 40 family of the malaria parasite *Plasmodium falciparum*. *IUBMB Life*, **63**(12): 1081–1086.

Sachs, J., Malaney, P. (2002). The economic and social burden of malaria. *Nature*, **415**: 680-685.

Sadlish, H., Rampelt, H., Shorter, J., Wegrzyn, R. D., Andréasson, C., Lindquist, S., Bukau, B. (2008). Hsp110 chaperones regulate prion formation and propagation in S. cerevisiae by two discrete activities. *PLoS ONE*, **3**: 0001763.

Saibil, H. (2013). Chaperone machines for protein folding, unfolding and disaggregation. *Nat Rev Mol Cell Biol*, **14**: 630–642.

Saigal, S., Kapoor, G., Gurjar, M., Singh, D. K. (2014). Diffuse alveolar hemorrhage due to *Plasmodium falciparum* : A rare entity — Are steroids indicated ? *J Vector Borne Dis*, **51**: 66-8.66–68.

Sanchez, Y., Taulien, J., Borkovich, K., Lindquist, S. L. (1990). Hsp104 is required for tolerance to many forms of stress. *Science*, **248**: 1112-1115.

Saridaki, T., Sanchez, C. P., Pfahler, J. Lanzer, M. (2008). A conditional export system provides new insights into protein export in *Plasmodium falciparum*-infected erythrocytes. *Cell Microbiol,* **10**: 2483–2495.

Sarbeng, E. B., Liu, Q., Tian, X., Yang, J., Li, H., Wong, J. L. (2015). A functional Dnak dimer is essential for the efficient interaction with heat shock protein 40kda (Hsp40). *J Biol Chem*, **290**: 8849-62.

© University of Venda

Sargeant, T. J., Marti, M., Caler, E., Carlton, J. M., Simpson, K., Speed, T. P., and Cowman, A. F. (2006) Lineage-specific expansion of proteins exported to erythrocytes in malaria parasites. *Genome Biol,* **7**: R12.

Sato, S., Wilson, R.J. (2004). The use of DsRED in single- and dual-color fluorescence labeling of mitochondrial and plastid organelles in *Plasmodium falciparum*. *Mol Biochem Parasitol*, 134:175-9.

Sato, S., Rangachari, K., Wilson, R.J.M. (2003). Targeting GFP to the malarial mitochondrion. *Mol Biochem Parasitol,* **130**: 155-158

Saxena, A., Banasavadi-Siddegowda, Y. K., Fan, Y., Bhattacharya, S., Roy, G., Giovannucci, D. R., Frizzell, R.A., Wang, X. (2012). Human heat shock protein 105/110 kDa (Hsp105/110) regulates biogenesis and quality control of misfolded cystic fibrosis transmembrane conductance regulator at multiple levels. *J Biol Chem*, **287**: 19158–19170.

Sayeed, S. K., Shah, V., Chaubey, S., Singh, M., Alampalli, S. V, Tatu, U. S. (2014). Identification of heat shock factor binding protein in *Plasmodium falciparum*. *Malar J*, **13**: 118.

Schäfer, U., Beck, K., Müller, M. (1999). Skp, a molecular chaperone of gram-negative bacteria, is required for the formation of soluble periplasmic intermediates of outer membrane proteins. *J Biol Chem*, **274**: 24567-74.

Scherf, A., Lopez-Rubio, J.J., Riviere, L. (2008). Antigenic variation in *Plasmodium falciparum*. *Annu Rev Microbiol*, **62**: 445-70.

Scheufler, C., Brinker, A., Bourenkov, G., Pegoraro, S., Moroder, L., Bartunik, H., Hartl, F. U., Moarefi, I. (2000). Structure of TPR domain-peptide complexes: critical elements in the assembly of the Hsp70-Hsp90 multichaperone machine. *Cell*, **101**: 199-210.

Schmid, A.B., Lagleder, S., Gräwert, M.A., Röhl, A., Hagn, F., Wandinger, S.K., Cox, M.B., Demmer, O., Richter, K., Groll, M., Kessler, H., Buchner, J. (2012). The architecture of functional modules in the Hsp90 co-chaperone Sti1/Hop. *EMBO J,* **31**: 1506-1517.

Schneider, D., Shahabuddin, M. (2000). Malaria parasite development in a *Drosophila* model. *Science***, 288**: 2376-9

Schuermann, J. P., Jiang, J., Cuellar, J., Llorca, O., Wang, L., Gimenez, L. E., Jin, S., Taylor, A. B., Demeler, B., Morano, K. A., Hart, P. J., Valpuesta, J. M., Lafer, E. M., Sousa, R. (2008). Structure of the Hsp110:Hsc70 nucleotide exchange machine. *Mol Cell,* **31**: 232–243.

Schulze, J., Kwiatkowski, M., Borner, J., Schlüter, H., Bruchhaus, I., Burmester, T., Spielmann, T., Pick, C. (2015). The *Plasmodium falciparum* exportome contains non-canonical PEXEL/HT proteins. *Mol Microbiol,* **97**: 301-14.

Senczuk, A.M., Reeder, J.C., Kosmala, M.M., Ho, M. (2001). *Plasmodium falciparum* erythrocyte membrane protein 1 functions as a ligand for P-selectin. *Blood,* **98**:3132-5.

© University of Venda

Sergeant N, Delacourte A, Buee L. (2005). Tau protein as a differential biomarker of tauopathies. *Biochim Biophys Acta,* **1739**: 179–197.

Shaner, L. Morano, K.A. (2007). All in the family: atypical Hsp70 chaperones are conserved modulators of Hsp70 activity. *Cell stress and Chaperones,* **12** 1-8.

Shaner, L., Trott, A., Goeckeler, J.L., Brodsky, J.L., Morano, K.A. (2004). The function of the yeast molecular chaperone Sse1 is mechanistically distinct from the closely related Hsp70 family. *J Biol Chem* **279**: 21992–22001.

Sharma, Y. D. (1992). Structure and possible function of heat-shock proteins in *Plasmodium falciparum. Comp Biochem Physiol B,* **102**: 437–444.

Shannon, P., Markiel, A., Ozier, O., Baliga, N. S., Wang, J. T., Ramage, D., Amin, N., Schwikowski, B., Ideker, T. (2003). Cytoscape : A software environment for integrated models of biomolecular interaction networks Cytoscape : A software environment for integrated models of biomolecular interaction networks. *Genome Res*, **13**: 2498-504.

Sharma, D., Masison, D. C. (2009). Hsp70 structure, function, regulation and influence on yeast prions. *Protein Pept Lett*, **16**, 571–581.

Shomura, Y., Dragovic, Z., Chang, H.C., Tzvetkov, N., Young, J.C., Brodsky, J.L., Guerriero, V., Hartl, F.U., Bracher, A. (2005). Regulation of Hsp70 function by HspBP1: Structural analysis reveals an alternate mechanism for Hsp70 nucleotide exchange. *Mol Cell,* **17**:367–379.

Shonhai, A. (2010). Plasmodial heat shock proteins: targets for chemotherapy. *FEMS Immunol Med Microbiol,* **58**: 61-74.

Shonhai, A. (2014). Role of Hsp70s in development and pathogenicity of plasmodium species: In: Shonhai A, Blatch G, Editors. *Heat Shock Proteins of Malaria*, Springer New York; pp 47–70.

Shonhai, A., Boshoff, A., Blatch, G.L. (2007). The structural and functional diversity of Hsp70 proteins from *Plasmodium falciparum*. *Protein Sci,* **16:** 1803-1818.

Shonhai, A., Boshoff, A., Blatch, G. L. (2005). *Plasmodium falciparum* heat shock protein 70 is able to suppress the thermosensitivity of an *Escherichia coli* DnaK mutant strain. *Mol Genet Genomics*, **274**: 70–78.

Shonhai, A., Botha, M., de Beer, T.A.P., Boshoff, A., Blatch, G.L. (2008). Structure-function study of *Plasmodium falciparum* Hsp70 using three dimensional modelling and in-vitro analyses. *Protein Pept Lett*, **15**: 1117-1125.

Shonhai, A., Maier, A. G., Przyborski, J. M., Blatch, G. L. (2011). Intracellular protozoan parasites of humans: the role of molecular chaperones in development and pathogenesis. *Protein Pept Lett*, **18**: 143–157.

© University of Venda

Shorter, J. (2011). The Mammalian Disaggregase Machinery: Hsp110 Synergizes with Hsp70 and Hsp40 to Catalyze Protein Disaggregation and Reactivation in a Cell-Free System. *PLoS ONE*, **6**: e26319.

Siegert, R., Leroux, M.R., Scheufler, C., Hartl, F.U., Moarefi, I. (2000). Structure of the molecular chaperone prefoldin: unique interaction of multiple coiled coil tentacles with unfolded proteins. *Cell*, **103**:621-32.

Silberg, J. J., Vickery, L. E. (2000) Kinetic characterization of the ATPase cycle of the molecular chaperone Hsc66 from *Escherichia coli*. *J Biol Chem,* **275**: 7779−7786.

Silva, M.D., Cooke, B.M., Guillotte, M., Buckingham, D.W., Sauzet, J.P., Le Scanf, C., Contamin, H., David, P., Mercereau-Puijalon, O., Bonnefoy, S. (2005). A role for the *Plasmodium falciparum* RESA protein in resistance against heat shock demonstrated using gene disruption. *Mol Microbiol*, **56**: 990-1003.

Singh, B., Kim Sung, L., Matusop, A., Radhakrishnan, A., Shamsul, S.S., Cox-Singh, J., Thomas, A., Conway, D.J. (2004a). A large focus of naturally acquired *Plasmodium knowlesi* infections in human beings. *Lancet,* **363**: 1017-24.

Singh, G.P. Chandra, B.R., Bhattacharya, A., Akhouri R.R., Singh, S.K., Sharma, A. (2004b). Hyper-expansion of asparagines correlates with an abundance of proteins with prion-like domains in *Plasmodium falciparum*. *Mol Biochem Parasitol,* **137**: 307-319.

Smythe, W., Joiner, K., Hoppe, H. C. (2008). Actin is required for endocytic trafficking in the malaria parasite *Plasmodium falciparum*. *Cell Microb*, **10**: 452–464.

Sondermann, H., Scheufler, C., Schneider, C., Hohfeld, J., Hartl, F.U., Moarefi, I. (2001). Structure of a Bag/Hsc70 complex: Convergent functional evolution of Hsp70 nucleotide exchange factors. *Science*, **291**:1553–1557.

Song, Y., Wu, Y. X., Jung, G., Tutar, Y., Eisenberg, E., Greene, L. E., Masison, D. C. (2005). Role for Hsp70 chaperone in *Saccharomyces cerevisiae* prion seed replication. *Eukaryot Cel,* **4**: 289-297.

Sommer, M.S., Gould, S.B., Lehmann, P., Gruber, A., Przyborski, J.M. Maier, U.G. (2007). Der1-mediated preprotein import into the periplastid compartment of chromalveolates? *Mol Biol Evol*, **24**: 918–928.

Spielmann, T., Gilberger, T.W. (2010). Protein export in malaria parasites: do multiple export motifs add up to multiple export pathways? *Trends Parasitol,* **26**: 6–10.

Spielmann, T., Hawthorne, P.L., Dixon, M.W., Hannemann, M., Klotz, K., Kemp, D.J., Klonis, N., Tilley, L., Trenholme, K.R., Gardiner, D.L. (2006). A cluster of ring stage-specific genes linked to a locus implicated in cytoadherence in Plasmodium falciparum codes for PEXEL-negative and PEXEL positive proteins exported into the host cell. *Mol Biol Cell*, **17**: 3613–3624.

© University of Venda

Spycher, C., Klonis, N., Spielmann, T., Kump, E., Steiger, S., Tilley, L., Beck, H. P. (2003). MAHRP-1, a novel *Plasmodium falciparum* histidine-rich protein, binds ferriprotoporphyrin IX and localizes to the Maurer's clefts. *J Biol Chem*, **278**, 35373–35383.

Spycher, C., Rug, M., Klonis, N., Ferguson, D.J., Cowman, A.F, Beck, H.P., Tilley, L. (2006). Genesis of and trafficking to the Maurer's clefts of *Plasmodium falciparum*-infected erythrocytes. *Mol Cell Biol*, **26**: 4074-85.

Squires, C. (1992). The Clp proteins: proteolysis regulators or molecular chaperones. *J Bacteriol,* **174**: 1081-1085.

Sreerama, N., Venyaminov, S. Y., Woody, R. W. (2000). Estimation of protein secondary structure from circular dichroism spectra: inclusion of denatured proteins with native proteins in the analysis. *Anal Biochem*, 287: 243–251.

Steel, G.J., Fullerton, D.M., Tyson, J.R., Stirling, C.J. (2004). Coordinated activation of Hsp70 chaperones. *Science*, **303**: 98–101.

Stephens, L. L., Shonhai, A., Blatch, G. L. (2011). Co-expression of the *Plasmodium falciparum* molecular chaperone, PfHsp70, improves the heterologous production of the antimalarial drug target GTP cyclohydrolase I, PfGCHI. *Prot Expr Purif,* **77:** 159–165.

Su, X., Kirkman, L.A., Fujioka, H., Wellems, T.E. (1997). Complex polymorphisms in anapproximately 330 kDa protein are linked to chloroquine-resistant *P. falciparum* in Southeast Asia and Africa. *Cell*, **91**: 593-603.

Su, X.Z., Wellems, T.E. (1994). Sequence, transcript characterization and polymorphisms of a *Plasmodium falciparum* gene belonging to the heat-shock protein (HSP) 90 family. *Gene*, **151**: 225-230.

Szabo A., Langer, T., Schröder, H., Flanagan, J., Bukau,B. Hartl,F.U. (1994). The ATP hydrolysis-dependent reaction cycle of the *Escherichia coli* Hsp70 system—DnaK, DnaJ and GrpE. *Proc Natl Acad Sci USA,* **91**: 10345–10349.

Tai, P. K.K., Albers, M. W., Chang, H., Faber, L.E, Schreiber, S.L. (1992). Association of a 50-kilodalton immunophilin with the glucocorticoid receptor complex. *Science*, **256**: 1315-1318.

Tardieux, I., Baines, I., Mossakowska, M., Ward, G. E. (1998a). Actin-binding proteins of invasive malaria parasites and the regulation of actin polymerization by a complex of 32/34-kDa proteins associated with heat shock protein 70kDa. *Mol Biochem Parasitol*, **93**: 295–308.

Tardieux, I., Liu, X., Poupel, O., Parzy, D., Dehoux, P., Langsley, G. (1998b). A *Plasmodium falciparum* novel gene encoding a coronin-like protein which associates with actin filaments. *FEBS Lett*, **441**: 251–256.

Tokumasu, F., Crivat, G., Ackerman, H., Hwang, J. Wellems T.E. (2014). Inward cholesterol gradient of the membrane system in *P. falciparum*-infected erythrocytes involves a dilution effect from parasite-produced lipids. *Biol Open,* **3**: 529–541.

© University of Venda

Torrente M. P., Shorter J. (2013). The metazoan protein disaggregase and amyloid depolymerase system: Hsp110, Hsp70, Hsp40, and small heat shock proteins. *Prion,* **7**: 457–463.

Trager, W., Jensen, J.B. (1997). Human malaria parasites in continuous culture. *Science*, **193**: 673–675.

Tsutsumi, S., Mollapour, M., Prodromou, C., Lee, C.T., Panaretou, B., Yoshida, S., Mayer, M.P., Neckers, L.M. (2012). Charged linker sequence modulates eukaryotic heat shock protein 90 (Hsp90) chaperone activity. *Proc Natl Acad Sci U S A*, **109**: 2937-42.

Tuteja, R., Pradhan, A. (2009). Isolation and functional characterization of eIF4F components and poly(A)-binding protein from *Plasmodium falciparum*. *Parasitol Int*, **58**: 481–5.

Ueno, T., Taguchi, H., Tadakuma, H., Yoshida, M., Funatsu, T. (2004). GroEL mediates protein folding with a two successive timer mechanism. *Mol Cell*, **14**: 423-434.

Vaina, G.M.R., Machado, R.L,D., Calvosa, V.S.P., Povoa, M.M. (2006). Mutations in the pfmdr1, cg2, and pfcrt genes in *Plasmodium falciparum* samples from endemic malaria areas in Rondonia and Pará State, Brazilian Amazon Region. *Cad Saúde Pública*, **22**: 2703-2711.

Vale, R.D. (2000). AAA proteins: Lords of the ring. *J Cell Biology*, **150**: F13–F19.

van der Heyde, H.C., Nolan, J., Combes, V., Gramaglia I, Grau, G.E. (2006). A unified hypothesis for the genesis of cerebral malaria: sequestration, inflammation and hemostasis leading to microcirculatory dysfunction. *Trends Parasitol,* **22**: 503-8.

Van Schalkwyk, D. A., Sutherland, C. J. (2015). Malaria resistance to non-artemisinin partner drugs: how to reACT. *Lancet Infect Dis*, **15**(6): 621–623.

Viitanen, P. V., Lubben, T. H., Reed, J., Goloubinoff, P., O'Keefe, D. P., Lorimer, G. H. (1990). Chaperonin facilitated refolding of ribulosebisphosphate carboxylase and ATP hydrolysis by chaperonin 60 (groEL) are K+ dependent. *Biochemistry*, **29**: 5665-5671.

Vilasi, S., Carrotta, R., Mangione, M. R., Campanella, C., Librizzi, F., Randazzo, L., Martorana,V., Gammazza, A.M., Ortore, M.G., Vilasi, A., Pocsfalvi, G., Burgio, G., Corona, D., Piccionello, A.P., Zummo, G., Bulone, D., de Macario, E.C., Macario, A.J.L., San Biagio, P.L., Cappello, F. (2014). Human Hsp60 with its mitochondrial import signal occurs in solution as heptamers and tetradecamers remarkably stable over a wide range of concentrations. *PLoS ONE*, **9**: e97657.

Vincensini, L., Richert, S., Blisnick, T., Van Dorsselaer, A., Leize-Wagner, E., Rabilloud, T., Braun, B.C. (2005). Proteomic analysis identifies novel proteins of the Maurer's clefts, a secretory compartment delivering *Plasmodium falciparum* proteins to the surface of its host cell. *Mol Cell Proteomics*, **4**: 582–593.

Vogel, M., Mayer, M. P., Bukau, B. (2006). Allosteric regulation of Hsp70 chaperones involves a conserved interdomain linker. *J Biol Chem*, **281**: 38705–38711.

© University of Venda

Voss, K., Combs, B., Patterson, K., Binder, L. I., Chris, T. (2013). Hsp70 alters tau function and aggregation in an isoform specific manner. *Biochemistry*, **51**: 888–898.

Waller, K.L., Nunomura, W., An, X., Cooke, B.M., Mohandas, N., Coppel, R.L. (2003). Mature parasite-infected erythrocyte surface antigen (MESA) of *Plasmodium falciparum* binds to the 30-kDa domain of protein 4.1 in malaria-infected red blood cells. *Blood*, **102**:1911-4.

Wang, T., Bisson, W.H., Maser, P., Scapozza, L., Picard, D. (2014). Differences in conformational dynamics between *plasmodium falciparum* and human Hsp90 Orthologues enable the structure based discovery of pathogen-selective inhibitors. *J Med Chem*, **57**: 2524-2535.

Wang, X. Y., Kazim, L., Repasky, E. A., Subjeck, J. R. (2001). Characterization of heat shock protein 110 and glucose-regulated protein 170 as cancer vaccines and the effect of fever-range hyperthermia on vaccine activity. *J Immunol*, **166**: 490–497.

Walsh, P., Bursac, D., Law, Y.C., Cyr, D., Lithgow, T. (2004). The J-protein family: modulating protein assembly, disassembly and translocation. *EMBO Rep,* **5**: 567-571.

Wiech, H., Buchner, J., Zimmermann, R., Jakob, U. (1992). Hsp90 chaperones protein folding in vitro. *Nature*, **358**: 169-70.

Weng, H., Guo, X., Papoin, J., Wang, J., Coppel, R., Mohandas, N., An, X. (2014). Interaction of *Plasmodium falciparum* knob-associated histidine-rich protein (KAHRP) with erythrocyte ankyrin R is required for its attachment to the erythrocyte membrane. *BBA - Biomembranes*, **1838**: 185–192.

Whitmore, L., Wallace, B. (2004). DICHROWEB, an online server for protein secondary structure analyses from circular dichroism spectroscopic data. *Nucleic Acids Res*, **32**: 668–673.

WHO (2012). World Health Organisation Global Malaria report http://www.who.int/malaria/world_malaria_report_2012/worldmalariareport2012.pdf.

WHO (2013). World Health Organisation Global Malaria report

http://www.who.int/malaria/world_malaria_report_2013/en/index.html

WHO (2014). World Health Organisation Global Malaria report http://www.who.int/malaria/world_malaria_report_2014/worldmalariareport2014.pdf.

Wickham, M. E., Rug, M., Ralph, S. A., Klonis, N., McFadden, G. I., Tilley, L., Cowman, A. F. (2001). Trafficking and assembly of the cytoadherence complex in *Plasmodium falciparum*-infected human erythrocytes. *EMBO J*, **20**: 5636–5649.

Winkler, J., Tyedmers, J., Bukau, B., Mogk, A. (2012). Hsp70 targets Hsp100 chaperones to substrates for protein disaggregation and prion fragmentation. *J Cell Biol*, **198**: 387–404.

Witkowski, B., Berry, A., Benoit-Vical, F. (2009), Resistance to antimalarial compounds: methods and applications. *Drug Resist Updat*, **12**: 42–50.

© University of Venda

Witkowski, B., Lelie`vre, J., Nicolau-Travers, M-L., Iriart, X., Njomnang Soh, P., Bousejra-ElGarah, F., Meunier, B., Berry, A., Benoit-Vica, F. (2012). Evidence for the contribution of the hemozoin synthesis pathway ofthe murine *Plasmodium yoelii* to the resistance to artemisinin-related drugs. *PLoS ONE,* **7**: e32620.

Wisniewska, M., Karlberg, T, Lehtio, L., Johansson, I., Kotenyova, T., Moche,, M., Schuler, H. (2010). Crystal Structures of the ATPase Domains of Four Human Hsp70 Isoforms: HSPA1L/Hsp70-hom, HSPA2/Hsp70-2, HSPA6/Hsp70B', and HSPA5/BiP/GRP78. *PLoS ONE*, **5**: e8625

Wynn, R. M., Davie, J. R., Cox, R. P., Chuang, D. T. (1994). Molecular chaperones: heat-shock proteins, foldases, and matchmakers. *J Lab Clin Med*, **124**: 31–36.

Xiao, J., Kim, L. S., Graham, T. R. (2006). Dissection of Swa2p/Auxilin domain requirements for co-chaperoning Hsp70 clathrin-uncoating activity *in vivo*. *Mol Biol Cell,* **17**: 3281-3290.

Xu, X., Sarbeng, E.B., Vorvis, C., Kumar, D.P., Zhou, L., Liu, Q. (2012). Unique peptide substrate binding properties of 110-kDa Heat-shock protein (Hsp110) determine its distinct chaperone activity. *J Biol Chem*, **287**: 5661-5672.

Xu, X., Efremov. A.K., Li, A., Lai, L., Dao, M., Lim, C.T., Cao, J. (2013). Probing the cytoadherence of malaria infected red blood cells under flow. *PLoS ONE,* **8**: e64763.

Yam, A.Y.W., Albanese, V., Lin, H.T.J., Frydman, J. (2005). Hsp110 Cooperates with Different Cytosolic Hsp70 Systems in a Pathway for de Novo Folding. *J Biol Chem*. **280**: 41252–41261.

Yang, C., Wang, H., Zhu, D., Hong, C.S., Dmitriev, P., Zhang, C., Li, Y., Ikejiri, B., Brady, R.O., Zhuang, Z. (2015). Mutant glucocerebrosidase in Gaucher disease recruits Hsp27 to the Hsp90 chaperone complex for proteasomal degradation. *Proc Natl Acad Sci U S A*, **112**: 1137-42.

Yoon, J., Blumer, A., Lee, K. (2006). An algorithm for modularity analysis of directed and weighted biological networks based on edge-betweenness centrality. *Bioinformatics*, **22**: 3106–3108.

Young, J. C., Agashe, V.R., Siegers, K., Hartl, F. U. (2004). Pathways of chaperone-mediated protein folding in the cytosol. *Nature Rev Mol Cell Biol,* **5**: 781-791.

Yu, Y. (2011). The discovery of artemisinin (ginghaosu) and gifts from Chinese medicine. *Nat Medicne* **17**: 1217-1220.

Zhang, P., Leu, J. I.-J., Murphy, M. E., George, D. L., Marmorstein, R. (2014). Crystal structure of the stress-inducible human heat shock protein 70 substrate-binding domain in complex with peptide substrate. *PloS ONE*, **9**, e103518.

Zhao, R., Davey, M., Hsu, Y.C., Kaplanek, P., Tong, A., Parsons, A.B., Krogan, N., Cagney, G., Mai, D., Greenblatt, J., Boone, C., Emili, A., Houry, W.A. (2005). Navigating the chaperone network: an integrative map of physical and genetic interactions mediated by the Hsp90 chaperone. *Cell*, **120**: 715-27.

© University of Venda

Zhu, X., Zhao, X., Burkholder, W. F., Gragerov, A., Ogata, C. M., Gottesman, M. E., Hendrickson, W. A. (1996). Structural analysis of substrate binding by the molecular chaperone DnaK. *Science*, **272**: 1606–1614.

Zhuravleva, A., Gierasch, L. M. (2011). Allosteric signal transmission in the nucleotide-binding domain of 70-kDa heat shock protein (Hsp70) molecular chaperones. *Proc Natl Acad Sci U S A*, **108**: 6987–6992.

Zininga, T., Achilonu, I., Hoppe, H., Prinsloo, E., Dirr, H. W., Shonhai, A. (2015a). Overexpression, Purification and Characterisation of the *Plasmodium falciparum* Hsp70-z (PfHsp70-z) Protein. *PloS ONE*, **10**: e0129445.

Zininga, T., Shonhai, A. (2014). Are heat shock proteins druggable candidates? *Am J Biochem Biotechnol*, **10**: 211- 213.

Zininga, T., Makumire, S., Gitau, G. W., Njunge, J. M., Pooe, O. J., Klimek, H., Scheurr, R., Raifer, H., Prinsloo, E., Przyborski, J.M., Hoppe, H., Shonhai, A. (2015b). *Plasmodium falciparum* Hop (PfHop) interacts with the Hsp70 chaperone in a nucleotide-dependent fashion and exhibits ligand Selectivity. *PloS ONE*, **10**: e0135326.

Zorzi, E., Bonvini, P. (2011). Inducible Hsp70 in the regulation of cancer cell survival: Analysis of chaperone induction, expression and activity. *Cancers*, **3**: 3921–3956.

© University of Venda

APPENDIX

SUPPLEMENTARY DATA, GENERAL EXPERIMENTAL PROCEDURES AND LIST OF SPECIALISED REAGENTS

© University of Venda

APPENDIX A: GENERAL EXPERIMENTAL PROCEDURES

A1 Extraction of plasmid DNA

Plasmid DNA was extracted using Zyppy™ Plasmid Miniprep Kit according to manufacturer's protocol.

A2 Restriction digest of Plasmid DNA using enzymes

Plasmid DNA was digested using the desired diagnostic restriction enzymes following the method described below. The reagents were set up as follows: Sterile deionised water (16 µl), 10x restriction buffer (2 µl) and DNA (100-200 ng) 2 µl. The reaction was initiated by addition of two units of restriction enzymes. The restriction was allowed to proceed for 2-3 hours at 37 °C. The reaction was stopped by addition of 4 µl of 10x DNA loading buffer (0.25 %) bromophenol blue and 30 % glycerol). The product was then analysed by agarose gel electrophoresis as described in (Appendix A. 5).

A3 Agarose gel electrophoresis

To prepare 0.8 % (w/v) agarose gel, the required amount of agarose was completely dissolved in 1x TAE buffer (40 mM, 20 mM acetic acid and 1 mM EDTA) by heating with frequent agitation. The agarose was then cooled to 55ºC prior to addition of ethidium bromide (0.5 µg/ml). The agarose gel was allowed to polymerise for 15-30 minutes at room temperature. The gel was placed in the electrophoresis chamber and covered with 1x TAE buffer. Volume of 4 µl of 10x DNA loading buffer (0.25% bromophenol blue + 30% glycerol) was added to 20 µl of sample followed by loading of the samples into the wells. Electrophoresis was conducted at 100 volts for one hour. The gel was then visualised using UV light (GeneGenius Bioimaging System (Syngene), USA).

A4 Preparation of competent *E. coli* XL1/JM109 Blue cells

Colony of E. *coli* XL1/JM109 Blue was inoculated in 5ml 2YT broth (1.6 % (w/v) tryptone, 1.0% (w/v) yeast, 1.5 % (w/v) agar, 0.5 % (w/v) NaCl in deionised water) broth and grown overnight with shaking at 37 °C. The overnight culture was diluted 1:100 into 50 ml 2YT broth and thereafter grown with shaking to early log phase of absorbance 0.3-0.6 measured at 600 nm. The cells were harvested by centrifuging at 5,000 g for 10 minutes at 4 °C. The

© University of Venda

cells were kept on ice from this point onwards. The cells were resuspended in 10 ml 0.1 M $MgCl_2$ and left on ice for 30 minutes. The suspension was centrifuged for 10 minutes at 2700 g at 4 °C. The cells were pelleted as before and gently resuspended in 10 ml ice cold 0.1 M $CaCl_2$ and then followed by incubation on ice for 4 hours. Centrifugation was carried out at 2700 g at 4 °C for 10 minutes. The competent cells were aliquoted by adding one volume of sterile 30 % (v/v) glycerol mixing and stored at -80 °C until use.

A5 Transformation of competent cells

A volume of 2 µl (equivalent to about 10 ng) of plasmid DNA was added into an aliquot of 100 µl of competent cell. The cells were then incubated on ice for 30 minutes followed by heat shocking at 42 °C for 45 seconds and immediately placed on ice for 10 minutes. Volume of 900 µl of 2YT broth was added and then incubated at 37 °C for one hour with gently agitation. The cells were transferred on 2YT plates containing the desired antibiotics followed by incubation at 37 °C overnight.

A6 Sodium dodecyl polyacrylamide gel electrophoresis (SDS-PAGE)

Proteins were treated by boiling in SDS sample buffer (0.25% Coomasie Brilliant blue (R250), 2% SDS, 10 % glycerol (v/v), 100 mM tris, and 1 % β-mercaptoethanol) in a ratio of 4:1 for 5 minutes at 95 °C and resolved using 12 % acrylamide resolving gel prepared as shown below (Table A.1). The gel is then transferred into the electrophoresis tank and electrophoresis buffer (25 mM Tris, pH 8.3 250 mM glycine and 0.1% (w/v) SDS) was added. The boiled samples were loaded in respective wells and prestained protein molecular weight markers (ThermoFisher Scientific, USA) were also loaded. The electrophoresis was performed at 150 volts for one hour using the Bio-Rad Mini protein electrophoresis system (Biorad, U.S.A).

Table A1 Preparation of SDS-PAGE

Reagent (ml)	5 % Stacking gel	12 % Separating gel
30 % Bis/acrylamide	0.235	2.08
10 % Ammonium persulphate	0.00875	0.025
1.5 M Tris (pH 8.8)	-	1.25
1.0 M Tris (pH 6.8)	0.437	-
10 % SDS	0.0175	0.05
Distilled water	1.05	1.58
TEMED	0.03	0.0020

© University of Venda

A7 Western Blot

Proteins were resolved in 12% acrylamide gel as described above (Appendix A.7). Removal of SDS-PAGE gel from the glass plates after completion of electrophoresis process and cutting off of the stacking gel was done. The Whatman filter papers, gel, two scotchbrite fibre pads and nitrocellulose were emmersed in western transfer paper and left to equilibrate at 8 °C for 30 minutes. Preparation of the gel for transfer was done as follows: filter paper was placed on a scotch brite pad; Gel was placed on the filter paper ensuring no air bubbles are trapped; nitrocellulose was placed over the gel; another filter paper was laid on top of the nitrocellulose, followed by another scotch brite pad. The transfer of the protein on the nitrocellulose membrane was performed by running at 100 volts for one hour. The membrane was removed from the sandwich and rinsed using transfer buffer as well as removal of adhering gel on the nitrocellulose membrane using a cotton swab. The blot was stained with ponceau stain to determine the success of the transfer followed by visualising the band using chemiluminescence. The membrane was blocked in 10 ml of (5 % non-fat milk in TBS) for one hour on a rotary shaker set at 1 rpm. The membrane was washed three times in TBS-Tween for 10 minutes followed by incubation of the membrane with primary antibody for one hour. Unbound primary antibody were removed by washing of the membrane three times using TBS-Tween for 10 minutes each wash. The membrane was incubated with secondary antibody for one hour followed by washing of the membrane three times using TBS-Tween.

A8 Enhanced ChemiLumescent (ECL)

The Thermo Scientific Pierce ECL Western Blotting Substrate is a highly sensitive nonradioactive, enhanced luminol-based chemiluminescent substrate for the detection of horseradish peroxidase (HRP) on immunoblots.

1. Remove blot from the transfer apparatus and block nonspecific sites with Blocking Reagent for 60 minutes at room temperature (RT) with shaking. If desired, block overnight at 2-8 °C without shaking. 2. Remove the Blocking Reagent and add the primary antibody working dilution. Incubate blot for 1 hour at RT with shaking or overnight at 2-8 °C without shaking.

3. Briefly rinse membrane in Wash Buffer two times.

© University of Venda

4. Wash membrane by suspending it in Wash Buffer and agitating for ≥ 5 minutes. Replace Wash Buffer at least 4-6 times. Increasing the Wash Buffer volume, the number of washes and wash duration may help minimize background signal.

5. Incubate blot with the HRP-conjugate working dilution for one hour at RT with shaking.

6. Repeat Steps 3 and 4 to remove nonbound HRP-conjugate. Note: Membrane MUST be thoroughly washed after incubation with the HRP-conjugate.

7. Prepare the substrate working solution by mixing equal parts of Detection Reagents 1 and 2. Use 0.125 mL Working Solution per cm^2 of membrane. Note: For best results prepare working solution immediately before use. The working solution is stable for one hour at RT.

8. Incubate blot with working solution for one minute at RT.

9. Remove blot from working solution and place it in a plastic sheet protector or clear plastic wrap. Use an absorbent tissue to remove excess liquid and to carefully press out any bubbles from between the blot and the membrane protector.

A9 Determination of protein concentration using Bradford assay

Protein concentration was determined by Bradford's method (Bradford, 1976). Bovine serum albumen (BSA) standards were prepared using concentration ranging from 0 to 1 mg/ml in 0.15 M NaCl. Bradfords reagent 200 µl (Sigma Aldrich, USA) was added to 10 µl of protein and the reaction incubated in the dark at room temperature for five minutes. Absorbance was read at 595 nm using (SpectraMax M3, Molecular devices USA).The recombinant protein was similarly treated and the protein concentration determined by extrapolation from the standard curve as indicated in (Appendix B3; Figure B1). The readings were prepared in triplicate and the average obtained.

A10 Determination of protein concentration using Christoph-Leidig webtool assay

Protein concentration was determined using the Christoph-leidig webtool (http://christoph-leidig.de/tprot.html) using the following formula

$A = c \times d \times \varepsilon$ Equation 1

$m = n \times M$ Equation 2

© University of Venda

where A: Absorbance at 280 nm

c: concentration (mol/l)

d: cuvette length (cm)

ε: extinction coefficient (L/mol x cm)

m: mass (g)

n: quantity (mol)

M: molecular unit (g/mol)

A11 determination of CD molar residue ellipticity

The analysis of the CD spectrum was conducted by conversion of ellipticity units from the CD spectrometer to molar residue ellipticity. This was achieved using the following formula

$[\theta] = (100 \times \theta) / CMR \times l$ Equation 3

Where [θ]: molar residue ellipticity ($deg.cm^2.dmol^{-1}$)

100: constant converting path length in meters

θ: ellipticity (mdeg)

l: cuvette path length

CMR: mean residue concentration

$CMR = c \times N$ Equation 4

Where c: Protein concentration (mol)

N: number of amino acids on the protein

A12 BioRad GLC chip activation and regeneration protocol

The GLC sensor chip was conditioned (Appendix B4), Pre-concentration of ligand (Appendix B5); immobilization of ligand (Appendix B6) and stabilised following the manufacturer's protocol BioRad bulletin 6414.

© University of Venda

A13 BioRad HTE chip activation and regeneration protocol

The HTE sensor chip was conditioned (Appendix B11) activated and immobilization of ligand (Appendix B12) following the manufacturer's protocol BioRad bulletin 6044.

A14 SDS-PAGE Silver staining

After running the SDS-PAGE the gel is carefully removed from the casting plates then placed into staining trays. The polyacrylamide gel was stained using Pierce® Silver Stain Kit, the protocol was followed as per manufacturer's instructions as follows

1. Wash gel in ultrapure water for five minutes. Replace the water and wash for another five minutes.
2. Fix gel in 30 % ethanol: 10 % acetic acid solution for 15 minutes. Replace the solution and fix for another 15 minutes.
3. Wash gel in 10 % ethanol solution for 5 minutes. Replace solution and wash for another five minutes.
4. Wash gel in ultrapure water for 5 minutes. Replace water and wash for another five minutes.
5. Prepare Sensitizer Working Solution by mixing 1 part Silver Stain Sensitizer with 500 parts ultrapure water.
6. Incubate gel in Sensitizer Working Solution for exactly one minute, then wash with two changes of ultrapure water for one minute each.
7. Prepare Stain Working Solution by mixing one part Silver Stain Enhancer with 50 parts Silver Stain.
8. Incubate gel in Stain Working Solution for 30 minutes.
9. Prepare Developer Working Solution by mixing one part Silver Stain Enhancer with 50 parts Silver Stain Developer.
10. Prepare 5 % acetic acid solution as a Stop Solution.
11. Quickly wash gel with two changes of ultrapure water for 20 seconds each.
12. Immediately add Developer Working Solution and incubate until protein bands appear (2-3 minutes).
13. When the desired band intensity is reached, replace Developer Working Solution with prepared Stop Solution (5 % acetic acid). Wash gel briefly, then replace Stop Solution and incubate for 10 minutes.

© University of Venda

A15 Immunoprecipitation using Pierce® Protein A/G Magnetic Beads

Immunoprecipitation was conducted using Pierce® Protein A/G Magnetic Beads (ThermoScientific, USA), with minor modifications as follows:

1. Combine the antigen sample with 10 µg of antibody. Adjust the reaction volume to 500 µL with the Cell Lysis Buffer (25 mM Tris-HCl pH 7.5, 150 mM NaCl, 1 mM EDTA, 1 % (v/v) Tween-20, and containing 1 mM PMSF). Incubate the reaction for 2 hours at room temperature or overnight at 4 °C with mixing.

2. Place 25 µL (0.25 mg) of Pierce Protein A/G Magnetic Beads into a 1.5 mL microcentrifuge tube.

3. Add 175 µL of Wash Buffer to the beads and gently vortex to mix.

4. Place the tube into a magnetic stand to collect the beads against the side of the tube. Remove and discard the supernatant

5. Add 1 mL of Wash Buffer to the tube. Invert the tube several times or gently vortex to mix for 1 minute. Collect beads with magnetic stand. Remove and discard the supernatant.

6. Add the antigen sample/antibody mixture to a 1.5 mL microcentrifuge tube containing pre-washed magnetic beads and incubate at room temperature for 1 hour with mixing.

7. Collect the beads with a magnetic stand and then remove the flow-through and save for analysis.

8. Add 500 µL of Wash Buffer to the tube and gently mix. Collect the beads and discard the supernatant. Repeat wash twice.

9. Add 500 µL of purified water to the tube and gently mix. Collect the beads on a magnetic stand and discard the supernatant.

10. Low-pH Elution: Add 100 µL of Low-pH Elution Buffer to the tube. Incubate the tube at room temperature with mixing for 10 minutes. Magnetically separate the beads and save the supernatant containing target antigen. To neutralize the low pH, add 10 µL of Neutralization Buffer for each 100 µL of eluate.

© University of Venda

APPENDIX B SUPPLEMENTARY DATA

B1 Conservation level of Hsp110 homologues and orthologues

Table B.1 Conservation level of Hsp110 homologues and orthologues

	Pf	Pv	Pk	Pc	Pcy	Pb	Py	Tb	Tc	Lm	La	Lb	HH	mH	Sse1
Pf	-	68.4 (84.4)	67.9 (83.3)	64.4 (78.8)	67.7 (83.6)	65.0 (80.3)	65.2 (80.8)	19.1 (37.8)	19.9 (36.5)	19.6 (37.1)	19.6 (37.0)	18.6 (36.7)	22.4 (43.9)	22.2 (44.9)	19.4 (36.0)
Pv	68.4 (84.4)	-	88.2 (94.7)	64.6 (78.7)	91.5 (95.5)	64.2 (80.5)	64.9 (80.5)	19.7 (37.0)	19.8 (36.5)	19.0 (37.1)	19.0 (37.1)	18.5 (36.3)	22.2 (43.8)	22.3 (43.9)	19.4 (35.0)
Pk	67.9 (83.3)	88.2 (94.7)	-	63.2 (77.9)	89.0 (95.0)	64.1 (79.7)	64.3 (80.3)	19.0 (36.5)	19.6 (36.3)	18.7 (36.8)	18.8 (37.0)	18.2 (36.0)	22.4 (44.1)	22.5 (44.0)	19 (35.0)
Pc	64.4 (78.8)	64.6 (78.7)	63.2 (77.9)	-	64.0 (77.7)	89.1 (95.2)	84.0 (95.0)	19.8 (37.0)	19.9 (36.0)	19.9 (37.1)	20.0 (37.1)	19.1 (36.9)	23.5 (42.3)	23.2 (42.7)	21.4 (37.6)
Pcy	67.7 (83.6)	91.5 (95.5)	89.0 (95.0)	64.0 (77.7)	-	63.1 (79.2)	63.9 (79.7)	18.9 (36.0)	18.7 (35.8)	18.9 (36.4)	18.9 (36.5)	17.9 (35.5)	21.9 (43.4)	21.8 (43.4)	19.0 (34.6)
Pb	65.0 (80.3)	64.2 (80.5)	64.1 (79.7)	89.1 (95.2)	63.1 (79.2)	-	96.5 (98.1)	20.3 (38.0)	20.1 (36.8)	19.8 (37.9)	19.9 (37.9)	19.2 (37.6)	23.9 (43.4)	23.1 (43.7)	21.4 (37.5)
Py	65.2 (80.8	64.9 (80.5)	64.3 (80.3)	84.0 (95.0	63.9 (79.7)	96.5 (98.1)	-	20.1 (37.9)	20.2 (36.8)	19.9 (37.7)	20.0 (37.7)	19.5 (37.6)	24.4 (44.1)	23.8 (44.6)	21.5 (37.4)
Tb	19.1 (37.8)	19.7 (37.0)	19.0 (36.5)	19.8 (37.0)	18.9 (36.0)	20.3 (38.0)	20.1 (37.9)	-	70.7 (81.0)	53.6 (69.7)	53.9 (69.7)	54.7 (68.9)	25.5 (43.3)	25.8 (43.7)	26.2 (42.6)
Tc	19.9 (36.5)	19.8 (36.5)	19.6 (36.3)	19.9 (36.0)	18.7 (35.8)	20.1 (36.8)	20.2 (36.8)	70.7 (81.0)	-	55.7 (69.6)	56.2 (69.7)	56.3 (69.1)	27.0 (45.3)	26.8 (44.8)	26.1 40.8)
Lm	19.6 (37.1)	19.0 (37.1)	18.7 (36.8)	19.9 (37.1)	18.9 (36.4)	19.8 (37.9)	19.9 (37.7)	53.6 (69.7)	55.7 (69.6)	-	98.1 (99.0)	84.5 (90.9)	24.8 (44.2)	24.6 (43.9)	22.9 (40.7)
La	19.6 (37.0)	19.0 (37.1)	18.8 (37.0)	20.0 (37.1)	18.9 (36.5)	19.9 (37.9)	20.0 (37.7)	53.9 (69.7)	56.2 (69.7)	98.1 (99.0)	-	84 (90.6)	25.0 (44.2)	24.8 (43.9)	23.2 (40.8)
Lb	18.6 (36.7)	18.5 (36.3)	18.2 (36.0)	19.1 (36.9)	17.9 (35.5)	19.2 (37.6)	19.5 (37.6)	54.7 (68.9)	56.3 (69.1)	84.5 (90.9)	84 (90.6)	-	24.5 (43.1)	24.4 (42.9)	23.4 (40.1)
HH	22.4 (43.9)	22.2 (43.8)	22.4 (44.1)	23.5 (42.3)	21.9 (43.4)	23.9 (43.4)	24.4 (44.1)	25.5 (43.3)	27.0 (45.3)	24.8 (44.2)	25.0 (44.2)	24.5 (43.1)	-	93.2 (96.6)	31.8 (47.5)
mH	22.2 (44.9)	22.3 (43.9)	22.5 (44.0)	23.2 (42.7)	21.8 (43.4)	23.1 (43.7)	23.8 (44.6)	25.8 (43.7)	26.8 (44.8)	24.6 (43.9)	24.8 (43.9)	24.4 (42.9)	93.2 (96.6)	-	31.5 (48.0)
Sse1	19.4 (36.0)	19.4 (35.0)	19 (35.0)	21.4 (37.6)	19.0 (34.6)	21.4 (37.5)	21.5 (37.4)	26.2 (42.6)	26.1 40.8)	22.9 (40.7)	23.2 (40.8)	23.4 (40.1)	31.8 (47.5)	31.5 (48.0)	-

Table Legend; sequence identities and similarities are in parenthesis as percentages of Hsp110 homologues from Pf; PfHsp70-z; Pv, *PvHsp110;* Pk, PkHsp110; Pc, PcHsp110; Pb, PbHsp110; Py, PyHsp110; Pcy, PcyHsp110; HH, HSPH1; mH, mHsp105; Sse1; Tb, TbHsp110; Tc, TcHsp110; Lm, LmHsp110; La, LaHsp110; Lb, LbHsp110. The accession numbers are indicated in Figure 2.1.

© University of Venda

B2 Predicted PfHsp70-z peptide epitopes

Table B2 Predicted PfHsp70-z peptide epitopes

No	Start	Antigenic Determinant	Length	Antigenicity/Surface/ Hydrophilicity	Coil	Amphipathic	Synthesis
1	564	CKDQTNDNNMNEKDT	14	3.33/1.00/1.23	Y	N	N
2	533	CIKSKDEKKKADDKT	14	2.91/0.93/2.06	Y	N	N
3	322	CEDLDCQGSINRETF	14	2.19/0.71/0.52	Y	Y	N
4	226	ADSNLGGRNLDNELC	14	2.15/0.79/0.42	Y	Y	N
5	280	CTASDQQNGINNKVR	14	2.09/0.71/0.34	Y	Y	N
6	71	IGKIGTDVKDDIEIC	14	2.08/0.64/0.69	Y	Y	N
7	669	CKNFVMDDERDRILL	14	1.93/0.64/0.69	Y	Y	N
8	768	CSLQEQEKNKPLYEP	14	1.64/0.79/0.62	Y	Y	N
9	417	CYKVKEYECVEKVTH	14	1.60/0.57/0.58	Y	Y	N
10	743	CQCSNKPSDESQNII	14	1.51/0.79/0.53	Y	Y	N
11	458	CKKVKKIVIPEKGHI	14	1.36/0.50/0.69	Y	Y	N
12	630	CSEQEINMQHSDILE	14	1.35/0.71/0.31	Y	N	N
13	301	CIKTKKVLSANNEAS	14	1.20/0.64/0.34	Y	Y	N
14	39	VGFTEKERLIGDSAC	14	1.19/0.64/0.45	Y	Y	N

Table legend. An extra "C" (highlighted as green) is added to the C terminus (or N terminus) to facilitate conjugation. Positive charged residues (K, R, H) are in blue. Negative charged residues (D, E) are in red. Synthesis: "N" means this peptide is easy to synthesize. "Y" means it has difficulty to synthesize.

B.3 Bradford assay standard curve

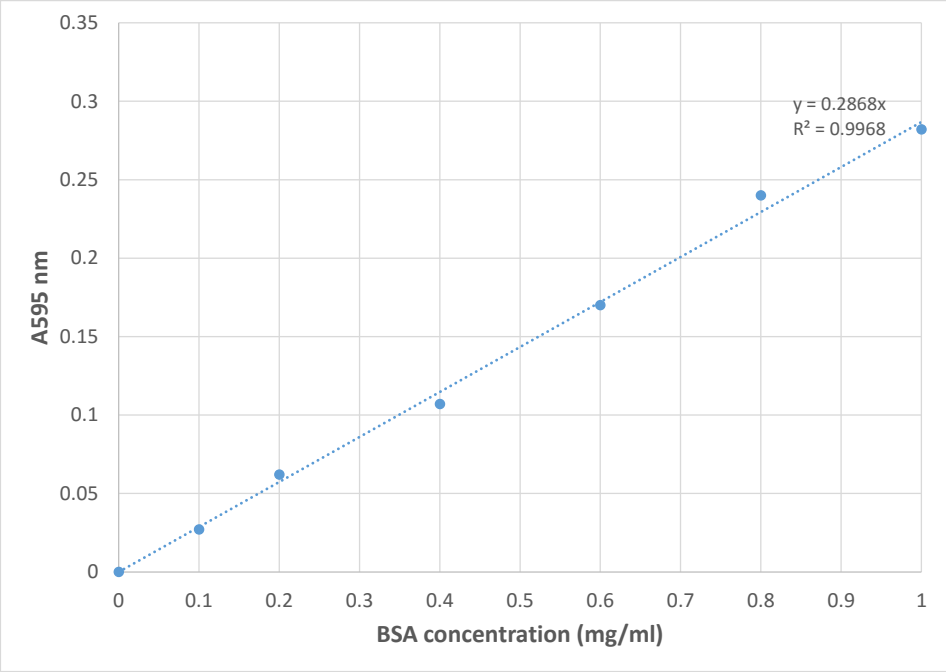

Figure B1 Bradford standard curve for protein concentration determination
Bovine serum albumen (BSA) standards of concentration ranging from 0 to 1 mg/ml were prepared and absorbance was read at 595 nm using (Biorad, U.S.A). The linear equation: y = 0.2868x; R^2 = 0.997 was used to calculate the protein concentration. The protein concentration determined using Bradford were confirmed with Christoph-Leidig method Appendix A10

© University of Venda

B4. GLC sensor chip conditioning

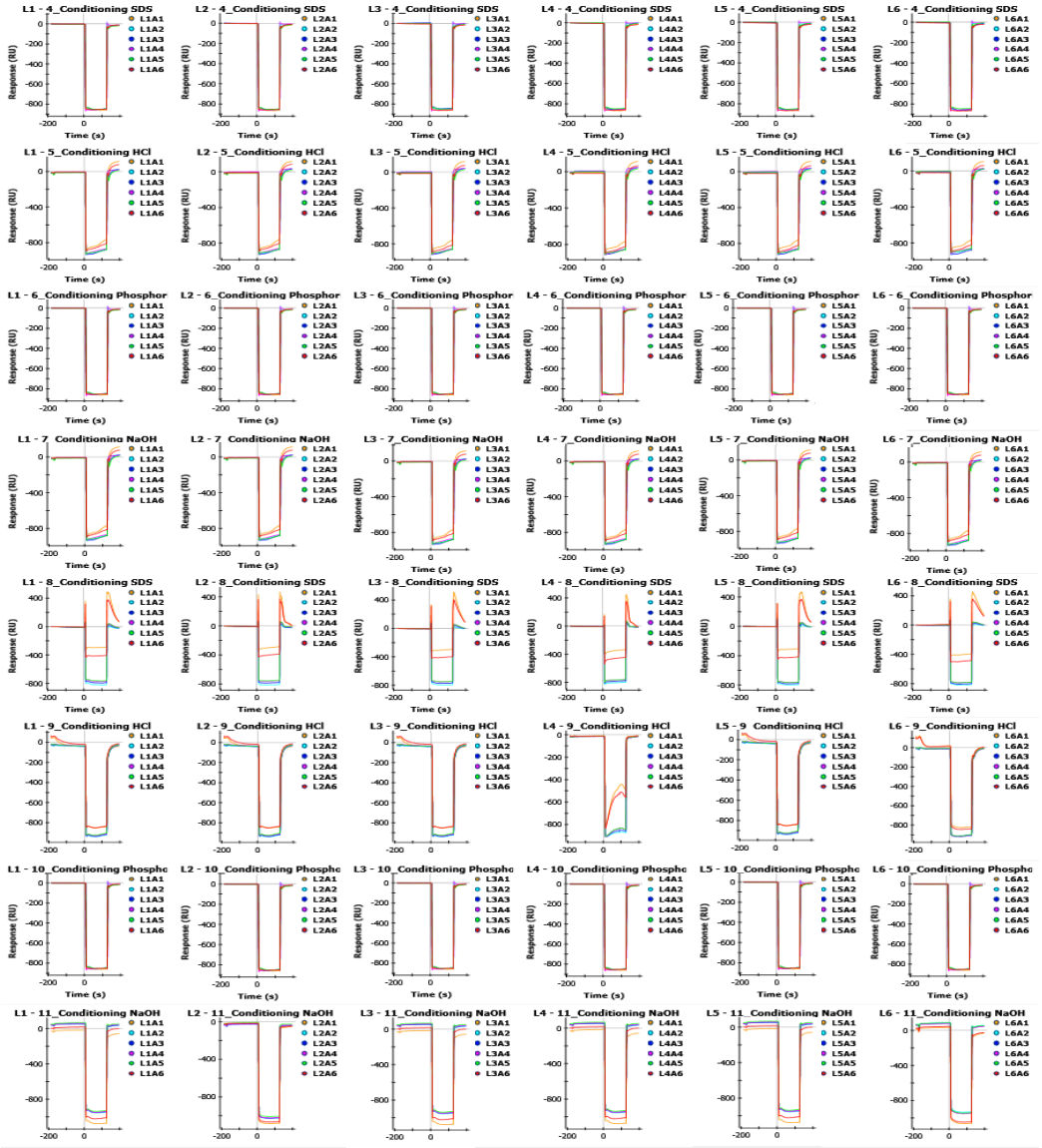

Figure B2. GLC sensor chip Conditioning

The GLC sensor chip was conditioned in horizontal orientation 0.5 % (w/v) SDS, 100 mM HCl, 0.85 % (v/v) Phosphoric acid, 50 mM NaOH, and in vertical orientation 0.5 % (w/v) SDS, 100 mM HCl, 0.85 % (v/v) Phosphoric acid and 50 mM NaOH. These injections were done for all the 6 horizontal (L1-L6) X 6 vertical (A1-A6) channels on the sensor chip

© University of Venda

B5. Ligand pre-concentration

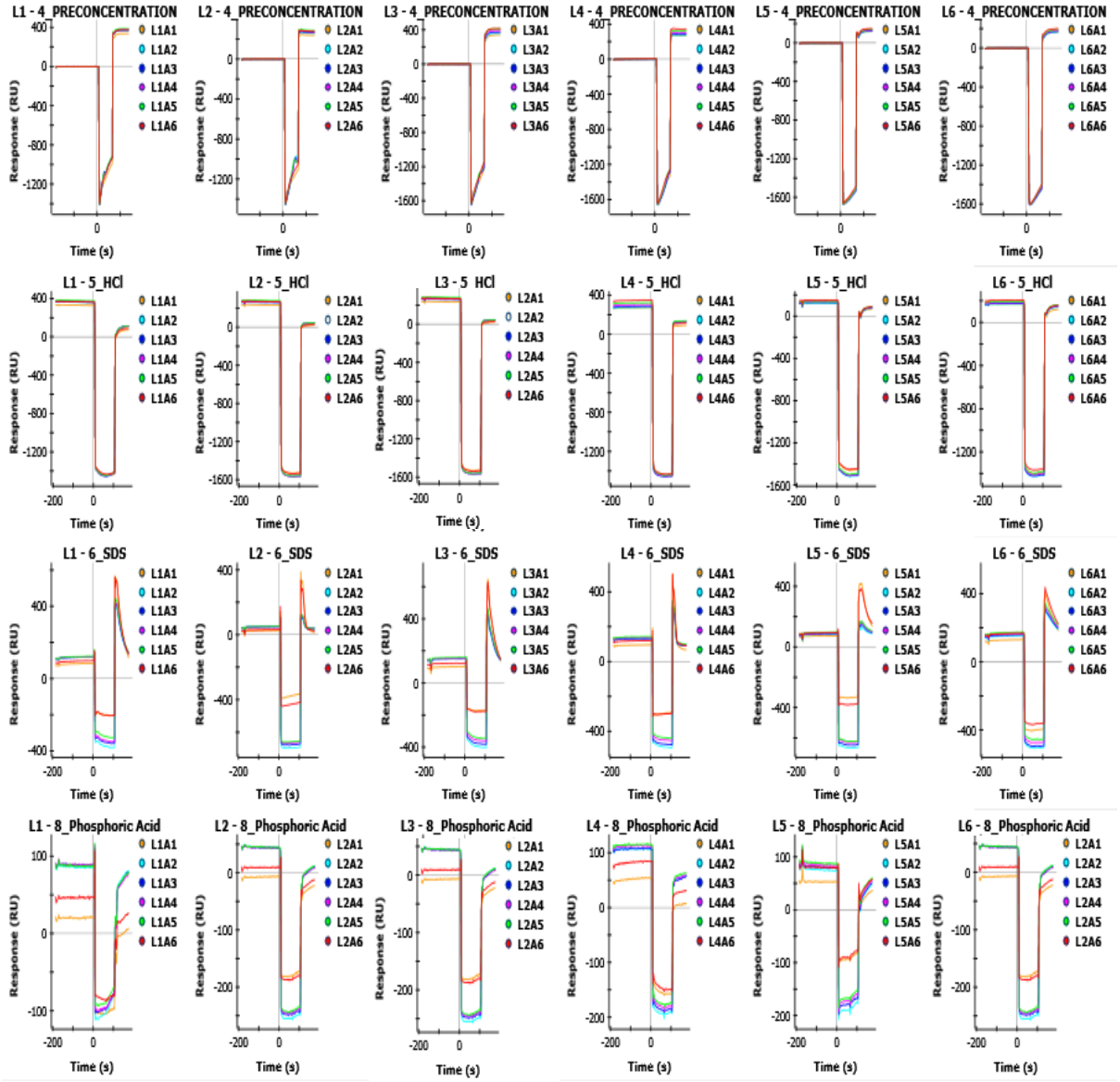

Figure B3. GLC sensor chip ligand pre-concentration

The ligand pre-concentration analysis was conducted to determine the optimum pH for immobilisation using 10 mM Sodium Acetate buffers at pH 4.0 and pH 4.5. This was followed by reconditioning of the chip using 100 mM HCl, 0.5 % (w/v) SDS and 0.85 % (v/v) Phosphoric acid.

© University of Venda

B6. Ligand immobilisation

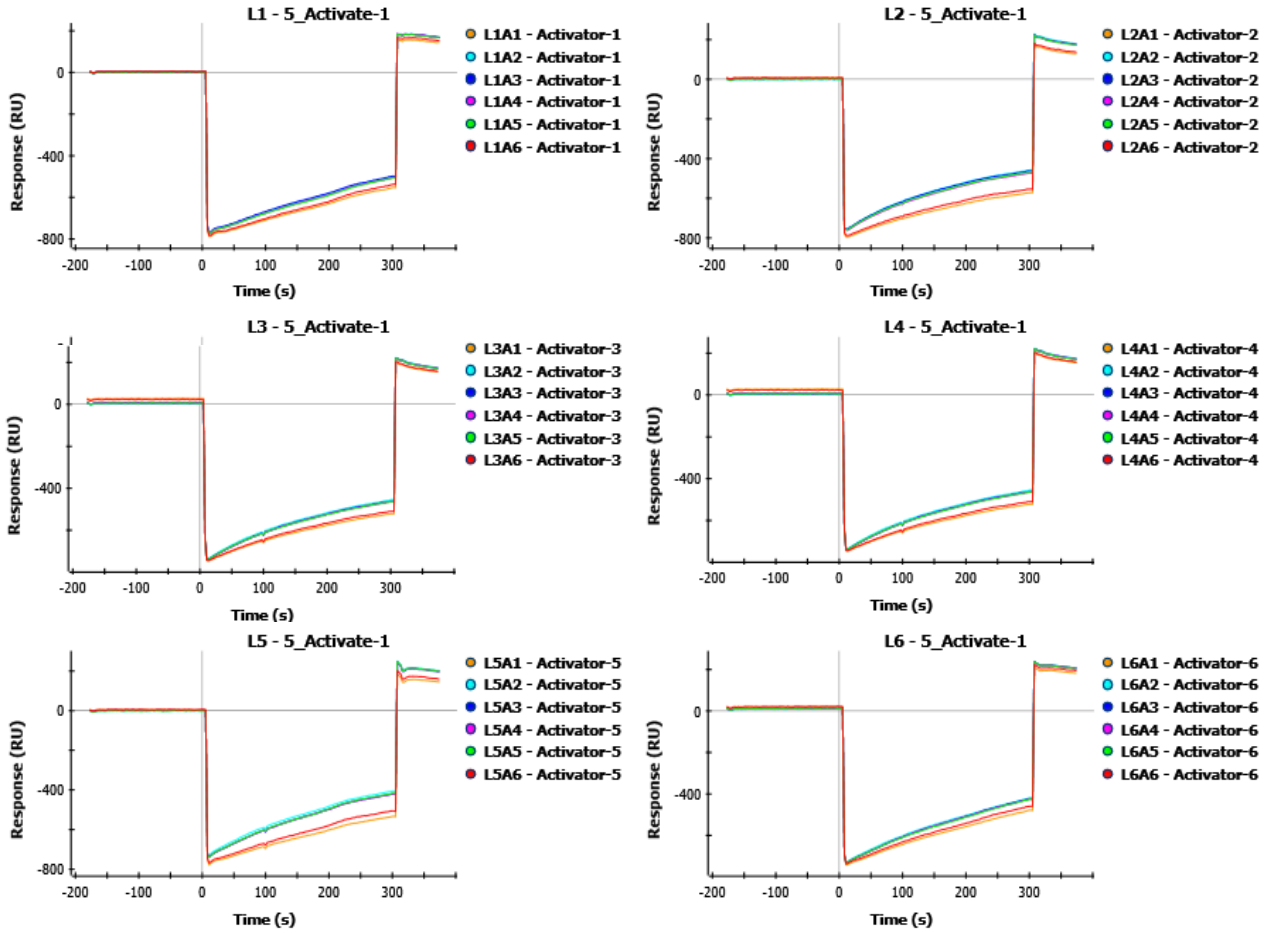

Figure B4. GLC sensor chip ligand immobilisation

The ligand immobilisation on the GLC surface analysis was conducted first the chip was activated with 1-ethyl-3-(3-dimethylaminopropyyl) carbodiimide hydrochroride and N-hydroxysulfosuccirimide. After activation the protein 0.5-1 µg/ml in 10 mM Sodium acetate buffer pH4.0 was injected at a flow rate of 30 µL/s with contact time of 30 seconds. The Chip was subsequently deactivated using 1M ethanolamine HCl pH8.5 to block any remaining carboxy groups on the chip surface.

© University of Venda

B7 Phosphate standard curve

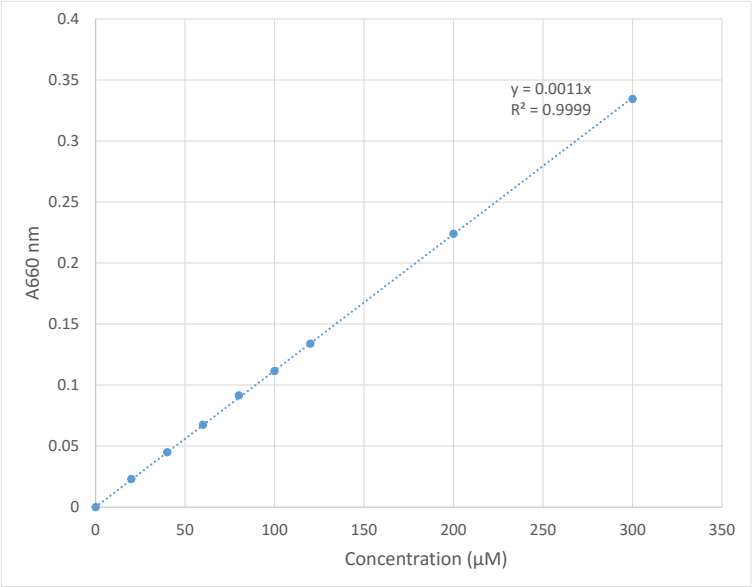

Figure B5 Phosphate standard curve for ATP hydrolysis analysis
Phosphate standards of concentration ranging from 0 to 300 µM were prepared and absorbance was read at 660 nm using (SpectraMax M3, Molecular Devices, U.S.A). The linear equation: y = 0.0011x; R^2 = 0.9999 was used to calculate inorganic phosphate released during ATP hydrolysis.

B8 Thermal stability of chaperone compared to luciferase

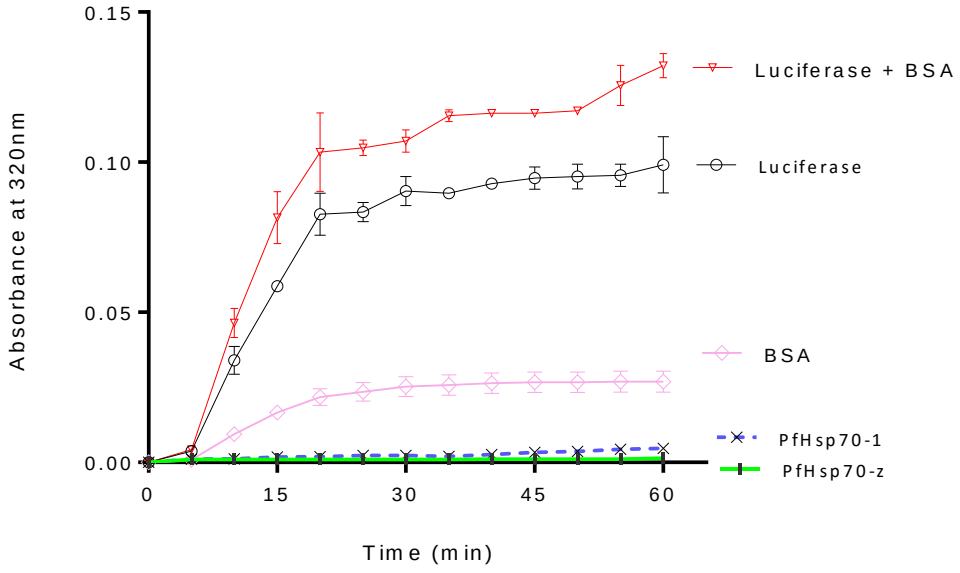

Figure B6. Thermal stability of chaperones compared to luciferase
Heat stability of the recombinant proteins was assessed by the presence of heat induced aggregates measured by increase in absorbance at 320 nm for luciferase using M3 Spectramax (Moleculer Devices). Recombinant proteins PfHsp70-z and PfHsp70-1, substrate luciferase, and BSA as a control. Error bars represent standard deviations obtained from three replicates of each assay.

© University of Venda

B9 Thermal stability of chaperone compared to malate dehydrogenase

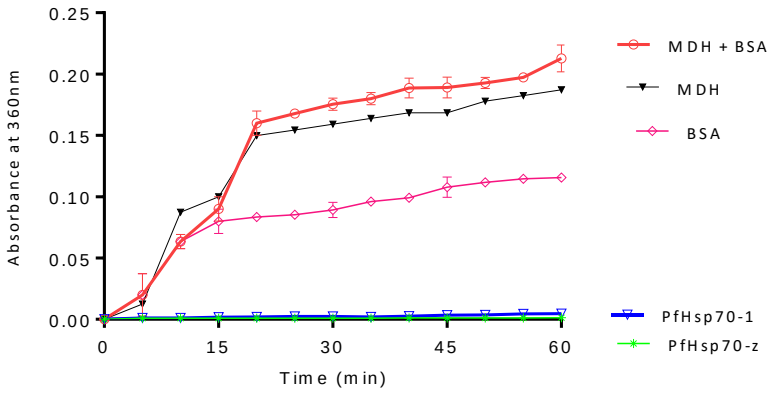

Figure B7. Thermal stability of chaperones compared to MDH
Heat stability of the recombinant proteins was assessed by the presence of heat induced aggregates measured by increase in absorbance at 360 nm for MDH using M3 Spectramax (Moleculer Devices). Recombinant proteins PfHsp70-z and PfHsp70-1, substrate MDH, and BSA as a control. Error bars represent standard deviations obtained from three replicates of each assay.

B10 Antibody specificity determination

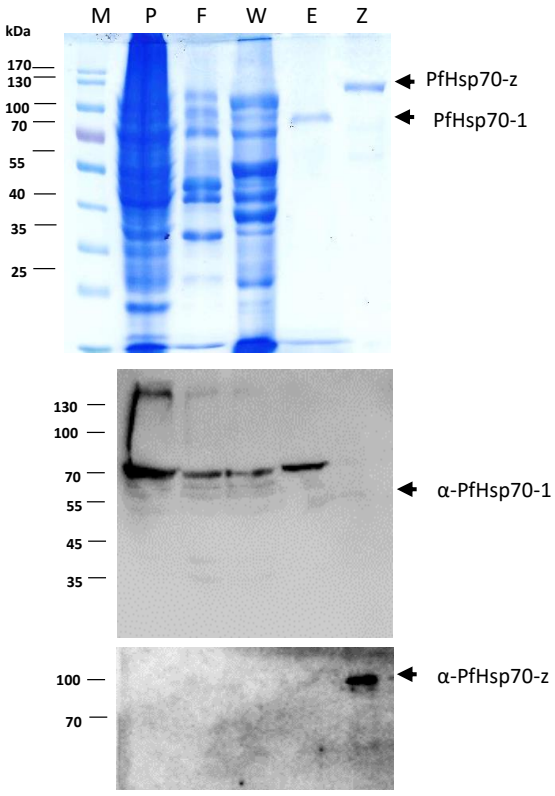

Figure B8. Validation for antibody specificity against PfHsp70-1 and PfHsp70-z
SDS-PAGE (12%) and western analysis of the purification of PfHsp70-1. Lane M – Page ruler (Thermo Scientific) in kDa is shown on the left hand side; lane P, S – the pellet and soluble fraction of total E. coli lysate, lane F – flow through, lane W - wash, lane E – PfHsp70-1 eluted using 500 mM imidazole, lane Z- purified PfHsp70-z. The western Blots were probed using α-PfHsp70-1 and α-PfHsp70-z

© University of Venda

Appendix B11 HTE sensor chip conditioning

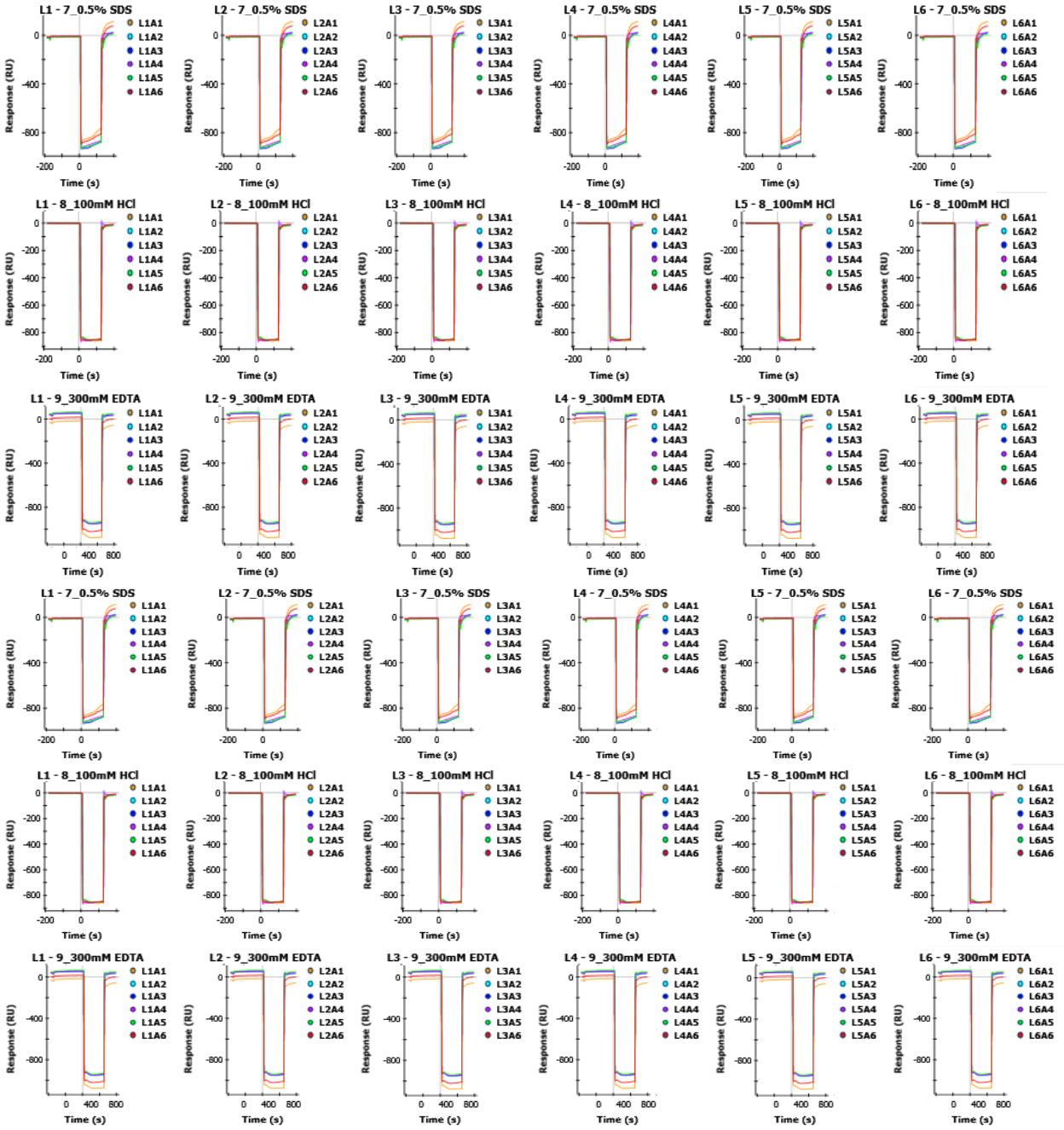

Figure B9. HTE sensor chip conditioning

The HTE sensor chip conditioning was conducted by 0.5 % (w/v) SDS, 100 mM HCl, 300 mM EDTA pH 8.5, for both Horizontal and vertical orientation. The flow rate was maintained at 30 µl/min.

© University of Venda

Appendix B12 Ligand Immobilisation on HTE Chip

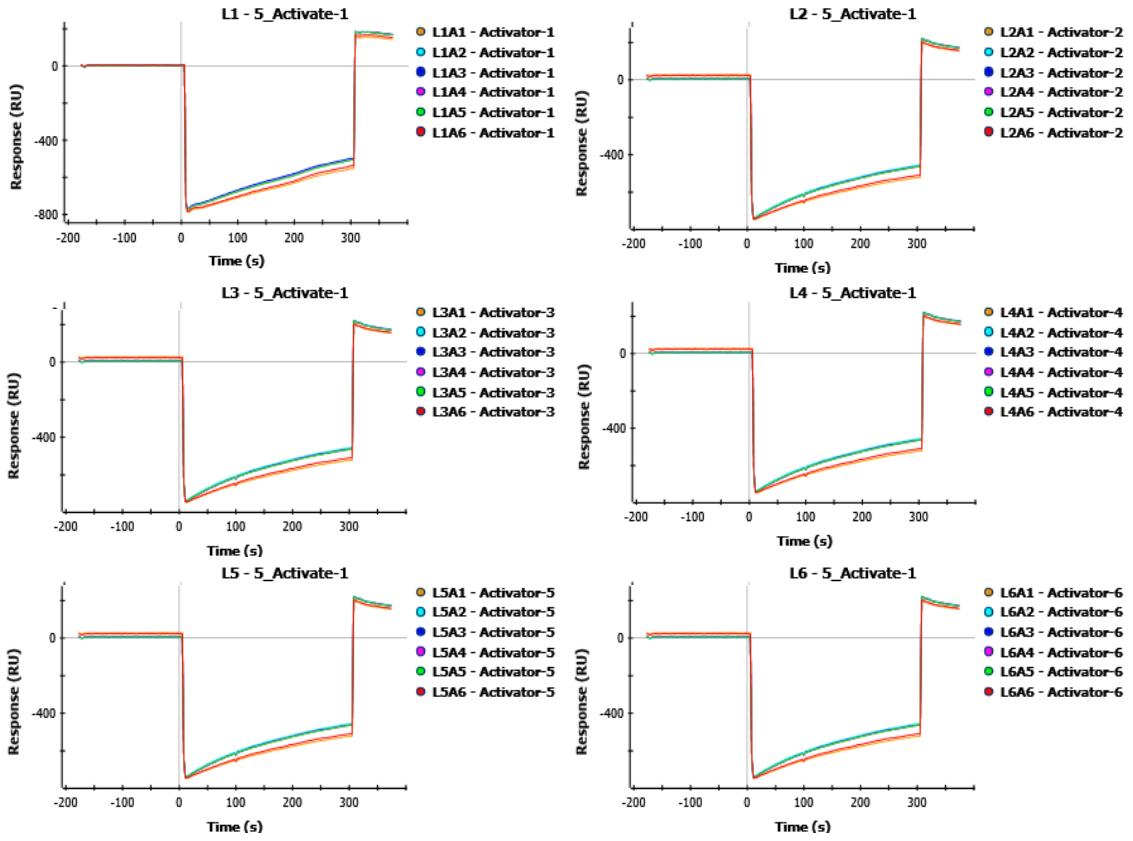

Figure B10. HTE sensor chip activation and ligand immobilisation

The ligand immobilisation on the HTE surface analysis was conducted first the chip was activated with 10 mM $NiSO_4$, pH 6.0. The Ligand was immobilised at 0.5 and 1 µg/ml at a flow rate of 30 µl/min. The Chip was subsequently stabilised using blank buffer (PBST) injections including regeneration (300 mM EDTA, pH 8.5) injections at 100µl/min).

© University of Venda

Appendix C: Specialised reagents

Table C. 1 List of materials and specialised reagents

REAGENT	SUPPLIER
Acetic acid	Merck, Germany
Adenosine triphosphate	Sigma, U.S.A
Agarose	Whitehead scientific, South Africa
Ammonium molybdate	Merck, Germany
Ammonium persulphate	Merck, Germany
Ampicillin	Sigma, U.S.A
Bovine serum albumin	Sigma, U.S.A
Bromophenol blue	Sigma, U.S.A
Calcium chloride	Merck, Germany
Chloramphenicol	Sigma, U.S.A
Coomasie brilliant blue R250	Merck, Germany
Diethiothreitol	Sigma, U.S.A
DreamTaq master mix	Thermo Scientific, U.S.A
Ethidium bromide	Sigma, U.S.A
Glacial acetic acid	Merck, Germany
Glycerol	Merck, Germany
Glycine	Merck, Germany
Imidazole	Sigma, U.S.A
Isopropyl-1-thio-D-galacopyranoside	Sigma, U.S.A
Lysozyme	Merck, Germany
Magnesium chloride	Merck, Germany
Methanol	Merck, Germany
Monoclonal anti-His_6-HRP antibodies	Sigma, U.S.A
Ni-NTA resin	Thermo Scientific, U.S.A
Nitrocellulose membrane	Pierce, U.S.A
PagerRuler Prestained Protein Ladder	Thermo Scientific, U.S.A
Peptone	Merck, Germany
Phenylmethylsufonyl fluoride	Sigma, U.S.A
Polyacrylamide	Merck, Germany
Polyethylene glycol 2000	Sigma, U.S.A
Polyethylenimine	Sigma, U.S.A

© University of Venda

Ponceau S	Sigma, U.S.A
Potassium chloride	Merck, Germany
Potassium dihydrogen phosphate	Merck, Germany
Proteinase-K	Sigma, U.S.A
Rapid ligation buffer	Promega, Germany
Restriction enzymes	Thermo Scientific, U.S.A
Snakeskin™ pleated dialysis tubing	Pierce, U.S.A
Sodium chloride	Merck, Germany
Sodium dodecyl sulphate	Merck, Germany
Sodium hydroxide	Merck, Germany
TEMED	Sigma, U.S.A
Tris	Merck, Germany
Tryptone	Merck, Germany
Tween 20	Merck, Germany
Urea	Melford, UK
Yeast extract powder	Merck, Germany
β-mercaptoethanol	Sigma, U.S.A

© University of Venda